Antragstyp	Schwerpunktprogramm - Einzelantrag - Neuantrag
Type of Proposal	Priority Programme - Individual Proposal - New Proposal
Antragsdauer / Requested Duration	36 Monate / 36 months
Fach	Mathematik
Subject Area	Mathematics
Rahmenprojekt / Framework Project	SPP 2171
Titel	**Steuerbare Substrate: Von mikroskopischen zu makroskopischen Modellen**
Title	**Switchable substrates: From micro to macro models**
Geschäftszeichen / Reference No.	**ME 5355/1-1**
	DFG-Erstantrag / First-Time Applicant
Antragsteller / Applicant	**Dr. Stefan Metzger** Friedrich-Alexander-Universität Erlangen-Nürnberg Department Mathematik Lehrstuhl für Angewandte Mathematik I Erlangen
Kooperationspartnerinnen und Kooperationspartner / Cooperation Partners	Professor Dr. Günther Grün Friedrich-Alexander-Universität Erlangen-Nürnberg Department Mathematik Lehrstuhl für Angewandte Mathematik I Erlangen

Beantragte Mittel / Budget Request:

	Beantragt / Requested		
Dauer [Monate] / Duration [Months]			**36**
ME 5355/1-1			
Summe / Total [Euro]			**186.969**
Dr. Stefan Metzger			
	Anz. / No.	**Dauer / Duration**	**Euro**
Personalmittel / Funding for Staff			**164.369**
Doktorandin/Doktorand und Vergleichbare 75 % / Doctoral Researcher or Comparable 75 %	1	36	145.100

Personal (pauschal) / Other Staff			19.269
Sachmittel / Direct Project Costs			**22.600**
Gäste / Visiting Researchers			3.000
Reisen / Travel			19.600

Zusammenfassung

Durch das Aufbringen von Beschichtungen lassen sich die Benetzungseigenschaften von Oberflächen verändern. Da sich die Mikrostuktur in den Beschichtungen durch externe Felder beeinflussen lassen können, lassen sich schaltbare Oberflächen realisieren. Ziel dieses Projekts im Rahmen des Schwerpunktprogramms 2171 ist die Modellierung solcher Beschichtungen und ihrer Wechselwirkungen mit benetzenden Filmen. In einem ersten Schritt sollen die Beschichtungen mikroskopisch als nematische Fluide modelliert werden. Dies erzeugt verschiedene räumliche und zeitliche Skalen in den Modellgleichungen. Durch Trennung der verschiedenen Skalen sollen anschließend die Modelle vereinfacht werden. Zielsetzung ist die Herleitung neuer, effektiver Modelle, die die wichtigsten Wechselwirkungen zwischen den Beschichtungen, den externen Felder und dem benetzenden Fluiden erfassen ohne die Mikrostuktur komplett auflösen zu müssen.
Neben der analytischen Behandlung der Modelle ist eine numerische Validierung geplant. Dazu sollen die effektiven Modelle sowohl mit den im ersten Schritt erarbeiteten mikroskopischen Modellen, als auch mit den experimentellen Resultaten unserer Kooperationspartner verglichen werden.

Summary

The wetting properties of substrates can be changed by coating layers. As the microstructure of such coating layers may be influenced by external fields, switchable substrates become technically feasible. It is the scope of this project to model such kind of layers together with their interactions with wetting fluid films. In the first part of the project, we plan to describe these layers as nematic liquid crystals. This gives rise to different spatial and temporal scales in the modeling equations. By an appropriate separation of scales, a simplification of the models is envisaged. The scope is to derive novel, effective models which capture the dominant interactions between the coating layers, the external fields and the wetting fluids without requiring a complete resolution of microstructures.
Besides analytical studies of the newly derived models, we focus on their numerical validation. For this purpose, the effective models shall be compared both with the complete microscopic models and with the experimental results of our cooperation partners.

Bemerkung der Geschäftsstelle / Comment by the DFG Head Office

Es liegt ein befristeter Arbeitsvertrag vor, der am 20.08.2020 ausläuft.
Eine Weiterbeschäftigung ist beabsichtigt.
The applicant’s fixed-term contract will expire on 20.08.2020 .
A continued employement is intended.

Project Description – Project Proposals

Stefan Metzger, Friedrich-Alexander-Universität Erlangen-Nürnberg

Switchable substrates: From micro to macro models

Project Description

1 State of the art and preliminary work

1.1 State of the art

When it comes to designing microfluidic hardware, it is in general not possible to scale down conventional devices to the micro-scale. In order to control droplets on this scale, influencing the wettability of the substrate is important. This dynamic process of liquids wetting or dewetting various substrates is an important part in many technological applications. Here, the wetting process depends predominantly on the properties of the liquid-substrate and liquid-air interfaces. One way to influence the wetting process is altering the properties of the liquid-substrate interface by applying thin coatings on the substrate which change the liquid-substrate interfacial energy. Depending on its components, the coating my exhibit internal structures which can be changed by external electric or magnetic fields. This gives rise to switchable substrates. However, the origins of the wettability variation are still not sufficiently understood, although several mechanisms have already been proposed in literature [21].

From the mathematical point of view, the description of wetting or dewetting processes on such switchable coatings contains several challenges. The strong coupling between (de)wetting hydrodynamics and processes in the coating typically introduces additional time and length scales that do not exist in the (de)wetting of inert and rigid substrates. Strong couplings may also impact the mechanisms of energy dissipation and thereby alter the dynamics on a global scale. The numerical treatment of micro-scale models describing these effects precisely is in general very expensive. On the other hand, macroscopic models describing the setting in less detail are often derived as an approximation of the microscopic models under the assumption of a quasi-stationary state. Therefore, the reliability of these models is questionable when the system is far from equilibrium.
The aim of this project is to bridge the gap between precise, microscopic descriptions and approximate coarse scale descriptions.

1.1.1 Two-phase flow

For the description of two-phase flow, there are different modeling approaches at hand. The interface between the two fluids can either be described by a sharp defined interface or by a smooth transition area between the fluids. We start by recalling the governing equations for the two-phase incompressible fluid flow in a classical sharp interface model. Away from the interface the flow is governed by

$$\operatorname{div} \boldsymbol{v} = 0\,, \tag{1.1}$$

$$\partial_t(\rho \boldsymbol{v}) + \operatorname{div}\{\rho \boldsymbol{v} \otimes \boldsymbol{v}\} = \operatorname{div} \boldsymbol{S}\,, \tag{1.2}$$

were $\boldsymbol{v}$ is the fluid velocity, ρ is the mass density and

$$\boldsymbol{S} = -p\mathbb{1} + \eta(\nabla \boldsymbol{v} + (\nabla \boldsymbol{v})^T) \tag{1.3}$$

is the symmetric stress tensor with the fluid viscosity η. Across the fluidic interface Γ, the jump conditions

$$[\boldsymbol{v}] = 0\,, \qquad [-\boldsymbol{S}]\boldsymbol{n}_\Gamma = \hat{\sigma}\kappa\boldsymbol{n}_\Gamma \tag{1.4}$$

hold true. Here, the jump across the interface is denoted by [.] and $\boldsymbol{n}_\Gamma$ is the unit normal on the interface. $\hat{\sigma}$ is the surface energy density and κ denotes the mean curvature. When both fluids touch a solid wall, a three phase contact line occurs and the corresponding contact angle Θ is given by

$$\hat{\sigma}\cos(\Theta) = -\Delta\sigma_{fs}\,, \tag{1.5}$$

where $\Delta\sigma_{fs}$ denotes the difference between the fluid-solid interfacial energies of the wetting fluids. If this difference becomes too large, i.e. $|\Delta\sigma_{fs}| > \sigma > 0$, complete wetting or dewetting occurs and one fluid detaches from the solid wall.
As topological changes, like droplet break-up, droplet coalescence, or detachment from a wall, are hard to capture with a sharp interface model, approaches based diffuse interface methods became popular in the last decades ([1,22,42,43,56]). In [3], a diffuse interface for incompressible two-phase flows with different mass densities was derived. This model combines the advantage of a solenoidal velocity field with a thermodynamically consistent and frame indifferent description of the two-phase flow. The bulk equations in the spatial domain Ω read

$$\rho(\phi)\partial_t\boldsymbol{v} + \left(\left(\rho(\phi)\boldsymbol{v} - \partial_\phi\rho(\phi)m(\phi)\nabla\mu\right)\cdot\nabla\right)\boldsymbol{v} - \operatorname{div}\left\{\eta(\phi)\left(\nabla\boldsymbol{v} + (\nabla\boldsymbol{v})^T\right)\right\} + \nabla p = \mu\nabla\phi\,, \tag{1.6a}$$

$$\operatorname{div}\boldsymbol{v} = 0\,, \tag{1.6b}$$

$$\partial_t\phi + \boldsymbol{v}\cdot\nabla\phi + \operatorname{div}\left\{m(\phi)\nabla\mu\right\} = 0\,, \tag{1.6c}$$

$$\mu = -\sigma\delta\Delta\phi + \sigma\delta^{-1}W'(\phi)\,, \tag{1.6d}$$

and are accompanied by the boundary conditions

$$\boldsymbol{v} = 0\,, \tag{1.6e}$$

$$m(\phi)\nabla\mu\cdot\boldsymbol{n} = 0\,, \tag{1.6f}$$

$$\sigma\delta\nabla\phi\cdot\boldsymbol{n} = \gamma'(\phi)\,. \tag{1.6g}$$

on $\partial\Omega$. Here, $\rho(\phi)$ is a linear interpolation between the mass densities of the two fluids, η is an interpolation of the viscosity, m is the mobility, δ is a parameter connected to the width of the transition region, and σ relates to the surface energy density via $\hat{\sigma} = c_W\sigma$, where c_W is a constant depending on the choice of double-well potential W. The function γ interpolates between the fluid-solid interfacial energy densities. Therefore, the boundary condition (1.6g) is a diffuse interface formulation of Young's formula for the contact angle (1.5) (cf. [65]). The existence of weak solutions was established in [2] and in [33]and [P6], where convergent finite element schemes were presented. This model was later extended by Campillo-Funolet et. al. in [16] to include dissolved ions which interact with external electric fields. The numerical treatment of the arising model was investigated by the applicant in [P7] and [P2] (see also Section 1.1.4 below).

1.1.2 Micro-macro models

For the description of the thin coating, there are different approaches at hand which differ in accuracy, complexity, and the underlying assumptions (cf. [25]). In the most accurate description, the so called Doi or Doi–Hess model [13,23,39,44], liquid-crystalline systems are described as an ensemble of rods which evolve due to thermal motion and pairwise interactions. In these models the state of the liquid-crystalline system is given by a function $f(\boldsymbol{x}, \boldsymbol{d}, t)$ describing the probability that a molecule at point $\boldsymbol{x}$ and a time t is aligned in direction $\boldsymbol{d}$ which is an element of the unit sphere $\mathbb{S}^2$, i.e. $|\boldsymbol{d}| = 1$. In the case of head-to-tail symmetric, nonpolar, rodlike molecules, one cannot distinguish between the orientations $\boldsymbol{d}$ and $-\boldsymbol{d}$. This gives rise to the additional symmetry assumption $f(\boldsymbol{x}, \boldsymbol{d}, t) = f(\boldsymbol{x}, -\boldsymbol{d}, t)$ for all spatial points $\boldsymbol{x}$ in the given spatial domain Ω, all times t, and all orientations $\boldsymbol{d} \in \mathbb{S}^2$. In absence of a velocity field, the evolution of the probability density f is governed by

$$\frac{\partial f}{\partial t} = \frac{1}{\mathrm{De}} \mathcal{R} \cdot \left(f \mathcal{R} \left(\frac{\delta F}{\delta f}[f] \right) \right) , \tag{1.7}$$

where $\mathcal{R} := \boldsymbol{d} \times \frac{\partial}{\partial \boldsymbol{d}}$ denotes the gradient with respect to $\boldsymbol{d}$ restricted to the sphere and $\frac{\delta F}{\delta f}$ denotes the variational derivative of the free energy F with respect to f. In other words, the evolution of f is described by the gradient flow of the free energy functional F which acts as a Lyapunov-type function. This property is the cornerstone for the mathematical analysis of the arising equations. The free energy consists of an entropic term $f \log f - f$, the contribution of the mean-field interactions of the molecules F_{MI}, and interactions with possible external fields F_{ext}. The mean field interactions are described by

$$F_{MI}(\boldsymbol{x}, \boldsymbol{d}, t) := f(\boldsymbol{x}, \boldsymbol{d}, t) \int_\Omega \int_{\mathbb{S}^2} \alpha(\boldsymbol{x} - \hat{\boldsymbol{x}}) \beta(\boldsymbol{d}, \hat{\boldsymbol{d}}) f(\hat{\boldsymbol{x}}, \hat{\boldsymbol{d}}, t) \mathrm{d}\hat{\boldsymbol{d}} \, \mathrm{d}\hat{\boldsymbol{x}} . \tag{1.8}$$

Here, α denotes a suitable localization term modeling the range of the interactions and the integral kernel β describes how the molecules interact with each other. In the case of unpolar, rod-like molecules, typical choices for β are Onsager's potential [61]

$$\beta(\boldsymbol{d}, \hat{\boldsymbol{d}}) = c|\boldsymbol{d} \times \hat{\boldsymbol{d}}| \tag{1.9}$$

with the constant $c > 0$ representing the coupling strength [20, 45], and the Maier–Saupe potential [57]

$$\beta(\boldsymbol{d}, \hat{\boldsymbol{d}}) \sim -(\boldsymbol{d} \cdot \hat{\boldsymbol{d}})^2 , \tag{1.10}$$

which is considered as an approximation (for small angles) of the cross product in (1.9). For the description of the interactions of "dipole-like" crystals, i.e. rods without head-to-tail symmetry, one may also use

$$\beta(\boldsymbol{d}, \hat{\boldsymbol{d}}) \sim -\boldsymbol{d} \cdot \hat{\boldsymbol{d}} . \tag{1.11}$$

In presence of an external magnetic field $\boldsymbol{H}$, F_{ext} can be written as

$$F_{ext}(\boldsymbol{x}, \boldsymbol{d}, t) = -(\chi_\parallel - \chi_\perp)(\boldsymbol{d} \cdot \boldsymbol{H})^2 f(\boldsymbol{x}, \boldsymbol{d}, t) \tag{1.12}$$

with susceptibilities $\chi_\parallel$ and $\chi_\perp$ parallel and perpendicular to the direction $\boldsymbol{d}$.
In the absence of external forces, the mathematical theorie is well established. Constantin et. al. proved the existence of solutions to (1.7) in [17], while the structure of stationary solutions was investigated in [55]. The inhomogeneous case which occurs, e.g., as a result of an externally imposed flow field with an $\boldsymbol{x}$-dependend velocity gradient is also well-understood: In [64], Otto and Tazavaras proved the existence of strong solutions to the Doi–Hess model coupled to a Stokes type equations. In [5, 6], Bae and Trivisa proved global existence of weak solutions and extended this result to compressible fluid flow.

We want to highlight that the structure of the Doi model is very similar to the micro-macro models used for the description of dilute polymeric solutions, where the mean-field interactions F_{MI} are neglected and the constraint $|\boldsymbol{d}| \equiv 1$ is replaced by a relative entropy penalizing deviations of f from a certain preferred distribution. These models are also well-understood, see e.g. [8,10] for analytical results and [9,11] for the discussion of discrete schemes. These results were extended to the case of two-phase flow by Grün and Metzger in [P5]. Using Onsager's variational principle [59,60], they derived a thermodynamically consistent multiscale model. In this model f was not interpreted as a probability density with a marginal equal to one. Instead, Grün and Metzger interpreted f as a number density for the polymer chains and therefore the marginal provides the time-dependent number of polymers at a spatial point $\boldsymbol{x}$. The existence of weak solutions to the aforementioned model was also established in [P5] and an energy stable, convergent finite element scheme was proposed in [P1] together with simulations in two and three spatial dimensions (cf. Section 1.1.4 and Fig 2).

Instead of considering the dynamics of the probability density f, which depends on the high-dimensional product space $\Omega \times \mathbb{S}^2$, one can simplify the model by considering only the evolution of the lowest-order moment of f [20]. For nonpolar particles the first moment $\int_{\mathbb{S}^2} \boldsymbol{d} f(\boldsymbol{x}, \boldsymbol{d}, t) \mathrm{d}\boldsymbol{d}$ vanishes for all spatial points $\boldsymbol{x}$ at all times t. Therefore, it suffices to consider the evolution of the second moment $Q(\boldsymbol{x}, t) := \int_{\mathbb{S}^2} \left(\boldsymbol{d} \otimes \boldsymbol{d} - \frac{1}{3}\mathbb{1}\right) f(\boldsymbol{x}, \boldsymbol{d}, t) \mathrm{d}\boldsymbol{d}$ which gives rise to the so called Q-tensor theory [7,20,40]. At this point, we want to highlight that a stress tensor with a similar structure can be obtained by coarse graining density based descriptions of dilute polymeric solutions (cf. [P5], [P3]).

Under the assumption of uniaxial nematic states, which typically holds only for liquid crystals at low molecular weights (cf. [13]), the structural orientation in the liquid-crystalline systems can be fully described by the normalized eigenvector $\boldsymbol{d}$ to the eigenvalue with the largest absolute value This eigenvector is unique up to a multiplication with -1. This approach dates back to the results of Ericksen [26,27], Leslie [46–48], Oseen [63], and Franck [29]. Similar to the probability distribution f in the Doi-Hess description, the evolution of the nematic director $\boldsymbol{d}$ is governed by a free energy. Leslie [47] suggested to use the free energy density

$$F(\boldsymbol{d}, \nabla \boldsymbol{d}) := k_1(\nabla \cdot \boldsymbol{d})^2 + k_2(\boldsymbol{d} \cdot \nabla \times \boldsymbol{d})^2 + k_3|\boldsymbol{d} \times \nabla \times \boldsymbol{d}|^2 + (k_2 + k_4)(\mathrm{tr}(\nabla \boldsymbol{d})^2 - (\nabla \cdot \boldsymbol{d})^2)\,, \tag{1.13}$$

an expression introduced by Oseen and Franck with the splay, twist, and bend elastic constants k_1, k_2, and k_3, and $(k_2 + k_4)$ describing the so called saddle-splay. To include an external magnetic field, one may follow the approach by de Gennes [20] and expand (1.13) by adding

$$F_{ext}(\boldsymbol{d}) = -\chi_\perp |\boldsymbol{H}|^2 - (\chi_\parallel - \chi_\perp)(\boldsymbol{d} \cdot \boldsymbol{H})^2 \tag{1.14}$$

with an externally controlled magnetic field $\boldsymbol{H}$ and susceptibilities $\chi_\parallel$ and $\chi_\perp$ parallel and perpendicular to the director $\boldsymbol{d}$. A frequently used simplification of the Oseen-Franck free energy (1.13) is the so called "one-constant-approximation" with $k_1 = k_2 = k_3 = \frac{\gamma}{2}$ and $k_4 = 0$. In this case, the free energy density simplifies to

$$F(\boldsymbol{d}, \nabla \boldsymbol{d}) = \frac{1}{2}|\nabla \boldsymbol{d}|^2 \tag{1.15}$$

(cf. [20,66]). A further simplification was introduced by Lin and Liu in [49], where they removed the algebraic restriction $|\boldsymbol{d}| = 1$ and rather added a Ginzburg–Landau penalty functional to the free energy density. In this case the free energy functional reads

$$F_\varepsilon(\boldsymbol{d}, \nabla \boldsymbol{d}) = \frac{1}{2}|\nabla \boldsymbol{d}|^2 + \frac{1}{4\varepsilon^2}\left(|\boldsymbol{d}|^2 - 1\right)^2 . \tag{1.16}$$

Coupled with Navier–Stokes equations describing the evolution of the momentum, the arising model reads

$$\frac{\partial \boldsymbol{d}}{\partial t} + (\boldsymbol{v} \cdot \nabla)\, \boldsymbol{d} - \boldsymbol{d} \cdot \nabla \boldsymbol{v} = \Delta \boldsymbol{d} - \frac{1}{\varepsilon^2}\left(|\boldsymbol{d}|^2 - 1\right) \boldsymbol{d}\,, \tag{1.17a}$$

$$\frac{\partial \boldsymbol{v}}{\partial t} + (\boldsymbol{v} \cdot \nabla)\, \boldsymbol{v} + \nabla p - \eta \Delta \boldsymbol{v} = -\nabla \cdot \left(\nabla \boldsymbol{d}^T \nabla \boldsymbol{d}\right)\,, \tag{1.17b}$$

$$\nabla \cdot \boldsymbol{v} = 0\,, \tag{1.17c}$$

where η denotes the viscosity of the ambient fluid. Existence of strong solution to a simplified model was first established in [49] and later extended to a more general case in [50].
While the Doi–Hess model arises from molecular kinetic theory, the Q-tensor theory and the Ericksen–Leslie theory are phenomenological [38] and rely on phenomenological parameters which are often hard to determine from experimental results. Therefore, the connection of the later theories to the Doi–Hess model was intensely studied in the recent years [24, 38, 45, 67], as it allows to derive the unknown parameters from molecular quantities. However, the derivation of the Q-tensor theory and the Ericksen–Leslie theory from the Doi–Hess description relies on appropriate closure conditions and requires the system to be close to equilibrium [38, 67]. Consequently, it is not clear how the dynamics of these models relate in a state far from equilibrium.

1.1.3 Lubrication approximation of thin films

Dimension reduced models offer a pathway to reduce the numerical costs of computer simulations while still capturing significant features of wetting processes. In recent decades, various classes of thin-film type equaions have been derived by lubrication approximation under the general assumption that the ratio between typical vertical and horizontal length scales is small and that the liquid viscosity is sufficiently high (see [35, 62] and the references therein).

In many cases, they come along with a gradient structure

$$\frac{\partial h}{\partial t} = \nabla \left[Q(h) \nabla \left(\frac{\delta F}{\delta h} \right) \right] \,, \tag{1.18}$$

where h is to describe the height of the liquid film above a substrate. $Q(.)$ is a usually degenerate mobility function – depending on the flow condition at the liquid–substrate interface, for instance $Q(h) \sim h^3$ in case of a no-slip condition. The underlying physics are captured by the energy

$$F(h) = \int_\Omega \tfrac{\gamma}{2} |\nabla h|^2 + f(h)\,. \tag{1.19}$$

Here, the Dirichlet integral models the energy of the liquid-gas interface and f my be used to include further effects – for instance long-range van der Waals-interactions with a – possibly heterogeneous substrate. During the last 25 years, these fourth-order degenerate parabolic equations have been studied or are still under investigation. Concerning rigorous mathematical analysis, global existence of solutions has been studied ([14, 15, 18, 32]) as well as the evolution of free-boundaries ([19, 31]) or the regularity of free boundaries ([30]). Convergent numerical schemes ([36, 37]) have been used to validate thin-film models ([12, 58]) and to predict new dewetting scenarios.

Thin films models have successfully been applied to the structure formation in thin liquid-liquid films. In that case, systems of degenerate fourth-oder parabolic equations are considered – and similarly as in the single-layer case, integral estimates become crucial both for analysis and numerics (for an overview, see [41] and the references therein).

In the recent years also a few results concerning liquid-crystalline films were obtained (see [51,52] and the references therein). However, these results differ concerning a possible stabilizing or destabilizing effect of the elastic energy on the film. Those differences were recently traced back by Lin et. al. [51] to incompatible stress balance conditions at the free interface, which neglected the elastic stresses. By deriving a lubrication approximation for a thin film of nematic liquid crystal with strong anchoring conditions in two spatial dimension, Lin et. al. established the stabilizing effect for the case of compatible interface conditions. In [52], Lin et. al. derived a

Figure 1: Ionic droplet in an electric field (published in [P2]): Droplet shape (left) and cross section with dissolved ions (right).

lubrication approximation for a thin liquid-crystalline film and investigated the influence of the anchoring direction on the substrate on the spreading of the film. However, the instantaneous adjustment of the directors to their unique steady state was used as a key assumption in order to avoid dealing with multiple time scales. It is not clear whether this assumption is also appropriate for more intricate scenarios which include interactions with am additional wetting fluid and external fields.

1.1.4 Preliminary work on the numerical treatment of micro-macro models and electric effects

The importance of stable and efficient schemes for the simulation of complex flow problems is undeniable. First, the different involved length scales lead to high-dimensional systems which can not be treated monolithically. Secondly, the interactions between different physical components (like coating and wetting fluids) induce a strong coupling in the arising partial differential equations. To reduce these couplings, specific discretization techniques are necessary. In [P6] a special time approximation of the transport velocity was used to drive a convergent numerical scheme for two-phase flow which decouples the Cahn–Hilliard and Navier–Stokes equations and thereby reduces the computation time drastically. This approach was refined in [P7] and [P2] for a Cahn–Hilliard–Poisson–Nernst–Planck–Navier–Stokes system. The resulting finite element scheme then allows for a sequential treatment of the different blocks of the model and thereby omits the employment of a fixed point method. To show the practicality of the schemes, simulations of ion induced topology changes were performed. Due to the electric field induced by the electrodes depicted as red and blue lines on right-hand side of Fig. 1, the uncharged molecules (green) decompose to charged ions (red and blue) which move towards the electrodes. Thereby, the droplet gets stretched and finally breaks.

Special attention has also to be paid to artificial diffusion induced by the numerical scheme. As shown in [P2], a reduction of artificial diffusion allows for larger time increments without loss of accuracy. Based on these techniques, the applicant derived a convergent finite element scheme for a Cahn–Hilliard–Fokker–Planck–Navier–Stokes system describing two-phase flow of dilute polymeric solutions. To investigate the influence of the dissolved polymer chains on the oscillatory behavior of a droplet, simulations in two and three spatial dimensions were made. The resulting pictures, which show the oscillating droplet and the additional stresses induced by the deformation of the polymer chains, are depicted in Fig. 2.

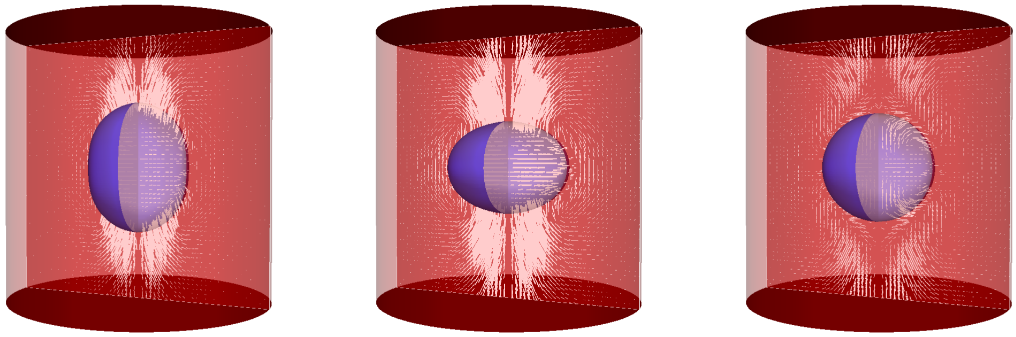

Figure 2: Simulation of two-phase flow of dilute polymeric solutions (published in [P1]).

1.2 Project-related publications

1.2.1 Articles published by outlets with scientific quality assurance, book publications, and works accepted for publication but not yet published.

[P1] S. Metzger, *On convergent schemes for two-phase flow of dilute polymeric solutions*, ESAIM: Mathematical Modelling and Numerical Analysis, Forthcoming article, accepted 2018, 52 pages.

[P2] S. Metzger, *On stable, dissipation reducing splitting schemes for two-phase flow of electrolyte solutions*, Numerical Algorithms, Forthcoming article, accepted 2018, 32 pages.

[P3] G. Grün, S. Metzger, *Micro-Macro-Models for Two-Phase Flow of Dilute Polymeric Solutions: Macroscopic Limit, Analysis, and Numerics*, Chapter in Transport Processes at Fluidic Interfaces, Springer International Publishing, 2017, 291–304.

[P4] H. Abels, H. Garcke, G. Grün, and S. Metzger, *Diffuse interface models for incompressible two-phase flows with different densities*, Chapter in Transport Processes at Fluidic Interfaces, Springer International Publishing, 2017, 203–229.

[P5] G. Grün, S. Metzger, *On micro-macro-models for two-phase flow with dilute polymeric solutions – modeling and analysis*, Mathematical Models and Methods in Applied Sciences **26** (2016), no. 05, 823–866.

[P6] G. Grün, F. Guillén-González, and S. Metzger, *On fully decoupled, convergent schemes for diffuse interface models for two-phase flow with general mass densities*, Communications in Computational Physics **19**, (2016), no. 5, 1473–1502.

[P7] S. Metzger, *On numerical schemes for phase-field models for electrowetting with electrolyte solutions*, Proceedings in Applied Mathematics and Mechanics **15** (2015), no. 1, 715–718.

1.2.2 Other publications

Not applicable.

1.3 Patents

Not applicable.

2 Objectives and work programme

2.1 Anticipated total duration of the project

The project's intended duration is 6 years. The application period is 36 month.

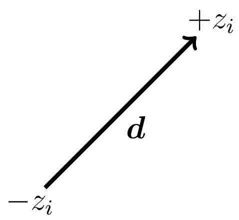

Figure 3: Sketch of a dipole.

2.2 Objectives

This project aims for a better understanding of wetting phenomena on flexible and switchable substrates. The properties of theses substrates are often dominated by thin coatings covering their surface. As the size of the structures in these coatings is significantly smaller than the lateral extension of the wetting droplet, different length scales are inherent to the problem. This makes monolithic numerical simulations very expensive, as the size of the computational domain is prescribed by a macroscopic length scale (e.g. the diameter of the wetting droplet), while the resolution is prescribed by a microscopic length scale (e.g. size of the structures in the coating) which is magnitudes smaller. In addition, changes on the microscopic length scale may happen very fast in comparison to the macroscopic evolution of the droplet. Therefore, resolving these changes leads to severe restrictions on the size of the time increment. As a consequence, identifying and separating the involved spatial and temporal scales is of great importance.

The aim of our project is threefold:

- We wish to provide a better understanding of the microscopic interactions at the fluid-solid contact line and – in particular – at the three phase contact line. For this reason, we will derive thermodynamically consistent microscopic models which are able to capture the interactions between the structures of the coating and the ambient fluid. Here, we will adapt liquid crystal models (cf. Section 1.1.2) to describe the coating, as these models include the orientation of structures as well as their interactions.
- Secondly, we shall derive effective macroscopic models which still include the main dynamics from the micro scale but allow for a more efficient treatment.
- Finally, we will derive stable and efficient numerical schemes for the aforementioned models and aim for a comparison of numerical and experimental results.

2.2.1 Micro-macro models for fluid-substrate interactions

As a first part of the project, we will derive thermodynamically consistent models describing the interactions between the wetting fluid and the underlying switchable substrate. Thereby, we will concentrate on the setting depicted in Fig. 4: A solid substrate Ω_s is coated by a thin nematic layer Ω_c of height l. On top of this layer, two immiscible fluids are placed. At the three phase contact line, the fluids form the contact angle θ, which depends on the surface tension between the fluids and the phase-dependent interfacial energy density on the fluid-coating interface $\Gamma_{c,f}$. The peculiarity of this approach is that the interfacial energy density on $\Gamma_{c,f}$ depends not only on the fluid phases but also on the orientation of microstructures in the nematic coating. To influence the orientation of liquid-crystalline structures, we will employ an external electric field.

In a first step, we shall adapt the approaches by Campillo et. al. [16], Fontelos et. al. [28] and by Grün and Metzger [P5] to derive a Doi-type model. In addition to the spatial domain which is denoted by $\Omega \subset \mathbb{R}^3$, we consider a larger domain $\Omega^* \supset \Omega$ for the electric field in order to reduce the bias introduced to the electric field by the finite size of the domain. The orientation of a rod-like liquid crystal molecule is described by the probability density function f which depends on the spatial coordinate $\boldsymbol{x} \in \Omega$, the time t and the orientation vector $\boldsymbol{d} \in \mathbb{S}^2$ with $\mathbb{S}^2$ denoting the unit sphere. These molecules are assumed to have electric dipole properties, i.e. positive and negative bound charges occur which, for simplicity, are assumed to be at the endpoints of the rod. Therefore, we may describe the polarization of a molecule by $z\boldsymbol{d}$, where $z \geq 0$ denotes the magnitude of the occurring charges in one molecule (cf. Fig. 3). The derivation of the model starts from balance equations for the probability density and the momentum, and Gauss's and Ampére's laws describing the electric field. Assuming that the fluid is incompressible and that magnetic fields can be neglected, we have the balance equation

$$\partial_t f + \operatorname{div}_{\boldsymbol{x}} \{\boldsymbol{v} \nabla_{\boldsymbol{x}} f\} + \operatorname{div}_{\mathcal{R}} \{\boldsymbol{d} \times \nabla_{\boldsymbol{x}} \boldsymbol{v} \boldsymbol{d} \psi\} + \operatorname{div}_{\boldsymbol{x}} \{\boldsymbol{J}_{f,\boldsymbol{x}}\} + \operatorname{div}_{\mathcal{R}} \{\boldsymbol{J}_{f,\boldsymbol{d}}\} = 0 \tag{2.1a}$$

for the density f on $\Omega \times \mathbb{S}^2$ with the rotational differential operator $\mathcal{R} := \boldsymbol{d} \times \frac{\partial}{\partial \boldsymbol{d}}$ and the correspondingly defined divergence operator $\operatorname{div}_{\mathcal{R}}$. The momentum balance with incompressibility condition is given as

$$\begin{aligned} \partial_t \boldsymbol{v} + \operatorname{div}_{\boldsymbol{x}} \{\boldsymbol{v} \otimes \boldsymbol{v}\} - \operatorname{div}_{\boldsymbol{x}} \boldsymbol{S} + \nabla_{\boldsymbol{x}} p - \boldsymbol{k} = 0\,, && (2.1\text{b}) \\ \operatorname{div}_{\boldsymbol{x}} \boldsymbol{v} = 0 && (2.1\text{c}) \end{aligned}$$

in Ω, and the electric field is governed by Ampére's and Gauss's laws

$$\begin{aligned} \epsilon \partial_t \boldsymbol{E} + \chi_\Omega \int_{\mathbb{S}^2} z \boldsymbol{d} \partial_t f = 0\,, && (2.1\text{d}) \\ \operatorname{div}_{\boldsymbol{x}} \{\epsilon \boldsymbol{E}\} = - \operatorname{div}_{\boldsymbol{x}} \left\{ \chi_\Omega z \int_{\mathbb{S}^2} \boldsymbol{d} f \right\} && (2.1\text{e}) \end{aligned}$$

in $\Omega^* \supset \Omega$. Here, χ_Ω denotes the characteristic function of Ω. A powerful tool for the determination of the unknown quantities in (2.1), which are the fluxes $\boldsymbol{J}_{f,\boldsymbol{x}}$ and $\boldsymbol{J}_{f,\boldsymbol{d}}$, the symmetric stress tensor $\boldsymbol{S}$, and the force term $\boldsymbol{k}$, is Onsager's variational principle [59, 60] – an approach which has already been applied successfully in [3, 16, 65] and [P5]. Separating the terms which only contribute to the work and do not produce entropy, provide an expression for $\boldsymbol{k}$. To determine the remaining, entropy producing terms, we apply Onsager's variational principle.

This principle states that the first variation δ with respect to $\boldsymbol{J}_{f,\boldsymbol{x}}$, $\boldsymbol{J}_{f,\boldsymbol{d}}$, and $\boldsymbol{S}$ of the sum of the rate of energy $\mathcal{E}$ and a dissipation functional Φ disappears. In particular, it states

$$\delta \left(\frac{\mathrm{d}\mathcal{E}}{\mathrm{d}t} + \Phi \right) \stackrel{!}{=} 0\,. \tag{2.2}$$

Concerning the energy, we want to consider the following contributions: The kinetic energy $\frac{1}{2} \int_\Omega |\boldsymbol{v}|^2$, the (negative) entropy $\int_\Omega \int_{\mathbb{S}^2} f \log f - f$, the contribution of the electric field $\frac{1}{2} \int_{\Omega^*} \epsilon |\boldsymbol{E}|^2$, the orientation energy of the dipoles $\int_\Omega \int_{\mathbb{S}^2} \boldsymbol{E} \cdot \boldsymbol{d} z f$, and the interaction of potential of the molecules which has the form

$$\frac{1}{2} \int_\Omega \int_\Omega \int_{\mathbb{S}^2} \int_{\mathbb{S}^2} \alpha(\boldsymbol{x} - \hat{\boldsymbol{x}}) \beta(\boldsymbol{d}, \hat{\boldsymbol{d}}) f(\hat{\boldsymbol{x}}, \hat{\boldsymbol{d}}, t) f(\boldsymbol{x}, \boldsymbol{d}, t) \, \mathrm{d}\hat{\boldsymbol{d}} \, \mathrm{d}\boldsymbol{d} \, \mathrm{d}\hat{\boldsymbol{x}} \, \mathrm{d}\boldsymbol{x} \tag{2.3}$$

with an appropriate localization term α and β defined in (1.10) or (1.11), depending on whether the influence of the charges on the mean-field interactions is negligible or not. In combination with the the mass conserving boundary conditions

$$\begin{aligned} \boldsymbol{v} =& 0\,, && (2.4) \\ \boldsymbol{J}_{f,\boldsymbol{x}} \cdot \boldsymbol{n}_{\boldsymbol{x}} =& 0 && (2.5) \end{aligned}$$

on $\partial\Omega$ and the dissipation functional

$$\Phi\left(\boldsymbol{J}_{f,\boldsymbol{x}},\boldsymbol{J}_{f,\boldsymbol{d}},\boldsymbol{S}\right) := \int_\Omega\int_{\mathbb{S}^2}\frac{\left|\boldsymbol{J}_{f,\boldsymbol{x}}\right|^2}{2fD_{\boldsymbol{x}}} + \int_\Omega\int_{\mathbb{S}^2}\frac{\left|\boldsymbol{J}_{f,\boldsymbol{d}}\right|^2}{2fD_{\boldsymbol{d}}} + \int_\Omega\frac{\left|\boldsymbol{S}\right|^2}{4\eta}\,, \tag{2.6}$$

this approach gives rise to the following set of equations. The evolution of the density f is governed by

$$\partial_t f + \boldsymbol{v}\cdot\nabla_{\boldsymbol{x}} f + \operatorname{div}_{\mathcal{R}}\left\{\boldsymbol{d}\times\nabla_{\boldsymbol{x}}\boldsymbol{v}\boldsymbol{d}f\right\} = \operatorname{div}_{\boldsymbol{x}}\left\{D_{\boldsymbol{x}}f\nabla_{\boldsymbol{x}}\mu_f\right\} + \operatorname{div}_{\mathcal{R}}\left\{D_{\boldsymbol{d}}f\mathcal{R}\mu_f\right\} \tag{2.7a}$$

on $\Omega\times\mathbb{S}^2$. The chemical potential μ_f is the first variation of the free energy with respect to f, i.e.

$$\begin{aligned}\mu_f(\boldsymbol{x},\boldsymbol{d},t) =& 2\nabla_{\boldsymbol{x}}V(\boldsymbol{x},t)\cdot\boldsymbol{d}z + \log f(\boldsymbol{x},\boldsymbol{d},t) + \tfrac{1}{\epsilon}\left(\int_{\mathbb{S}^2} zf(\boldsymbol{x},\hat{\boldsymbol{d}},t)\,\mathrm{d}\hat{\boldsymbol{d}}\right)\cdot\boldsymbol{d}z\\ &+\int_\Omega\int_{\mathbb{S}^2}\alpha(\boldsymbol{x}-\hat{\boldsymbol{x}})\beta(\boldsymbol{d},\hat{\boldsymbol{d}})f(\hat{\boldsymbol{x}},\hat{\boldsymbol{d}},t)\,\mathrm{d}\hat{\boldsymbol{d}}\,\mathrm{d}\hat{\boldsymbol{x}}\,.\end{aligned} \tag{2.7b}$$

For the momentum, we obtain the Navier–Stokes equations with an additonal stress tensor depending on the microstructures.

$$\begin{aligned}\partial_t\boldsymbol{v} + \operatorname{div}_{\boldsymbol{x}}\left\{\boldsymbol{v}\otimes\boldsymbol{v}\right\} - \operatorname{div}_{\boldsymbol{x}}\left\{\eta\left(\nabla\boldsymbol{v}+(\nabla\boldsymbol{v})^T\right)\right\} + \nabla_{\boldsymbol{x}}p&\\ = \int_{\mathbb{S}^2}\mu_f\nabla_{\boldsymbol{x}}\psi + \operatorname{div}_{\boldsymbol{x}}\left\{\int_{\mathbb{S}^2}\left(\boldsymbol{d}\times\mathcal{R}\mu_f\right)\otimes\boldsymbol{d}f\right\}&\,,\end{aligned} \tag{2.7c}$$

$$\operatorname{div}_{\boldsymbol{x}}\boldsymbol{v} = 0\,, \tag{2.7d}$$

in Ω. Finally, the electrostatic potential V, which prescribes the electric field via $\boldsymbol{E} = -\nabla_{\boldsymbol{x}}V$, is given by

$$\operatorname{div}_{\boldsymbol{x}}\left\{\epsilon\nabla_{\boldsymbol{x}}V\right\} = \operatorname{div}_{\boldsymbol{x}}\left\{\chi_\Omega\int_{\mathbb{S}^2} zf\boldsymbol{d}\right\} \tag{2.7e}$$

in Ω^*. In order to include anchoring conditions in (2.7), we will add

$$\int_\Omega\int_{\mathbb{R}^3\setminus\Omega}\int_{\mathbb{S}^2}\int_{\mathbb{S}^2}\alpha(\boldsymbol{x}-\hat{\boldsymbol{x}})\beta(\boldsymbol{d},\hat{\boldsymbol{d}})\psi(\hat{\boldsymbol{x}},\hat{\boldsymbol{d}},t)f(\boldsymbol{x},\boldsymbol{d},t)\,\mathrm{d}\hat{\boldsymbol{d}}\,\mathrm{d}\boldsymbol{d}\,\mathrm{d}\hat{\boldsymbol{x}}\,\mathrm{d}\boldsymbol{d} \tag{2.8}$$

where ψ is the extension of the preferred orientation on $\partial\Omega$. The interplay between the wetting fluid and the internal structures of the liquid crystalline film can the be included by making the extension ψ fluid dependent.

The numerical treatment of the Doi–Hess model derived above is expected to be rather expensive as the evolution is governed by a Fokker–Planck type equation on the high-dimensional product space $\Omega\times\mathbb{S}^2$ and includes the non-local contributions of the interaction potential (2.3). However, when deriving a simpler looking director field model, the standard approach [54] yields

$$\partial_t\boldsymbol{d} + \left(\boldsymbol{v}\cdot\nabla\right)\boldsymbol{d} - \boldsymbol{d}\cdot\nabla\boldsymbol{v} = -\frac{\delta F}{\delta\boldsymbol{d}}\,, \tag{2.9}$$

i.e. the director $\boldsymbol{d}$ is governed by an L^2-gradient flow of the free energy F. This approach captures the long-time behavior of the liquid-crystalline film, but not the current dynamic evolution. Therefore, we intend to derive a director model which includes the variation of the energy not only by an L^2-gradient flow, and therefore will capture the dynamic evolution of the system in addition to its long time behavior. We will also investigate the existence of weak solutions to the arising partial differential equations. The construction of weak solutions is usually based

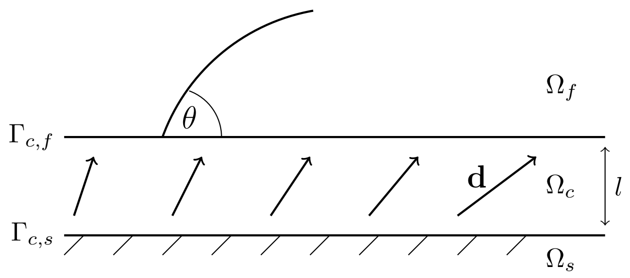

Figure 4: Sketch of a droplet on a switchable coating.

on global energy estimates and suitable (weak) compactness methods and therefore requires an understanding of the underlying structure of the model and the identification of important quantities that can be controlled by energy estimates. Consequently, establishing the existence of weak solutions will not only prove the well-posedness of the derived model, but will also indicate which properties of the model should be conserved in the subsequent coarse-graining process.

To validate the freshly derived microscopic model, we shall derive stable numerical schemes and compare our simulations of microscopic phenomena to experimental results which can be provided by the group of J. Hussong and E. Gurevich. Based on our experience (see Figure 2) with the numerical treatment high-dimensional, microscopic problems [P1], we intend to derive stable finite element schemes. As we expect the simulations to be very costly, it will be crucial to improve the splitting techniques successfully used in [P6], [P1], and [P2] to decouple as many parts of the model as possible without losing stability. In this part of the project, we intend to collaborate with the group of R. Stannarius and E. Eremin concerning the modeling of the interactions between the liquid-crystalline film and the wetting fluid, and with C. Liu concerning the derivation of improved Ericksen-Leslie type models.

2.2.2 From multi-scale to effective models

The second part of the project aims for a better understanding of the different involved spatial and temporal scales. By separating the different scales it is often possible to simplify the model by using macroscopic, averaged quantities without losing the information from the microscopic scale completely.

As we assume the liquid-crystalline film to be very thin in comparison to its lateral extension, there is an obvious difference in the occurring spatial length scales. We intend to make use of this difference in the length scales and employ a lubrication approximation. This is a standard approach for the description of thin films (cf. Section 1.1.3). However, we do not expect the approximation to be as straightforward as in e.g. [51] and [52], as the instantaneous adjustment of the directors to their steady state was a key assumption in these publications. Hence, considering only the time scale corresponding to the evolution of the film is sufficient and the faster time scale corresponding to the evolution of the director can be neglected. In our case, i.e. in presence of external forces and interactions with the additional Newtonian film, it is not clear whether the director field attains the global or a possible local energetic minimum, and therefore, whether the fast time scale can be completely neglected. To overcome this obstacle, we shall consider also a faster time scale reflecting the changes in the orientation of the director. Adapting an approach from homogenization, we assume local periodicity in lateral direction. This allows us to split the model into multiple decoupled fine scale problems describing evolution of the director on the fast time scale, and a coarse scale problem describing the evolution of the coating and the wetting Newtonian film on the larger time scale.

We intend to investigate the resulting equations numerically.

At this point we want to highlight that the focus of this project is not on the spreading of the liquid-crystalline thin film or the occurrence of precursor layers, but on the interplay between the anchoring conditions on the solid substrate, the influence of external magnetic or electric fields, and the anchoring conditions on the fluid-coating interface which give rise to switchable boundary conditions for the overlying film of a simple liquid.

2.3 Work programme incl. proposed research methods

2.3.1 Microscopic models

To derive the microscopic models for liquid-crystalline films, we apply an energetic variational approach [53]. The evolution of the director is governed by the deformation induced by a flow field $\boldsymbol{v}$. In particular, the evolution equation for the deformation tensor $\boldsymbol{\mathcal{F}}$ in the observer's coordinates reads

$$\partial_t \boldsymbol{\mathcal{F}} + \boldsymbol{v} \cdot \nabla \boldsymbol{\mathcal{F}} = \nabla \boldsymbol{v} \boldsymbol{\mathcal{F}} \,. \tag{2.10}$$

As the director $\boldsymbol{d}$ depends on its initial data $\boldsymbol{d}_0$ via $\boldsymbol{d} = \boldsymbol{\mathcal{F}} \boldsymbol{d}_0$ the kinematic equation for the director reads

$$\partial_t \boldsymbol{d} + \boldsymbol{v} \cdot \nabla \boldsymbol{d} - \boldsymbol{d} \cdot \nabla \boldsymbol{v} = 0 \tag{2.11}$$

with an a priori unknown velocity field $\boldsymbol{v}$. Here, $\boldsymbol{v}$ Combining the least action principle with Onsager's maximum dissipation principle will allow us to determine the velocity field based on the total energy and the dissipation of the system (see e.g. [68]).

2.3.2 Lubrication approximations

In the second year of the funding period, we will derive a lubrication approximation of the aforementioned models. We will use an asymptotic expansion and approximate the problem by considering the leading order terms. This will be a collaboration with G. Grün.

2.3.3 Numerical simulations

We plan to start with the numerical study of the microscopic models derived in Section 2.2.1 at the beginning of the second year of the funding period. We will implement the finite element schemes in our inhouse package `EconDrop` [4, 34],[P1],[P2]. `EconDrop`, which was developed in the group of G. Grün, is a finite element framework written in `C++` and allows for adaptivity in space and time. In the past various schemes for different models including two-phase flow [4], [P6], [P2] and micro-macro models [P1] have been implemented successfully in `EconDrop`.
The investigation of the numerical treatment of the coarse grained models derived in Section 2.2.2 will start at the end of the second year of the first funding period. Again, we plan to use the framework of `EconDrop` for the implementation, as it was also already used successfully used for simulations based the (stochastic) thin film equation.

2.4 Data handling

Not applicable.

2.5 Other information

2.6 Descriptions of proposed investigations involving experiments on humans, human materials or animals as well as dual use research of concern

Not applicable.

2.7 Information on scientific and financial involvement of international cooperation partners

Not applicable.

3 Bibliography

[1] H. Abels. Existence of weak solutions for a diffuse interface model for viscous incompressible fluids with general densities. *Comm. Math. Phys.*, 289(1):45–73, 2009.

[2] H. Abels, D. Depner, and H. Garcke. Existence of weak solutions for a diffuse interface model for two-phase flows of incompressible fluids with different densities. *Journal of Mathematical Fluid Mechanics*, 15(3):453–480, 2013.

[3] H. Abels, H. Garcke, and G. Grün. Thermodynamically consistent, frame indifferent diffuse interface models for incompressible two-phase flows with different densities. *Mathematical Models and Methods in Applied Sciences*, 22(3):1150013, 2012.

[4] S. Aland, S. Boden, A. Hahn, F. Klingbeil, M. Weismann, and S. Weller. Quantitative comparison of Taylor flow simulations based on sharp-interface and diffuse-interface models. *International Journal for Numerical Methods in Fluids*, 73(4):344–361, 2013.

[5] H. Bae and K. Trivisa. On the doi model for the suspensions of rod-like molecules in compressible fluids. *Math. Mod. Meth. Appl. S.*, 22(10):1250027, 2012.

[6] H. Bae and K. Trivisa. On the doi model for the suspensions of rod-like molecules: global-in-time existence. *Commun. Math. Sci.*, 11(3):831, 2013.

[7] J.M. Ball and A. Majumdar. Nematic liquid crystals: From maier-saupe to a continuum theory. *Molecular Crystals and Liquid Crystals*, 525(1):1–11, 2010.

[8] J. W. Barrett, C. Schwab, and E. Süli. Existence of global weak solutions for some polymeric flow models. *Mathathematical Models and Methods in Applied Sciences*, 15:939–983, 2005.

[9] J. W. Barrett and E. Süli. Finite element approximation of kinetic dilute polymer models with microscopic cut-off. *ESAIM: Mathematical Modelling and Numerical Analysis*, 45:39–89, 2011.

[10] J. W. Barrett and E. Süli. Existence and equilibration of global weak solutions to Hookean-type bead-spring chain models for dilute polymers. *Mathathematical Models and Methods in Applied Sciences*, 2012.

[11] J. W. Barrett and E. Süli. Finite element approximation of finitely extensible nonlinear elastic dumbbell models for dilute polymers. *ESAIM: Mathematical Modelling and Numerical Analysis*, 46:949–978, 2012.

[12] J. Becker, G. Grün, R. Seemann, H. Mantz, K. Jacobs, K.R. Mecke, and R. Blossey. Complex dewetting scenarios captured by thin-film models. *Nature Materials*, 2:59–63, 2003.

[13] A.N. Beris and B.J. Edwards. *Thermodynamics of Flowing Systems: with Internal Microstructure.* Oxford Engineering Science Series. Oxford University Press, 1994.

[14] F. Bernis and A. Friedman. Higher Order Nonlinear Degenerate Parabolic Equations. *J. Differential Equations*, 83:179–206, 1990.

[15] A. Bertozzi and M. Pugh. The lubrication approximation for thin viscous films: the moving contact line with a 'porous media' cut-off of van der waals interactions. *Nonlinearity*, 7(6):1535, 1994.

[16] E. Campillo-Funollet, G. Grün, and F. Klingbeil. On modeling and simulation of electrokinetic phenomena in two-phase flow with general mass densities. *SIAM Journal on Applied Mathematics*, 72(6):1899–1925, 2012.

[17] P. Constantin, I. Kevrekidis, and E.S. Titi. Remarks on a smoluchowski equation. *Discrete and Continuous Dynamical Systems*, 11:101–112, 2004.

[18] R. Dal Passo, H. Garcke, and G. Grün. On a Fourth-Order Degenerate Parabolic Equation: Global Entropy Estimates, Existence, and Qualitative Behavior of Solutions. *SIAM J. Math. Anal.*, 29(2):321–342, 1998.

[19] R. Dal Passo, L. Giacomelli, and G. Grün. A waiting time phenomenon for thin film equations. *Ann. Sc. Norm. Super. Pisa Cl. Sci. (4)*, 30, n^o 2:437–463, 2001.

[20] P. G. de Gennes and J. Prost. *The Physics of Liquid Crystals.* International Series of Monographs on Physics. Clarendon Press, 1995.

[21] N. Delorme, J.-F. Bardeau, A. Bulou, and F. Poncin-Epaillard. Azobenzene-Containing Monolayer with Photoswitchable Wettability. *Langmuir*, 21(26):12278–12282, 2005.

[22] H. Ding, P. D. M. Spelt, and C. Shu. Diffuse interface model for incompressible two-phase flows with large density ratios. *J.Comput.Phys.*, 226:2078–2095, 2007.

[23] M. Doi and S.F. Edwards. *The Theory of Polymer Dynamics.* Comparative Pathobiology - Studies in the Postmodern Theory of Education. Clarendon Press, 1988.

[24] W. E and P. Zhang. A molecular kinetic theory of inhomogeneous liquid crystal flow and the small deborah number limit. *Methods Appl. Anal.*, 13(2):181–198, 06 2006.

[25] E. Emmrich, S.H.L. Klapp, and R. Lasarzik. Nonstationary models for liquid crystals: A fresh mathematical perspective. *Journal of Non-Newtonian Fluid Mechanics*, 259:32 – 47, 2018.

[26] J. L. Ericksen. Conservation laws for liquid crystals. *Transactions of the Society of Rheology*, 5(1):23–34, 1961.

[27] J.L. Ericksen. Continuum theory of liquid crystals of nematic type. *Molecular Crystals*, 7(1):153–164, 1969.

[28] M.A. Fontelos, G. Grün, and S. Jörres. On a phase-field model for electrowetting and other electrokinetic phenomena. *SIAM Journal on Mathematical Analysis*, 43(1):527–563, 2011.

[29] F. C. Frank. I. liquid crystals. on the theory of liquid crystals. *Discuss. Faraday Soc.*, 25:19–28, 1958.

[30] L. Giacomelli, H. Knüpfer, and F Otto. Smooth zero-contact-angle solutions to a thin-film equation around the steady state. *J. Differential Equations*, 245:1454–1506, 2008.

[31] L. Giacomelli and A. Shishkov. Propagation of support in one-dimensional convected thin-film flow. *Indiana Univ. Math. J.*, 54(4):1181–1215, 2005.

[32] G. Grün. On the convergence of entropy consistent schemes for lubrication-type equations in multiple space dimensions. *Math. Comput.*, 72:1251–1279, 2003.

[33] G. Grün. On convergent schemes for diffuse interface models for two-phase flow of incompressible fluids with general mass densities. *SIAM Journal on Numerical Analysis*, 51(6):3036–3061, 2013.

[34] G. Grün and F. Klingbeil. Two-phase flow with mass density contrast: stable schemes for a thermodynamic consistent and frame-indifferent diffuse-interface model. *J.Comput.Phys.*, 257, Part A:708–725, 2014.

[35] G. Grün, K. Mecke, and M. Rauscher. Thin-Film Flow Influenced by Thermal Noise . *J. Stat. Phys.*, 122(6):1261–1291, 2006.

[36] G. Grün and M. Rumpf. Nonnegativity preserving convergent schemes for the thin film equation. *Numerische Mathematik*, 87:113–152, 2000.

[37] Günther Grün. On the Convergence of Entropy Consistent Schemes for Lubrication Type Equations in Multiple Space Dimensions. *Math. Comp.*, 72(243):1251–1279, 2003.

[38] J. Han, Y. Luo, W. Wang, P. Zhang, and Z. Zhang. From microscopic theory to macroscopic theory: a systematic study on modeling for liquid crystals. *Archive for Rational Mechanics and Analysis*, 215(3):741–809, Mar 2015.

[39] S. Hess. *Tensors for Physics.* Undergraduate Lecture Notes in Physics. Springer International Publishing, 2015.

[40] J. Huang and S. Ding. Global well-posedness for the dynamical q-tensor model of liquid crystals. *Science China Mathematics*, 58(6):1349–1366, Jun 2015.

[41] S. Jachalski, D. Peschka, S. Bommer, R. Seemann, and B. Wagner. *Structure Formation in Thin Liquid-Liquid Films*, pages 531–576. Springer International Publishing, Cham, 2017.

[42] D. Jacqmin. Calculation of two-phase Navier–Stokes flows using phase-field modeling. *J.Comput.Phys.*, 155:96–127, 1999.

[43] J. Kim, K. Kang, and J. Lowengrub. Conservative multigrid methods for Cahn–Hilliard fluids. *J.Comput.Phys.*, 193:511–543, 2004.

[44] N. Kuzuu and M. Doi. Constitutive equation for nematic liquid crystals under weak velocity gradient derived from a molecular kinetic equation. *Journal of the Physical Society of Japan*, 52(10):3486–3494, 1983.

[45] N. Kuzuu and M. Doi. Constitutive equation for nematic liquid crystals under weak velocity gradient derived from a molecular kinetic equation. *Journal of the Physical Society of Japan*, 52(10):3486–3494, 1983.

[46] F.M. Lelsie. Some constitutive equations for anisotropic fluids. *The Quarterly Journal of Mechanics and Applied Mathematics*, 19(3):357–370, 1966.

[47] F.M. Leslie. Some constitutive equations for liquid crystals. *Archive for Rational Mechanics and Analysis*, 28(4):265–283, Jan 1968.

[48] F.M. Leslie. Continuum theory for nematic liquid crystals. *Continuum Mechanics and Thermodynamics*, 4(3):167–175, Sep 1992.

[49] F.-H. Lin and C. Liu. Nonparabolic dissipative systems modeling the flow of liquid crystals. *Communications on Pure and Applied Mathematics*, 48(5):501–537, 1995.

[50] F.-H. Lin and C Liu. Existence of solutions for the ericksen-leslie system. *Archive for Rational Mechanics and Analysis*, 154(2):135–156, 2000.

[51] T.-S. Lin, L. J. Cummings, A. J. Archer, L. Kondic, and U. Thiele. Note on the hydrodynamic description of thin nematic films: strong anchoring model. *Phys. Fluids*, 25:082102, 2013.

[52] T.-S. Lin, L. Kondic, U. Thiele, and L. J. Cummings. Modelling spreading dynamics of nematic liquid crystals in three spatial dimensions. *J. Fluid Mech.*, 729:214–230, 2013.

[53] C. Liu. An introduction of elastic complex fluids: An energetic variational approach. In T. Y. Hou, C. Liu, and J.-G. Liu, editors, *Multi-Scale Phenomena in Complex Fluids*, volume 2, pages 286–337. World Scientific Publishing Company, Singapore, 2009.

[54] C. Liu and H. Sun. On energetic variational approaches in modeling the nematic liquid crystal flows. *Discrete & Continuous Dynamical Systems - A*, 23(1078-0947_2009_1/2_455):455, 2009.

[55] H. Liu, H. Zhang, and P. Zhang. Axial symmetry and classification of stationary solutions of doi–onsager equation on the sphere with maier–saupe potential. *Commun. Math. Sci*, 3(2):201–218, 2005.

[56] J. Lowengrub and L. Truskinovsky. Quasi-incompressible Cahn–Hilliard fluids and topological transitions. *Proceeding of the Royal Society A*, 454(1978):2617–2654, 1998.

[57] W. Maier and A. Saupe. Eine einfache molekulare theorie des nematischen kristallinflüssigen zustandes. *Z. Naturforsch. A*, 13(7):564–566, 1958.

[58] C. Neto, K. Jacobs, R. Seemann, R. Blossey, J. Becker, and G. Grün. Satellite hole formation during dewetting: experiment and simulation. *J. Phys.: Condensed Matter*, 15(19):3355–3366, 2003.

[59] L. Onsager. Reciprocal relations in irreversible processes. I. *Phys. Rev.*, 37(4):405–426, Feb 1931.

[60] L. Onsager. Reciprocal relations in irreversible processes. II. *Phys. Rev.*, 38(12):2265–2279, December 1931.

[61] L. Onsager. The effects of shape on the interaction of colloidal particles. *Annals of the New York Academy of Sciences*, 51(4):627–659, 1949.

[62] A. Oron, S. H. Davis, and S. G. Bankoff. Long-scale evolution of thin liquid films. *Rev. Modern Phys.*, 69:932–977, 1997.

[63] C. W. Oseen. The theory of liquid crystals. *Trans. Faraday Soc.*, 29:883–899, 1933.

[64] F. Otto and A.E. Tzavaras. Continuity of velocity gradients in suspensions of rod–like molecules. *Comm. Math.l Phys.*, 277(3):729–758, 2008.

[65] T. Qian, X. Wang, and P. Sheng. A variational approach to the moving contact line hydrodynamics. *Journal of Fluid Mechanics*, 564:333–360, 2006.

[66] I.W. Stewart. *The Static and Dynamic Continuum Theory of Liquid Crystals: A Mathematical Introduction*. Liquid Crystals Book Series. CRC Press, 2004.

[67] W. Wang, P. Zhang, and Z. Zhang. From microscopic theory to macroscopic theory: dynamics of the rod-like liquid crystal molecules. *ArXiv e-prints*, 2013.

[68] S. Xu, P. Sheng, and C. Liu. An energetic variational approach for ion transport. *Communications in Mathematical Sciences*, 12(4):779–789, 2014.

4 Requested modules/funds

4.1 Basic Module

4.1.1 Funding for Staff

To carry out the research programme, we apply for funding of the following positions.

Official position	Number	Duration	Salary	Total Cost
Doctoral researcher	0.75	36 months	TV-L E13	145.125 Euro
Student assistant (B. Sc.)	1	36 months		19.269 Euro

4.1.2 Funding for direct project costs

4.1.3 Module Project-Specific Workshop

For travelling to the SPP2171 related meetings, we apply for 19.600 Euro.
To present results on conferences and invite other scientist, we apply for an assistance of 3000 Euro.

5 Project requirements

5.1 Employment status information

Stefan Metzger
Research associate A13 (for at least three years starting on August 20, 2019), University of Erlangen-Nürnberg

5.2 First-time proposal data

Stefan Metzger

5.3 Composition of the project group

5.4 Cooperation with other researchers

5.4.1 Researchers with whom you have agreed to cooperate on this project

J. Hussong and E. Gurevich for a comparison of numerical and experimental results.
R. Stannarius and E. Eremin for modeling of liquid crystal - fluid interactions. C. Liu for the derivation of Ericksen–Leslie type models. G. Grün for the derivation a lubrication approximation.

5.4.2 Researchers with whom you have collaborated scientifically within the past three years

H. Abels and H. Garcke (Regensburg University), G. Grün (Friedrich–Alexander University of Erlangen–Nürnberg), F. Guillen-Gonzalez (University of Sevilla, Spain), P. Knabner (Friedrich–Alexander University of Erlangen–Nürnberg), I. Rybak (University of Stuttgart), E. Süli (Oxford University, UK).

5.5 Scientific equipment

For numerical simulations, the PI has direct access to the computer infrastructure of Chair of Applied Mathematics 1 at Erlangen University which includes two workstations (2×6 cores, 48 GB RAM, and 2×10 cores, 128 GB RAM, respectively) and a compute server (4×10 cores, 512 GB RAM).

5.6 Project-relevant cooperation with commerical enterprises

Not applicable.

6 Additional information

G. Grün will also assist in the supervision of Ph.D. candidates.

Stefan Metzger
✉ *stefan.metzger@fau.de*

October 15, 2018

Office of Human Resources
Illinois Institute of Technology
10 West 35th Street
Chicago, IL 60616

Dear Hiring Committee:

with this letter I am applying for a postdoc position at the Department of Applied Mathematics at the Illinois Institute of Technology. I finished my Ph.D. in applied mathematics at the Friedrich–Alexander University of Erlangen–Nuremberg (Germany) in 2017. During my research visit with Professor Chun Liu (chair of the Department of Applied Mathematics) in March 2018, we discussed a possibility for future collaboration and he encouraged me to apply.

My research interests are mathematical modeling, analysis and numerical simulation in fluid mechanics, in particular two-phase flows, electrolyte solutions, and micro-macro-models for complex fluids. Currently, I am working on model development and simulation of two-phase flow in porous media. These topics fit perfectly for the Department of Applied Mathematics. For example, the core subject of my Ph.D. thesis, which is modeling, analysis and numerical treatment of two-phase flow of electrolyte or dilute polymeric solutions, is within the research interests of Professor Chun Liu. In addition, I see possible collaboration with Associate Professor Shuwang Li, who is working on multicomponent flows.

During my Ph.D. studies, I also gained teaching experience by preparing assignments and solutions for diverse lectures, giving tutorial lectures and programming courses, and supervising teaching assistants.

I think my research interests and teaching experience fit well to the Department of Applied Mathematics. The postdoc position at the IIT will give me an excellent chance to extend my expertise on modeling and analysis of complex flows and to collaborate with renown researchers.

For further information, please feel free to contact me at anytime.

Yours sincerly

Stefan Metzger

Stefan Metzger

Ph.D. in Mathematics

✉ *stefan.metzger@fau.de*

Work experience and distinctions

2019–2021 **GAMM junior**.

since 10/2018 **Staedler-Promotionspreis**.

since 08/2018 **Research associate**, *Illionois Institute of Technology, Chicago*, USA, Department of Applied Mathematics, Group of Prof. Chun Liu.

2017–2018 **Research associate**, *Friedrich–Alexander University of Erlangen–Nuremberg*, Germany, Chair of Applied Mathematics I.

2013–2017 **Research associate**, *Friedrich–Alexander University of Erlangen–Nuremberg*, Germany, Group of Prof. Dr. Günther Grün.

2011–2013 **Research assistant**, *Friedrich–Alexander University of Erlangen–Nuremberg*, Germany, Group of Prof. Dr. Günther Grün.

Education

06/2013-02/2017 **Ph.D. in Mathematics**, *Friedrich-Alexander University Erlangen-Nuremberg*, Germany, *Grade* 'summa cum laude'.
Ph.D. thesis: 'Diffuse interface models for complex flow scenarios: Modeling, analysis, and simulation'
(Supervisor: Prof. Dr. Günther Grün; additional referees: Prof. Dr. Eberhard Bänsch, Prof. Dr. Thomas Richter)

10/2011-05/2013 **M.Sc. Mathematics**, *Friedrich–Alexander University of Erlangen–Nuremberg*, Germany, *Grade* 1.0.
Master's thesis: 'Diffuse interface models for transport processes at fluidic interfaces: Modeling and simulation' (in German)
(Supervisor: Prof. Dr. Günther Grün)

10/2008-9/2011 **B.Sc. Technomathematics**, *Friedrich–Alexander University of Erlangen–Nuremberg*,
Germany, *Grade* 1.3.
Bachelor's thesis: 'Hyperelastic limiting process of the Cosserat rod to a generalized string and regularized numerical schemes for low Mach numbers' (in German)
(Supervisor: Prof. Dr. Nicole Marheineke)

2007–2008 Compulsory civilian service

2007 **Abitur** (general qualification for university entrance), *Naturwissenschaftlich-technologisches und Sprachliches Gymnasium (secondary school)*, Feuchtwangen (Germany), *Grade* 1.0.

Projects

2011–2017 Participation in the **Priority Program 'SPP1506: Transport Processes at Fluidic Interfaces'**, *funded by the German Research Foundation DFG*.
- Modeling, analysis, and simulation of dilute polymeric solutions
- Supervision of the C++ software project **EconDrop**

Computer skills

Software	Matlab, Paraview
Programming languages	C++, Java
Miscellaneous	LaTeX

Conference and Workshop Talks

2018 **'Upscaling two-phase flow in porous media including droplet topology'**, *Computational Methods In Water Resources XXII*, Saint-Malo (France).

2017 **'On a convergent, decoupled splitting scheme for DIMs for two-phase flow with general mass densities'**, *International Conference on Elliptic and Parabolic Problems*, Gaeta (Italy).

'Complex transport processes at fluidic interfaces – numerical simulations based on thermodynamically consistent models', *Workshop: Dynamics of Interfaces in Complex Fluids and Complex Flows*, Erlangen (Germany).

2016 **'On micro-macro models for two-phase flow with dilute polymeric solutions'**, *4th Workshop of the GAMM Activity Group on Analysis of Partial Differential Equations*, Dortmund (Germany).

'On stable splitting schemes for phase-field models with ion transport', *11th AIMS Conference on Dynamical Systems, Differential Equations and Applications*, Orlando (USA).

2015 **'Simulation of ion induced fluid motion and droplet break-up'**, *Joint International Conference and Autumn School*, Darmstadt (Germany).

'On numerical schemes for phase-field models for electrowetting with electrolyte solutions', *GAMM 86th Annual Scientific Conference*, Lecce (Italy).

2014 **'On a convergent, decoupled splitting scheme for DIMs for two-phase flow with general mass densities'**, *2nd International Conference on Numerical Methods in Multiphase Flows*, Darmstadt (Germany).

2013 **'Diffuse interface modells for transport processes on fluidic interfaces'**, *ITN-Springschool: Optimization in PDE, Reaction-diffusion Systems and Phase-field Models*, Saint Raphael (France).

Posters

2014 **'On a convergent, decoupled splitting scheme for DIMs for two-phase flow with general mass densities'**, *International Conference: Modeling, Analysis and Computing in Nonlinear PDEs*, Liblice (Czech Republic).

Publications

[1] S. Metzger, *On convergent schemes for two-phase flow of dilute polymeric solutions*, ESAIM: Mathematical Modelling and Numerical Analysis (2018), published online first.

[2] S. Metzger, *On stable, dissipation reducing splitting schemes for two-phase flow of electrolyte solutions*, Numerical Algorithms (2018), published online first, DOI 10.1007/s11075-018-0530-2.

[3] H. Abels, H. Garcke, G. Grün, and S. Metzger, *Diffuse interface models for incompressible two-phase flows with different densities*, In Advances in Mathematical Fluid Mechanics (2017), DOI 978-3-319-56602-3_8.

[4] G. Grün and S. Metzger, *Micro-macro-models for two-phase flow of dilute polymeric solutions: Macroscopic limit, analysis, and numerics*, In Advances in Mathematical Fluid Mechanics (2017), DOI 978-3-319-56602-3_12.

[5] G. Grün, F. Guillén-González, and S. Metzger, *On fully decoupled, convergent schemes for diffuse interface models for two-phase flow with general mass densities*, Communications in Computational Physics **19** (2016), no. 5, 1473–1502, DOI:10.4208/cicp.scpde14.39s.

[6] G. Grün and S. Metzger, *On micro-macro-models for two-phase flow with dilute polymeric solutions – modeling and analysis*, Mathematical Models and Methods in Applied Sciences **26** (2016), no. 05, 823–866, DOI: 10.1142/S0218202516500196.

[7] S. Metzger, *On numerical schemes for phase-field models for electrowetting with electrolyte solutions*, Proceedings in Applied Mathematics and Mechanics **15** (2015), no. 1, 715–718, DOI: 10.1002/pamm.201510346.

ESAIM: M2AN
https://doi.org/10.1051/m2an/2018042

ESAIM: Mathematical Modelling and Numerical Analysis
www.esaim-m2an.org

ON CONVERGENT SCHEMES FOR TWO-PHASE FLOW OF DILUTE POLYMERIC SOLUTIONS

Stefan Metzger[1,*]

Abstract. We construct a Galerkin finite element method for the numerical approximation of weak solutions to a recent micro-macro bead-spring model for two-phase flow of dilute polymeric solutions derived by methods from nonequilibrium thermodynamics ([Grün, Metzger, *M3AS* **26** (2016) 823–866]). The model consists of Cahn–Hilliard type equations describing the evolution of the fluids and the unsteady incompressible Navier–Stokes equations in a bounded domain in two or three spatial dimensions for the velocity and the pressure of the fluids with an elastic extra-stress tensor on the right-hand side in the momentum equation which originates from the presence of dissolved polymer chains. The polymers are modeled by dumbbells subjected to a finitely extensible, nonlinear elastic (FENE) spring-force potential. Their density and orientation are described by a Fokker–Planck type parabolic equation with a center-of-mass diffusion term. We perform a rigorous passage to the limit as the spatial and temporal discretization parameters simultaneously tend to zero, and show that a subsequence of these finite element approximations converges towards a weak solution of the coupled Cahn–Hilliard–Navier–Stokes–Fokker–Planck system. To underline the practicality of the presented scheme, we provide simulations of oscillating dilute polymeric droplets and compare their oscillatory behaviour to the one of Newtonian droplets.

Mathematics Subject Classification. 35Q30, 35Q35, 35Q84, 65M12, 65M60, 76A05, 82D60, 76T99.

Received April 19, 2017. Accepted June 25, 2018.

1. Introduction

In this paper, we present a stable, fully discrete finite-element scheme for a diffuse interface model for two-phase flow of dilute polymeric solutions and establish convergence for the case of equal fluid mass densities. Allowing for different solubility properties which are modelled by some phase dependent cost functional β, the presented model covers the case of two dilute polymeric solutions as well as the case of one dilute polymeric solution and one pure Newtonian fluid. In contrast to other approaches (see *e.g.* [7,8]) our scheme solely relies on standard finite element functions. In particular, it does not include simplices with curved edges or faces. The presented results are excerpts from the author's Ph.D. thesis [25].

Keywords and phrases. Convergence of finite-element schemes, existence of weak solutions, polymeric flow model, two-phase flow, diffuse interface models, Navier–Stokes equations, Fokker–Planck equations, Cahn–Hilliard equations, FENE.

[1] Department Mathematik, Friedrich-Alexander-Universität Erlangen-Nürnberg, Cauerstr. 11, 91058 Erlangen, Germany.
*Corresponding author: `stefan.metzger@fau.de`

The aforementioned model derived by G. Grün and Metzger ([18]) combines a diffuse interface model for two-phase flow of incompressible, viscous fluids (*cf.* [1]) for the description of the immiscible fluids in an open domain $\Omega \subset \mathbb{R}^d$, $d = 2$ or 3, with a FENE-dumbbell description of the dissolved polymer chains. That is a polymer chain is represented by two beads connected by a massless spring (*cf.* [5, 22]) and can be described by the position of its barycenter and the configurational vector $\mathbf{q}$ connecting the beads. Using the so called FENE spring potential (FENE: acronym for *f*initely *e*xtensible, *n*onlinear *e*lastic), which reads

$$U\left(\tfrac{1}{2}|\mathbf{q}|^2\right) = -\tfrac{Q_{\max}^2}{2}\ln\left(1 - \tfrac{|\mathbf{q}|^2}{Q_{\max}^2}\right), \tag{1.1}$$

restricts the admissible polymer elongations to

$$\mathbf{q} \in D := B(0, Q_{\max}), \tag{1.2}$$

where $B(0, Q_{\max})$ is a bounded, open, origin centered ball with radius $Q_{\max}$. Associated with the potential, there comes the Maxwellian

$$M(\mathbf{q}) := \frac{\exp\left(-U\left(\frac{1}{2}|\mathbf{q}|^2\right)\right)}{\int_D \exp\left(-U\left(\frac{1}{2}|\overline{\mathbf{q}}|^2\right)\right)\,\mathrm{d}\overline{\mathbf{q}}}, \tag{1.3}$$

which provides the energetically most favorable probability density of the elongation of a polymer chain. A straight forward computation shows that

$$M\nabla_{\mathbf{q}}M^{-1} = -M^{-1}\nabla_{\mathbf{q}}M = U'\mathbf{q}. \tag{1.4}$$

As shown in [5], the FENE-potential defined in (1.1) and the Maxwellian satisfy the following properties on the corresponding set of admissible elongations D.

(P1) $\mathbf{q} \mapsto U\left(\frac{1}{2}|\mathbf{q}|^2\right) \in C^\infty(D)$, nonnegative;

(P2) $\mathbf{q} \mapsto U'\left(\frac{1}{2}|\mathbf{q}|^2\right)$ is positive on D;

(P3) there exist constants $c_i > 0$ $(i = 1, \dots, 5)$ such that for $\kappa = \frac{Q_{\max}^2}{2}$ the following inequalities hold true:

$$c_1[\operatorname{dist}(\mathbf{q}, \partial D)]^\kappa \le M(\mathbf{q}) \le c_2[\operatorname{dist}(\mathbf{q}, \partial D)]^\kappa \qquad \forall \mathbf{q} \in D,$$
$$c_3 \le [\operatorname{dist}(\mathbf{q}, \partial D)]U'\left(\tfrac{1}{2}|\mathbf{q}|^2\right) \le c_4, \qquad [\operatorname{dist}(\mathbf{q}, \partial D)]^2\left|U''\left(\tfrac{1}{2}|\mathbf{q}|^2\right)\right| \le c_5 \qquad \forall \mathbf{q} \in D,$$

(P4) $\int_D \left[1 + \left(1 + |\mathbf{q}|^2\right)\left((U)^2 + |\mathbf{q}|^2 (U')^2\right)\right] M\,\mathrm{d}\mathbf{q} < \infty.$

Under the additional assumption $Q_{\max} > \sqrt{2}$, the FENE-potential additionally satisfies the following estimates:

(P5) There exist constants c_6, $c_7 > 0$, such that for $B(0, (\frac{d}{c_7})^{1/2}) \subset\subset D$

$$(U')^2 - U'' \quad \ge c_6 \quad \forall \mathbf{q} \in D \qquad \text{and} \qquad (U')^2 - U'' \ge 2c_7 U' \quad \forall \mathbf{q} \in D\,:\, |\mathbf{q}|^2 \ge \tfrac{d}{c_7}.$$

In [18], spatial distribution and configuration of the polymer chains is described by the configurational density $\psi\,:\,\Omega \times D \times \mathbb{R}_0^+ \to \mathbb{R}_0^+$. Following the approach in [7], we define the scaled configurational density function $\hat{\psi} := \frac{\psi}{M}$. As the scaled configurational density is defined on the product space of the spatial domain Ω and the configurational space D, we introduce two different variables, $\mathbf{x} \in \Omega$ and $\mathbf{q} \in D$, to determine the position in the spatial domain Ω and the configurational space D. Consequently, we denote the gradient and the divergence operators with respect to $\mathbf{x}$ and $\mathbf{q}$ by $\nabla_{\mathbf{x}}$, $\nabla_{\mathbf{q}}$, $\operatorname{div}_{\mathbf{x}}$, and $\operatorname{div}_{\mathbf{q}}$. Using this notation, the model reads as follows:

$$\partial_t\phi + \mathbf{u}\cdot\nabla_{\mathbf{x}}\phi - \operatorname{div}_{\mathbf{x}}\left\{m(\phi)\nabla_{\mathbf{x}}\mu_\phi\right\} = 0, \tag{1.5a}$$

$$\mu_\phi = -\delta\sigma\Delta_{\mathbf{x}}\phi + \tfrac{\sigma}{\delta}W'(\phi) + \beta'(\phi)\mathcal{J}_\varepsilon\left\{\int_D M\hat{\psi}\right\}, \tag{1.5b}$$

$$\begin{aligned} &M\partial_t\hat{\psi} + M\mathbf{u}\cdot\nabla_{\mathbf{x}}\hat{\psi} + \mathrm{div}_{\mathbf{q}}\left\{M\hat{\psi}\nabla_{\mathbf{x}}\boldsymbol{\mathcal{J}}_\varepsilon\{\mathbf{u}\}\cdot\mathbf{q}\right\} \\ &\qquad = \mathrm{div}_{\mathbf{q}}\left\{c_{\mathbf{q}}M\nabla_{\mathbf{q}}\hat{\psi}\right\} + \mathrm{div}_{\mathbf{x}}\left\{c_{\mathbf{x}}M\hat{\psi}\nabla_{\mathbf{x}}\Big(g'(\hat{\psi}) + \mathcal{J}_\varepsilon\{\beta(\phi)\}\Big)\right\}, \end{aligned} \tag{1.5c}$$

$$\begin{aligned} &\rho(\phi)\partial_t\mathbf{u} + ((\rho(\phi)\mathbf{u} - m(\phi)\rho'\nabla_{\mathbf{x}}\mu_\phi)\cdot\nabla_{\mathbf{x}})\mathbf{u} - \mathrm{div}_{\mathbf{x}}\left\{2\eta(\phi)\mathbf{D}\mathbf{u}\right\} + \nabla_{\mathbf{x}}p \\ &\qquad = \mu_\phi\nabla_{\mathbf{x}}\phi + \int_D M\Big(g'(\hat{\psi}) + \mathcal{J}_\varepsilon\{\beta(\phi)\}\Big)\nabla_{\mathbf{x}}\hat{\psi} + \mathrm{div}_{\mathbf{x}}\left\{\mathfrak{J}_\varepsilon\left\{\int_D M\nabla_{\mathbf{q}}\hat{\psi}\otimes\mathbf{q}\right\}\right\}, \end{aligned} \tag{1.5d}$$

$$\mathrm{div}_{\mathbf{x}}\,\mathbf{u} = 0 \tag{1.5e}$$

on $\Omega\times\mathbb{R}^+$ (or $\Omega\times D\times\mathbb{R}^+$, respectively) with the boundary conditions

$$\nabla_{\mathbf{x}}\phi\cdot\mathbf{n}_{\mathbf{x}} = 0 \qquad \text{on } \partial\Omega\times\mathbb{R}^+, \tag{1.5f}$$

$$\nabla_{\mathbf{x}}\mu_\phi\cdot\mathbf{n}_{\mathbf{x}} = 0 \qquad \text{on } \partial\Omega\times\mathbb{R}^+, \tag{1.5g}$$

$$M\hat{\psi}\nabla_{\mathbf{x}}\Big(g'(\hat{\psi}) + \mathcal{J}_\varepsilon\{\beta(\phi)\}\Big)\cdot\mathbf{n}_{\mathbf{x}} = 0 \qquad \text{on } \partial\Omega\times D\times\mathbb{R}^+, \tag{1.5h}$$

$$\Big(M\hat{\psi}\nabla_{\mathbf{x}}\boldsymbol{\mathcal{J}}_\varepsilon\{\mathbf{u}\}\cdot\mathbf{q} - c_{\mathbf{q}}M\nabla_{\mathbf{q}}\hat{\psi}\Big)\cdot\mathbf{n}_{\mathbf{q}} = 0 \qquad \text{on } \Omega\times\partial D\times\mathbb{R}^+, \tag{1.5i}$$

$$\mathbf{u} = 0 \qquad \text{on } \partial\Omega\times\mathbb{R}^+. \tag{1.5j}$$

The Cahn–Hilliard type phase-field equations (1.5a) and (1.5b) describe the evolution of two immiscible fluids in terms of the phase-field parameter ϕ and its chemical potential μ_ϕ. Thereby, m is the mobility and W is a double-well potential with minima in ±1, representing the pure phases $\phi\equiv\pm1$. The parameters σ and δ denote the surface tension and the width of the diffuse interface, respectively. Throughout this paper, we will set $\sigma=\delta=1$ for the ease of notation and assume a constant mobility, *i.e.* $m\equiv1$. In contrast to other publications (see *e.g.* [23, 24]), the coefficient $c_{\mathbf{x}}$ of the center-of-mass diffusion term is kept as it guarantees parabolicity of the Fokker–Planck type equation (1.5c) (*cf.* [5]). The tuple $(\mathbf{u},p)$ stands for the velocity and pressure field, respectively, and

$$\rho(\phi) := \frac{\tilde{\rho}_2+\tilde{\rho}_1}{2} - \frac{\tilde{\rho}_2-\tilde{\rho}_1}{2}\phi \tag{1.6}$$

is the phase-field dependent mass density of the fluids, where $\tilde{\rho}_1$ and $\tilde{\rho}_2$ denote the mass densities of the pure phases.

Formal computations (*cf.* Lem. B.1) show that the energy

$$\begin{aligned} \mathcal{E}(\phi,\hat{\psi},\mathbf{u}) := &\int_\Omega \tfrac{\sigma\delta}{2}\left|\nabla_{\mathbf{x}}\phi\right|^2 + \int_\Omega \tfrac{\sigma}{\delta}W(\phi) + \int_{\Omega\times D} Mg\Big(\hat{\psi}\Big) + \int_{\Omega\times D} M\mathcal{J}_\varepsilon\{\beta(\phi)\}\hat{\psi} \\ &+ \int_\Omega \tfrac12\rho(\phi)\left|\mathbf{u}\right|^2 \end{aligned} \tag{1.7}$$

is not increasing over time. Thereby, the first two terms are the so-called Cahn–Hilliard free energy and describe the contributions of the fluid-fluid contact area. The next two terms describe the properties of the polymers. Introducing the entropic functional $g(s) := s\log s - s$, the first one measures the deviation of the configurational density ψ from the Maxwellian M. The second one, the so-called Henry energy, describes the solubility properties in the different fluids: High values of β indicate a poor solubility of polymers, while low values indicate good solubility properties in the corresponding fluid. The last term in (1.7) is the kinetic energy of the fluids. By $\mathcal{J}_\varepsilon : L^1(\Omega)\to W^{2,\infty}(\Omega)$ (or $\boldsymbol{\mathcal{J}}_\varepsilon : \boldsymbol{L}^1(\Omega)\to\boldsymbol{W}^{2,\infty}(\Omega)$, respectively), we denote the isotropic mollifier which is defined as

$$\mathcal{J}_\varepsilon\{f\}(\mathbf{x}) := \int_\Omega \zeta_\varepsilon(\mathbf{x}-\mathbf{y})f(\mathbf{y})\mathrm{d}\mathbf{y} \qquad \forall\mathbf{x}\in\Omega, \qquad \forall f\in L^1(\Omega), \tag{1.8}$$

where $\zeta_\varepsilon(\mathbf{x}) := \varepsilon^{-d}\zeta\big(\varepsilon^{-1}\mathbf{x}\big)$ with $\zeta \in W^{2,\infty}\big(\mathbb{R}^d\big)$ being nonnegative and rotationally symmetric, satisfying $\operatorname{supp}\zeta \subset \overline{B(0,1)}$ and having mass one. This mollifier satisfies the following properties.

$$\|\mathcal{J}_\varepsilon\{f\}\|_{L^2(\Omega)} \leq \|f\|_{L^2(\Omega)} \qquad \forall f \in L^2(\Omega), \tag{1.9a}$$

$$\|(I-\mathcal{J}_\varepsilon)\{f\}\|_{L^2(\Omega)} \to 0 \quad \text{as } \varepsilon \searrow 0 \qquad \forall f \in L^2(\Omega), \tag{1.9b}$$

$$\int_\Omega \mathcal{J}_\varepsilon\{f\}g \,\mathrm{d}\mathbf{x} = \int_\Omega f\mathcal{J}_\varepsilon\{g\} \,\mathrm{d}\mathbf{x} \qquad \forall f,g \in L^2(\Omega), \tag{1.9c}$$

$$\partial_{x_i}\mathcal{J}_\varepsilon\{f\} = \mathcal{J}_\varepsilon\{\partial_{x_i}f\} \qquad \forall f \in H^1_0(\Omega),\ i=1,\dots,d, \tag{1.9d}$$

$$\|\mathcal{J}_\varepsilon\{f\}\|_{H^1(\Omega)} \leq \|f\|_{H^1(\Omega)} \qquad \forall f \in H^1_0(\Omega), \tag{1.9e}$$

$$\|\mathcal{J}_\varepsilon\{f\}\|_{W^{2,\infty}(\Omega)} \leq C(\varepsilon)\,\|f\|_{L^1(\Omega)} \qquad \forall f \in L^1(\Omega). \tag{1.9f}$$

Restricting (1.5) to the case of a single-phase flow, *i.e.* ϕ, ρ, and η constant, allows to recover the set of equations derived by Barrett and Süli [5]. Convergent numerical schemes for this single-phase model can be found in [7,8]. Neglecting the mollifier and using simplices with curved edges or faces, J.W. Barrett and E. Süli showed convergence towards weak solutions of a regularized single-phase model (*cf.* [7]) and, by passing to the limit in space and time separately, convergence towards weak solutions of the original model (*cf.* [8] and [6]).

A first existence result for the two-phase flow model (1.5) was already established by Grün and Metzger in [18]. In this paper, we suggest a stable numerical scheme for (1.5) and establish the convergence of discrete solutions for the case of equal fluid mass densities. It turns out, that the resulting existence result is comparable to the one established in [18].

The outline of the paper is as follows. In Section 2, we introduce the discrete function spaces and operators used in the discrete scheme. In Section 3, we introduce the fully discrete finite element scheme for the case of different mass densities and prove a first stability result which suffices to establish the existence of discrete solutions. Restricting ourselves to the case of equal mass densities, we use Section 4 to establish regularity results for discrete solutions, which are independent of the discretization parameters. In Section 5, we pass to the limit as the spatial discretization parameter h and the time step parameter τ tend to zero.

Based on the regularity results of Section 4, we are able to identify subsequences of discrete solutions converging towards weak solutions of (1.5).

As a proof of concept, we present simulations of oscillating non-Newtonian droplets in two and three spatial dimensions in the last section.

Notation 1.1. In this paper, Ω denotes the spatial domain of the flow, and D stands for the configuration space, both sets being contained in $\mathbb{R}^d$ with $d \in \{2,3\}$. By "$\cdot$", we denote the Euclidean scalar product on $\mathbb{R}^d$. Sometimes, we write Ω_T for the space-time cylinder $\Omega \times (0,T)$. By $W^{k,p}(\Omega)$, we denote the space of k-times weakly differentiable functions with weak derivatives in $L^p(\Omega)$. The symbol $W^{k,p}_0(\Omega)$ stands for the closure of $C^\infty_0(\Omega)$ in $W^{k,p}(\Omega)$. For $p=2$, we will denote $W^{k,2}(\Omega)$ by $H^k(\Omega)$ and $W^{k,2}_0(\Omega)$ by $H^k_0(\Omega)$. Corresponding spaces of vector- and matrix-valued functions are denoted in boldface. A similar notation is used for function spaces defined on D or $\Omega \times D$. The space of solenoidal functions with homogeneous Dirichlet boundary data will be denoted by $\boldsymbol{H}^1_{0,\mathrm{div}}(\Omega) := \{\mathbf{w} \in \boldsymbol{H}^1_0 : \operatorname{div}_{\mathbf{x}}\mathbf{w} = 0\}$, its dual space by $\big(\boldsymbol{H}^1_{0,\mathrm{div}}(\Omega)\big)'$, and the duality pairing between $\big(\boldsymbol{H}^1_{0,\mathrm{div}}(\Omega)\big)'$ and $\boldsymbol{H}^1_{0,\mathrm{div}}(\Omega)$ by $\langle .,.\rangle$. To describe the regularity properties of the scaled configurational density $\hat{\psi}$, we introduce the Maxwellian-weighted Lebesgue and Sobolev spaces

$$L^2(\Omega \times D; M) := \Big\{\theta \in L^1_{\mathrm{loc}}(\Omega \times D) \,:\, \|\theta\|_{L^2(\Omega\times D;M)} < \infty\Big\}, \tag{1.10a}$$

$$\hat{X} := H^1(\Omega \times D; M) := \Big\{\theta \in L^1_{\mathrm{loc}}(\Omega \times D) \,:\, \|\theta\|_{H^1(\Omega\times D;M)} < \infty\Big\}, \tag{1.10b}$$

$$\hat{X}_+ := \Big\{\theta \in \hat{X} \,:\, \theta(\mathbf{x},\mathbf{q}) \geq 0 \text{ for a.e. } (\mathbf{x},\mathbf{q}) \in \Omega \times D\Big\}, \tag{1.10c}$$

with the associated norms

$$\|\theta\|_{L^2(\Omega\times D;M)} := \left(\int_{\Omega\times D} M\,|\theta|^2\right)^{1/2}, \tag{1.11a}$$

$$\|\theta\|_{H^1(\Omega\times D;M)} := \left(\int_{\Omega\times D} M\Big[|\theta|^2 + |\nabla_{\mathbf{x}}\theta|^2 + |\nabla_{\mathbf{q}}\theta|^2\Big]\right)^{1/2}. \tag{1.11b}$$

For a Banach space Y and a time interval I, the symbol $L^p(I;Y)$ stands for the parabolic space of L^p-integrable functions on I with values in Y.

2. Technical preliminaries

This section addresses the discretization techniques used in the presented scheme. We introduce discrete function spaces, list the essential estimates for the used approximation, interpolation, and projection operators, and introduce a discrete version of the mollifier $\mathcal{J}_\varepsilon$.

2.1. Discretization in space and time

Concerning the discretization with respect to time, we assume that

(T) the time interval $I := [0,T)$ is subdivided in intervals $I_k := [t_k, t_{k+1})$ with $t_{k+1} = t_k + \tau_k$ for time increments $\tau_k > 0$ and $k = 0,\dots,N-1$ with $t_N = T$. For simplicity, we take $\tau_k \equiv \tau = \frac{T}{N}$ for $k = 0,\dots,N-1$.

From now on, we consider the two-phase problem on a bounded, convex polygonal (or polyhedral, respectively) spatial domain $\Omega \subset \mathbb{R}^d$ in spatial dimensions $d \in \{2,3\}$. As the mollifier $\mathcal{J}_\varepsilon$ includes a convolution on $\mathbb{R}^d$, we also consider a likewise bounded, convex polygonal (or polyhedral, respectively) superset Ω^* of Ω such that $\operatorname{dist}(\partial\Omega^*, \Omega) \geq \varepsilon$, *i.e.* $\operatorname{supp}\zeta_\varepsilon(\mathbf{x} - .) \subset \Omega^*$ for all $\mathbf{x} \in \Omega$. We introduce partitions $\mathcal{T}_h^{\mathbf{x}}$ and $\mathcal{T}_h^{\mathbf{x}*}$ of Ω and Ω^* depending on a spatial discretization parameter $h > 0$ satisfying the following assumptions:

(S1) Let $\{\mathcal{T}_h^{\mathbf{x}*}\}_{h>0}$ be a quasiuniform family (in the sense of [9]) of partitions of Ω^* into disjoint, open, nonobtuse simplices $\kappa_{\mathbf{x}}$, so that

$$\overline{\Omega^*} \equiv \bigcup_{\kappa_{\mathbf{x}}\in\mathcal{T}_h^{\mathbf{x}*}} \overline{\kappa_{\mathbf{x}}} \quad \text{with} \quad h_{\mathbf{x}} := \max_{\kappa_{\mathbf{x}}\in\mathcal{T}_h^{\mathbf{x}*}} \operatorname{diam}(\kappa_{\mathbf{x}}) \leq \operatorname{diam}(\Omega^*)h.$$

(S2) Let $\{\mathcal{T}_h^{\mathbf{x}}\}_{h>0}$ be a quasiuniform family of partitions of Ω into disjoint, open, nonobtuse simplices with $\mathcal{T}_h^{\mathbf{x}} \subset \mathcal{T}_h^{\mathbf{x}*}$, so that $\overline{\Omega} \equiv \bigcup_{\kappa_{\mathbf{x}}\in\mathcal{T}_h^{\mathbf{x}}} \overline{\kappa_{\mathbf{x}}}$.

Instead of working with the configurational space $D := B_{Q_{\max}} \subset \mathbb{R}^d$ and simplices with curved edges or faces (see *e.g.* [7]), we use a bounded polygonal (or polyhedral, respectively) domain $\mathfrak{D} \supset D$. A suitable choice for $\mathfrak{D}$ might be *e.g.* the cube of side length $2Q_{\max}$ which includes D. We make the following assumptions on the partitions of $\mathcal{T}_h^{\mathbf{q}}$ of $\mathfrak{D}$.

(S3) Let $\{\mathcal{T}_h^{\mathbf{q}}\}_{h>0}$ be a quasiuniform family (in the sense of [9]) of partitions of $\mathfrak{D}$ into disjoint open nonobtuse simplices $\kappa_{\mathbf{q}}$, so that

$$\overline{\mathfrak{D}} \equiv \bigcup_{\kappa_{\mathbf{q}}\in\mathcal{T}_h^{\mathbf{q}}} \overline{\kappa_{\mathbf{q}}} \quad \text{with} \quad h_{\mathbf{q}} := \max_{\kappa_{\mathbf{q}}\in\mathcal{T}_h^{\mathbf{q}}} \operatorname{diam}(\kappa_{\mathbf{q}}) \leq \operatorname{diam}(\mathfrak{D})h.$$

Combining (S1) and (S3), we immediately obtain

$$c_1 h \leq h_{\mathbf{x}} \leq c_2 h, \qquad c_3 h \leq h_{\mathbf{q}} \leq c_4 h, \qquad \frac{h_{\mathbf{x}}}{h_{\mathbf{q}}} + \frac{h_{\mathbf{q}}}{h_{\mathbf{x}}} \leq c_5 \tag{2.1}$$

as $h \searrow 0$ with c_i $(i = 1, \dots, 5)$ independent of h. For both, $\mathcal{T}_h^{\mathbf{x}*}$ and $\mathcal{T}_h^{\mathbf{q}}$, we use the same standard reference simplex $\tilde{\kappa}$ with vertices $\{\tilde{\mathbf{P}}_i\}_{i=0,\dots,d}$, where $\tilde{\mathbf{P}}_0$ is the origin and the $\tilde{\mathbf{P}}_i$ are such that the jth component of $\tilde{\mathbf{P}}_i$ is δ_{ij} for $i, j = 1, \dots, d$.

We denote the vertices of an element $\kappa_{\mathbf{x}} \in \mathcal{T}_h^{\mathbf{x}*}$ by $\{\mathbf{P}_{\kappa_{\mathbf{x}},i}\}_{i=0,\dots,d}$ and define $\mathbf{B}_{\kappa_{\mathbf{x}}} \in \mathbb{R}^{d\times d}$ such that the mapping $\mathcal{B}_{\kappa_{\mathbf{x}}} : \mathbb{R}^d \ni y \mapsto \mathbf{P}_{\kappa_{\mathbf{x}},0} + \mathbf{B}_{\kappa_{\mathbf{x}}} y$ maps the vertex $\tilde{\mathbf{P}}_i$ to $\mathbf{P}_{\kappa_{\mathbf{x}},i}$ $(i = 0, \dots, d)$ and hence $\tilde{\kappa}$ to $\kappa_{\mathbf{x}}$. The quantities $\{\mathbf{P}_{\kappa_{\mathbf{q}},i}\}_{i=0,\dots,d}$, $\mathcal{B}_{\kappa_{\mathbf{q}}}$, and $\mathbf{B}_{\kappa_{\mathbf{q}}}$ are defined analogously.

2.2. Discrete function spaces and interpolation operators

For the approximation of the phase-field parameter ϕ and its chemical potential μ_ϕ, we introduce the space $U_h^{\mathbf{x}}$ of continuous, piecewise linear finite element functions on $\mathcal{T}_h^{\mathbf{x}}$. The extension of $U_h^{\mathbf{x}}$ to $\mathcal{T}_h^{\mathbf{x}*}$ is denoted by $U_h^{\mathbf{x}*}$. Pressure and velocity field are approximated with the lowest order Taylor–Hood elements, *i.e.* we define the space $\boldsymbol{W}_h \subset \boldsymbol{H}_0^1(\Omega)$ of continuous, piecewise quadratic finite element functions on $\mathcal{T}_h^{\mathbf{x}}$ together with the spaces

$$S_h := \left\{ \theta_h^{\mathbf{x}} \in U_h^{\mathbf{x}} \,:\, \int_\Omega \theta_h^{\mathbf{x}} \,\mathrm{d}\mathbf{x} = 0 \right\}, \tag{2.2}$$

$$\boldsymbol{W}_{h,\mathrm{div}} := \left\{ \mathbf{w}_h \in \boldsymbol{W}_h \,:\, \int_\Omega \mathrm{div}_{\mathbf{x}}\, \mathbf{w}_h \theta_h^{\mathbf{x}} = 0 \quad \forall \theta_h^{\mathbf{x}} \in S_h \right\}. \tag{2.3}$$

Those spaces enjoy the following properties (see [14] and [21] in combination with the regularity results of [12]):

(TH1) The Babuška–Brezzi condition is satisfied, *i.e.* a positive constant C exists such that

$$\sup_{\mathbf{w}_h \in \boldsymbol{W}_h} \frac{(q_h, \mathrm{div}_{\mathbf{x}}\, \mathbf{w}_h)}{\|\mathbf{w}_h\|_{\boldsymbol{H}_0^1(\Omega)}} \geq C \|q_h\|_{L^2(\Omega)} \tag{2.4}$$

for all $q_h \in S_h$.

(TH2) The L^2-projector $\mathcal{Q}_h : \boldsymbol{H}^1_{0,\mathrm{div}}(\Omega) \to \boldsymbol{W}_{h,\mathrm{div}}$ defined by

$$\int_\Omega (\mathbf{v} - \mathcal{Q}_h[\mathbf{v}]) \cdot \mathbf{w}_h = 0 \qquad\qquad \forall \mathbf{w}_h \in \boldsymbol{W}_{h,\mathrm{div}},\ \mathbf{v} \in \boldsymbol{H}^1_{0,\mathrm{div}}(\Omega)$$

is uniformly $H^1(\Omega)$-stable, *i.e.*

$$\|\mathcal{Q}_h[\mathbf{v}]\|_{H^1(\Omega)} \leq C \|\mathbf{v}\|_{H^1(\Omega)},$$

and satisfies

$$\|\mathbf{v} - \mathcal{Q}_h[\mathbf{v}]\|_{L^2(\Omega)} + h_{\mathbf{x}} \|\nabla_{\mathbf{x}}(\mathbf{v} - \mathcal{Q}_h[\mathbf{v}])\|_{L^2(\Omega)} \leq C h_{\mathbf{x}}^2 \|\mathbf{v}\|_{H^2(\Omega)}$$

for all $\mathbf{v} \in \boldsymbol{H}^1_{0,\mathrm{div}}(\Omega) \cap \boldsymbol{H}^2(\Omega)$.

Similarly to $U_h^{\mathbf{x}*}$ and $U_h^{\mathbf{x}}$, we denote the space of continuous, piecewise linear finite element functions on $\mathcal{T}_h^{\mathbf{q}}$ by $U_h^{\mathbf{q}}$. To approximate $\hat{\psi}$ on $\Omega \times \mathfrak{D}$, we introduce the space $\hat{X}_h := U_h^{\mathbf{x}} \times U_h^{\mathbf{q}}$. That is for a given basis $\{\chi_{h,i}^{\mathbf{x}}\}_{i=1,\dots,\dim U_h^{\mathbf{x}}}$ of $U_h^{\mathbf{x}}$ and a given basis $\{\chi_{h,j}^{\mathbf{q}}\}_{j=1,\dots,\dim U_h^{\mathbf{q}}}$ of $U_h^{\mathbf{q}}$, $\hat{X}_h$ is defined as the span of $\left\{\chi_{h,i}^{\mathbf{x}} \chi_{h,j}^{\mathbf{q}}\right\}_{i=1,\dots,\dim U_h^{\mathbf{x}}}^{j=1,\dots,\dim U_h^{\mathbf{q}}}$.

We define the nodal interpolation operator $\mathcal{I}_h^{\mathbf{x}}$ from $C^0(\overline{\Omega^*})$ to $U_h^{\mathbf{x}*}$ by

$$\mathcal{I}_h^{\mathbf{x}}\{a\} := \sum_{i=1}^{\dim U_h^{\mathbf{x}*}} a(\mathbf{x}_i) \chi_{h,i}^{\mathbf{x}}, \tag{2.5}$$

where the functions $\{\chi^{\mathbf{x}}_{h,i}\}_{i=1,\dots,\dim U_h^{\mathbf{x}*}}$ form a dual basis to the vertices $\{\mathbf{x}_i\}_{i=1,\dots,\dim U_h^{\mathbf{x}*}}$ of $\mathcal{T}_h^{\mathbf{x}*}$, *i.e.* $\chi^{\mathbf{x}}_{h,i}(\mathbf{x}_j) = \delta_{ij}$ for $i,j = 1,\dots,\dim U_h^{\mathbf{x}*}$. In a slight misuse of notation, we also denote the nodal interpolation from $C^0(\overline{\Omega})$ to $U_h^{\mathbf{x}}$ by $\mathcal{I}_h^{\mathbf{x}}$. In the context of the discrete mollifier (see (2.38)), we will introduce a second spatial variable $\mathbf{y}$ and the corresponding operator $\mathcal{I}_h^{\mathbf{y}}$ which is defined analogously to $\mathcal{I}_h^{\mathbf{x}}$.

Similarly, we define

$$\mathcal{I}_h^{\mathbf{q}} : C^0\big(\overline{\mathfrak{D}}\big) \to U_h^{\mathbf{q}}, \qquad a \mapsto \mathcal{I}_h^{\mathbf{q}}\{a\} := \sum_{i=1}^{\dim U_h^{\mathbf{q}}} a(\mathbf{q}_i)\chi^{\mathbf{q}}_{h,i}, \tag{2.6}$$

where the functions $\{\chi^{\mathbf{q}}_{h,i}\}_{i=1,\dots,\dim U_h^{\mathbf{q}}}$ form a dual basis to the vertices $\{\mathbf{q}_i\}_{i=1,\dots,\dim U_h^{\mathbf{q}}}$ of $\mathcal{T}_h^{\mathbf{q}}$. Combining these operators defines the nodal interpolation operator

$$\mathcal{I}_h^{\mathbf{xq}} : C^0\big(\overline{\Omega\times\mathfrak{D}}\big) \to \hat{X}_h, \quad a \mapsto \mathcal{I}_h^{\mathbf{xq}}\{a\} := \mathcal{I}_h^{\mathbf{x}}\{\mathcal{I}_h^{\mathbf{q}}\{a\}\} = \mathcal{I}_h^{\mathbf{q}}\{\mathcal{I}_h^{\mathbf{x}}\{a\}\}. \tag{2.7}$$

Sometimes, we write $\mathcal{I}_h^{\mathbf{x}}\{\mathbf{a}\}$ (or $\mathcal{I}_h^{\mathbf{x}}\{\mathbf{A}\}$) with $\mathbf{a} \in \big(C^0(\overline{\Omega})\big)^d$ (or $\mathbf{A} \in \big(C^0(\overline{\Omega})\big)^{d\times d}$) when we apply $\mathcal{I}_h^{\mathbf{x}}$ to each component of $\mathbf{a}$ (or $\mathbf{A}$, respectively). We also use similar conventions for $\mathcal{I}_h^{\mathbf{q}}$ and $\mathcal{I}_h^{\mathbf{xq}}$.

We define the discrete Laplacian $\Delta_h\phi_h \in S_h$ for all $\phi_h \in U_h^{\mathbf{x}}$ by

$$\int_\Omega \mathcal{I}_h^{\mathbf{x}}\{\Delta_h\phi_h\theta_h^{\mathbf{x}}\} = -\int_\Omega \nabla_{\mathbf{x}}\phi_h \cdot \nabla_{\mathbf{x}}\theta_h^{\mathbf{x}} \quad \forall\theta_h^{\mathbf{x}} \in U_h^{\mathbf{x}}. \tag{2.8}$$

Using the nodal interpolation operator $\mathcal{I}_h^{\mathbf{x}}$, we define the norm $\|.\|_h$ *via*

$$\|\theta^{\mathbf{x}}\|_h^2 := \int_\Omega \mathcal{I}_h^{\mathbf{x}}\Big\{|\theta^{\mathbf{x}}|^2\Big\}, \qquad \text{for all } \theta^{\mathbf{x}} \in C^0(\overline{\Omega}). \tag{2.9}$$

It is well-known that this norm is equivalent to the $L^2(\Omega)$-norm on $U_h^{\mathbf{x}}$, *i.e.* there exist constants $c, C > 0$ such that

$$c\,\|.\|_h \le \|.\|_{L^2(\Omega)} \le C\,\|.\|_h\,. \tag{2.10}$$

Similarly, the following inequalities for the $L^4(\Omega)$- and $L^6(\Omega)$-norm hold true for all $\theta_h^{\mathbf{x}} \in U_h^{\mathbf{x}}$ (*cf.* [25]).

$$c\int_\Omega \mathcal{I}_h^{\mathbf{x}}\Big\{|\theta_h^{\mathbf{x}}|^4\Big\} \le \int_\Omega |\theta_h^{\mathbf{x}}|^4 \le C\int_\Omega \mathcal{I}_h^{\mathbf{x}}\Big\{|\theta_h^{\mathbf{x}}|^4\Big\}, \tag{2.11a}$$

$$c\int_\Omega \mathcal{I}_h^{\mathbf{x}}\Big\{|\theta_h^{\mathbf{x}}|^6\Big\} \le \int_\Omega |\theta_h^{\mathbf{x}}|^6 \le C\int_\Omega \mathcal{I}_h^{\mathbf{x}}\Big\{|\theta_h^{\mathbf{x}}|^6\Big\}. \tag{2.11b}$$

For future reference, we collect additional useful estimates related to the nodal interpolation operators.

Lemma 2.1. *Let $\{\mathcal{T}_h^{\mathbf{x}*}\}_{h>0}$ and $\{\mathcal{T}_h^{\mathbf{q}}\}_{h>0}$ satisfy (S1)–(S3). Then the following estimates hold true for all $\kappa_{\mathbf{x}} \in \mathcal{T}_h^{\mathbf{x}*}$, $\kappa_{\mathbf{q}} \in \mathcal{T}_h^{\mathbf{q}}$, and $1 \le p < \infty$.*

$$|\mathcal{I}_h^{\mathbf{x}}\{\theta^{\mathbf{x}}\}(\mathbf{x})|^p \le \mathcal{I}_h^{\mathbf{x}}\{|\theta^{\mathbf{x}}|^p\}(\mathbf{x}) \qquad \forall\mathbf{x} \in \kappa_{\mathbf{x}} \qquad \forall\theta^{\mathbf{x}} \in C^0(\overline{\kappa_{\mathbf{x}}}), \tag{2.12a}$$

$$|\mathcal{I}_h^{\mathbf{q}}\{\theta^{\mathbf{q}}\}(\mathbf{q})|^p \le \mathcal{I}_h^{\mathbf{q}}\{|\theta^{\mathbf{q}}|^p\}(\mathbf{q}) \qquad \forall\mathbf{q} \in \kappa_{\mathbf{q}} \qquad \forall\theta^{\mathbf{q}} \in C^0(\overline{\kappa_{\mathbf{q}}}), \tag{2.12b}$$

$$|\mathcal{I}_h^{\mathbf{xq}}\{\theta\}(\mathbf{x},\mathbf{q})|^p \le \mathcal{I}_h^{\mathbf{xq}}\{|\theta|^p\}(\mathbf{x},\mathbf{q}) \qquad \forall(\mathbf{x},\mathbf{q}) \in \kappa_{\mathbf{x}}\times\kappa_{\mathbf{q}} \qquad \forall\theta \in C^0(\overline{\kappa_{\mathbf{x}}\times\kappa_{\mathbf{q}}}). \tag{2.12c}$$

Additionally, we have for affine linear functions $\theta_h^{\mathbf{x}}$ and $\theta_h^{\mathbf{q}}$

$$\|\theta_h^{\mathbf{x}}\|_{L^\infty(\kappa_{\mathbf{x}})}^2 \leq C h_{\mathbf{x}}^{-d} \int_{\kappa_{\mathbf{x}}} |\theta_h^{\mathbf{x}}|^2 \,\mathrm{d}\mathbf{x}, \tag{2.13a}$$

$$\|\theta_h^{\mathbf{q}}\|_{L^\infty(\kappa_{\mathbf{q}})}^2 \leq C h_{\mathbf{q}}^{-d} \int_{\kappa_{\mathbf{q}}} |\theta_h^{\mathbf{q}}|^2 \,\mathrm{d}\mathbf{q}, \tag{2.13b}$$

$$\int_{\kappa_{\mathbf{x}}} |\nabla_{\mathbf{x}}\theta_h^{\mathbf{x}}|^2 \,\mathrm{d}\mathbf{x} \leq C h_{\mathbf{x}}^{-2} \int_{\kappa_{\mathbf{x}}} |\theta_h^{\mathbf{x}}|^2 \,\mathrm{d}\mathbf{x} \leq C h_{\mathbf{x}}^{-2} \int_{\kappa_{\mathbf{x}}} \mathcal{I}_h^{\mathbf{x}}\Big\{|\theta_h^{\mathbf{x}}|^2\Big\} \,\mathrm{d}\mathbf{x}, \tag{2.13c}$$

$$\int_{\kappa_{\mathbf{q}}} |\nabla_{\mathbf{q}}\theta_h^{\mathbf{q}}|^2 \,\mathrm{d}\mathbf{q} \leq C h_{\mathbf{q}}^{-2} \int_{\kappa_{\mathbf{q}}} |\theta_h^{\mathbf{q}}|^2 \,\mathrm{d}\mathbf{q} \leq C h_{\mathbf{q}}^{-2} \int_{\kappa_{\mathbf{q}}} \mathcal{I}_h^{\mathbf{q}}\Big\{|\theta_h^{\mathbf{q}}|^2\Big\} \,\mathrm{d}\mathbf{q}. \tag{2.13d}$$

Proof. The inequalities (2.12) are a direct consequence of Jensen's inequality. Standard inverse estimates (see *e.g.* [9], Lem. 4.5.3) yield (2.13a) and (2.13b), as well as the first inequalities in (2.13c) and (2.13d). The second inequalities in (2.13c) and (2.13d) are a consequence of (2.12a) and (2.12b). □

Using the nodal interpolation operator $\mathcal{I}_h^{\mathbf{q}}$ mentioned above, we define a discrete version M_h of the Maxwellian M. We start by defining an extension of M on $\mathfrak{D}$ *via*

$$\hat{M}(\mathbf{q}) := \begin{cases} M(\mathbf{q}) & \text{if } \mathbf{q} \in D, \\ 0 & \text{if } \mathbf{q} \in \mathfrak{D} \setminus D, \end{cases} \tag{2.14}$$

and continue with its finite element approximation

$$M_h(\mathbf{q}) := c_{h_{\mathbf{q}}} \mathcal{I}_h^{\mathbf{q}}\Big\{\hat{M}\Big\}(\mathbf{q}) \qquad \text{for all } \mathbf{q} \in \mathfrak{D}, \tag{2.15}$$

with $c_{h_{\mathbf{q}}} := [\int_{\mathfrak{D}} \mathcal{I}_h^{\mathbf{q}}\{\hat{M}\} \,\mathrm{d}\mathbf{q}]^{-1}$. As shown in [25], the following lemma holds true which in particular states that $\hat{M}$ is continuous and therefore that M_h is well-defined.

Lemma 2.2. *Let the spring potential U and its associated Maxwellian M satisfy the properties (P1)–(P5) with $\kappa > 1$. Then the extension $\hat{M}$ of the Maxwellian on $\mathfrak{D}$ (see (2.14)) and its discrete approximation M_h defined* via (2.15) *have the following properties:*

- $\hat{M} \in C^1(\overline{\mathfrak{D}})$ *with* $\hat{M}\Big|_{\partial\mathfrak{D}} = 0$.
- *The constant $c_{h_{\mathbf{q}}}$ is bounded from below by some constant $c_M > 0$ independently of $h_{\mathbf{q}}$.*
- *For $h_{\mathbf{q}}$ small enough, $c_{h_{\mathbf{q}}}$ is bounded from above by some constant and we have $\Big\|M_h - \hat{M}\Big\|_{L^\infty(\mathfrak{D})} \leq C h_{\mathbf{q}}$.*

The proof of the lemma above can be found in the Appendix A.

For future reference, we state the following Maxwellian-weighted approximation results for the interpolation operators.

Lemma 2.3. *Let M_h be the finite element approximation of the Maxwellian M defined* via (2.15) *and let $\{\mathcal{T}_h^{\mathbf{x}}\}_{h>0}$ and $\{\mathcal{T}_h^{\mathbf{q}}\}_{h>0}$ satisfy (S1)–(S3). Then the following estimates hold true for all $\kappa_{\mathbf{x}} \in \mathcal{T}_h^{\mathbf{x}}$, $\kappa_{\mathbf{q}} \in \mathcal{T}_h^{\mathbf{q}}$ and for all $\hat{\theta}_h, \tilde{\theta}_h \in \hat{X}_h$.*

$$\int_{\kappa_{\mathbf{x}} \times \kappa_{\mathbf{q}}} \Big| M_h (I - \mathcal{I}_h^{\mathbf{x}}) \Big\{ \nabla_{\mathbf{q}} \hat{\theta}_h \cdot \nabla_{\mathbf{q}} \tilde{\theta}_h \Big\} \Big| \,\mathrm{d}\mathbf{q}\,\mathrm{d}\mathbf{x}$$
$$\leq C h_{\mathbf{x}} \left(\int_{\kappa_{\mathbf{x}} \times \kappa_{\mathbf{q}}} M_h \left| \nabla_{\mathbf{q}} \hat{\theta}_h \right|^2 \,\mathrm{d}\mathbf{q}\,\mathrm{d}\mathbf{x} \right)^{1/2} \left(\sum_{i=1}^{d} \sum_{j=1}^{d} \int_{\kappa_{\mathbf{x}} \times \kappa_{\mathbf{q}}} M_h \left| \partial_{\mathbf{x}_i} \partial_{\mathbf{q}_j} \tilde{\theta}_h \right|^2 \,\mathrm{d}\mathbf{q}\,\mathrm{d}\mathbf{x} \right)^{1/2} \tag{2.16a}$$

$$\int_{\kappa_{\mathbf{x}}\times\kappa_{\mathbf{q}}} \left| M_h (I - \mathcal{I}_h^{\mathbf{q}}) \left\{ \nabla_{\mathbf{x}} \hat{\theta}_h \cdot \nabla_{\mathbf{x}} \tilde{\theta}_h \right\} \right| \, \mathrm{d}\mathbf{q}\, \mathrm{d}\mathbf{x}$$
$$\leq C h_{\mathbf{q}} \left(\int_{\kappa_{\mathbf{x}}\times\kappa_{\mathbf{q}}} M_h \left| \nabla_{\mathbf{q}} \hat{\theta}_h \right|^2 \, \mathrm{d}\mathbf{q}\, \mathrm{d}\mathbf{x} \right)^{1/2} \left(\sum_{i=1}^{d} \sum_{j=1}^{d} \int_{\kappa_{\mathbf{x}}\times\kappa_{\mathbf{q}}} M_h \left| \partial_{\mathbf{x}_i} \partial_{\mathbf{q}_j} \tilde{\theta}_h \right|^2 \, \mathrm{d}\mathbf{q}\, \mathrm{d}\mathbf{x} \right)^{1/2} \tag{2.16b}$$

$$\int_{\kappa_{\mathbf{x}}\times\kappa_{\mathbf{q}}} \left| M_h (I - \mathcal{I}_h^{\mathbf{xq}}) \left\{ \hat{\theta}_h \tilde{\theta}_h \right\} \right| \, \mathrm{d}\mathbf{q}\, \mathrm{d}\mathbf{x}$$
$$\leq C h_{\mathbf{x}}^2 \left(\int_{\kappa_{\mathbf{x}}\times\kappa_{\mathbf{q}}} M_h \left| \nabla_{\mathbf{x}} \hat{\theta}_h \right|^2 \, \mathrm{d}\mathbf{q}\, \mathrm{d}\mathbf{x} \right)^{1/2} \left(\int_{\kappa_{\mathbf{x}}\times\kappa_{\mathbf{q}}} M_h \left| \nabla_{\mathbf{x}} \tilde{\theta}_h \right|^2 \, \mathrm{d}\mathbf{q}\, \mathrm{d}\mathbf{x} \right)^{1/2}$$
$$+ C h_{\mathbf{q}}^2 \left(\int_{\kappa_{\mathbf{x}}\times\kappa_{\mathbf{q}}} M_h \left| \nabla_{\mathbf{q}} \hat{\theta}_h \right|^2 \, \mathrm{d}\mathbf{q}\, \mathrm{d}\mathbf{x} \right)^{1/2} \left(\int_{\kappa_{\mathbf{x}}\times\kappa_{\mathbf{q}}} M_h \left| \nabla_{\mathbf{q}} \tilde{\theta} \right|^2 \, \mathrm{d}\mathbf{q}\, \mathrm{d}\mathbf{x} \right)^{1/2}. \tag{2.16c}$$

In Lemma 2.3, we denoted the identity operator mapping scalar-valued functions onto themselves by I. For a Proof of Lemma 2.3 we refer to the Appendix A or to [25] or [7]. In contrast to the proof presented in the latter publication, the Proof of Lemma 2.3 uses (2.1) to obtain $\int_{\kappa_{\mathbf{x}}\times\kappa_{\mathbf{q}}} M_h |\nabla_{\mathbf{q}} \hat{\theta}|^2$ on the right hand-side of (2.16b). Similar computations yield the following result.

Lemma 2.4. *Let $\{\mathcal{T}_h^{\mathbf{x}}\}_{h>0}$ and $\{\mathcal{T}_h^{\mathbf{q}}\}_{h>0}$ satisfy (S1)–(S3). Then, for all $\kappa_{\mathbf{x}} \in \mathcal{T}_h^{\mathbf{x}}$, $\kappa_{\mathbf{q}} \in \mathcal{T}_h^{\mathbf{q}}$, and for all $f_h, \tilde{f}_h \in U_h^{\mathbf{x}}$ and $g_h, \tilde{g}_h \in U_h^{\mathbf{q}}$, we have that*

$$\int_{\kappa_{\mathbf{x}}} \left| (I - \mathcal{I}_h^{\mathbf{x}}) \left\{ f_h \tilde{f}_h \right\} \right| \, \mathrm{d}\mathbf{x} \leq C h_{\mathbf{x}}^2 \left\| \nabla_{\mathbf{x}} f_h \right\|_{L^2(\kappa_{\mathbf{x}})} \left\| \nabla_{\mathbf{x}} \tilde{f}_h \right\|_{L^2(\kappa_{\mathbf{x}})}. \tag{2.17}$$
$$\int_{\kappa_{\mathbf{x}}} \left| (I - \mathcal{I}_h^{\mathbf{x}}) \left\{ f_h \tilde{f}_h \right\} \right| \, \mathrm{d}\mathbf{x} \leq C h_{\mathbf{x}} \left\| f_h \right\|_{L^2(\kappa_{\mathbf{x}})} \left\| \nabla_{\mathbf{x}} \tilde{f}_h \right\|_{L^2(\kappa_{\mathbf{x}})}, \tag{2.18}$$
$$\int_{\kappa_{\mathbf{q}}} \left| M_h (I - \mathcal{I}_h^{\mathbf{q}}) \{ g_h \tilde{g}_h \} \right| \, \mathrm{d}\mathbf{q} \leq C h_{\mathbf{q}}^2 \left(\int_{\kappa_{\mathbf{q}}} M_h \left| \nabla_{\mathbf{q}} g_h \right|^2 \, \mathrm{d}\mathbf{q} \right)^{1/2} \left(\int_{\kappa_{\mathbf{q}}} M_h \left| \nabla_{\mathbf{q}} \tilde{g}_h \right|^2 \, \mathrm{d}\mathbf{q} \right)^{1/2}. \tag{2.19}$$

2.3. Discrete versions of the chain rule

As the regularity results in Section 4 will heavily rely on the validity of the formal identities

$$g''(\hat{\psi})^{-1} \nabla_{\mathbf{q}} g'(\hat{\psi}) = \nabla_{\mathbf{q}} \hat{\psi}, \quad g''(\hat{\psi})^{-1} \nabla_{\mathbf{x}} g'(\hat{\psi}) = \nabla_{\mathbf{x}} \hat{\psi}, \text{ and } \quad \hat{\psi} \nabla_{\mathbf{x}} \hat{\psi} = \tfrac{1}{2} \nabla_{\mathbf{x}} |\hat{\psi}|^2, \tag{2.20}$$

we extend the ideas of G. Grün and M. Rumpf (*cf.* [19]) and J.W. Barrett and E. Süli (*cf.* [7, 8]) to establish discrete counterparts of (2.20). As we are not able to guarantee $\hat{\psi} \geq 0$ in the discrete setting, we start by defining a regularized version of the entropic function g *via*

$$g_\nu(s) := \begin{cases} s \log s - s & \text{if } s \geq \nu, \\ \frac{s^2 - \nu^2}{2\nu} + (\log \nu - 1) s & \text{if } s < \nu, \end{cases} \tag{2.21a}$$
$$g'_\nu(s) = \begin{cases} \log s & \text{if } s \geq \nu, \\ \frac{s}{\nu} + \log \nu - 1 & \text{if } s < \nu, \end{cases} \tag{2.21b}$$
$$g''_\nu(s) = \max\{\nu, s\}^{-1}, \tag{2.21c}$$

for all $s \in \mathbb{R}$ and some regularization parameter $\nu > 0$. Additionally, we define a function $f_\nu : \mathbb{R} \to \mathbb{R}^+$ with $f_\nu'(s) = (g_\nu''(s))^{-1}$ *via*

$$f_\nu(s) := \begin{cases} \frac{1}{2}s^2 & \text{if } s \geq \nu, \\ \nu s - \frac{1}{2}\nu^2 & \text{if } s < \nu, \end{cases} \tag{2.22a}$$

$$f_\nu'(s) = \max\{\nu, s\}. \tag{2.22b}$$

Using the ideas from [19] and [7], we define for a given function $\theta_h \in \hat{X}_h$ and a given element $\kappa_{\mathbf{x}} \in \mathcal{T}_h^{\mathbf{x}}$ a diagonal matrix $\hat{\Xi}_\nu^{\mathbf{x}}[\theta_\mathrm{h}]$ by

$$\left[\hat{\Xi}_\nu^{\mathbf{x}}[\theta_\mathrm{h}]\right]_{ii}(\mathbf{q}) = \begin{cases} \frac{\theta_h(\mathbf{P}_{\kappa_{\mathbf{x}},i},\mathbf{q}) - \theta_h(\mathbf{P}_{\kappa_{\mathbf{x}},0},\mathbf{q})}{g_\nu'(\theta_h(\mathbf{P}_{\kappa_{\mathbf{x}},i},\mathbf{q})) - g_\nu'(\theta_h(\mathbf{P}_{\kappa_{\mathbf{x}},0},\mathbf{q}))} & \text{if } \theta_h(\mathbf{P}_{\kappa_{\mathbf{x}},i},\mathbf{q}) \neq \theta_h(\mathbf{P}_{\kappa_{\mathbf{x}},0},\mathbf{q}), \\ \frac{1}{g_\nu''(\theta_h(\mathbf{P}_{\kappa_{\mathbf{x}},0},\mathbf{q}))} & \text{if } \theta_h(\mathbf{P}_{\kappa_{\mathbf{x}},i},\mathbf{q}) = \theta_h(\mathbf{P}_{\kappa_{\mathbf{x}},0},\mathbf{q}), \end{cases} \tag{2.23a}$$

for any $\mathbf{q} \in \mathfrak{D}$. Incorporating the affine mapping from $\tilde{\kappa}$ to $\kappa_{\mathbf{x}}$, we define the matrix-valued operator $\Xi_\nu^{\mathbf{x}}[.]$ *via*

$$\Xi_\nu^{\mathbf{x}}[\theta_\mathrm{h}](\mathbf{q})\big|_{\kappa_{\mathbf{x}}} := \mathbf{B}_{\kappa_{\mathbf{x}}}^{-T} \cdot \hat{\Xi}_\nu^{\mathbf{x}}[\theta_\mathrm{h}](\mathbf{q}) \cdot \mathbf{B}_{\kappa_{\mathbf{x}}}^T \tag{2.23b}$$

for $\theta_h \in \hat{X}_h$. Analogously, we define $\Lambda_\nu^{\mathbf{x}}[.]$ *via*

$$\left[\hat{\Lambda}_\nu^{\mathbf{x}}[\theta_\mathrm{h}]\right]_{ii}(\mathbf{q}) = \begin{cases} \frac{f_\nu(\theta_h(\mathbf{P}_{\kappa_{\mathbf{x}},i},\mathbf{q})) - f_\nu(\theta_h(\mathbf{P}_{\kappa_{\mathbf{x}},0},\mathbf{q}))}{\theta_h(\mathbf{P}_{\kappa_{\mathbf{x}},i},\mathbf{q}) - \theta_h(\mathbf{P}_{\kappa_{\mathbf{x}},0},\mathbf{q})} & \text{if } \theta_h(\mathbf{P}_{\kappa_{\mathbf{x}},i},\mathbf{q}) \neq \theta_h(\mathbf{P}_{\kappa_{\mathbf{x}},0},\mathbf{q}), \\ f_\nu'(\theta_h(\mathbf{P}_{\kappa_{\mathbf{x}},0},\mathbf{q})) & \text{if } \theta_h(\mathbf{P}_{\kappa_{\mathbf{x}},i},\mathbf{q}) = \theta_h(\mathbf{P}_{\kappa_{\mathbf{x}},0},\mathbf{q}), \end{cases} \tag{2.23c}$$

$$\Lambda_\nu^{\mathbf{x}}[\theta_\mathrm{h}](\mathbf{q})\big|_{\kappa_{\mathbf{x}}} := \mathbf{B}_{\kappa_{\mathbf{x}}}^{-T} \cdot \hat{\Lambda}_\nu^{\mathbf{x}}[\theta_\mathrm{h}](\mathbf{q}) \cdot \mathbf{B}_{\kappa_{\mathbf{x}}}^T, \tag{2.23d}$$

on every $\kappa_{\mathbf{x}} \in \mathcal{T}_h^{\mathbf{x}}$ for $\theta_h \in \hat{X}_h$ and $\mathbf{q} \in \mathfrak{D}$. $\Xi_\nu^{\mathbf{q}}[.]$ is defined *via*

$$\left[\hat{\Xi}_\nu^{\mathbf{q}}[\theta_\mathrm{h}]\right]_{ii}(\mathbf{x}) = \begin{cases} \frac{\theta_h(\mathbf{x},\mathbf{P}_{\kappa_{\mathbf{q}},i}) - \theta_h(\mathbf{x},\mathbf{P}_{\kappa_{\mathbf{q}},0})}{g_\nu'(\theta_h(\mathbf{x},\mathbf{P}_{\kappa_{\mathbf{q}},i})) - g_\nu'(\theta_h(\mathbf{x},\mathbf{P}_{\kappa_{\mathbf{q}},0}))} & \text{if } \theta_h(\mathbf{x},\mathbf{P}_{\kappa_{\mathbf{q}},i}) \neq \theta_h(\mathbf{x},\mathbf{P}_{\kappa_{\mathbf{q}},0}), \\ \frac{1}{g_\nu''(\theta_h(\mathbf{x},\mathbf{P}_{\kappa_{\mathbf{q}},0}))} & \text{if } \theta_h(\mathbf{x},\mathbf{P}_{\kappa_{\mathbf{q}},i}) = \theta_h(\mathbf{x},\mathbf{P}_{\kappa_{\mathbf{q}},0}), \end{cases} \tag{2.23e}$$

$$\Xi_\nu^{\mathbf{q}}[\theta_\mathrm{h}](\mathbf{x})\big|_{\kappa_{\mathbf{q}}} := \mathbf{B}_{\kappa_{\mathbf{q}}}^{-T} \cdot \hat{\Xi}_\nu^{\mathbf{q}}[\theta_\mathrm{h}](\mathbf{x}) \cdot \mathbf{B}_{\kappa_{\mathbf{q}}}^T, \tag{2.23f}$$

on every $\kappa_{\mathbf{q}} \in \mathcal{T}_h^{\mathbf{q}}$ for $\theta_h \in \hat{X}_h$ and $\mathbf{x} \in \Omega$.

Remark 2.5. For a simplex $\kappa_{\mathbf{x}}$, which has a vertex $\mathbf{P}_{\kappa_{\mathbf{x}},0}$ with the property that any two edges intersecting each other in $\mathbf{P}_{\kappa_{\mathbf{x}},0}$ form a right angle, we may define the mapping $\mathcal{B}_{\kappa_{\mathbf{x}}}$ in a way that $\mathbf{B}_{\kappa_{\mathbf{x}}}$ is orthogonal, *i.e.* $\mathbf{B}_{\kappa_{\mathbf{x}}}^T \cdot \mathbf{B}_{\kappa_{\mathbf{x}}}$ is a diagonal matrix. In this case $\Xi_\nu^{\mathbf{x}}[.](.)\big|_{\kappa_{\mathbf{x}}}$ and $\Lambda_\nu^{\mathbf{x}}[.](.)\big|_{\kappa_{\mathbf{x}}}$ are symmetric matrices with eigenvalues greater than or equal to ν.
As we will only consider nonobtuse simplices, $\Xi_\nu^{\mathbf{x}}[.](.)\big|_{\kappa_{\mathbf{x}}}$ and $\Lambda_\nu^{\mathbf{x}}[.](.)\big|_{\kappa_{\mathbf{x}}}$ may not be assumed to be symmetric. Nevertheless, their eigenvalues are still greater than or equal to ν.

Similar considerations apply to $\Xi_\nu^{\mathbf{q}}[.](.)\big|_{\kappa_{\mathbf{q}}}$ and the shape of $\kappa_{\mathbf{q}}$.

As shown in the following lemma, those operators allow for a discrete version of (2.20).

Lemma 2.6. *Let $\Xi_\nu^{\mathbf{q}}[.]$, $\Xi_\nu^{\mathbf{x}}[.]$, and $\Lambda_\nu^{\mathbf{x}}[.]$ be matrix-valued operators on $\Omega \times \mathfrak{D}$ which are defined* via (2.23)*. Then the following identities hold true for $\theta_h \in \hat{X}_h$.*

$$\mathcal{I}_h^{\mathbf{q}}\{\Xi_\nu^{\mathbf{x}}[\theta_\mathrm{h}]\nabla_{\mathbf{x}}\mathcal{I}_h^{\mathbf{xq}}\{g_\nu'(\theta_h)\}\} = \nabla_{\mathbf{x}}\theta_h, \tag{2.24a}$$

$$\mathcal{I}_h^{\mathbf{q}}\{\Lambda_\nu^{\mathbf{x}}[\theta_\mathrm{h}]\nabla_{\mathbf{x}}\theta_h\} = \nabla_{\mathbf{x}}\mathcal{I}_h^{\mathbf{xq}}\{f_\nu(\theta_h)\}, \tag{2.24b}$$

$$\mathcal{I}_h^{\mathbf{x}}\{\Xi_\nu^{\mathbf{q}}[\theta_\mathrm{h}]\nabla_{\mathbf{q}}\mathcal{I}_h^{\mathbf{xq}}\{g_\nu'(\theta_h)\}\} = \nabla_{\mathbf{q}}\theta_h. \tag{2.24c}$$

Proof. Restricting ourselves to $\tilde{\kappa} \times \kappa_{\mathbf{q}}$ with the vertices $\{(\tilde{\mathbf{P}}_i, \mathbf{P}_{\kappa_{\mathbf{q}},j})\}_{i,j=0,\ldots d}$, we note that the $\mathbf{x}$-gradient of $\mathcal{I}_h^{\mathbf{xq}}\{g'_\nu(\theta_h(\mathbf{x},\mathbf{q}))\}$ for some $\theta_h \in \hat{X}$ may be written as

$$\nabla_{\mathbf{x}} \mathcal{I}_h^{\mathbf{xq}}\{g'_\nu(\theta_h(\mathbf{x},\mathbf{q}))\} = \sum_{i=1}^{d} [g'_\nu(\theta_h(\tilde{\mathbf{P}}_i,\mathbf{q})) - g'_\nu(\theta_h(\tilde{\mathbf{P}}_0,\mathbf{q}))]\mathbf{e}_i, \tag{2.25}$$

for all $\mathbf{x} \in \tilde{\kappa}$ and $\mathbf{q} \in \kappa_{\mathbf{q}}$. Therefore, we may compute on each $\kappa_{\mathbf{x}} \times \kappa_{\mathbf{q}} \in \mathcal{T}_h^{\mathbf{x}} \otimes \mathcal{T}_h^{\mathbf{q}}$

$$\begin{aligned}
&\Xi_\nu^{\mathbf{x}}[\theta_{\mathrm{h}}]\big(\mathbf{P}_{\kappa_{\mathbf{q}},j}\big)\nabla_{\mathbf{x}}\mathcal{I}_h^{\mathbf{xq}}\big\{g'_\nu\big(\theta_h(\mathbf{x},\mathbf{P}_{\kappa_{\mathbf{q}},j})\big)\big\} \\
&\quad = \mathbf{B}_{\kappa_{\mathbf{x}}}^{-T} \cdot \hat{\Xi}_\nu^{\mathbf{x}}[\theta_{\mathrm{h}}]\big(\mathbf{P}_{\kappa_{\mathbf{q}},j}\big) \cdot \mathbf{B}_{\kappa_{\mathbf{x}}}^{T} \cdot \mathbf{B}_{\kappa_{\mathbf{x}}}^{-T} \sum_{i=1}^{d} \big[g'_\nu\big(\theta_h\big(\mathbf{P}_{\kappa_{\mathbf{x}},i},\mathbf{P}_{\kappa_{\mathbf{q}},j}\big)\big) - g'_\nu\big(\theta_h\big(\mathbf{P}_{\kappa_{\mathbf{x}},0},\mathbf{P}_{\kappa_{\mathbf{q}},j}\big)\big)\big]\mathbf{e}_i \\
&\quad = \mathbf{B}_{\kappa_{\mathbf{x}}}^{-T} \sum_{i=1}^{d} \big[\theta_h\big(\mathbf{P}_{\kappa_{\mathbf{x}},i},\mathbf{P}_{\kappa_{\mathbf{q}},j}\big) - \theta_h\big(\mathbf{P}_{\kappa_{\mathbf{x}},0},\mathbf{P}_{\kappa_{\mathbf{q}},j}\big)\big]\mathbf{e}_i = \nabla_{\mathbf{x}}\theta_h(\mathbf{x},\mathbf{P}_{\kappa_{\mathbf{q}},j}),
\end{aligned} \tag{2.26}$$

where $\{\mathbf{P}_{\kappa_{\mathbf{q}},j}\}_{j=0,\ldots,d}$ denote the vertices of $\kappa_{\mathbf{q}}$, which proves (2.24a). Similar arguments yield (2.24b) and (2.24c). ☐

By definition, the smallest eigenvalues of $\Xi_\nu^{\mathbf{x}}[.]$, $\Lambda_\nu^{\mathbf{x}}[.]$, and $\Xi_\nu^{\mathbf{q}}[.]$ are bounded from below by ν. As we will also stumble upon the largest eigenvalues of those matrices in Section 4, we define piecewise constant functions $\sigma^{\Xi_\nu^{\mathbf{x}}[.]}(\mathbf{x},\mathbf{q})$, $\sigma^{\Lambda_\nu^{\mathbf{x}}[.]}(\mathbf{x},\mathbf{q})$, and $\sigma^{\Xi_\nu^{\mathbf{q}}[.]}(\mathbf{x},\mathbf{q})$ as the supremum on $\kappa_{\mathbf{x}} \times \kappa_{\mathbf{q}} \ni (\mathbf{x},\mathbf{q})$ of the largest eigenvalues of $\Xi_\nu^{\mathbf{x}}[.]\big|_{\kappa_{\mathbf{x}}\times\kappa_{\mathbf{q}}\ni(\mathbf{x},\mathbf{q})}$, $\Lambda_\nu^{\mathbf{x}}[.]\big|_{\kappa_{\mathbf{x}}\times\kappa_{\mathbf{q}}\ni(\mathbf{x},\mathbf{q})}$, and $\Xi_\nu^{\mathbf{q}}[.]\big|_{\kappa_{\mathbf{x}}\times\kappa_{\mathbf{q}}\ni(\mathbf{x},\mathbf{q})}$, respectively.

Lemma 2.7. *Let $\Xi_\nu^{\mathbf{q}}[.]$, $\Xi_\nu^{\mathbf{x}}[.]$, and $\Lambda_\nu^{\mathbf{x}}[.]$ be matrix-valued operators on $\Omega \times \mathfrak{D}$ which are defined* via (2.23) *and let $\mathcal{T}_h^{\mathbf{x}}$ and $\mathcal{T}_h^{\mathbf{q}}$ be quasiuniform triangulations. Then, for $\theta_h \in \hat{X}_h$, $\kappa_{\mathbf{x}} \in \mathcal{T}_h^{\mathbf{x}}$, $\kappa_{\mathbf{q}} \in \mathcal{T}_h^{\mathbf{q}}$, and any nonnegative $M_h \in U_h^{\mathbf{q}}$, the estimates*

$$\int_{\kappa_{\mathbf{x}}\times\kappa_{\mathbf{q}}} M_h \mathcal{I}_h^{\mathbf{x}}\{\Xi_\nu^{\mathbf{q}}[\theta_{\mathrm{h}}] : \Xi_\nu^{\mathbf{q}}[\theta_{\mathrm{h}}]\} \le C\int_{\kappa_{\mathbf{x}}\times\kappa_{\mathbf{q}}} M_h \nu^2 + C\int_{\kappa_{\mathbf{x}}\times\kappa_{\mathbf{q}}} M_h \mathcal{I}_h^{\mathbf{xq}}\Big\{|\theta_h|^2\Big\}, \tag{2.27a}$$

$$\int_{\kappa_{\mathbf{x}}\times\kappa_{\mathbf{q}}} M_h \mathcal{I}_h^{\mathbf{q}}\{\Xi_\nu^{\mathbf{x}}[\theta_{\mathrm{h}}] : \Xi_\nu^{\mathbf{x}}[\theta_{\mathrm{h}}]\} \le C\int_{\kappa_{\mathbf{x}}\times\kappa_{\mathbf{q}}} M_h \nu^2 + C\int_{\kappa_{\mathbf{x}}\times\kappa_{\mathbf{q}}} M_h \mathcal{I}_h^{\mathbf{xq}}\Big\{|\theta_h|^2\Big\}, \tag{2.27b}$$

$$\int_{\kappa_{\mathbf{x}}\times\kappa_{\mathbf{q}}} M_h \mathcal{I}_h^{\mathbf{q}}\{\Lambda_\nu^{\mathbf{x}}[\theta_{\mathrm{h}}] : \Lambda_\nu^{\mathbf{x}}[\theta_{\mathrm{h}}]\} \le C\int_{\kappa_{\mathbf{x}}\times\kappa_{\mathbf{q}}} M_h \nu^2 + C\int_{\kappa_{\mathbf{x}}\times\kappa_{\mathbf{q}}} M_h \mathcal{I}_h^{\mathbf{xq}}\Big\{|\theta_h|^2\Big\}, \tag{2.27c}$$

$$\int_{\kappa_{\mathbf{x}}\times\kappa_{\mathbf{q}}} M_h \left|\sigma^{\Xi_\nu^{\mathbf{q}}[\theta_{\mathrm{h}}]}(\mathbf{x},\mathbf{q})\right|^2 \le C\int_{\kappa_{\mathbf{x}}\times\kappa_{\mathbf{q}}} M_h \nu^2 + C\int_{\kappa_{\mathbf{x}}\times\kappa_{\mathbf{q}}} M_h \mathcal{I}_h^{\mathbf{xq}}\Big\{|\theta_h|^2\Big\}, \tag{2.27d}$$

$$\int_{\kappa_{\mathbf{x}}\times\kappa_{\mathbf{q}}} M_h \left|\sigma^{\Xi_\nu^{\mathbf{x}}[\theta_{\mathrm{h}}]}(\mathbf{x},\mathbf{q})\right|^2 \le C\int_{\kappa_{\mathbf{x}}\times\kappa_{\mathbf{q}}} M_h \nu^2 + C\int_{\kappa_{\mathbf{x}}\times\kappa_{\mathbf{q}}} M_h \mathcal{I}_h^{\mathbf{xq}}\Big\{|\theta_h|^2\Big\}, \tag{2.27e}$$

$$\int_{\kappa_{\mathbf{x}}\times\kappa_{\mathbf{q}}} M_h \left|\sigma^{\Lambda_\nu^{\mathbf{x}}[\theta_{\mathrm{h}}]}(\mathbf{x},\mathbf{q})\right|^2 \le C\int_{\kappa_{\mathbf{x}}\times\kappa_{\mathbf{q}}} M_h \nu^2 + C\int_{\kappa_{\mathbf{x}}\times\kappa_{\mathbf{q}}} M_h \mathcal{I}_h^{\mathbf{xq}}\Big\{|\theta_h|^2\Big\} \tag{2.27f}$$

hold true with some $C > 0$ independent of h, M_h, ν, and θ_h.

Proof. To prove (2.27a)–(2.27c), we will use the well-known estimates

$$\big\|\mathbf{B}_{\kappa_{\mathbf{x}}}^{-T}\big\|\,\big\|\mathbf{B}_{\kappa_{\mathbf{x}}}^{T}\big\| \le C, \quad \Big\|\mathbf{B}_{\kappa_{\mathbf{q}}}^{-T}\Big\|\,\Big\|\mathbf{B}_{\kappa_{\mathbf{q}}}^{T}\Big\| \le C, \tag{2.28}$$

with the Frobenius matrix norm $\|.\|$, which hold true for quasiuniform triangulations (*cf.* [11]). Denoting the supremum on $\kappa_{\mathbf{x}} \times \kappa_{\mathbf{q}}$ of the largest eigenvalue of $\hat{\Xi}_\nu^{\mathbf{q}}[\theta_{\rm h}]$ by $\sigma^{\hat{\Xi}_\nu^{\mathbf{q}}[\theta_{\rm h}]}$, we compute

$$\begin{aligned}\int_{\kappa_{\mathbf{x}}\times\kappa_{\mathbf{q}}} M_h \mathcal{I}_h^{\mathbf{x}}\{\Xi_\nu^{\mathbf{q}}[\theta_{\rm h}] : \Xi_\nu^{\mathbf{q}}[\theta_{\rm h}]\} &\leq C \int_{\kappa_{\mathbf{x}}\times\kappa_{\mathbf{q}}} \left\|\mathbf{B}_{\kappa_{\mathbf{q}}}^{-T}\right\|^2 \left\|\mathbf{B}_{\kappa_{\mathbf{q}}}^{T}\right\|^2 M_h \mathcal{I}_h^{\mathbf{x}}\left\{\hat{\Xi}_\nu^{\mathbf{q}}[\theta_{\rm h}] : \hat{\Xi}_\nu^{\mathbf{q}}[\theta_{\rm h}]\right\} \\ &\leq C \int_{\kappa_{\mathbf{x}}\times\kappa_{\mathbf{q}}} M_h d \left|\sigma^{\hat{\Xi}_\nu^{\mathbf{q}}[\theta_{\rm h}]}(\mathbf{x},\mathbf{q})\right|^2 = C \int_{\kappa_{\mathbf{x}}\times\kappa_{\mathbf{q}}} M_h d \left|\sigma^{\Xi_\nu^{\mathbf{q}}[\theta_{\rm h}]}(\mathbf{x},\mathbf{q})\right|^2, \end{aligned} \tag{2.29}$$

as $\Xi_\nu^{\mathbf{q}}[\theta_{\rm h}]$ and $\hat{\Xi}_\nu^{\mathbf{q}}[\theta_{\rm h}]$ share the same eigenvalues. Combining (2.23e) with the mean value theorem yields

$$\left|\sigma^{\Xi_\nu^{\mathbf{q}}[\theta_{\rm h}]}(\mathbf{x},\mathbf{q})\right|^2 = \left|\sigma^{\hat{\Xi}_\nu^{\mathbf{q}}[\theta_{\rm h}]}(\mathbf{x},\mathbf{q})\right|^2 \leq \left|\max\left\{\nu, \max_{\kappa_{\mathbf{x}}\times\kappa_{\mathbf{q}}} \theta_h\right\}\right|^2 \leq \nu^2 + \max_{\kappa_{\mathbf{x}}\times\kappa_{\mathbf{q}}} |\theta_h|^2 . \tag{2.30}$$

Due to the structure of $\hat{X}_h$, this maximum is attained in one of the vertices of $\kappa_{\mathbf{x}} \times \kappa_{\mathbf{q}}$. The estimate

$$\int_{\kappa_{\mathbf{x}}\times\kappa_{\mathbf{q}}} M_h \max_{\kappa_{\mathbf{x}}\times\kappa_{\mathbf{q}}} \{\theta_h\}^2 \leq \int_{\kappa_{\mathbf{x}}\times\kappa_{\mathbf{q}}} M_h \sum_{i,j=0}^{d} \left|\theta_h(\mathbf{P}_{\kappa_{\mathbf{x}},i}, \mathbf{P}_{\kappa_{\mathbf{q}},j})\right|^2 \leq C \int_{\kappa_{\mathbf{x}}\times\kappa_{\mathbf{q}}} M_h \mathcal{I}_h^{\mathbf{xq}}\left\{|\theta_h|^2\right\} \tag{2.31}$$

finally yields (2.27a) and (2.27d). Analogous arguments show (2.27b), (2.27c), (2.27e), and (2.27f). ☐

As already indicated by their definition, the quantities $\Xi_\nu^{\mathbf{q}}[\theta_{\rm h}]$, $\Xi_\nu^{\mathbf{x}}[\theta_{\rm h}]$, and $\Lambda_\nu^{\mathbf{x}}[\theta_{\rm h}]$ are meant to be local approximations of $\theta_h \in \hat{X}_h$. The following lemma characterizes the quality of the approximation. As $\Xi_\nu^{\mathbf{q}}[\theta_{\rm h}]$, $\Xi_\nu^{\mathbf{x}}[\theta_{\rm h}]$, and $\Lambda_\nu^{\mathbf{x}}[\theta_{\rm h}]$ are positive definite matrices, the quality of the approximation will naturally depend on the negative fraction

$$[.]_- \;:\; s \mapsto [s]_- := \min\{0, s\} \tag{2.32}$$

of θ_h.

Lemma 2.8. *Let $\Xi_\nu^{\mathbf{q}}[.]$, $\Xi_\nu^{\mathbf{x}}[.]$, and $\Lambda_\nu^{\mathbf{x}}[.]$ be matrix-valued operators on $\Omega \times \mathfrak{D}$ which are defined* via (2.23) *and let the triangulations $\mathcal{T}_h^{\mathbf{x}}$ and $\mathcal{T}_h^{\mathbf{q}}$ be quasiuniform. Then, for $\theta_h \in \hat{X}_h$, $\kappa_{\mathbf{x}} \in \mathcal{T}_h^{\mathbf{x}}$, $\kappa_{\mathbf{q}} \in \mathcal{T}_h^{\mathbf{q}}$, and any nonnegative $M_h \in U_h^{\mathbf{q}}$, the following estimates hold true*

$$\int_{\kappa_{\mathbf{x}}\times\kappa_{\mathbf{q}}} M_h \mathcal{I}_h^{\mathbf{x}}\left\{|\Xi_\nu^{\mathbf{q}}[\theta_{\rm h}] - \theta_h \mathbb{1}|^2\right\} \leq C\left(h_{\mathbf{q}}^2 \int_{\kappa_{\mathbf{x}}\times\kappa_{\mathbf{q}}} M_h \mathcal{I}_h^{\mathbf{x}}\left\{|\nabla_{\mathbf{q}}\theta_h|^2\right\} + \int_{\kappa_{\mathbf{x}}\times\kappa_{\mathbf{q}}} M_h \nu^2 + \int_{\kappa_{\mathbf{x}}\times\kappa_{\mathbf{q}}} M_h \mathcal{I}_h^{\mathbf{xq}}\left\{[\theta_h]_-^2\right\}\right), \tag{2.33a}$$

$$\int_{\kappa_{\mathbf{x}}\times\kappa_{\mathbf{q}}} M_h \mathcal{I}_h^{\mathbf{q}}\left\{|\Xi_\nu^{\mathbf{x}}[\theta_{\rm h}] - \theta_h \mathbb{1}|^2\right\} \leq C\left(h_{\mathbf{x}}^2 \int_{\kappa_{\mathbf{x}}\times\kappa_{\mathbf{q}}} M_h \mathcal{I}_h^{\mathbf{q}}\left\{|\nabla_{\mathbf{x}}\theta_h|^2\right\} + \int_{\kappa_{\mathbf{x}}\times\kappa_{\mathbf{q}}} M_h \nu^2 + \int_{\kappa_{\mathbf{x}}\times\kappa_{\mathbf{q}}} M_h \mathcal{I}_h^{\mathbf{xq}}\left\{[\theta_h]_-^2\right\}\right), \tag{2.33b}$$

$$\int_{\kappa_{\mathbf{x}}\times\kappa_{\mathbf{q}}} M_h \mathcal{I}_h^{\mathbf{q}}\left\{|\Lambda_\nu^{\mathbf{x}}[\theta_{\rm h}] - \theta_h \mathbb{1}|^2\right\} \leq C\left(h_{\mathbf{x}}^2 \int_{\kappa_{\mathbf{x}}\times\kappa_{\mathbf{q}}} M_h \mathcal{I}_h^{\mathbf{q}}\left\{|\nabla_{\mathbf{x}}\theta_h|^2\right\} + \int_{\kappa_{\mathbf{x}}\times\kappa_{\mathbf{q}}} M_h \nu^2 + \int_{\kappa_{\mathbf{x}}\times\kappa_{\mathbf{q}}} M_h \mathcal{I}_h^{\mathbf{xq}}\left\{[\theta_h]_-^2\right\}\right), \tag{2.33c}$$

$$\int_{\kappa_{\mathbf{x}}\times\kappa_{\mathbf{q}}} M_h \mathcal{I}_h^{\mathbf{q}}\left\{|\Xi_\nu^{\mathbf{x}}[\theta_{\rm h}] - \Lambda_\nu^{\mathbf{x}}[\theta_{\rm h}]|^2\right\} \leq C h_{\mathbf{x}}^2 \int_{\kappa_{\mathbf{x}}\times\kappa_{\mathbf{q}}} M_h \mathcal{I}_h^{\mathbf{q}}\left\{|\nabla_{\mathbf{x}}\theta_h|^2\right\}, \tag{2.33d}$$

where $\mathbb{1}$ denotes the unit matrix in $\mathbb{R}^{d\times d}$.

Proof. We start with the estimate

$$\begin{aligned}&\int_{\kappa_{\mathbf{x}}\times\kappa_{\mathbf{q}}} M_h \mathcal{I}_h^{\mathbf{x}}\left\{|\Xi_\nu^{\mathbf{q}}[\theta_{\rm h}] - \theta_h \mathbb{1}|^2\right\} \\ &\qquad \leq C \int_{\kappa_{\mathbf{x}}\times\kappa_{\mathbf{q}}} M_h \mathcal{I}_h^{\mathbf{x}}\left\{\left|\Xi_\nu^{\mathbf{q}}[\theta_{\rm h}] - g_\nu''(\theta_h)^{-1}\mathbb{1}\right|^2\right\} + C \int_{\kappa_{\mathbf{x}}\times\kappa_{\mathbf{q}}} M_h \mathcal{I}_h^{\mathbf{x}}\left\{\left|g_\nu''(\theta_h)^{-1}\mathbb{1} - \theta_h \mathbb{1}\right|^2\right\} \\ &\qquad =: I + II. \end{aligned} \tag{2.34}$$

Similarly to the proof of Lemma 2.7, we use (2.28) to gain access to the entries of the diagonal matrix $\hat{\Xi}^{\mathbf{q}}_{\nu}[\theta_{\mathrm{h}}]$. Then, we use the affine linearity of θ_h with respect to $\mathbf{q}$ to compute

$$\begin{aligned}
I \leq & C \int_{\kappa_{\mathbf{x}}\times\kappa_{\mathbf{q}}} M_h \left\|\mathbf{B}_{\kappa_{\mathbf{x}}}^T\right\|^2 \left\|\mathbf{B}_{\kappa_{\mathbf{x}}}^{-T}\right\|^2 \mathcal{I}_h^{\mathbf{x}}\left\{\left|\hat{\Xi}^{\mathbf{q}}_{\nu}[\theta_{\mathrm{h}}] - \max\left\{\nu, \theta_h\right\}\mathbb{1}\right|^2\right\} \\
\leq & C \int_{\kappa_{\mathbf{x}}\times\kappa_{\mathbf{q}}} M_h d\mathcal{I}_h^{\mathbf{x}}\left\{\left|\max_{j=1,\ldots,d} \max\left\{\nu, \theta_h(\mathbf{x}, \mathbf{P}_{\kappa_{\mathbf{q}},j})\right\} - \min_{j=1,\ldots,d} \max\left\{\nu, \theta_h(\mathbf{x}, \mathbf{P}_{\kappa_{\mathbf{q}},j})\right\}\right|^2\right\} \\
\leq & C \int_{\kappa_{\mathbf{x}}\times\kappa_{\mathbf{q}}} M_h d\mathcal{I}_h^{\mathbf{x}}\left\{\left|\max_{j=1,\ldots,d} \theta_h(\mathbf{x}, \mathbf{P}_{\kappa_{\mathbf{q}},j}) - \min_{j=1,\ldots,d} \theta_h(\mathbf{x}, \mathbf{P}_{\kappa_{\mathbf{q}},j})\right|^2\right\} \\
\leq & C \int_{\kappa_{\mathbf{x}}\times\kappa_{\mathbf{q}}} M_h h_{\mathbf{q}}^2 \left\|\nabla_{\mathbf{q}}\theta_h\right\|^2_{L^\infty(\kappa_{\mathbf{x}}\times\kappa_{\mathbf{q}})} \leq C h_{\mathbf{q}}^2 \int_{\kappa_{\mathbf{x}}\times\kappa_{\mathbf{q}}} M_h \sum_{i=1}^d \left|\nabla_{\mathbf{q}}\theta_h(\mathbf{P}_{\kappa_{\mathbf{x}},i}, \mathbf{q})\right|^2 \\
\leq & C h_{\mathbf{q}}^2 \int_{\kappa_{\mathbf{x}}\times\kappa_{\mathbf{q}}} M_h \mathcal{I}_h^{\mathbf{x}}\left\{\left|\nabla_{\mathbf{q}}\theta_h\right|^2\right\},
\end{aligned} \tag{2.35}$$

where we used that $\nabla_{\mathbf{q}}\theta_h$ is constant with respect to $\mathbf{q}$ on each simplex. Concerning the second term, we use that $g_\nu''(s)^{-1} \equiv s$ for $s \geq \nu$.

$$\begin{aligned}
II \leq & \, d \int_{\kappa_{\mathbf{x}}\times\kappa_{\mathbf{q}}} M_h \left\|\nu - [\theta_h]_-\right\|^2_{L^\infty(\kappa_{\mathbf{x}}\times\kappa_{\mathbf{q}})} \leq C \int_{\kappa_{\mathbf{x}}\times\kappa_{\mathbf{q}}} M_h \left\|\nu^2 + [\theta_h]_-^2\right\|_{L^\infty(\kappa_{\mathbf{x}}\times\kappa_{\mathbf{q}})} \\
\leq & \, C \int_{\kappa_{\mathbf{x}}\times\kappa_{\mathbf{q}}} M_h \nu^2 + C \int_{\kappa_{\mathbf{x}}\times\kappa_{\mathbf{q}}} M_h \sum_{i,j=0}^d \left[\theta_h(\mathbf{P}_{\kappa_{\mathbf{x}},i}, \mathbf{P}_{\kappa_{\mathbf{q}},j})\right]_-^2 \\
\leq & \, C \int_{\kappa_{\mathbf{x}}\times\kappa_{\mathbf{q}}} M_h \nu^2 + C \int_{\kappa_{\mathbf{x}}\times\kappa_{\mathbf{q}}} M_h \mathcal{I}_h^{\mathbf{xq}}\left\{[\theta_h]_-^2\right\}.
\end{aligned} \tag{2.36}$$

Therefore, (2.33a) is proven. Analogous computations yield (2.33b) and (2.33c). Noting $g_\nu''(\theta_h)^{-1} \equiv f_\nu'(\theta_h)$, the last inequality follows from

$$\begin{aligned}
&\int_{\kappa_{\mathbf{x}}\times\kappa_{\mathbf{q}}} M_h \mathcal{I}_h^{\mathbf{q}}\left\{\left|\Xi^{\mathbf{x}}_{\nu}[\theta_{\mathrm{h}}] - \Lambda^{\mathbf{x}}_{\nu}[\theta_{\mathrm{h}}]\right|^2\right\} \\
&\qquad \leq C \int_{\kappa_{\mathbf{x}}\times\kappa_{\mathbf{q}}} M_h \mathcal{I}_h^{\mathbf{q}}\left\{\left|\Xi^{\mathbf{x}}_{\nu}[\theta_{\mathrm{h}}] - g_\nu''(\theta_h)^{-1}\mathbb{1}\right|^2\right\} + C \int_{\kappa_{\mathbf{x}}\times\kappa_{\mathbf{q}}} M_h \mathcal{I}_h^{\mathbf{q}}\left\{\left|f_\nu'(\theta_h)\mathbb{1} - \Lambda^{\mathbf{x}}_{\nu}[\theta_{\mathrm{h}}]\right|^2\right\}
\end{aligned} \tag{2.37}$$

with arguments similar to (2.35). □

2.4. A discrete mollifier

In this subsection, we introduce a finite element version of the continuous mollifier $\mathcal{J}_\varepsilon$. It will turn out that a suitable weak formulation (or discrete scheme, respectively) allows to drop the properties (1.9a)–(1.9e). Therefore, we only demand that the discrete mollifier satisfies an inequality similar to (1.9f) and converges towards $\mathcal{J}_\varepsilon$ in a suitable sense (*cf.* Lem. 2.11).

We define a discrete mollification operator $\mathcal{J}_{\varepsilon,h}$ analogously to (1.8). Again, we start with a nonnegative, rotationally symmetric $\zeta \in W^{2,\infty}(\mathbb{R}^d)$ satisfying $\operatorname{supp}\zeta \subset \overline{B(0,1)}$ with mass one. We then define $\zeta_\varepsilon(\mathbf{x}) := \varepsilon^{-d}\zeta(\varepsilon^{-1}\mathbf{x})$ and finally $\mathcal{J}_{\varepsilon,h}$ *via*

$$\mathcal{J}_{\varepsilon,h}\{f\}(\mathbf{x}) := c_{\mathcal{J}}(\mathbf{x}) \int_{\Omega} \mathcal{I}_h^{\mathbf{y}}\{\zeta_\varepsilon(\mathbf{x}-\mathbf{y})\} f(\mathbf{y}) \,\mathrm{d}\mathbf{y}, \tag{2.38}$$

for $f \in L^1(\Omega)$ with the nodal interpolation operator $\mathcal{I}_h^{\mathbf{y}}$ which is equivalent to $\mathcal{I}_h^{\mathbf{x}}$ but works on the spatial variable $\mathbf{y}$. The weight function $c_{\mathcal{J}}(\mathbf{x}) := \left[\int_{\mathbb{R}^d} \mathcal{I}_h^{\mathbf{y}}\{\zeta_\varepsilon(\mathbf{x}-\mathbf{y})\}\,\mathrm{d}\mathbf{y}\right]^{-1}$ reduces the impact of the triangulation on $\mathcal{J}_{\varepsilon,h}$ but inhibits a property similar to (1.9c). As we defined Ω^* such that $\operatorname{dist}(\Omega, \partial\Omega^*) \geq \varepsilon$, it suffices to write $c_{\mathcal{J}}$ in a practically more convenient way as

$$c_{\mathcal{J}}(\mathbf{x}) := \left[\int_{\Omega^*} \mathcal{I}_h^{\mathbf{y}}\{\zeta_\varepsilon(\mathbf{x}-\mathbf{y})\}\,\mathrm{d}\mathbf{y}\right]^{-1}. \tag{2.39}$$

Lemma 2.9. *Let $\{\mathcal{T}_h^{\mathbf{x}*}\}_{h>0}$ and $\{\mathcal{T}_h^{\mathbf{q}}\}_{h>0}$ satisfy (S1)–(S3) and let $c_{\mathcal{J}}$ be the weight function defined* via (2.39)*. Then there exists $C>0$ independent of $h_{\mathbf{x}}$ such that*

$$\|c_{\mathcal{J}}\|_{W^{1,\infty}(\Omega)} \leq C(\varepsilon), \tag{2.40}$$

for $h_{\mathbf{x}}$ small enough.

Proof. Using $\int_{\Omega^*} \zeta_\varepsilon(\mathbf{x}-\mathbf{y})\,\mathrm{d}\mathbf{y} \equiv 1$ for all $\mathbf{x} \in \Omega$ and the standard error estimates for the interpolation operator (see *e.g.* Thm. 4.4.4 and Them. 4.4.20 in [9]), we obtain

$$\begin{aligned}
\int_{\Omega^*} \mathcal{I}_h^{\mathbf{y}}\{\zeta_\varepsilon(\mathbf{x}-\mathbf{y})\}\,\mathrm{d}\mathbf{y} &= \int_{\Omega^*} \zeta_\varepsilon(\mathbf{x}-\mathbf{y})\,\mathrm{d}\mathbf{y} + \int_{\Omega^*} \left(\mathcal{I}_h^{\mathbf{y}}\{\zeta_\varepsilon(\mathbf{x}-\mathbf{y})\} - \zeta_\varepsilon(\mathbf{x}-\mathbf{y})\right)\mathrm{d}\mathbf{y} \\
&\geq 1 - \sum_{\kappa_{\mathbf{x}} \in \mathcal{T}_h^{\mathbf{x}*}} |\kappa_{\mathbf{x}}| \, \|\zeta_\varepsilon(\mathbf{x}-\,.\,) - \mathcal{I}_h^{\mathbf{y}}\{\zeta_\varepsilon(\mathbf{x}-\,.\,)\}\|_{L^\infty(\kappa_{\mathbf{x}})} \\
&\geq 1 - \sum_{\kappa_{\mathbf{x}} \in \mathcal{T}_h^{\mathbf{x}*}} |\kappa_{\mathbf{x}}| \, C h_{\mathbf{x}}^2 \, |\zeta_\varepsilon(\mathbf{x}-\,.\,)|_{W^{2,\infty}(\kappa_{\mathbf{x}})} \\
&\geq 1 - C\,|\Omega^*|\,h_{\mathbf{x}}^2\,|\zeta_\varepsilon|_{W^{2,\infty}(\mathbb{R}^d)} \geq 1 - C(\varepsilon) h_{\mathbf{x}}^2 \geq \tilde{C}(\varepsilon) > 0,
\end{aligned} \tag{2.41}$$

for $h_{\mathbf{x}}$ small enough. Therefore, $\|c_{\mathcal{J}}\|_{L^\infty(\Omega)}$ is bounded from above by $\tilde{C}(\varepsilon)^{-1}$. Combining this result with

$$\begin{aligned}
|\partial_{\mathbf{x}_i} c_{\mathcal{J}}(\mathbf{x})| &\leq \left[\int_{\Omega^*} \mathcal{I}_h^{\mathbf{y}}\{\zeta_\varepsilon(\mathbf{x}-\mathbf{y})\}\,\mathrm{d}\mathbf{y}\right]^{-2} \left|\partial_{\mathbf{x}_i} \int_{\Omega^*} \mathcal{I}_h^{\mathbf{y}}\{\zeta_\varepsilon(\mathbf{x}-\mathbf{y})\}\,\mathrm{d}\mathbf{y}\right| \\
&= c_{\mathcal{J}}^2(\mathbf{x}) \left|\int_{\Omega^*} \sum_{j=1}^{\dim U_h^{\mathbf{x}*}} \partial_{\mathbf{x}_i} \zeta_\varepsilon(\mathbf{x}-\mathbf{y}_j) \chi_{h,j}^{\mathbf{y}}(\mathbf{y})\,\mathrm{d}\mathbf{y}\right| \leq c_{\mathcal{J}}^2(\mathbf{x})\,|\Omega^*|\,\|\partial_{\mathbf{x}_i}\zeta_\varepsilon\|_{L^\infty(\mathbb{R}^d)}
\end{aligned} \tag{2.42}$$

for all $i = 1, \dots, d$, where $\{\chi_{h,j}^{\mathbf{y}}\}_{j=1,\dots,\dim U_h^{\mathbf{x}*}}$ form a dual basis to the nodes $\{\mathbf{y}_j\}_{j=1,\dots,\dim U_h^{\mathbf{x}*}}$ with $\sum_{j=1}^{\dim U_h^{\mathbf{x}*}} \chi_{h,j}^{\mathbf{y}}(\mathbf{y}) \equiv 1$, yields the result. □

The mollifier $\mathcal{J}_\varepsilon$ was constructed as convolution with a $W^{2,\infty}(\mathbb{R}^d)$-kernel, which allowed for the estimate (1.9f). In the discrete setting, the interpolation operator $\mathcal{I}_h^{\mathbf{y}}$ decreases the regularity. However, we still have an analog to (1.9f) for the $W^{1,\infty}(\Omega)$-norm of the discrete mollifier.

Lemma 2.10. *Let $\{\mathcal{T}_h^{\mathbf{x}*}\}_{h>0}$ and $\{\mathcal{T}_h^{\mathbf{q}}\}_{h>0}$ satisfy (S1)–(S3) and let $c_{\mathcal{J}}$ be the weight function defined* via (2.39)*. Then, the discrete mollifier $\mathcal{J}_{\varepsilon,h}$ defined in* (2.38) *satisfies*

$$\|\mathcal{J}_{\varepsilon,h}\{f\}\|_{W^{1,\infty}(\Omega)} \leq C(\varepsilon)\,\|f\|_{L^1(\Omega)} \qquad \textit{for all } f \in L^1(\Omega), \tag{2.43}$$

with some $C(\varepsilon) > 0$ which is independent of $h_{\mathbf{x}}$.

Proof. We use the result of Lemma 2.9 and the regularity of ζ_ε to compute

$$\begin{aligned}\|\mathcal{J}_{\varepsilon,h}\{f\}\|_{L^\infty(\Omega)} &\leq \sup_{\mathbf{x}\in\Omega}\left(c_{\mathcal{J}}(\mathbf{x})\int_\Omega |\mathcal{I}_h^{\mathbf{y}}\{\zeta_\varepsilon(\mathbf{x}-\mathbf{y})\}|\,|f(\mathbf{y})|\;\mathrm{d}\mathbf{y}\right)\\ &\leq C\,\|\zeta_\varepsilon\|_{L^\infty(\mathbb{R}^d)}\int_\Omega |f(\mathbf{y})|\;\mathrm{d}\mathbf{y} \leq C(\varepsilon)\,\|f\|_{L^1(\Omega)}.\end{aligned} \tag{2.44}$$

Applying the product rule on the derivative of $\mathcal{J}_{\varepsilon,h}\{f\}$ yields

$$\begin{aligned}|\partial_{\mathbf{x}_i}\mathcal{J}_{\varepsilon,h}\{f\}| \leq{}& |\partial_{\mathbf{x}_i}c_{\mathcal{J}}(\mathbf{x})|\int_\Omega |\mathcal{I}_h^{\mathbf{y}}\{\zeta_\varepsilon(\mathbf{x}-\mathbf{y})\}|\,|f(\mathbf{y})|\;\mathrm{d}\mathbf{y}\\ &+|c_{\mathcal{J}}(\mathbf{x})|\int_\Omega |\partial_{\mathbf{x}_i}\mathcal{I}_h^{\mathbf{y}}\{\zeta_\varepsilon(\mathbf{x}-\mathbf{y})\}|\,|f(\mathbf{y})|\;\mathrm{d}\mathbf{y}.\end{aligned} \tag{2.45}$$

The first summand is bounded from above by $C(\varepsilon)\,\|f\|_{L^1(\Omega)}$ due to Lemma 2.9 and the regularity of ζ_ε. Concerning the second summand, we have $\|c_{\mathcal{J}}\|_{L^\infty(\Omega)} \leq C(\varepsilon)$ and may apply the mean value theorem to obtain the desired result. ◻

With the following lemma, we prove the convergence of $\mathcal{J}_{\varepsilon,h}\{f\}$ towards $\mathcal{J}_\varepsilon\{f\}$ for $f\in L^1(\Omega)$.

Lemma 2.11. *Let be $\mathcal{J}_\varepsilon$ be the mollifier defined in (1.8) and $\mathcal{J}_{\varepsilon,h}$ the finite element version of $\mathcal{J}_\varepsilon$ which is defined in (2.38). Furthermore, let $\{\mathcal{T}_h^{\mathbf{x}*}\}_{h>0}$ and $\{\mathcal{T}_h^{\mathbf{q}}\}_{h>0}$ satisfy (S1)–(S3) and let $c_{\mathcal{J}}$ be the weight function defined* via *(2.39). Then, there exists $C>0$ independent of $h_{\mathbf{x}}$ such that*

$$\|\mathcal{J}_{\varepsilon,h}\{f\}-\mathcal{J}_\varepsilon\{f\}\|_{W^{1,\infty}(\Omega)} \leq C(\varepsilon)h_{\mathbf{x}}\,\|f\|_{L^1(\Omega)} \tag{2.46}$$

for $f\in L^1(\Omega)$ and $h_{\mathbf{x}}$ small enough.

Proof. We start with the estimate

$$\begin{aligned}\|\mathcal{J}_{\varepsilon,h}\{f\}-\mathcal{J}_\varepsilon\{f\}\|_{W^{1,\infty}(\Omega)} \leq{}& \left\|c_{\mathcal{J}}(.)\int_\Omega (\mathcal{I}_h^{\mathbf{y}}\{\zeta_\varepsilon(\,.\,-\mathbf{y})\}-\zeta_\varepsilon(\,.\,-\mathbf{y}))f(\mathbf{y})\;\mathrm{d}\mathbf{y}\right\|_{W^{1,\infty}(\Omega)}\\ &+\left\|(1-c_{\mathcal{J}}(.))\int_\Omega \zeta_\varepsilon(\,.\,-\mathbf{y})f(\mathbf{y})\;\mathrm{d}\mathbf{y}\right\|_{W^{1,\infty}(\Omega)} =: I+II.\end{aligned} \tag{2.47}$$

Applying the product rule on I yields

$$\begin{aligned}I \leq{}& \|c_{\mathcal{J}}\|_{W^{1,\infty}(\Omega)}\left\|\int_\Omega (\mathcal{I}_h^{\mathbf{y}}\{\zeta_\varepsilon(\,.\,-\mathbf{y})\}-\zeta_\varepsilon(\,.\,-\mathbf{y}))f(\mathbf{y})\;\mathrm{d}\mathbf{y}\right\|_{L^\infty(\Omega)}\\ &+\|c_{\mathcal{J}}\|_{L^\infty(\Omega)}\max_{i=1,..,d}\left\|\int_\Omega \partial_{\mathbf{x}_i}(\mathcal{I}_h^{\mathbf{y}}\{\zeta_\varepsilon(\,.\,-\mathbf{y})\}-\zeta_\varepsilon(\,.\,-\mathbf{y}))f(\mathbf{y})\;\mathrm{d}\mathbf{y}\right\|_{L^\infty(\Omega)}.\end{aligned} \tag{2.48}$$

Lemma 2.9 provides $\|c_{\mathcal{J}}\|_{W^{1,\infty}(\Omega)} \leq C(\varepsilon)$. To control the second factors in the terms on the right-hand side of (2.48), we denote the dual basis to the nodes $\{\mathbf{y}_j\}_{j=1,\ldots,\dim U_h^{\mathbf{x}*}}$ by $\left\{\chi_{h,j}^{\mathbf{y}}\right\}_{j=1,\ldots,\dim U_h^{\mathbf{x}*}}$. Noting $\sum_{j=1}^{\dim U_h^{\mathbf{x}*}}\chi_{h,j}^{\mathbf{y}}(\mathbf{y})\equiv 1$ for $\mathbf{y}\in\Omega$, we compute for $\mathbf{x}\in\Omega$

$$\begin{aligned}\sup_{\mathbf{y}\in\Omega}|(\mathcal{I}_h^{\mathbf{y}}\{\zeta_\varepsilon(\mathbf{x}-\mathbf{y})\}-\zeta_\varepsilon(\mathbf{x}-\mathbf{y}))| &= \sup_{\mathbf{y}\in\Omega}\left|\sum_{j=1}^{\dim U_h^{\mathbf{x}}}(\zeta_\varepsilon(\mathbf{x}-\mathbf{y}_j)-\zeta_\varepsilon(\mathbf{x}-\mathbf{y}))\chi_{h,j}^{\mathbf{y}}(\mathbf{y})\right|\\ &\leq \sup_{\mathbf{y}\in\Omega}\max_{j\,:\,\mathbf{y}\in\operatorname{supp}\chi_{h,j}^{\mathbf{y}}}|\zeta_\varepsilon(\mathbf{x}-\mathbf{y}_j)-\zeta_\varepsilon(\mathbf{x}-\mathbf{y})| \leq C(\varepsilon)h_{\mathbf{x}},\end{aligned} \tag{2.49}$$

where we used $0 \leq \chi^{\mathbf{y}}_{h,j} \leq 1$ for $j = 1, \ldots, \dim U^{\mathbf{x}}_h$, $|\zeta_\varepsilon(\tilde{\mathbf{x}}) - \zeta_\varepsilon(\tilde{\mathbf{y}})| \leq C(\varepsilon)\,|\tilde{\mathbf{x}} - \tilde{\mathbf{y}}|$ for $\tilde{\mathbf{x}}, \tilde{\mathbf{y}} \in \Omega$ (as $\zeta_\varepsilon \in W^{2,\infty}(\mathbb{R}^d)$), and $\max_{j=1,\ldots,\dim U^{\mathbf{x}}_h} \operatorname{diam}\left(\operatorname{supp} \chi^{\mathbf{y}}_{h,j}\right) \leq C h_{\mathbf{x}}$. Similarly, we compute for $i = 1, \ldots, d$ and $\mathbf{x} \in \Omega$

$$\sup_{\mathbf{y}\in\Omega} \left|\partial_{\mathbf{x}_i}\left(\mathcal{I}^{\mathbf{y}}_h\{\zeta_\varepsilon(\mathbf{x}-\mathbf{y})\} - \zeta_\varepsilon(\mathbf{x}-\mathbf{y})\right)\right| \leq C(\varepsilon) h_{\mathbf{x}}. \tag{2.50}$$

Combining (2.48) with Lemma 2.9, (2.49), and (2.50) yields

$$I \leq C(\varepsilon) h_{\mathbf{x}} \left\|f\right\|_{L^1(\Omega)}. \tag{2.51}$$

To control II, we compute

$$II \leq C \left\|1 - c_{\mathcal{J}}(.)\right\|_{W^{1,\infty}(\Omega)} \left\|\mathcal{J}_\varepsilon\{f\}\right\|_{W^{1,\infty}(\Omega)}. \tag{2.52}$$

As (1.9f) yields $\left\|\mathcal{J}_\varepsilon\{f\}\right\|_{W^{1,\infty}(\Omega)} \leq \left\|\mathcal{J}_\varepsilon\{f\}\right\|_{W^{2,\infty}(\Omega)} \leq C(\varepsilon) \left\|f\right\|_{L^1(\Omega)}$, it remains to show that $\left\|1 - c_{\mathcal{J}}(.)\right\|_{W^{1,\infty}(\Omega)} \leq h_{\mathbf{x}} C(\varepsilon)$. From (2.41), we have $\int_{\Omega^*} \mathcal{I}^{\mathbf{y}}_h\{\zeta_\varepsilon(\mathbf{x}-\mathbf{y})\}\,\mathrm{d}\mathbf{y} \geq 1 - C(\varepsilon) h_{\mathbf{x}}^2$ for $\mathbf{x} \in \Omega$. Analogously, we may compute $\int_{\Omega^*} \mathcal{I}^{\mathbf{y}}_h\{\zeta_\varepsilon(\mathbf{x}-\mathbf{y})\}\,\mathrm{d}\mathbf{y} \leq 1 + C(\varepsilon) h_{\mathbf{x}}^2$. Hence, we have for $h_{\mathbf{x}}$ small enough

$$\left\|1 - c_{\mathcal{J}}(.)\right\|_{L^\infty(\Omega)} = \left\|\frac{\int_{\Omega^*} \mathcal{I}^{\mathbf{y}}_h\{\zeta_\varepsilon(\,.\,-\mathbf{y})\}\,\mathrm{d}\mathbf{y} - 1}{\int_{\Omega^*} \mathcal{I}^{\mathbf{y}}_h\{\zeta_\varepsilon(\,.\,-\mathbf{y})\}\,\mathrm{d}\mathbf{y}}\right\|_{L^\infty(\Omega)} \leq \frac{C(\varepsilon) h_{\mathbf{x}}^2}{1 - C(\varepsilon) h_{\mathbf{x}}^2} \leq C(\varepsilon) h_{\mathbf{x}}^2. \tag{2.53}$$

Noting $\int_{\Omega^*} \zeta_\varepsilon(\mathbf{x}-\mathbf{y})\,\mathrm{d}\mathbf{y} = 1$ for all $\mathbf{x} \in \Omega$ and reusing the idea of (2.50), we obtain

$$\begin{aligned} &\left\|\partial_{\mathbf{x}_i}(1 - c_{\mathcal{J}}(.))\right\|_{L^\infty(\Omega)} \\ &\quad\leq \left\|c_{\mathcal{J}}\right\|^2_{L^\infty(\Omega)} |\Omega^*| \sup_{\mathbf{y}\in\Omega^*,\,\mathbf{x}\in\Omega} \left|\partial_{\mathbf{x}_i}\left(\mathcal{I}^{\mathbf{y}}_h\{\zeta_\varepsilon(\mathbf{x}-\mathbf{y})\} - \zeta_\varepsilon(\mathbf{x}-\mathbf{y})\right)\right| \leq C(\varepsilon) h_{\mathbf{x}} \end{aligned} \tag{2.54}$$

for $i = 1, \ldots, d$, which completes the proof. □

By applying $\mathcal{J}_{\varepsilon,h}$ on each component of a vector-valued function $\mathbf{f} \in \boldsymbol{L}^1(\Omega)$, we obtain a discrete version of $\boldsymbol{\mathcal{J}}_\varepsilon$ denoted by $\boldsymbol{\mathcal{J}}_{\varepsilon,h}$ which satisfies a vector-valued version of Lemma 2.10 and Lemma 2.11. As we will not consider the limit $\varepsilon \searrow 0$, we suppress the dependence of constants on ε and denote the discrete mollifiers by $\mathcal{J}_h$ and $\boldsymbol{\mathcal{J}}_h$.

3. A stable, discrete scheme

In this section, we introduce a stable, fully discrete finite element scheme allowing to approximate the solutions of (1.5) in the case of different mass densities and establishing an *a priori* stability result for possible solutions. An existence result may easily be deduced using Brouwer's fixed point theorem.

As we show in the subsequent sections, the presented scheme is convergent in the case of equal mass densities.

As the mass density function ρ depends affine linearly on the phase-field parameter ϕ, it is positive as long as ϕ stays in the interval $(-\mathfrak{At}^{-1}, \mathfrak{At}^{-1})$ with $\mathfrak{At} := \left|\frac{\tilde{\rho}_2 - \tilde{\rho}_1}{\tilde{\rho}_2 + \tilde{\rho}_1}\right| < 1$ denoting the Atwood number. Since there is no mechanism guaranteeing that ϕ stays in this region, we introduce a regularized mass density function (*cf.* [15]). Picking some parameter $\overline{\phi} \in (1, \mathfrak{At}^{-1})$, we approximate the mass density of the two-phase flow by a smooth, monotonously increasing (or decreasing, respectively), strictly positive function $\overline{\rho}$ satisfying

$$\overline{\rho}(\phi)\big|_{(-\overline{\phi},+\overline{\phi})} = \tfrac{\tilde{\rho}_2 + \tilde{\rho}_1}{2} - \tfrac{\tilde{\rho}_2 - \tilde{\rho}_1}{2}\phi, \tag{3.1a}$$

$$\overline{\rho}(\phi)\big|_{(-\infty,-\overline{\phi}]} \equiv \text{const}, \qquad \overline{\rho}(\phi)\big|_{[+\overline{\phi},+\infty)} \equiv \text{const}. \tag{3.1b}$$

As the original mass density ρ depends affine linearly on the phase-field parameter, we introduce $\frac{\delta\overline{\rho}}{\delta\phi} := \frac{\tilde{\rho}_2 - \tilde{\rho}_1}{2}$ as an approximation of the derivative of $\overline{\rho}$ (*cf.* [15]).

Similarly to [16], we make the following assumption on the general structure of the double-well potential W.

(W1) $W \in C^1(\mathbb{R};\mathbb{R}_0^+)$ with $\left|W(s)s^{-3}\right| \to \infty$ for $|s| \to \infty$ such that W' is piecewise C^1 and that its derivatives have at most quadratic growth for $|s| \to \infty$.

We allow for different discrete approximations of the derivative W' which we denote by $W_h' : \mathbb{R}^2 \to \mathbb{R}_0^+$. Thereby, we will assume that the following conditions hold true.

(W2) There is a positive constant C such that for all $a, b \in \mathbb{R}$

$$|W_h'(a,b)| \leq C\Big(1 + |a|^3 + |b|^3\Big).$$

(W3) $W_h'(a,b)(a-b) \geq W(a) - W(b)$ for all $a, b \in \mathbb{R}$.
(W4) $W_h'(a,a) = W'(a)$ for all $a \in \mathbb{R}$.
(W5) There is a positive constant C, such that for all $a, b, c \in \mathbb{R}$

$$|W_h'(a,b) - W_h'(b,c)| \leq C(a^2 + b^2 + c^2)(|a-b| + |b-c|).$$

Remark 3.1. In the simulations presented in Section 6, we will consider a polynomial double-well potential with penalty terms which reads

$$W(\phi) = \tfrac{1}{4}(1-\phi^2)^2 + \tfrac{1}{\delta'}\max\{|\phi| - 1, 0\}^2 \tag{3.2}$$

with some penalty parameter $0 < \delta' \ll 1$. This approach often suffices to confine the phase-field parameter to an interval close to the physical meaningful interval $[-1, +1]$. The double-well potential defined in (3.2) satisfies (W1). Suitable choices for $W_h'(\,.\,,\,.\,)$ satisfying (W2)–(W5) are *e.g.* discretizations using a difference quotient or the classical convex-concave splitting (*cf.* [16]).

For the approximation of β', we use a difference quotient, *i.e.* we define β'_{DQ} by

$$\beta'_{DQ}(a,b) := \begin{cases} \frac{\beta(a)-\beta(b)}{a-b} & \text{if } a \neq b, \\ \beta'(a) & \text{if } a = b, \end{cases} \tag{3.3}$$

for all $a, b \in \mathbb{R}$, which immediately yields $\beta'_{DQ}(a,b)(a-b) = \beta(a) - \beta(b)$ for all $a, b \in \mathbb{R}$.

Denoting the backward difference quotient in time by ∂_τ^- and using the above definitions, we introduce the following discrete scheme. Given $\phi_h^{n-1} \in U_h^{\mathbf{x}}$, $\hat{\psi}_h^{n-1} \in \hat{X}_h$, and $\mathbf{u}_h^{n-1} \in \boldsymbol{W}_{h,\mathrm{div}}$, we compute a quadruple $\left\{\phi_h^n,\, \mu_{\phi,h}^n,\, \hat{\psi}_h^n, \mathbf{u}_h^n\right\} \in U_h^{\mathbf{x}} \times U_h^{\mathbf{x}} \times \hat{X}_h \times \boldsymbol{W}_{h,\mathrm{div}}$ solving

$$\begin{aligned} &\int_\Omega \mathcal{I}_h^{\mathbf{x}}\{\partial_\tau^- \phi_h^n \theta_h^{\mathbf{x}}\} - \int_\Omega \phi_h^{n-1}\mathbf{u}_h^{n-1}\cdot\nabla_{\mathbf{x}}\theta_h^{\mathbf{x}} \\ &\quad + \tau\int_\Omega \left(\min\overline{\rho}_h^{n-1}\right)^{-1}\left|\phi_h^{n-1}\right|^2 \nabla_{\mathbf{x}}\mu_{\phi,h}^n\cdot\nabla_{\mathbf{x}}\theta_h^{\mathbf{x}} + \int_\Omega \nabla_{\mathbf{x}}\mu_{\phi,h}^n\cdot\nabla_{\mathbf{x}}\theta_h^{\mathbf{x}} = 0 \qquad \forall \theta_h^{\mathbf{x}} \in U_h^{\mathbf{x}}, \end{aligned} \tag{3.4a}$$

$$\begin{aligned} \int_\Omega \mathcal{I}_h^{\mathbf{x}}\{\mu_{\phi,h}^n\theta_h^{\mathbf{x}}\} &= \int_\Omega \mathcal{I}_h^{\mathbf{x}}\{W_h'(\phi_h^n,\phi_h^{n-1})\theta_h^{\mathbf{x}}\} + \int_\Omega (\vartheta\nabla_{\mathbf{x}}\phi_h^n + (1-\vartheta)\nabla_{\mathbf{x}}\phi_h^{n-1})\cdot\nabla_{\mathbf{x}}\theta_h^{\mathbf{x}} \\ &\quad + \int_\Omega \mathcal{I}_h^{\mathbf{x}}\Big\{\mathcal{J}_h\{\mathcal{I}_h^{\mathbf{x}}\{\beta'_{DQ}(\phi_h^n,\phi_h^{n-1})\theta_h^{\mathbf{x}}\}\}\int_{\mathfrak{D}}(M_h + \mathfrak{m})\hat{\psi}_h^{n-1}\Big\} \qquad \forall \theta_h^{\mathbf{x}} \in U_h^{\mathbf{x}}, \end{aligned} \tag{3.4b}$$

$$
\begin{aligned}
\int_{\Omega\times\mathfrak{D}} (M_h+\mathfrak{m})\mathcal{I}_h^{\mathbf{xq}}\Big\{\partial_\tau^-\hat{\psi}_h^n\theta_h\Big\} - \int_{\Omega\times\mathfrak{D}} M_h\mathbf{u}_h^n\cdot\mathcal{I}_h^{\mathbf{q}}\Big\{\Lambda_\nu^{\mathbf{x}}[\hat{\psi}_{\mathrm{h}}^{\mathrm{n}}]\nabla_{\mathbf{x}}\theta_h\Big\} \\
-\int_{\Omega\times\mathfrak{D}} (\nabla_{\mathbf{x}}\mathcal{I}_h^{\mathbf{x}}\{\boldsymbol{\mathcal{J}}_h\{\mathbf{u}_h^n\}\}\cdot\mathcal{I}_h^{\mathbf{q}}\{\mathbf{q}M_h\})\cdot\mathcal{I}_h^{\mathbf{x}}\Big\{\Xi_\nu^{\mathbf{q}}[\hat{\psi}_{\mathrm{h}}^{\mathrm{n}}]\nabla_{\mathbf{q}}\theta_h\Big\} \\
+(1-\gamma)\int_{\Omega\times\mathfrak{D}} c_{\mathbf{x}}M_h\mathcal{I}_h^{\mathbf{q}}\Big\{\Big(\Xi_\nu^{\mathbf{x}}[\hat{\psi}_{\mathrm{h}}^{\mathrm{n}}]\nabla_{\mathbf{x}}\mathcal{I}_h^{\mathbf{xq}}\Big\{g_\nu'(\hat{\psi}_h^n)+\mathcal{J}_h\{\mathcal{I}_h^{\mathbf{x}}\{\beta(\phi_h^n)\}\}\Big\}\Big)\cdot\nabla_{\mathbf{x}}\theta_h\Big\} \\
+\gamma\int_{\Omega\times\mathfrak{D}} c_{\mathbf{x}}M_h\mathcal{I}_h^{\mathbf{q}}\Big\{\Big(\Lambda_\nu^{\mathbf{x}}[\hat{\psi}_{\mathrm{h}}^{\mathrm{n}}]\nabla_{\mathbf{x}}\mathcal{I}_h^{\mathbf{xq}}\Big\{g_\nu'(\hat{\psi}_h^n)+\mathcal{J}_h\{\mathcal{I}_h^{\mathbf{x}}\{\beta(\phi_h^n)\}\}\Big\}\Big)\cdot\nabla_{\mathbf{x}}\theta_h\Big\} \\
+\int_{\Omega\times\mathfrak{D}} c_{\mathbf{q}}M_h\mathcal{I}_h^{\mathbf{x}}\Big\{\nabla_{\mathbf{q}}\hat{\psi}_h^n\cdot\nabla_{\mathbf{q}}\theta_h\Big\} = 0 \\
\forall\theta_h\in\hat{X}_h,
\end{aligned}
\tag{3.4c}
$$

$$
\begin{aligned}
\int_\Omega \tfrac12\big(\overline{\rho}_h^n+\overline{\rho}_h^{n-1}\big)\partial_\tau^-\mathbf{u}_h^n\cdot\mathbf{w}_h + \tfrac12\int_\Omega \partial_\tau^-\overline{\rho}_h^n\mathbf{u}_h^{n-1}\cdot\mathbf{w}_h \\
+\tfrac12\int_\Omega \overline{\rho}_h^n\Big((\nabla_{\mathbf{x}}\mathbf{u}_h^n)^T\cdot\mathbf{w}_h\Big)\cdot\mathbf{u}_h^{n-1} - \tfrac12\int_\Omega \overline{\rho}_h^n\Big((\nabla_{\mathbf{x}}\mathbf{w}_h)^T\cdot\mathbf{u}_h^n\Big)\cdot\mathbf{u}_h^{n-1} \\
+\tfrac12\int_\Omega \tfrac{\delta\overline{\rho}}{\delta\phi}\Big((\nabla_{\mathbf{x}}\mathbf{u}_h^n)^T\cdot\mathbf{w}_h\Big)\cdot\nabla_{\mathbf{x}}\mu_{\phi,h}^n - \tfrac12\int_\Omega \tfrac{\delta\overline{\rho}}{\delta\phi}\Big((\nabla_{\mathbf{x}}\mathbf{w}_h)^T\cdot\mathbf{u}_h^n\Big)\cdot\nabla_{\mathbf{x}}\mu_{\phi,h}^n \\
+\int_\Omega 2\mathcal{I}_h^{\mathbf{x}}\{\eta(\phi_h^n)\}\mathbf{D}\mathbf{u}_h^n:\mathbf{D}\mathbf{w}_h = -\int_\Omega \phi_h^{n-1}\nabla_{\mathbf{x}}\mu_{\phi,h}^n\cdot\mathbf{w}_h \\
-\int_{\Omega\times\mathfrak{D}} M_h\mathbf{w}_h\cdot\mathcal{I}_h^{\mathbf{q}}\Big\{\Lambda_\nu^{\mathbf{x}}[\hat{\psi}_{\mathrm{h}}^{\mathrm{n}}]\nabla_{\mathbf{x}}\mathcal{I}_h^{\mathbf{xq}}\Big\{g_\nu'(\hat{\psi}_h^n)+\mathcal{J}_h\{\mathcal{I}_h^{\mathbf{x}}\{\beta(\phi_h^n)\}\}\Big\}\Big\} \\
-\int_{\Omega\times\mathfrak{D}} (\nabla_{\mathbf{x}}\mathcal{I}_h^{\mathbf{x}}\{\boldsymbol{\mathcal{J}}_h\{\mathbf{w}_h\}\}\cdot\mathcal{I}_h^{\mathbf{q}}\{\mathbf{q}M_h\})\cdot\nabla_{\mathbf{q}}\hat{\psi}_h^n \\
\forall\mathbf{w}_h\in\boldsymbol{W}_{h,\mathrm{div}},
\end{aligned}
\tag{3.4d}
$$

with some fixed $\vartheta\in(0.5,1]$, $\gamma\in(0,1)$ and some regularization parameter $\mathfrak{m}>0$. To simplify the notation, we used the abbreviation $\overline{\rho}_h^n := \mathcal{I}_h^{\mathbf{x}}\{\overline{\rho}(\phi_h^n)\}$. For better readability, we introduce the discrete version of the chemical potential of the polymer densities as

$$
\mu_{\psi,h,\nu}^n := \mathcal{I}_h^{\mathbf{xq}}\Big\{g_\nu'(\hat{\psi}_h^n)+\mathcal{J}_h\{\beta(\phi_h^n)\}\Big\}\in\hat{X}_h \tag{3.5}
$$

for $n=1,\dots,N$.

Remark 3.2. As (3.4a) and (3.4b) do not depend on $\hat{\psi}_h^n$ and $\mathbf{u}_h^n$, it is possible to compute ϕ_h^n and $\mu_{\phi,h}^n$ separately before advancing to (3.4c) and (3.4d). To maintain stability, the third term in (3.4a) was added. Similar splitting ideas have previously been used in [3], [20], and [26] for a model of magnetohydrodynamics and for diffuse interface models for multi-phase and two-phase flows, respectively. For the case of a pure two-phase flow with different mass densities without any additional species, convergence of this splitting approach has been established in [16].

Remark 3.3. For time-discretizations of $\int_\Omega \nabla_{\mathbf{x}}\phi\cdot\nabla_{\mathbf{x}}\theta^{\mathbf{x}}$, we have chosen a compromise between

$$
\nabla_{\mathbf{x}}\phi_h^n\cdot\nabla_{\mathbf{x}}\partial_\tau^-\phi_h^n = \tfrac{1}{2\tau}\left|\nabla_{\mathbf{x}}\phi_h^n\right|^2 + \tfrac{1}{2\tau}\left|\nabla_{\mathbf{x}}\phi_h^n-\nabla_{\mathbf{x}}\phi_h^{n-1}\right|^2 - \tfrac{1}{2\tau}\left|\nabla_{\mathbf{x}}\phi_h^{n-1}\right|^2
$$

and

$$
\tfrac12\big(\nabla_{\mathbf{x}}\phi_h^n+\nabla_{\mathbf{x}}\phi_h^{n-1}\big)\cdot\nabla_{\mathbf{x}}\partial_\tau^-\phi_h^n = \tfrac{1}{2\tau}\left|\nabla_{\mathbf{x}}\phi_h^n\right|^2 - \tfrac{1}{2\tau}\left|\nabla_{\mathbf{x}}\phi_h^{n-1}\right|^2,
$$

to reduce the numerical dissipation of the scheme (*cf.* Sect. 4.2 in [25]). Although the scheme is still stable for $\vartheta = 0.5$, the presented proof of convergence requires $\vartheta > 0.5$, as we need to control $\tau^{-1}\sum_{k=1}^{n}\int_{\Omega}\left|\nabla_{\mathbf{x}}\phi_h^k - \nabla_{\mathbf{x}}\phi_h^{k-1}\right|^2$ (*cf.* Lem. 5.1).

Remark 3.4. The choice of $\Lambda_\nu^{\mathbf{x}}[\hat{\psi}_{\mathrm{h}}^{\mathrm{n}}]$ as an approximation for $\hat{\psi}$ in the $\mathbf{x}$-convective term in (3.4c) allows to establish improved regularity results for the scaled configurational density $\hat{\psi}$ (*cf.* Lem. 4.5). Unfortunately, this enforces the application of $\Lambda_\nu^{\mathbf{x}}[\hat{\psi}_{\mathrm{h}}^{\mathrm{n}}]$ on the right-hand side of (3.4d). As a result, we will need control over

$$\int_{\Omega\times\mathfrak{D}} M_h \mathcal{I}_h^{\mathbf{q}}\Big\{\Big(\Lambda_\nu^{\mathbf{x}}[\hat{\psi}_{\mathrm{h}}^{\mathrm{n}}]\nabla_{\mathbf{x}}\mu_{\psi,h,\nu}^n\Big)\cdot\nabla_{\mathbf{x}}\mu_{\psi,h,\nu}^n\Big\}$$

to prove compactness in time for the velocity field (*cf.* Lem. 4.8). Therefore, the approximation of $\hat{\psi}$ by $(1-\gamma)\Xi_\nu^{\mathbf{x}}[\hat{\psi}_{\mathrm{h}}^{\mathrm{n}}] + \gamma\Lambda_\nu^{\mathbf{x}}[\hat{\psi}_{\mathrm{h}}^{\mathrm{n}}]$ in the fourth and fifth term in (3.4c) is necessary.

Replacing $\Lambda_\nu^{\mathbf{x}}[\hat{\psi}_{\mathrm{h}}^{\mathrm{n}}]$ by $\Xi_\nu^{\mathbf{x}}[\hat{\psi}_{\mathrm{h}}^{\mathrm{n}}]$ also results in a stable scheme, but by now there is no technique at hand to improve the regularity of $\hat{\psi}$ and therefore to prove convergence of this version of (3.4).

As M_h vanishes on the majority of $\mathfrak{D}\backslash D$ for $h_{\mathbf{q}}$ small enough, we introduced the regularization parameter $\mathfrak{m}$ to prevent definition gaps in (3.4c).

Remark 3.5. By choosing weakly solenoidal test functions in (3.4d), we eliminated the pressure term, which is more convenient for the analysis of the scheme. As shown in ([14], Chap. 1, Sect. 4), the formulation in (3.4d) is equivalent to the straightforward approach using $\mathbf{w}\in\boldsymbol{W}_h$ and the pressure term $-\int_{\Omega} p_h^n \operatorname{div}_{\mathbf{x}}\mathbf{w}$, as $\boldsymbol{W}_h$ and S_h satisfy the inf-sup condition (*cf.* (TH1)).

After passing to the limit in Theorem 5.2, one may recover the pressure in a very weak sense following the procedure discussed in [28].

Remark 3.6. In the third term on the left-hand-side of (3.4c) and in the third term on the right-hand side of (3.4d) we used $\mathcal{I}_h^{\mathbf{q}}\{\mathbf{q}M_h\}$. At this point, the interpolation operator is neither necessary for stability nor for convergence, but it reduces the costs of an exact integration of these terms.

Testing (3.4a) and (3.4c) by 1 shows that solutions to (3.4), if they exists, satisfy the conservation properties

$$\int_{\Omega}\phi_h^n = \int_{\Omega}\phi_h^{n-1} \quad\text{and}\quad \int_{\Omega\times\mathfrak{D}}(M_h+\mathfrak{m})\hat{\psi}_h^n = \int_{\Omega\times\mathfrak{D}}(M_h+\mathfrak{m})\hat{\psi}_h^{n-1} \tag{3.6}$$

for all $n\in\{1,\ldots,N\}$.

As shown in the following lemma, the scheme presented in (3.4) is consistent with thermodynamics in the sense that the discrete version of the energy

$$\begin{aligned}\mathcal{E}_h(\phi_h^n,\hat{\psi}_h^n,\mathbf{u}_h^n) :=& \tfrac{1}{2}\int_{\Omega}|\nabla_{\mathbf{x}}\phi_h^n|^2 + \int_{\Omega}\mathcal{I}_h^{\mathbf{x}}\{W(\phi_h^n)\} + \int_{\Omega\times\mathfrak{D}}(M_h+\mathfrak{m})\mathcal{I}_h^{\mathbf{xq}}\Big\{g_\nu(\hat{\psi}_h^n)\Big\} \\ &+ \int_{\Omega\times\mathfrak{D}}(M_h+\mathfrak{m})\mathcal{I}_h^{\mathbf{x}}\Big\{\hat{\psi}_h^n\mathcal{J}_h\{\mathcal{I}_h^{\mathbf{x}}\{\beta(\phi_h^n)\}\}\Big\} + \tfrac{1}{2}\int_{\Omega}\overline{\rho}_h^n|\mathbf{u}_h^n|^2\end{aligned} \tag{3.7}$$

is not increasing. In particular, testing (3.4a) by $\tau\mu_{\phi,h}^n$, (3.4b) by $\tau\partial_\tau^-\phi_h^n$, (3.4c) by $\tau\mu_{\psi,h,\nu}^n$, and (3.4d) by $\tau\mathbf{u}_h^n$ yields the following result (*cf.* [25]).

Lemma 3.7. *Let W and W_h' satisfy (W1)–(W5). Furthermore, let (T) and (S1)–(S3) hold true. Assuming $\eta\geq c>0$ and $\beta\geq 0$, a solution $(\phi_h^n,\,\mu_{\phi,h}^n,\,\hat{\psi}_h^n,\mathbf{u}_h^n)\in U_h^{\mathbf{x}}\times U_h^{\mathbf{x}}\times\hat{X}_h\times\boldsymbol{W}_{h,\mathrm{div}}$ to (3.4), if exists, satisfies for $n=1,\ldots,N$*

$$\begin{aligned}
&\mathcal{E}_h(\phi_h^n,\hat{\psi}_h^n,\mathbf{u}_h^n)+\tfrac{2\vartheta-1}{2}\int_\Omega\left|\nabla_{\mathbf{x}}\phi_h^n-\nabla_{\mathbf{x}}\phi_h^{n-1}\right|^2+\tfrac14\int_\Omega\overline{\rho}_h^{n-1}\left|\mathbf{u}_h^n-\mathbf{u}_h^{n-1}\right|^2\\
&\quad+\tau\int_\Omega\left|\nabla_{\mathbf{x}}\mu_{\phi,h}^n\right|^2+\tau\int_\Omega 2\mathcal{I}_h^{\mathbf{x}}\{\eta(\phi_h^n)\}\left|\mathbf{D}\mathbf{u}_h^n\right|^2\\
&\quad+\tau\int_{\Omega\times\mathfrak{D}}c_{\mathbf{q}}M_h\mathcal{I}_h^{\mathbf{x}}\Big\{\Big(\Xi_\nu^{\mathbf{q}}[\hat{\psi}_{\mathrm{h}}^{\mathrm{n}}]\nabla_{\mathbf{q}}\mathcal{I}_h^{\mathbf{xq}}\Big\{g_\nu'(\hat{\psi}_h^n)\Big\}\Big)\cdot\nabla_{\mathbf{q}}\mathcal{I}_h^{\mathbf{xq}}\Big\{g_\nu'(\hat{\psi}_h^n)\Big\}\Big\}\\
&\quad+\tau\int_{\Omega\times\mathfrak{D}}c_{\mathbf{x}}M_h\mathcal{I}_h^{\mathbf{q}}\Big\{\Big(\Big((1-\gamma)\Xi_\nu^{\mathbf{x}}[\hat{\psi}_{\mathrm{h}}^{\mathrm{n}}]+\gamma\Lambda_\nu^{\mathbf{x}}[\hat{\psi}_{\mathrm{h}}^{\mathrm{n}}]\Big)\nabla_{\mathbf{x}}\mu_{\psi,h,\nu}^n\Big)\cdot\nabla_{\mathbf{x}}\mu_{\psi,h,\nu}^n\Big\}\\
&\quad\leq\mathcal{E}_h(\phi_h^{n-1},\hat{\psi}_h^{n-1},\mathbf{u}_h^{n-1})
\end{aligned}\tag{3.8}$$

with given initial data $(\phi_h^0,\hat{\psi}_h^0,\mathbf{u}_h^0)\in U_h^{\mathbf{x}}\times\hat{X}_h\times\boldsymbol{W}_{h,\mathrm{div}}$.

As we can not guarantee $\hat{\psi}_h^n\geq 0$ for $n\in\{1,\ldots,N\}$, the Henry energy, *i.e.* the term $\int_{\Omega\times\mathfrak{D}}(M_h+\mathfrak{m})\mathcal{I}_h^{\mathbf{x}}\Big\{\hat{\psi}_h^n\mathcal{J}_h\{\mathcal{I}_h^{\mathbf{x}}\{\beta(\phi_h^n)\}\}\Big\}$, may become arbitrarily negative and therefore Lemma 3.7 alone does not provide stability of the scheme. By enhancing the ideas of [7], we refine this result to guarantee stability.

Lemma 3.8. *Let initial data* $(\phi_h^0,\hat{\psi}_h^0,\mathbf{u}_h^0)\in U_h^{\mathbf{x}}\times\hat{X}_h\times\boldsymbol{W}_{h,\mathrm{div}}$ *be given, let* W *and* W_h' *satisfy (W1)–(W5), let (T) and (S1)–(S3) hold true, and let* $\eta\geq c>0$ *and* $\beta\geq 0$. *For* $n=1,\ldots,N$, *a solution* $(\phi_h^n,\,\mu_{\phi,h}^n,\,\hat{\psi}_h^n,\mathbf{u}_h^n)\in U_h^{\mathbf{x}}\times U_h^{\mathbf{x}}\times\hat{X}_h\times\boldsymbol{W}_{h,\mathrm{div}}$ *to* (3.4), *if exists, satisfies*

$$\begin{aligned}
&\tfrac12\int_\Omega\left|\nabla_{\mathbf{x}}\phi_h^n\right|^2+\int_\Omega\mathcal{I}_h^{\mathbf{x}}\{W(\phi_h^n)\}+\int_{\Omega\times\mathfrak{D}}(M_h+\mathfrak{m})\mathcal{I}_h^{\mathbf{xq}}\Big\{g_\nu(\hat{\psi}_h^n)\Big\}\\
&\qquad+\nu^{-1}\int_{\Omega\times\mathfrak{D}}(M_h+\mathfrak{m})\mathcal{I}_h^{\mathbf{xq}}\Big\{\big[\hat{\psi}_h^n\big]_-^2\Big\}+\tfrac12\int_\Omega\overline{\rho}_h^n\left|\mathbf{u}_h^n\right|^2\\
&\qquad+\tfrac{2\vartheta-1}{2}\sum_{k=1}^n\int_\Omega\left|\nabla_{\mathbf{x}}\phi_h^k-\nabla_{\mathbf{x}}\phi_h^{k-1}\right|^2+\tfrac14\sum_{k=1}^n\int_\Omega\overline{\rho}_h^{k-1}\left|\mathbf{u}_h^k-\mathbf{u}_h^{k-1}\right|^2\\
&\qquad+\tau\sum_{k=1}^n\int_\Omega\left|\nabla_{\mathbf{x}}\mu_\phi^k\right|^2+\tau\sum_{k=1}^n\int_\Omega 2\mathcal{I}_h^{\mathbf{x}}\{\eta(\phi_h^k)\}\left|\mathbf{D}\mathbf{u}_h^k\right|^2\\
&\qquad+\tau\sum_{k=1}^n\int_{\Omega\times\mathfrak{D}}c_{\mathbf{q}}M_h\mathcal{I}_h^{\mathbf{x}}\Big\{\Big(\Xi_\nu^{\mathbf{q}}[\hat{\psi}_{\mathrm{h}}^{\mathrm{k}}]\nabla_{\mathbf{q}}\mathcal{I}_h^{\mathbf{xq}}\Big\{g_\nu'(\hat{\psi}_h^k)\Big\}\Big)\cdot\nabla_{\mathbf{q}}\mathcal{I}_h^{\mathbf{xq}}\Big\{g_\nu'(\hat{\psi}_h^k)\Big\}\Big\}\\
&\qquad+\tau\sum_{k=1}^n\int_{\Omega\times\mathfrak{D}}c_{\mathbf{x}}M_h\mathcal{I}_h^{\mathbf{q}}\Big\{\Big(\Big((1-\gamma)\Xi_\nu^{\mathbf{x}}[\hat{\psi}_{\mathrm{h}}^{\mathrm{k}}]+\gamma\Lambda_\nu^{\mathbf{x}}[\hat{\psi}_{\mathrm{h}}^{\mathrm{k}}]\Big)\nabla_{\mathbf{x}}\mu_{\psi,h,\nu}^k\Big)\cdot\nabla_{\mathbf{x}}\mu_{\psi,h,\nu}^k\Big\}\\
&\qquad\leq C\mathcal{E}_h(\phi_h^0,\hat{\psi}_h^0,\mathbf{u}_h^0)+C,
\end{aligned}\tag{3.9}$$

with some constant $C>0$ *independent of* h, τ, $\mathfrak{m}$, *and* ν.

Proof. We consider a dual basis to the nodes $\{\mathbf{x}_i\}_{i=1,\ldots,\dim U_h^{\mathbf{x}}}$ and $\{\mathbf{q}_j\}_{j=1,\ldots,\dim U_h^{\mathbf{q}}}$ which is denoted by $\{\chi_{h,i}^{\mathbf{x}}\}_{i=1,\ldots,\dim U_h^{\mathbf{x}}}$ and $\{\chi_{h,j}^{\mathbf{q}}\}_{j=1,\ldots,\dim U_h^{\mathbf{q}}}$. Furthermore, we denote $\hat{\psi}_h^n(\mathbf{x}_i,\mathbf{q}_j)$ by $\hat{\psi}_{h,i,j}^n$ and define positive weights $\lambda_{ij}:=\int_{\Omega\times\mathfrak{D}}(M_h+\mathfrak{m})\chi_{h,i}^{\mathbf{x}}\chi_{h,j}^{\mathbf{q}}$ for all $i\in\{1,\ldots,\dim U_h^{\mathbf{x}}\}$, $j\in\{1,\ldots,\dim U_h^{\mathbf{q}}\}$. We compute

$$\begin{aligned}
\tfrac12\int_{\Omega\times\mathfrak{D}}(M_h+\mathfrak{m})\mathcal{I}_h^{\mathbf{xq}}\Big\{g_\nu(\hat{\psi}_h^n)\Big\}&=\tfrac12\sum_{i=1}^{\dim U_h^{\mathbf{x}}}\sum_{j=1}^{\dim U_h^{\mathbf{q}}}\lambda_{ij}g_\nu(\hat{\psi}_{h,i,j}^n)\\
&=\tfrac12\sum_{i,j\,:\,\hat{\psi}_{h,i,j}^n\geq 0}\lambda_{ij}g_\nu(\hat{\psi}_{h,i,j}^n)+\tfrac12\sum_{i,j\,:\,\hat{\psi}_{h,i,j}^n<0}\lambda_{ij}g_\nu(\hat{\psi}_{h,i,j}^n).
\end{aligned}\tag{3.10}$$

As there exists a ν-independent lower bound for g_ν, the first summand is bounded from below. From (2.21a), we have for negative $\hat{\psi}^n_{h,i,j}$

$$g_\nu(\hat{\psi}^n_{h,i,j}) = \frac{|\hat{\psi}^n_{h,i,j}|^2}{2\nu} - \frac{\nu}{2} + \hat{\psi}^n_{h,i,j}(\log\nu - 1) \geq \frac{1}{2\nu}\left[\hat{\psi}^n_{h,i,j}\right]_-^2 - \frac{\nu}{2}, \tag{3.11}$$

as $\left[\hat{\psi}^n_{h,i,j}\right]_-(\log\nu - 1) \geq 0$. Therefore, we have

$$\frac{1}{2}\int_{\Omega\times\mathfrak{D}} (M_h + \mathfrak{m})\mathcal{I}_h^{\mathbf{xq}}\Big\{g_\nu(\hat{\psi}^n_h)\Big\} \geq -C + \frac{1}{4\nu}\int_{\Omega\times\mathfrak{D}} (M_h + \mathfrak{m})\mathcal{I}_h^{\mathbf{xq}}\Big\{\left[\hat{\psi}^n_h\right]_-^2\Big\}. \tag{3.12}$$

On the other hand, we may apply Young's inequality to compute

$$\begin{aligned}\int_{\Omega\times\mathfrak{D}} (M_h + \mathfrak{m})\mathcal{I}_h^{\mathbf{x}}\Big\{\mathcal{J}_h\{\mathcal{I}_h^{\mathbf{x}}\{\beta(\phi_h^n)\}\}\hat{\psi}^n_h\Big\} &\geq \int_{\Omega\times\mathfrak{D}} (M_h + \mathfrak{m})\mathcal{I}_h^{\mathbf{xq}}\Big\{\mathcal{J}_h\{\mathcal{I}_h^{\mathbf{x}}\{\beta(\phi_h^n)\}\}\left[\hat{\psi}^n_h\right]_-\Big\}\\ &\geq -\delta\int_{\Omega\times\mathfrak{D}} (M_h + \mathfrak{m})\mathcal{I}_h^{\mathbf{xq}}\Big\{\left[\hat{\psi}^n_h\right]_-^2\Big\} - C_\delta,\end{aligned} \tag{3.13}$$

with $0 < \delta \ll 1$ independent of ν. Combining (3.12) and (3.13) provides

$$\begin{aligned}\left(\tfrac{1}{4\nu} - \delta\right)\int_{\Omega\times\mathfrak{D}} (M_h + \mathfrak{m})\mathcal{I}_h^{\mathbf{xq}}\Big\{\left[\hat{\psi}^n_h\right]_-^2\Big\} &\leq \int_{\Omega\times\mathfrak{D}} (M_h + \mathfrak{m})\mathcal{I}_h^{\mathbf{x}}\Big\{\mathcal{J}_h\{\mathcal{I}_h^{\mathbf{x}}\{\beta(\phi_h^n)\}\}\hat{\psi}^n_h\Big\}\\ &\quad + \tfrac{1}{2}\int_{\Omega\times\mathfrak{D}} (M_h + \mathfrak{m})\mathcal{I}_h^{\mathbf{xq}}\Big\{g_\nu(\hat{\psi}^n_h)\Big\} + C.\end{aligned} \tag{3.14}$$

Applying this on a discrete integration in time over the result of Lemma 3.7 provides the result. □

At this point, we want to emphasize that the constants in Lemma 3.8 does not depend on the mollification parameter ε. Combining the *a priori* estimates above with Brouwer's fixed point theorem, we obtain the existence of discrete solutions (*cf.* [25]).

Lemma 3.9. *Let the assumptions (W1)–(W5) hold true. Furthermore, let $\beta \in C^1(\mathbb{R}_0^+) \cap W^{1,\infty}(\mathbb{R})$ and $\eta \in C^1(\mathbb{R}) \cap W^{1,\infty}$ with $\eta \geq c > 0$, then for given $\left(\phi_h^{n-1}, \hat{\psi}_h^{n-1}, \mathbf{u}_h^{n-1}\right) \in U_h^{\mathbf{x}} \times \hat{X}_h \times \boldsymbol{W}_{h,\mathrm{div}}$ and a given time increment $\tau > 0$, there exists at least one quadruple $\left(\phi_h^n, \mu_{\phi,h}^n, \hat{\psi}_h^n, \mathbf{u}_h^n\right) \in U_h^{\mathbf{x}} \times U_h^{\mathbf{x}} \times \hat{X}_h \times \boldsymbol{W}_{h,\mathrm{div}}$ satisfying (3.4).*

4. Compactness in space and time

From now on, we restrict ourselves to the case of equal mass densities. Without loss of generality, we assume $\rho \equiv 1$. Furthermore, we make the following general assumptions

- **(A1)** The spring potential U and its associated Maxwellian M satisfy (P1)–(P5) with some $\kappa > 1$ such that Lemma 2.2 holds true.
- **(A2)** The discretization in time satisfies (T).
- **(A3)** Ω^* and Ω are bounded, convex polygonal (or polyhedral) domains with families of partitions $\{\mathcal{T}_h^{\mathbf{x}*}\}_{h>0}$ and $\{\mathcal{T}_h^{\mathbf{x}}\}_{h>0}$ satisfying (S1)–(S2).
  $\mathfrak{D}$ is a bounded polygonal (or polyhedral) domain with a family of partitions $\{\mathcal{T}_h^{\mathbf{q}}\}_{h>0}$ satisfying (S3).
- **(A4)** Assumptions (W1)–(W5) apply to the double-well potential W and the time-discrete approximations of its derivatives.
- **(A5)** The mollification operators $\mathcal{J}_\varepsilon$ and $\boldsymbol{\mathcal{J}}_\varepsilon$ are defined by (1.8), while their discrete counterparts $\mathcal{J}_h$ and $\boldsymbol{\mathcal{J}}_h$ are obtained *via* (2.38).

(A6) $\beta,\, \eta \in C^\infty(\mathbb{R}) \cap W^{2,\infty}(\mathbb{R})$, and there exist constants $c_1,\, c_2 > 0$ such that

$$0 \leq \beta(s) \leq c_2 \qquad c_1 \leq \eta(s) \leq c_2 \quad \forall s \in \mathbb{R}.$$

(A7) There is a constant $C > 0$ such that $h_{\mathbf{q}}^\kappa \leq C\mathfrak{m}$ with the $\kappa > 1$ used in assumption (A1). Furthermore, $h_{\mathbf{x}}$ and ν satisfy the relation $\frac{h_{\mathbf{x}}^2}{\nu} \to 0$, as $h_{\mathbf{x}}, \nu \searrow 0$.

(A8) Let initial data $\Phi^0 \in H^2(\Omega; [-1,1])$ and $\mathbf{U}^0 \in \boldsymbol{H}^1_{0,\mathrm{div}}(\Omega)$ be given such that we have for discrete initial data $\phi_h^0 = \mathcal{I}_h^{\mathbf{x}}\{\Phi^0\}$ and $\mathbf{u}_h^0 := \mathcal{Q}_h\{\mathbf{U}^0\}$ uniformly in $h > 0$ that

$$\left\|\mathbf{u}_h^0\right\|_{H^1(\Omega)} + \int_\Omega \left|\Delta_h \phi_h^0\right|^2 + \int_\Omega \left|\nabla_{\mathbf{x}} \phi_h^0\right|^2 + \int_\Omega \mathcal{I}_h^{\mathbf{x}}\{W(\phi_h^0)\} \leq C < \infty.$$

(A9) Let nonnegative initial data for the scaled configurational density be given as $\hat{\Psi}^0 \in L^2(\Omega \times \mathfrak{D})$. We compute discrete initial data $\hat{\psi}_h^0$ *via*

$$\begin{aligned}\int_{\Omega\times\mathfrak{D}} (M_h + \mathfrak{m})\mathcal{I}_h^{\mathbf{xq}}\Big\{\hat{\psi}_h^0 \theta_h\Big\} + \tau \int_{\Omega\times\mathfrak{D}} M_h \mathcal{I}_h^{\mathbf{q}}\Big\{\nabla_{\mathbf{x}} \hat{\psi}_h^0 \cdot \nabla_{\mathbf{x}} \theta_h\Big\} \\ + \tau \int_{\Omega\times\mathfrak{D}} M_h \mathcal{I}_h^{\mathbf{x}}\Big\{\nabla_{\mathbf{q}} \hat{\psi}_h^0 \cdot \nabla_{\mathbf{q}} \theta_h\Big\} = \int_{\Omega\times\mathfrak{D}} (M_h + \mathfrak{m})\hat{\Psi}^0 \theta_h \qquad \forall \theta_h \in \hat{X}_h.\end{aligned} \tag{4.1}$$

Remark 4.1. The definition of the discrete initial data is an adaption of the ideas used in [7]. As shown in [25], it is also possible to adapt (4.1) to allow for $\hat{\Psi}^0 \in L^2(\Omega \times \mathfrak{D}; \hat{M})$.

Lemma 4.2. *Under the assumptions (A1), (A3), (A7), and (A9) the discrete initial data $\hat{\psi}_h^0$ satisfies*

$$\int_{\Omega\times\mathfrak{D}} (M_h + \mathfrak{m})\mathcal{I}_h^{\mathbf{xq}}\left\{\left|\hat{\psi}_h^0\right|^2\right\} + \tau \int_{\Omega\times\mathfrak{D}} M_h \mathcal{I}_h^{\mathbf{q}}\left\{\left|\nabla_{\mathbf{x}} \hat{\psi}_h^0\right|^2\right\} + \tau \int_{\Omega\times\mathfrak{D}} M_h \mathcal{I}_h^{\mathbf{x}}\left\{\left|\nabla_{\mathbf{q}} \hat{\psi}_h^0\right|^2\right\} \leq C, \tag{4.2}$$

with some $C > 0$ independent of h, τ, $\mathfrak{m}$, and ν. In addition, we have

$$\hat{\psi}_h^0 \geq 0. \tag{4.3}$$

To prove this lemma, we need an additional result concerning the Maxwellian $\hat{M}$ and its discrete counterpart M_h.

Lemma 4.3. *Let (A1) and (A7) hold true. Then there is a positive constant c independent of h, τ, $\mathfrak{m}$, and ν such that*

$$\hat{M}(\mathbf{q}) \leq c(M_h(\mathbf{q}) + \mathfrak{m})$$

for all $\mathbf{q} \in \mathfrak{D}$.

Proof. Let $\mathcal{T}_{h,\mathrm{inner}}^{\mathbf{q}} \subset \mathcal{T}_h^{\mathbf{q}}$ be the set containing all $\kappa_{\mathbf{q}} \in \mathcal{T}_h^{\mathbf{q}}$ satisfying $\kappa_{\mathbf{q}} \subset D$ and $\mathrm{dist}\,(\kappa_{\mathbf{q}}, \partial D) \geq h_{\mathbf{q}}$. Then we have for every $\kappa_{\mathbf{q}} \in \mathcal{T}_{h,\mathrm{inner}}^{\mathbf{q}}$

$$\min_{\mathbf{q}\in\kappa_{\mathbf{q}}} \hat{M}(\mathbf{q}) \geq c_1 [\mathrm{dist}\,(\kappa_{\mathbf{q}}, \partial D)]^\kappa, \tag{4.4}$$

$$\max_{\mathbf{q}\in\kappa_{\mathbf{q}}} \hat{M}(\mathbf{q}) \leq c_2 [\mathrm{dist}\,(\kappa_{\mathbf{q}}, \partial D) + h_{\mathbf{q}}]^\kappa \leq c_2 2^\kappa [\mathrm{dist}\,(\kappa_{\mathbf{q}}, \partial D)]^\kappa \tag{4.5}$$

with $\kappa > 1$ due to (P3) and therefore

$$\hat{M} \leq \max_{\mathbf{q}\in\kappa_{\mathbf{q}}} \hat{M}(\mathbf{q}) \leq \tfrac{c_2 2^\kappa}{c_1} \tfrac{c_{h_{\mathbf{q}}}}{c_M} \min_{\mathbf{q}\in\kappa_{\mathbf{q}}} \hat{M}(\mathbf{q}) \leq \tfrac{c_2 2^\kappa}{c_1 c_M} M_h, \tag{4.6}$$

as $c_{h_{\mathbf{q}}} \geq c_M$ (see Lem. 2.2). We use (P3) and $h_{\mathbf{q}}^{\kappa} \leq C\mathfrak{m}$ on every $\kappa_{\mathbf{q}} \in \mathcal{T}_h^{\mathbf{q}} \setminus \mathcal{T}_{h,\text{inner}}^{\mathbf{q}}$ to compute

$$\max_{\mathbf{q}\in\kappa_{\mathbf{q}}} \hat{M}(\mathbf{q}) \leq C h_{\mathbf{q}}^{\kappa} \leq C\mathfrak{m}. \tag{4.7}$$

□

Proof of Lemma 4.2. Testing (4.1) by $\hat{\psi}_h^0 \in \hat{X}$ yields

$$(1-\delta c)\int_{\Omega\times\mathfrak{D}} (M_h+\mathfrak{m})\mathcal{I}_h^{\mathbf{xq}}\Big\{\left|\hat{\psi}_h^0\right|^2\Big\} + \tau\int_{\Omega\times\mathfrak{D}} M_h\mathcal{I}_h^{\mathbf{q}}\Big\{\left|\nabla_{\mathbf{x}}\hat{\psi}_h^0\right|^2\Big\} \\ +\tau\int_{\Omega\times\mathfrak{D}} M_h\mathcal{I}_h^{\mathbf{x}}\Big\{\left|\nabla_{\mathbf{q}}\hat{\psi}_h^0\right|^2\Big\} \leq C \tag{4.8}$$

and therefore (4.2) for δ small enough. The nonnegativity of $\hat{\psi}_h^0$ follows from standard arguments (cf*cf.* Chap. 11 in [29]). □

Combining Lemma 3.8 with the regularity assumptions on the initial data and noting

$$\left|\int_{\Omega\times\mathfrak{D}} (M_h+\mathfrak{m})\mathcal{I}_h^{\mathbf{xq}}\Big\{g_\nu(\hat{\psi}_h^0)\Big\}\right| \leq \int_{\Omega\times\mathfrak{D}} (M_h+\mathfrak{m})\mathcal{I}_h^{\mathbf{xq}}\Big\{\left|\hat{\psi}_h^0\right|^2\Big\} + C. \tag{4.9}$$

for $\hat{\psi}_h^0 \geq 0$, we obtain our first regularity result.

Lemma 4.4. *Let the assumptions (A1)–(A9) hold true. Then for $n = 1,\ldots,N$ a solution $\{\phi_h^n,\ \mu_{\phi,h}^n,\ \hat{\psi}_h^n, \mathbf{u}_h^n\} \in U_h^{\mathbf{x}} \times U_h^{\mathbf{x}} \times \hat{X}_h \times \boldsymbol{W}_{h,\text{div}}$ to the equal density version of (3.4) satisfies*

$$\int_\Omega |\nabla_{\mathbf{x}}\phi_h^n|^2 + \int_\Omega \mathcal{I}_h^{\mathbf{x}}\{W(\phi_h^n)\} + \int_{\Omega\times\mathfrak{D}} (M_h+\mathfrak{m})\mathcal{I}_h^{\mathbf{xq}}\Big\{g_\nu(\hat{\psi}_h^n)\Big\} + \nu^{-1}\int_{\Omega\times\mathfrak{D}} (M_h+\mathfrak{m})\mathcal{I}_h^{\mathbf{xq}}\Big\{[\hat{\psi}_h^n]_-^2\Big\} \\ + \int_\Omega |\mathbf{u}_h^n|^2 + \tfrac{2\vartheta-1}{2}\sum_{k=1}^n\int_\Omega \left|\nabla_{\mathbf{x}}\phi_h^k - \nabla_{\mathbf{x}}\phi_h^{k-1}\right|^2 + \sum_{k=1}^n\int_\Omega \left|\mathbf{u}_h^k - \mathbf{u}_h^{k-1}\right|^2 + \tau\sum_{k=1}^n\int_\Omega \left|\nabla_{\mathbf{x}}\mu_\phi^k\right|^2 \\ + \tau\sum_{k=1}^n\int_\Omega 2\mathcal{I}_h^{\mathbf{x}}\{\eta(\phi_h^k)\}\left|\mathbf{D}\mathbf{u}_h^k\right|^2 + \tau\sum_{k=1}^n\int_{\Omega\times\mathfrak{D}} M_h\mathcal{I}_h^{\mathbf{x}}\Big\{\Big(\Xi_\nu^{\mathbf{q}}[\hat{\psi}_{\text{h}}^{\text{k}}]\nabla_{\mathbf{q}}\mathcal{I}_h^{\mathbf{xq}}\Big\{g_\nu'(\hat{\psi}_h^k)\Big\}\Big)\cdot\nabla_{\mathbf{q}}\mathcal{I}_h^{\mathbf{xq}}\Big\{g_\nu'(\hat{\psi}_h^k)\Big\}\Big\} \\ + \tau\sum_{k=1}^n\int_{\Omega\times\mathfrak{D}} M_h\mathcal{I}_h^{\mathbf{q}}\Big\{\Big(\Big((1-\gamma)\Xi_\nu^{\mathbf{x}}[\hat{\psi}_{\text{h}}^{\text{k}}] + \gamma\Lambda_\nu^{\mathbf{x}}[\hat{\psi}_{\text{h}}^{\text{k}}]\Big)\nabla_{\mathbf{x}}\mu_{\psi,h,\nu}^k\Big)\cdot\nabla_{\mathbf{x}}\mu_{\psi,h,\nu}^k\Big\} \leq C, \tag{4.10}$$

with some constant $C > 0$ independent of h, τ, $\mathfrak{m}$, and ν.

Starting from this result, we use the specific discretization of the $\mathbf{x}$-convective term in (3.4c) to improve the regularity results for the scaled configurational density. In particular, we establish the following lemma.

Lemma 4.5. *Let the assumptions (A1)–(A9) hold true. Then for τ small enough, there is a positive constant $C > 0$ independent of h, τ, $\mathfrak{m}$, and ν such that*

$$\int_{\Omega\times\mathfrak{D}} (M_h+\mathfrak{m})\mathcal{I}_h^{\mathbf{xq}}\Big\{\left|\hat{\psi}_h^n\right|^2\Big\} + \sum_{k=1}^n\int_{\Omega\times\mathfrak{D}} (M_h+\mathfrak{m})\mathcal{I}_h^{\mathbf{xq}}\Big\{\left|\hat{\psi}_h^k - \hat{\psi}_h^{k-1}\right|^2\Big\} \\ +\tau\sum_{k=0}^n\int_{\Omega\times\mathfrak{D}} M_h\mathcal{I}_h^{\mathbf{q}}\Big\{\left|\nabla_{\mathbf{x}}\hat{\psi}_h^k\right|^2\Big\} + \tau\sum_{k=0}^n\int_{\Omega\times\mathfrak{D}} M_h\mathcal{I}_h^{\mathbf{x}}\Big\{\left|\nabla_{\mathbf{q}}\hat{\psi}_h^k\right|^2\Big\} \leq C \tag{4.11}$$

for all $n \in \{0,\ldots,N\}$.

Proof. By testing (3.4c) by $\hat{\psi}_h^n$ for $n \in \{1,\dots,N\}$, we obtain

$$\begin{aligned}
0 =& \int_{\Omega\times\mathfrak{D}} (M_h + \mathfrak{m})\mathcal{I}_h^{\mathbf{xq}}\Big\{\partial_\tau^- \hat{\psi}_h^n \hat{\psi}_h^n\Big\} - \int_{\Omega\times\mathfrak{D}} M_h \mathbf{u}_h^n \cdot \mathcal{I}_h^{\mathbf{q}}\Big\{\Lambda_\nu^{\mathbf{x}}[\hat{\psi}_{\mathrm{h}}^{\mathrm{n}}]\nabla_{\mathbf{x}}\hat{\psi}_h^n\Big\} \\
&- \int_{\Omega\times\mathfrak{D}} (\nabla_{\mathbf{x}}\mathcal{I}_h^{\mathbf{x}}\{\boldsymbol{\mathcal{J}}_h\{\mathbf{u}_h^n\}\} \cdot \mathcal{I}_h^{\mathbf{q}}\{\mathbf{q}M_h\}) \cdot \mathcal{I}_h^{\mathbf{x}}\Big\{\Xi_\nu^{\mathbf{q}}[\hat{\psi}_{\mathrm{h}}^{\mathrm{n}}]\nabla_{\mathbf{q}}\hat{\psi}_h^n\Big\} \\
&+ (1-\gamma)\int_{\Omega\times\mathfrak{D}} c_{\mathbf{x}} M_h \mathcal{I}_h^{\mathbf{q}}\Big\{\Big(\Xi_\nu^{\mathbf{x}}[\hat{\psi}_{\mathrm{h}}^{\mathrm{n}}]\nabla_{\mathbf{x}}\mu_{\psi,h,\nu}^n\Big) \cdot \nabla_{\mathbf{x}}\hat{\psi}_h^n\Big\} \\
&+ \gamma\int_{\Omega\times\mathfrak{D}} c_{\mathbf{x}} M_h \mathcal{I}_h^{\mathbf{q}}\Big\{\Big(\Lambda_\nu^{\mathbf{x}}[\hat{\psi}_{\mathrm{h}}^{\mathrm{n}}]\nabla_{\mathbf{x}}\mu_{\psi,h,\nu}^n\Big) \cdot \nabla_{\mathbf{x}}\hat{\psi}_h^n\Big\} + \int_{\Omega\times\mathfrak{D}} c_{\mathbf{q}} M_h \mathcal{I}_h^{\mathbf{x}}\Big\{\Big|\nabla_{\mathbf{q}}\hat{\psi}_h^n\Big|^2\Big\} \\
=:& I + II + III + IV + V + VI.
\end{aligned} \tag{4.12}$$

Combining (2.24b) with the weak solenoidality of $\mathbf{u}_h^n$, we obtain

$$II = -\int_{\Omega\times\mathfrak{D}} M_h \mathbf{u}_h^n \cdot \mathcal{I}_h^{\mathbf{q}}\Big\{\nabla_{\mathbf{x}}\mathcal{I}_h^{\mathbf{xq}}\Big\{f_\nu(\hat{\psi}_h^n)\Big\}\Big\} = 0. \tag{4.13}$$

Applying Young's inequality with $0 < \delta \ll 1$, Lemma 2.10, Lemma 4.4, and Lemma 2.7, we compute

$$\begin{aligned}
III + IV \geq& (1-\gamma)(c_{\mathbf{x}} - \delta)\int_{\Omega\times\mathfrak{D}} M_h \mathcal{I}_h^{\mathbf{q}}\Big\{\Big|\nabla_{\mathbf{x}}\hat{\psi}_h^n\Big|^2\Big\} - \delta\int_{\Omega\times\mathfrak{D}} M_h \mathcal{I}_h^{\mathbf{x}}\Big\{\Big|\nabla_{\mathbf{q}}\hat{\psi}_h^n\Big|^2\Big\} \\
&- C_\delta\Big[\int_{\Omega\times\mathfrak{D}} M_h \nu^2 + \int_{\Omega\times\mathfrak{D}} M_h \mathcal{I}_h^{\mathbf{xq}}\Big\{\Big|\hat{\psi}_h^n\Big|^2\Big\}\Big].
\end{aligned} \tag{4.14}$$

Applying similar arguments on the fifth term on the right-hand side of (4.12) yields

$$\begin{aligned}
V =& \gamma\int_{\Omega\times\mathfrak{D}} c_{\mathbf{x}} M_h \mathcal{I}_h^{\mathbf{q}}\Big\{\Big(\Lambda_\nu^{\mathbf{x}}[\hat{\psi}_{\mathrm{h}}^{\mathrm{n}}] \cdot \Xi_\nu^{\mathbf{x}}[\hat{\psi}_{\mathrm{h}}^{\mathrm{n}}]^{-1}\nabla_{\mathbf{x}}\hat{\psi}_h^n\Big) \cdot \nabla_{\mathbf{x}}\hat{\psi}_h^n\Big\} \\
&+ \gamma\int_{\Omega\times\mathfrak{D}} c_{\mathbf{x}} M_h \mathcal{I}_h^{\mathbf{q}}\Big\{\Big(\Lambda_\nu^{\mathbf{x}}[\hat{\psi}_{\mathrm{h}}^{\mathrm{n}}]\nabla_{\mathbf{x}}\mathcal{I}_h^{\mathbf{x}}\{\mathcal{J}_h\{\mathcal{I}_h^{\mathbf{x}}\{\beta(\phi_h^n)\}\}\}\Big) \cdot \nabla_{\mathbf{x}}\hat{\psi}_h^n\Big\} \\
\geq& -\gamma\delta\int_{\Omega\times\mathfrak{D}} M_h \mathcal{I}_h^{\mathbf{q}}\Big\{\Big|\nabla_{\mathbf{x}}\hat{\psi}_h^n\Big|^2\Big\} - \gamma C_\delta\Big[\int_{\Omega\times\mathfrak{D}} M_h \nu^2 + \int_{\Omega\times\mathfrak{D}} M_h \mathcal{I}_h^{\mathbf{xq}}\Big\{\Big|\hat{\psi}_h^n\Big|^2\Big\}\Big],
\end{aligned} \tag{4.15}$$

as $\Lambda_\nu^{\mathbf{x}}[\hat{\psi}_{\mathrm{h}}^{\mathrm{n}}] \cdot \Xi_\nu^{\mathbf{x}}[\hat{\psi}_{\mathrm{h}}^{\mathrm{n}}]^{-1}$ is positive definite. Combining the above results and multiplying by τ yields

$$\begin{aligned}
&\tfrac{1}{2}\int_{\Omega\times\mathfrak{D}} (M_h + \mathfrak{m})\mathcal{I}_h^{\mathbf{xq}}\Big\{\Big|\hat{\psi}_h^n\Big|^2\Big\} + \tfrac{1}{2}\int_{\Omega} (M_h + \mathfrak{m})\mathcal{I}_h^{\mathbf{xq}}\Big\{\Big|\hat{\psi}_h^n - \hat{\psi}_h^{n-1}\Big|^2\Big\} \\
&\quad + \tau(1-\gamma)\int_{\Omega\times\mathfrak{D}} c_{\mathbf{x}} M_h \mathcal{I}_h^{\mathbf{q}}\Big\{\Big|\nabla_{\mathbf{x}}\hat{\psi}_h^n\Big|^2\Big\} + \tau\int_{\Omega\times\mathfrak{D}} c_{\mathbf{q}} M_h \mathcal{I}_h^{\mathbf{x}}\Big\{\Big|\nabla_{\mathbf{q}}\hat{\psi}_h^n\Big|^2\Big\} \\
&\quad - \tau\delta\int_{\Omega\times\mathfrak{D}} M_h \mathcal{I}_h^{\mathbf{q}}\Big\{\Big|\nabla_{\mathbf{x}}\hat{\psi}_h^n\Big|^2\Big\} - \tau\delta\int_{\Omega\times\mathfrak{D}} M_h \mathcal{I}_h^{\mathbf{x}}\Big\{\Big|\nabla_{\mathbf{q}}\hat{\psi}_h^n\Big|\Big\} \\
&\quad \leq \tfrac{1}{2}\int_{\Omega\times\mathfrak{D}} (M_h + \mathfrak{m})\mathcal{I}_h^{\mathbf{xq}}\Big\{\Big|\hat{\psi}_h^{n-1}\Big|^2\Big\} + \tau C_0\int_{\Omega\times\mathfrak{D}} M_h \mathcal{I}_h^{\mathbf{xq}}\Big\{\Big|\hat{\psi}_h^n\Big|^2\Big\} + \tau C\int_{\Omega\times\mathfrak{D}} M_h \nu^2.
\end{aligned} \tag{4.16}$$

For δ small enough, we have $(1-\gamma)c_{\mathbf{x}} - \delta \geq c > 0$ and $c_{\mathbf{q}} - \delta \geq c > 0$. Therefore, a summation in time yields

$$\begin{aligned}\tfrac{1}{2}\int_{\Omega\times\mathfrak{D}} (M_h + \mathfrak{m})\mathcal{I}_h^{\mathbf{xq}}\Big\{\Big|\hat{\psi}_h^n\Big|^2\Big\} &+ \tfrac{1}{2}\sum_{k=1}^{n}\int_{\Omega\times\mathfrak{D}} (M_h + \mathfrak{m})\mathcal{I}_h^{\mathbf{xq}}\Big\{\Big|\hat{\psi}_h^k - \hat{\psi}_h^{k-1}\Big|^2\Big\} + c\tau\sum_{k=1}^{n}\int_{\Omega\times\mathfrak{D}} M_h\mathcal{I}_h^{\mathbf{q}}\Big\{\Big|\nabla_{\mathbf{x}}\hat{\psi}_h^k\Big|^2\Big\} \\ &+ c\tau\sum_{k=1}^{n}\int_{\Omega\times\mathfrak{D}} M_h\mathcal{I}_h^{\mathbf{x}}\Big\{\Big|\nabla_{\mathbf{q}}\hat{\psi}_h^k\Big|^2\Big\} \leq \tfrac{1}{2}\int_{\Omega\times\mathfrak{D}} (M_h + \mathfrak{m})\mathcal{I}_h^{\mathbf{xq}}\Big\{\Big|\hat{\psi}_h^0\Big|^2\Big\} \\ &+ \tau C_0\int_{\Omega\times\mathfrak{D}} M_h\mathcal{I}_h^{\mathbf{xq}}\Big\{\Big|\hat{\psi}_h^n\Big|^2\Big\} + \tau C\sum_{k=1}^{n-1}\int_{\Omega\times\mathfrak{D}} M_h\mathcal{I}_h^{\mathbf{xq}}\Big\{\Big|\hat{\psi}_h^k\Big|^2\Big\} + \tau nC. \qquad (4.17)\end{aligned}$$

As the constant C_0 on the right-hand side depends neither on τ nor on the solution itself, we may safely assume $\tau C_0 < \frac{1}{4}$. Absorbing $\tau C_0 \int_{\Omega\times\mathfrak{D}} M_h\mathcal{I}_h^{\mathbf{xq}}\Big\{\Big|\hat{\psi}_h^n\Big|^2\Big\}$ on the left-hand side and applying a discrete version of Gronwall's lemma (see *e.g.* [31]) shows

$$\begin{aligned}\int_{\Omega\times\mathfrak{D}} (M_h + \mathfrak{m})\mathcal{I}_h^{\mathbf{xq}}\Big\{\Big|\hat{\psi}_h^n\Big|^2\Big\} &+ \sum_{k=1}^{n}\int_{\Omega\times\mathfrak{D}} (M_h + \mathfrak{m})\mathcal{I}_h^{\mathbf{xq}}\Big\{\Big|\hat{\psi}_h^k - \hat{\psi}_h^{k-1}\Big|^2\Big\} \\ +\tau\sum_{k=1}^{n}\int_{\Omega\times\mathfrak{D}} M_h\mathcal{I}_h^{\mathbf{q}}\Big\{\Big|\nabla_{\mathbf{x}}\hat{\psi}_h^k\Big|^2\Big\} &+ \tau\sum_{k=1}^{n}\int_{\Omega\times\mathfrak{D}} M_h\mathcal{I}_h^{\mathbf{x}}\Big\{\Big|\nabla_{\mathbf{q}}\hat{\psi}_h^k\Big|^2\Big\} \leq C \qquad (4.18)\end{aligned}$$

for $n \in \{1, \ldots, N\}$. Combining (4.18) with Lemma 4.2 completes the proof. $\square$

Following the arguments in [15, 16, 18], we establish the following regularity results for the phase-field parameter.

Lemma 4.6. *Let the assumptions (A1)–(A9) hold true and let τ be small enough. Then there is $C > 0$ independent of h, τ, $\mathfrak{m}$, and ν such that*

$$\left|\int_\Omega \mu_{\phi,h}^n\right| + \sum_{k=0}^{n}\tau\left\|\Delta_h\phi_h^k\right\|_{L^2(\Omega)}^2 + \sum_{k=0}^{n}\tau\left\|\phi_h^k\right\|_{L^\infty(\Omega)}^4 \leq C \qquad (4.19)$$

for all $n \in \{1, \ldots, N\}$.

Lemma 4.7. *Let the assumptions (A1)–(A9) hold true and let τ be small enough. Then there is $C > 0$ independent of h, τ, $\mathfrak{m}$, and ν such that*

$$\tau\sum_{k=0}^{N-l}\left\|\phi_h^{k+l} - \phi_h^k\right\|_{L^2(\Omega)}^2 \leq Cl\tau \qquad (4.20)$$

for all $l \in \{1, \ldots, N\}$.

Proof of Lemma 4.6. A straightforward computation relying in particular on (2.11a), (W2), and the already established regularity results yields $\left|\int_\Omega \mu_{\phi,h}^n\right| \leq C$.
Therefore, the mean value of the chemical potential is bounded which allows to apply Poincaré's inequality.

We continue by testing (3.4b) by $-\Delta_h\phi_h^n$ and use the definition of the discrete Laplacian (2.8) to obtain

$$\begin{aligned}\vartheta\int_\Omega \mathcal{I}_h^{\mathbf{x}}\{\Delta_h\phi_h^n\Delta_h\phi_h^n\} &= -\int_\Omega \mathcal{I}_h^{\mathbf{x}}\{\mu_{\phi,h}^n\Delta_h\phi_h^n\} + \int_\Omega \mathcal{I}_h^{\mathbf{x}}\{W_h'(\phi_h^n,\phi_h^{n-1})\Delta_h\phi_h^n\}\\ &\quad + \int_{\Omega\times\mathfrak{D}} (M_h+\mathfrak{m})\mathcal{I}_h^{\mathbf{x}}\Big\{\mathcal{J}_h\big\{\mathcal{I}_h^{\mathbf{x}}\{\beta_{DQ}'(\phi_h^n,\phi_h^{n-1})\Delta_h\phi_h^n\}\big\}\hat{\psi}_h^{n-1}\Big\}\\ &\quad -(1-\vartheta)\int_\Omega \mathcal{I}_h^{\mathbf{x}}\big\{\Delta_h\phi_h^{n-1}\Delta_h\phi_h^n\big\}\\ &=: I+II+III+IV.\end{aligned} \tag{4.21}$$

Combining Hölder's inequality and Poincaré's inequality provides

$$|I| \le \left\|\mu_{\phi,h}^n\right\|_h \|\Delta_h\phi_h^n\|_h \le C\Big(\left\|\nabla_{\mathbf{x}}\mu_{\phi,h}^n\right\|_{L^2(\Omega)}+1\Big)\|\Delta_h\phi_h^n\|_h\,. \tag{4.22}$$

We infer from Hölder's inequality and (W2) that

$$II \le \left\|W_h'(\phi_h^n,\phi_h^{n-1})\right\|_h \|\Delta_h\phi_h^n\|_h \le C\|\Delta_h\phi_h^n\|_h\,. \tag{4.23}$$

To gain control over the third term, we combine Hölder's inequality and (2.10) with the results of Lemma 4.5, the results of Lemma 2.10, and (A6).

$$\begin{aligned}III &\le C\left\|\mathcal{J}_h\{\mathcal{I}_h^{\mathbf{x}}\{\beta_{DQ}'(\phi_h^n,\phi_h^{n-1})\Delta_h\phi_h^n\}\}\right\|_{L^2(\Omega)}\left(\int_{\Omega\times\mathfrak{D}}(M_h+\mathfrak{m})\mathcal{I}_h^{\mathbf{xq}}\Big\{\left|\hat{\psi}_h^{n-1}\right|^2\Big\}\right)^{1/2}\\ &\le C\int_\Omega\left|\mathcal{I}_h^{\mathbf{x}}\{\beta_{DQ}'(\phi_h^n,\phi_h^{n-1})\Delta_h\phi_h^n\}\right| \le C\|\Delta_h\phi_h^n\|_h\,.\end{aligned} \tag{4.24}$$

Concerning the fourth term,

$$|IV| \le (1-\vartheta)\|\Delta_h\phi_h^n\|_h\left\|\Delta_h\phi_h^{n-1}\right\|_h \tag{4.25}$$

holds true. Collecting the previous results, we obtain

$$\vartheta\|\Delta_h\phi_h^n\|_h \le C\left\|\nabla_{\mathbf{x}}\mu_{\phi,h}^n\right\|_{L^2(\Omega)} + C + (1-\vartheta)\left\|\Delta_h\phi_h^{n-1}\right\|_h\,. \tag{4.26}$$

As Young's inequality implies

$$(a+b+c)^2 = a^2+b^2+c^2+2ab+2ac+2bc \le C_\delta(a^2+b^2)+(1+2\delta)c^2 \tag{4.27}$$

for $a,b,c\in\mathbb{R}$ with $0<\delta\ll 1$, a discrete integration with respect to time over (4.26) yields

$$\vartheta^2\sum_{k=1}^n\tau\left\|\Delta_h\phi_h^k\right\|_h^2 \le C_\delta\left(\sum_{k=1}^n\left\|\nabla_{\mathbf{x}}\mu_{\phi,h}^k\right\|_{L^2(\Omega)}^2+T\right)+(1-\vartheta)^2(1+2\delta)\sum_{k=1}^n\tau\left\|\Delta_h\phi_h^{k-1}\right\|_h^2\,. \tag{4.28}$$

As we assumed $\vartheta\in(0.5,1]$, we have $\vartheta^2>(1-\vartheta)^2$. Therefore, we may choose $\delta>0$ such that $\vartheta^2-(1-\vartheta)^2(1+2\delta)=:\tilde{c}>0$. Noting the regularity assumptions on the initial data (*cf.* (A8)), we infer

$$\tilde{c}\sum_{k=0}^n\tau\left\|\Delta_h\phi_h^k\right\|_{L^2(\Omega)}^2 \le C_\delta(1+T)\,. \tag{4.29}$$

The last claim of Lemma 4.6 follows from Lemma 4.4 and the interpolation inequality

$$\|\chi_h\|_{L^\infty(\Omega)} \le C\|\Delta_h\chi_h\|_{L^2(\Omega)}^{1/2}\|\chi_h\|_{H^1(\Omega)}^{1/2}+\|\chi_h\|_{H^1(\Omega)} \qquad \text{for all } \chi_h\in U_h^{\mathbf{x}}, \tag{4.30}$$

which was proven in Corollary A.1 in [16]. □

Proof of Lemma 4.7. Following the lines of [18], we test (3.4a) by $\tau(\phi_h^{k+l}-\phi_h^k)$ with $0\le k\le N-l$ and sum from $n=k+1$ to $k+l$ to obtain

$$\begin{aligned}
0 =& \int_\Omega \mathcal{I}_h^{\mathbf{x}}\left\{\left|\phi_h^{k+l}-\phi_h^k\right|^2\right\} - \tau\sum_{n=k+1}^{k+l}\int_\Omega \phi_h^{n-1}\mathbf{u}_h^{n-1}\cdot\nabla_{\mathbf{x}}(\phi_h^{k+l}-\phi_h^k)\\
&+\tau^2\sum_{n=k+1}^{k+l}\int_\Omega\left|\phi_h^{n-1}\right|^2\nabla_{\mathbf{x}}\mu_{\phi,h}^n\cdot\nabla_{\mathbf{x}}(\phi_h^{k+l}-\phi_h^k)+\tau\sum_{n=k+1}^{k+l}\int_\Omega\nabla_{\mathbf{x}}\mu_{\phi,h}^n\cdot\nabla_{\mathbf{x}}(\phi_h^{k+l}-\phi_h^k)\\
=:& I+II+III+IV\,.
\end{aligned}\tag{4.31}$$

Using Hölder's inequality, the well-known Sobolev embedding theorem, and Poincaré's inequality, we compute

$$\begin{aligned}
|II| \le& \tau\sum_{n=k+1}^{k+l}\left\|\mathbf{u}_h^{n-1}\right\|_{L^6(\Omega)}\left\|\phi_h^{n-1}\right\|_{L^3(\Omega)}\left\|\nabla_{\mathbf{x}}\phi_h^{k+l}-\nabla_{\mathbf{x}}\phi_h^k\right\|_{L^2(\Omega)}\\
\le& C\sum_{m=0}^{l-1}\tau^{1/2}\left\|\nabla_{\mathbf{x}}\mathbf{u}_h^{k+m}\right\|_{L^2(\Omega)}\left\|\nabla_{\mathbf{x}}\phi_h^{k+m}\right\|_{L^2(\Omega)}\tau^{1/2}\left\|\nabla_{\mathbf{x}}\phi_h^{k+l}-\phi_h^k\right\|_{L^2(\Omega)}\,.
\end{aligned}\tag{4.32}$$

Noting the inequality $\left\|\phi_h^{n-1}\right\|_{L^\infty(\Omega)}\le C(1+\left\|\Delta_h\phi_h^{n-1}\right\|_{L^2(\Omega)})$, which is a direct consequence of the interpolation inequality (4.30) and Lemma 4.4 (see also [15]), we obtain

$$\begin{aligned}
|III| \le& \tau^2\sum_{n=k+1}^{k+l}\left\|\phi_h^{n-1}\right\|_{L^\infty(\Omega)}^2\left\|\nabla_{\mathbf{x}}\mu_{\phi,h}^n\right\|_{L^2(\Omega)}\left\|\nabla_{\mathbf{x}}\phi_h^{k+l}-\nabla_{\mathbf{x}}\phi_h^k\right\|_{L^2(\Omega)}^2\\
\le& C\sum_{m=0}^{l-1}\tau(1+\left\|\Delta_h\phi_h^{k+m}\right\|_{L^2(\Omega)})^2\tau^{1/2}\left\|\nabla_{\mathbf{x}}\mu_{\phi,h}^{k+m+1}\right\|_{L^2(\Omega)}\tau^{1/2}\left\|\nabla_{\mathbf{x}}\phi_h^{k+l}-\nabla_{\mathbf{x}}\phi_h^k\right\|_{L^2(\Omega)}\,.
\end{aligned}\tag{4.33}$$

We deduce by combining (4.31)–(4.33), multiplying by τ, summing from $k=0$ to $N-l$, and applying Hölder's inequality that

$$\begin{aligned}
\tau\sum_{k=0}^{N-l}\left\|\phi_h^{k+l}-\phi_h^k\right\|_h^2 \le& C\tau\sum_{m=0}^{l-1}\left(\sum_{k=0}^{N-l}\tau\left\|\nabla_{\mathbf{x}}\mathbf{u}_h^{k+m}\right\|_{L^2(\Omega)}^2\right)^{1/2}\left(\sup_{k=0,\dots,N-l}\left\|\nabla_{\mathbf{x}}\phi_h^{k+m}\right\|_{L^2(\Omega)}^2\right)^{1/2}\\
&\times\left(\sum_{k=0}^{N-l}\tau\left\|\nabla_{\mathbf{x}}\phi_h^{k+l}-\nabla_{\mathbf{x}}\phi_h^k\right\|_{L^2(\Omega)}^2\right)^{1/2}+C\tau\sum_{m=0}^{l-1}\left(\sum_{k=0}^{N-l}\tau\left(1+\left\|\Delta_h\phi_h^{k+m}\right\|_{L^2(\Omega)}\right)^2\right)\\
&\times\left(\sum_{k=0}^{N-l}\tau\left\|\nabla_{\mathbf{x}}\mu_{\phi,h}^{k+m+1}\right\|_{L^2(\Omega)}^2\right)^{1/2}\left(\sum_{k=0}^{N-l}\tau\left\|\nabla_{\mathbf{x}}\phi_h^{k+l}-\nabla_{\mathbf{x}}\phi_h^k\right\|_{L^2(\Omega)}^2\right)^{1/2}\\
&+C\tau\sum_{m=0}^{l-1}\left(\sum_{k=0}^{N-l}\tau\left\|\nabla_{\mathbf{x}}\mu_{\phi,h}^{k+m+1}\right\|_{L^2(\Omega)}^2\right)^{1/2}\left(\sum_{k=0}^{N-l}\tau\left\|\nabla_{\mathbf{x}}\phi_h^{k+l}-\nabla_{\mathbf{x}}\phi_h^k\right\|_{L^2(\Omega)}^2\right)^{1/2}.
\end{aligned}\tag{4.34}$$

Applying the results of Lemma 4.4 and Lemma 4.6 to the right-hand side of (4.34) and using the norm equivalence (2.10) yields the result. □

In a final step, we show compactness in time for the velocity field.

For this reason, we introduce the Helmholtz–Stokes operator $\boldsymbol{S} : \big(\boldsymbol{H}^1_{0,\mathrm{div}}(\Omega)\big)' \to \boldsymbol{H}^1_{0,\mathrm{div}}(\Omega)$, $\mathbf{v} \mapsto \boldsymbol{S}\{\mathbf{v}\}$, which is defined *via*

$$\int_\Omega \boldsymbol{S}\{\mathbf{v}\} \cdot \mathbf{w} \,\mathrm{d}\mathbf{x} + \int_\Omega \nabla_{\mathbf{x}} \boldsymbol{S}\{\mathbf{v}\} : \nabla_{\mathbf{x}} \mathbf{w} \,\mathrm{d}\mathbf{x} = \langle \mathbf{v}, \mathbf{w} \rangle \quad \forall \mathbf{w} \in \boldsymbol{H}^1_{0,\mathrm{div}}(\Omega), \tag{4.35}$$

where $\langle .,. \rangle$ denotes the duality pairing between $\big(\boldsymbol{H}^1_{0,\mathrm{div}}(\Omega)\big)'$ and $\boldsymbol{H}^1_{0,\mathrm{div}}(\Omega)$. This operator satisfies the following properties (see *e.g.* [5]).

(H1) $\langle \mathbf{v}, \boldsymbol{S}\{\mathbf{v}\} \rangle = \|\boldsymbol{S}\{\mathbf{v}\}\|^2_{H^1(\Omega)} \qquad \forall \mathbf{v} \in \big(\boldsymbol{H}^1_{0,\mathrm{div}}(\Omega)\big)'$,

(H2) $\|\boldsymbol{S}\{.\}\|_{H^1(\Omega)}$ is a norm on $\big(\boldsymbol{H}^1_{0,\mathrm{div}}(\Omega)\big)'$,

(H3) $\|\boldsymbol{S}\{\mathbf{v}\}\|^2_{L^2(\Omega)} + \|\nabla_{\mathbf{x}} \boldsymbol{S}\{\mathbf{v}\}\|^2_{L^2(\Omega)} \le \|\mathbf{v}\|^2_{L^2(\Omega)} \qquad \forall \mathbf{v} \in \boldsymbol{L}^2(\Omega)$,

(H4) $\|(\boldsymbol{I} - \boldsymbol{S})\{\mathbf{v}\}\|^2_{L^2(\Omega)} + \|\nabla_{\mathbf{x}} (\boldsymbol{I} - \boldsymbol{S})\{\mathbf{v}\}\|^2_{L^2(\Omega)} \le \|\nabla_{\mathbf{x}} \mathbf{v}\|^2_{L^2(\Omega)} \quad \forall \mathbf{v} \in \boldsymbol{H}^1_{0,\mathrm{div}}(\Omega)$,

where $\boldsymbol{I}$ denotes the identity operator on $\mathbb{R}^d$. Following the lines of [13], we also consider the orthogonal Stokes projector $\boldsymbol{R}_h : \boldsymbol{W}_{h,\mathrm{div}} \to \boldsymbol{H}^1_{0,\mathrm{div}}(\Omega)$ which is defined *via*

$$\int_\Omega \nabla_{\mathbf{x}} (\boldsymbol{R}_h\{\mathbf{v}_h\} - \mathbf{v}_h) : \nabla_{\mathbf{x}} \mathbf{w} = 0, \qquad \forall \mathbf{w} \in \boldsymbol{H}^1_{0,\mathrm{div}}(\Omega)\,. \tag{4.36}$$

Analogously to [13], where $\boldsymbol{R}_h$ is defined on a different finite element space, one can show that $\boldsymbol{R}_h$ satisfies the properties

$$\|\boldsymbol{R}_h\{\mathbf{v}_h\}\|_{H^1(\Omega)} \le C \|\mathbf{v}_h\|_{H^1(\Omega)}\,, \tag{4.37a}$$

$$\|\boldsymbol{R}_h\{\mathbf{v}_h\} - \mathbf{v}_h\|_{L^2(\Omega)} \le C h_{\mathbf{x}} \|\mathrm{div}_{\mathbf{x}}\, \mathbf{v}_h\|_{L^2(\Omega)}\,, \tag{4.37b}$$

$$\|\boldsymbol{R}_h\{\mathbf{v}_h\}\|_{(\boldsymbol{H}^1_{0,\mathrm{div}}(\Omega))'} \le C\Big(h_{\mathbf{x}} \|\mathrm{div}_{\mathbf{x}}\, \mathbf{v}_h\|_{L^2(\Omega)} + \|\mathbf{v}_h\|_{(\boldsymbol{H}^1_{0,\mathrm{div}}(\Omega))'} \Big) \tag{4.37c}$$

for $\mathbf{v}_h \in \boldsymbol{W}_{h,\mathrm{div}} \subset \boldsymbol{L}^2(\Omega) \subset \big(\boldsymbol{H}^1_{0,\mathrm{div}}(\Omega)\big)'$. To prove compactness in time for the velocity field, we start by establishing a bound, which is independent of h, τ, $\mathfrak{m}$, and ν, on the time derivative of the velocity in the dual space of $\boldsymbol{H}^1_{0,\mathrm{div}}(\Omega)$. Then we use this result to establish a regularity result for projected velocity field. In particular, we prove the following estimates.

Lemma 4.8. *Let the assumptions (A1)–(A9) hold true, let τ and $h_{\mathbf{x}}$ be small enough (such that Lem. 2.10 and Lem. 4.5 hold true), and let $\boldsymbol{S}$ be the Helmholtz–Stokes operator satisfying (H1)–(H4). Then there is a positive constant C independent of h, τ, $\mathfrak{m}$, and ν such that*

$$\sum_{k=1}^{N} \tau \left\| \boldsymbol{S}\{\partial_\tau^- \mathbf{u}_h^k\} \right\|^{4/\lambda}_{H^1(\Omega)} \le C \tag{4.38}$$

with $\lambda \in (2,4)$, if $d = 2$, or $\lambda = 3$, if $d = 3$.

Lemma 4.9. *Let the assumptions (A1)–(A9) hold true, let τ and $h_{\mathbf{x}}$ be small enough (such that Lem. 2.10 and Lem. 4.5 hold true), let $\boldsymbol{R}_h$ be the orthogonal Stokes projector satisfying (4.37). Then there is a positive constant C independent of h, τ, $\mathfrak{m}$, and ν such that*

$$\tau \sum_{k=0}^{N-l} \left\| \boldsymbol{R}_h\{\mathbf{u}_h^{k+l} - \mathbf{u}_h^k\} \right\|^2_{(\boldsymbol{H}^1_{0,\mathrm{div}}\Omega)'} \le C \tau l^{\lambda/4} + C h_{\mathbf{x}}^2$$

for all $l \in \{1, \dots, N\}$ with $\lambda \in (2,4)$, if $d = 2$, or $\lambda = 3$, if $d = 3$.

Noting that $\lambda/4<1$, these results will enable us to apply a "compactness by pertubation" result by Azérad and Guillén [4] and to identify strongly converging subsequences.

Proof of Lemma 4.8. $\boldsymbol{S}\{\partial_\tau^-\mathbf{u}_h^n\}\in\boldsymbol{H}^1_{0,\mathrm{div}}(\Omega)$ is well-defined as $\partial_\tau^-\mathbf{u}_h^n\in\boldsymbol{W}_{h,\mathrm{div}}\subset\boldsymbol{L}^2(\Omega)\subset(\boldsymbol{H}^1_{0,\mathrm{div}}(\Omega))'$. Recalling the H^1-stable L^2-projector $\mathcal{Q}_h$ from (TH2), we adapt the proof of a similar regularity result in [7] and test (3.4d) by $\mathcal{Q}_h[\boldsymbol{S}\{\partial_\tau^-\mathbf{u}_h^n\}]$.

$$\begin{aligned}
0=&\int_\Omega\partial_\tau^-\mathbf{u}_h^n\cdot\mathcal{Q}_h\big[\boldsymbol{S}\{\partial_\tau^-\mathbf{u}_h^n\}\big]-\tfrac12\int_\Omega\Big(\big(\nabla_{\mathbf{x}}\mathcal{Q}_h\big[\boldsymbol{S}\{\partial_\tau^-\mathbf{u}_h^n\}\big]\big)^T\cdot\mathbf{u}_h^n\Big)\cdot\mathbf{u}_h^{n-1}\\
&+\tfrac12\int_\Omega\Big((\nabla_{\mathbf{x}}\mathbf{u}_h^n)^T\cdot\mathcal{Q}_h\big[\boldsymbol{S}\{\partial_\tau^-\mathbf{u}_h^n\}\big]\Big)\cdot\mathbf{u}_h^{n-1}+\int_\Omega 2\mathcal{I}_h^{\mathbf{x}}\{\eta(\phi_h^n)\}\mathbf{D}\mathbf{u}_h^n:\mathbf{D}\mathcal{Q}_h\big[\boldsymbol{S}\{\partial_\tau^-\mathbf{u}_h^n\}\big]\\
&+\int_\Omega\phi_h^{n-1}\nabla_{\mathbf{x}}\mu_{\phi,h}^n\cdot\mathcal{Q}_h\big[\boldsymbol{S}\{\partial_\tau^-\mathbf{u}_h^n\}\big]+\int_{\Omega\times\mathfrak{D}}M_h\mathcal{Q}_h\big[\boldsymbol{S}\{\partial_\tau^-\mathbf{u}_h^n\}\big]\cdot\mathcal{I}_h^{\mathbf{q}}\Big\{\Lambda_\nu^{\mathbf{x}}[\hat\psi_h^n]\nabla_{\mathbf{x}}\mu_{\psi,h,\nu}^n\Big\}\\
&+\int_{\Omega\times\mathfrak{D}}\big(\nabla_{\mathbf{x}}\mathcal{I}_h^{\mathbf{x}}\big\{\boldsymbol{\mathcal{J}}_h\big\{\mathcal{Q}_h\big[\boldsymbol{S}\{\partial_\tau^-\mathbf{u}_h^n\}\big]\big\}\big\}\cdot\mathcal{I}_h^{\mathbf{q}}\{\mathbf{q}M_h\}\big)\cdot\nabla_{\mathbf{q}}\hat\psi_h^n\\
=:&\,I+II+III+IV+V+VI+VII\,.
\end{aligned}\tag{4.39}$$

We obtain from (TH2) and from (H1) that

$$I=\int_\Omega\partial_\tau^-\mathbf{u}_h^n\cdot\mathcal{Q}_h\big[\boldsymbol{S}\{\partial_\tau^-\mathbf{u}_h^n\}\big]=\big\|\boldsymbol{S}\{\partial_\tau^-\mathbf{u}_h^n\}\big\|_{H^1(\Omega)}^2\,.\tag{4.40}$$

Using Young's inequality together with the Gagliardo–Nirenberg inequality and Poincaré's inequality, we compute

$$\begin{aligned}
|II|&\le\delta\int_\Omega\big|\nabla_{\mathbf{x}}\mathcal{Q}_h\big[\boldsymbol{S}\{\partial_\tau^-\mathbf{u}_h^n\}\big]\big|^2+C_\delta\Big(\|\mathbf{u}_h^n\|_{L^4(\Omega)}^4+\big\|\mathbf{u}_h^{n-1}\big\|_{L^4(\Omega)}^4\Big)\\
&\le\delta\int_\Omega\big|\nabla_{\mathbf{x}}\mathcal{Q}_h\big[\boldsymbol{S}\{\partial_\tau^-\mathbf{u}_h^n\}\big]\big|^2+C_\delta\Big(\big\|\nabla_{\mathbf{x}}\mathbf{u}_h^{n-1}\big\|_{L^2(\Omega)}^d+\|\nabla_{\mathbf{x}}\mathbf{u}_h^n\|_{L^2(\Omega)}^d\Big)\,.
\end{aligned}\tag{4.41}$$

Young's inequality yields, together with Sobolev's embedding theorem,

$$|III|\le\delta\big\|\boldsymbol{S}\{\partial_\tau^-\mathbf{u}_h^n\}\big\|_{H^1(\Omega)}^2+C_\delta\big\|\big|\mathbf{u}_h^{n-1}\big|\,|\nabla_{\mathbf{x}}\mathbf{u}_h^n|\big\|_{L^{1+\sigma}(\Omega)}^2\tag{4.42}$$

with $\sigma\in(0,1)$ in the case $d=2$ and $\sigma=\frac15$ in the case $d=3$. Similarly to (4.77) in [7], we compute for $d=2$ and $\sigma=\frac{\lambda-2}{6-\lambda}$ by applying Hölder's inequality, the Gagliardo–Nirenberg inequality, Poincaré's inequality, and Young's inequality

$$\begin{aligned}
\big\|\big|\mathbf{u}_h^{n-1}\big|\,|\nabla_{\mathbf{x}}\mathbf{u}_h^n|\big\|_{L^{1+\sigma}(\Omega)}^2&\le\big\|\mathbf{u}_h^{n-1}\big\|_{L^{2(1+\sigma)/(1-\sigma)}(\Omega)}^2\|\nabla_{\mathbf{x}}\mathbf{u}_h^n\|_{L^2(\Omega)}^2\\
&\le C\big\|\mathbf{u}_h^{n-1}\big\|_{L^2(\Omega)}^{\frac{2(1-\sigma)}{1+\sigma}}\left(\|\nabla_{\mathbf{x}}\mathbf{u}_h^n\|_{L^2(\Omega)}^{\frac{2+6\sigma}{1+\sigma}}+\big\|\nabla_{\mathbf{x}}\mathbf{u}_h^{n-1}\big\|_{L^2(\Omega)}^{\frac{2+6\sigma}{1+\sigma}}\right)\\
&\le C\Big(\big\|\nabla_{\mathbf{x}}\mathbf{u}_h^{n-1}\big\|_{L^2(\Omega)}^\lambda+\|\nabla_{\mathbf{x}}\mathbf{u}_h^n\|_{L^2(\Omega)}^\lambda\Big),
\end{aligned}\tag{4.43}$$

where we used $\big\|\mathbf{u}_h^{n-1}\big\|_{L^2(\Omega)}\le C$ (*cf.* Lem. 4.4) in the last step. Analogously, we obtain for $d=3$

$$\begin{aligned}
\big\|\big|\mathbf{u}_h^{n-1}\big|\,|\nabla_{\mathbf{x}}\mathbf{u}_h^n|\big\|_{L^{6/5}(\Omega)}^2&\le C\big\|\mathbf{u}_h^{n-1}\big\|_{L^3(\Omega)}^2\|\nabla_{\mathbf{x}}\mathbf{u}_h^n\|_{L^2(\Omega)}^2\\
&\le C\big\|\mathbf{u}_h^{n-1}\big\|_{L^2(\Omega)}\Big(\big\|\nabla_{\mathbf{x}}\mathbf{u}_h^{n-1}\big\|_{L^2(\Omega)}^3+\|\nabla_{\mathbf{x}}\mathbf{u}_h^n\|_{L^2(\Omega)}^3\Big)\\
&\le C\Big(\big\|\nabla_{\mathbf{x}}\mathbf{u}_h^{n-1}\big\|_{L^2(\Omega)}^3+\|\nabla_{\mathbf{x}}\mathbf{u}_h^n\|_{L^2(\Omega)}^3\Big)\,.
\end{aligned}\tag{4.44}$$

Therefore,

$$|III| \leq \delta \left\|\boldsymbol{S}\{\partial_\tau^- \mathbf{u}_h^n\}\right\|_{H^1(\Omega)}^2 + C_\delta \Big(\left\|\nabla_{\mathbf{x}} \mathbf{u}_h^{n-1}\right\|_{L^2(\Omega)}^\lambda + \|\nabla_{\mathbf{x}} \mathbf{u}_h^n\|_{L^2(\Omega)}^\lambda \Big) . \tag{4.45}$$

As η is a bounded function, Young's inequality yields

$$|IV| \leq \delta \left\|\boldsymbol{S}\{\partial_\tau^- \mathbf{u}_h^n\}\right\|_{H^1(\Omega)}^2 + C_\delta \|\nabla_{\mathbf{x}} \mathbf{u}_h^n\|_{L^2(\Omega)}^2 . \tag{4.46}$$

Using Hölder's inequality, Sobolev's embedding theorem, Poincaré's inequality, the H^1-stability of $\mathcal{Q}_h$, Young's inequality, and the already established regularity results for ϕ_h^{n-1} (see Lem. 4.4), we compute for the fifth term on the right-hand side of (4.39)

$$\begin{aligned} |V| &\leq C \left\|\mathcal{Q}_h\big[\boldsymbol{S}\{\partial_\tau^- \mathbf{u}_h^n\}\big]\right\|_{H^1(\Omega)} \left\|\nabla_{\mathbf{x}} \phi_h^{n-1}\right\|_{L^2(\Omega)} \left\|\nabla_{\mathbf{x}} \mu_{\phi,h}^n\right\|_{L^2(\Omega)} \\ &\leq \delta \left\|\boldsymbol{S}\{\partial_\tau^- \mathbf{u}_h^n\}\right\|_{H^1(\Omega)}^2 + C_\delta \left\|\nabla_{\mathbf{x}} \mu_{\phi,h}^n\right\|_{L^2(\Omega)}^2 . \end{aligned} \tag{4.47}$$

In order to deal with the sixth term, we use an analogon of Young's inequality which is applicable in the case of matrix-valued coefficients. In particular, we apply the pointwise inequality

$$\begin{aligned} \mathcal{Q}_h\big[\boldsymbol{S}\{\partial_\tau^- \mathbf{u}_h^n\}\big] &\cdot \Big(\Lambda_\nu^{\mathbf{x}}[\hat{\psi}_{\mathrm{h}}^{\mathrm{n}}] \nabla_{\mathbf{x}} \mu_{\psi,h,\nu}^n\Big) \\ &\leq \delta \sigma^{\Lambda_\nu^{\mathbf{x}}[\hat{\psi}_{\mathrm{h}}^{\mathrm{n}}]} \left|\mathcal{Q}_h\big[\boldsymbol{S}\{\partial_\tau^- \mathbf{u}_h^n\}\big]\right|^2 + \tfrac{1}{4\delta} \Big(\sigma^{\Lambda_\nu^{\mathbf{x}}[\hat{\psi}_{\mathrm{h}}^{\mathrm{n}}]}\Big)^{-1} \left|\Lambda_\nu^{\mathbf{x}}[\hat{\psi}_{\mathrm{h}}^{\mathrm{n}}] \nabla_{\mathbf{x}} \mu_{\psi,h,\nu}^n\right|^2 \\ &\leq \delta \sigma^{\Lambda_\nu^{\mathbf{x}}[\hat{\psi}_{\mathrm{h}}^{\mathrm{n}}]} \left|\mathcal{Q}_h\big[\boldsymbol{S}\{\partial_\tau^- \mathbf{u}_h^n\}\big]\right|^2 + \tfrac{1}{4\delta} \Big(\Lambda_\nu^{\mathbf{x}}[\hat{\psi}_{\mathrm{h}}^{\mathrm{n}}] \nabla_{\mathbf{x}} \mu_{\psi,h,\nu}^n\Big) \cdot \nabla_{\mathbf{x}} \mu_{\psi,h,\nu}^n . \end{aligned} \tag{4.48}$$

Applying (4.48) to $|VI|$ yields

$$\begin{aligned} |VI| \leq\, & \tilde{\delta} \int_{\Omega\times\mathfrak{D}} M_h \left|\mathcal{Q}_h\big[\boldsymbol{S}\{\partial_\tau^- \mathbf{u}_h^n\}\big]\right|^2 \sigma^{\Lambda_\nu^{\mathbf{x}}[\hat{\psi}_{\mathrm{h}}^{\mathrm{n}}]}(\mathbf{x},\mathbf{q}) \\ &+ C_{\tilde{\delta}} \int_{\Omega\times\mathfrak{D}} M_h \mathcal{I}_h^{\mathbf{q}} \Big\{ \Big(\Lambda_\nu^{\mathbf{x}}[\hat{\psi}_{\mathrm{h}}^{\mathrm{n}}] \nabla_{\mathbf{x}} \mu_{\psi,h,\nu}^n\Big) \cdot \nabla_{\mathbf{x}} \mu_{\psi,h,\nu}^n \Big\}, \end{aligned} \tag{4.49}$$

where $\sigma^{\Lambda_\nu^{\mathbf{x}}[\hat{\psi}_{\mathrm{h}}^{\mathrm{n}}]}(\mathbf{x},\mathbf{q})$ denotes the supremum of the largest eigenvalue of $\Lambda_\nu^{\mathbf{x}}[\hat{\psi}_{\mathrm{h}}^{\mathrm{n}}]$ on $\kappa_{\mathbf{x}} \times \kappa_{\mathbf{q}} \ni (\mathbf{x},\mathbf{q})$. Recalling (2.27f), we obtain

$$\begin{aligned} \int_{\Omega\times\mathfrak{D}} & M_h \left|\mathcal{Q}_h\big[\boldsymbol{S}\{\partial_\tau^- \mathbf{u}_h^n\}\big]\right|^2 \sigma^{\Lambda_\nu^{\mathbf{x}}[\hat{\psi}_{\mathrm{h}}^{\mathrm{n}}]}(\mathbf{x},\mathbf{q}) \\ &\leq \bigg(\int_{\Omega\times\mathfrak{D}} M_h \left|\mathcal{Q}_h\big[\boldsymbol{S}\{\partial_\tau^- \mathbf{u}_h^n\}\big]\right|^4\bigg)^{1/2} \bigg(\int_{\Omega\times\mathfrak{D}} M_h \left|\sigma^{\Lambda_\nu^{\mathbf{x}}[\hat{\psi}_{\mathrm{h}}^{\mathrm{n}}]}(\mathbf{x},\mathbf{q})\right|^2\bigg)^{1/2} \\ &\leq C \left\|\mathcal{Q}_h\big[\boldsymbol{S}\{\partial_\tau^- \mathbf{u}_h^n\}\big]\right\|_{L^4(\Omega)}^2 \bigg(\int_{\Omega\times\mathfrak{D}} M_h \nu^2 + \int_{\Omega\times\mathfrak{D}} M_h \mathcal{I}_h^{\mathbf{xq}} \Big\{ \left|\hat{\psi}_h^n\right|^2 \Big\}\bigg)^{1/2} \\ &\leq C \left\|\boldsymbol{S}\{\partial_\tau^- \mathbf{u}_h^n\}\right\|_{H^1(\Omega)}^2 . \end{aligned} \tag{4.50}$$

Therefore, we have

$$|VI| \leq \delta \left\|\boldsymbol{S}\{\partial_\tau^- \mathbf{u}_h^n\}\right\|_{H^1(\Omega)}^2 + C_\delta \int_{\Omega\times\mathfrak{D}} M_h \mathcal{I}_h^{\mathbf{q}} \Big\{ \Big(\Lambda_\nu^{\mathbf{x}}[\hat{\psi}_{\mathrm{h}}^{\mathrm{n}}] \nabla_{\mathbf{x}} \mu_{\psi,h,\nu}^n\Big) \cdot \nabla_{\mathbf{x}} \mu_{\psi,h,\nu}^n \Big\}, \tag{4.51}$$

with some $0 < \delta \ll 1$. Due to our specific discretization (*cf.* Rem. 3.4), the stability result in Lemma 4.4 enables us to control the L^2-norm with respect to time of the second term.
As $\mathfrak{D}$ is bounded, we use Hölder's inequality to compute

$$|VII| \leq C\left(\int_{\Omega\times\mathfrak{D}} M_h \left|\nabla_{\mathbf{x}}\mathcal{I}_h^{\mathbf{x}}\big\{\boldsymbol{\mathcal{J}}_h\big\{\mathcal{Q}_h\big[\boldsymbol{S}\big\{\partial_\tau^- \mathbf{u}_h^n\big\}\big]\big\}\big\}\right|^2\right)^{1/2}\left(\int_{\Omega\times\mathfrak{D}} M_h\mathcal{I}_h^{\mathbf{x}}\left\{\left|\nabla_{\mathbf{q}}\hat{\psi}_h^n\right|^2\right\}\right)^{1/2}. \tag{4.52}$$

Due to the mean value theorem, Lemma 2.10, and the H^1-stability of $\mathcal{Q}_h$, we may compute

$$\begin{aligned}\left(\int_{\Omega\times\mathfrak{D}} M_h \left|\nabla_{\mathbf{x}}\mathcal{I}_h^{\mathbf{x}}\big\{\boldsymbol{\mathcal{J}}_h\big\{\mathcal{Q}_h\big[\boldsymbol{S}\big\{\partial_\tau^- \mathbf{u}_h^n\big\}\big]\big\}\big\}\right|^2\right)^{1/2} &\leq C\left\|\nabla_{\mathbf{x}}\boldsymbol{\mathcal{J}}_h\big\{\mathcal{Q}_h\big[\boldsymbol{S}\big\{\partial_\tau^- \mathbf{u}_h^n\big\}\big]\big\}\right\|_{L^\infty(\Omega)} \\ &\leq C\left\|\boldsymbol{S}\big\{\partial_\tau^- \mathbf{u}_h^n\big\}\right\|_{H^1(\Omega)}.\end{aligned} \tag{4.53}$$

Combining (4.52) with (4.53) and applying Young's inequality, we deduce

$$|VII| \leq \delta\left\|\boldsymbol{S}\big\{\partial_\tau^- \mathbf{u}_h^n\big\}\right\|_{H^1(\Omega)}^2 + C_\delta\int_{\Omega\times\mathfrak{D}} M_h\mathcal{I}_h^{\mathbf{x}}\left\{\left|\nabla_{\mathbf{q}}\hat{\psi}_h^n\right|^2\right\}. \tag{4.54}$$

Collecting the above results and taking the $\frac{2}{\lambda}$ power on both sides, we obtain

$$\begin{aligned}\left\|\boldsymbol{S}\big\{\partial_\tau^- \mathbf{u}_h^n\big\}\right\|_{H^1(\Omega)}^{4/\lambda} \leq\, & C + C\left\|\nabla_{\mathbf{x}}\mathbf{u}_h^{n-1}\right\|_{L^2(\Omega)}^2 + C\left\|\nabla_{\mathbf{x}}\mathbf{u}_h^n\right\|_{L^2(\Omega)}^2 + C\left\|\nabla_{\mathbf{x}}\mu_{\phi,h}^n\right\|_{L^2(\Omega)}^2 \\ &+ C\int_{\Omega\times\mathfrak{D}} M_h\mathcal{I}_h^{\mathbf{q}}\left\{\left(\Lambda_\nu^{\mathbf{x}}[\hat{\psi}_{\mathrm{h}}^{\mathrm{n}}]\nabla_{\mathbf{x}}\mu_{\psi,h,\nu}^n\right)\cdot\nabla_{\mathbf{x}}\mu_{\psi,h,\nu}^n\right\} \\ &+ C\int_{\Omega\times\mathfrak{D}} M_h\mathcal{I}_h^{\mathbf{x}}\left\{\left|\nabla_{\mathbf{q}}\hat{\psi}_h^n\right|^2\right\}.\end{aligned} \tag{4.55}$$

A discrete integration with respect to time, together with (A8) and the results of Lemma 4.4 and Lemma 4.5, finally provides the result. ☐

Proof of Lemma 4.9. From (4.37c) we obtain

$$\begin{aligned}&\tau\sum_{k=0}^{N-l}\left\|\boldsymbol{R}_h\big\{\mathbf{u}_h^{k+l}-\mathbf{u}_h^k\big\}\right\|_{(\boldsymbol{H}^1_{0,\mathrm{div}}(\Omega))'}^2 \\ &\qquad\leq C\tau\sum_{k=0}^{N-l}\left\|\mathbf{u}_h^{k+l}-\mathbf{u}_h^k\right\|_{(\boldsymbol{H}^1_{0,\mathrm{div}}(\Omega))'}^2 + Ch_{\mathbf{x}}^2\tau\sum_{k=0}^{N-l}\left\|\mathrm{div}_{\mathbf{x}}\big\{\mathbf{u}_h^{k+l}-\mathbf{u}_h^k\big\}\right\|_{L^2(\Omega)}^2.\end{aligned} \tag{4.56}$$

Applying Hölder's inequality and (H3) provides

$$\begin{aligned}&\tau\sum_{k=0}^{N-l}\left\|\mathbf{u}_h^{k+l}-\mathbf{u}_h^k\right\|_{(\boldsymbol{H}^1_{0,\mathrm{div}}(\Omega))'}^2 \\ &\qquad\leq\left(\tau\sum_{k=0}^{N-l}\left\|\mathbf{u}_h^{k+l}-\mathbf{u}_h^k\right\|_{(\boldsymbol{H}^1_{0,\mathrm{div}}(\Omega))'}^{4/\lambda}\right)^{\lambda/4}\left(\tau\sum_{k=0}^{N-l}\left\|\mathbf{u}_h^{k+l}-\mathbf{u}_h^k\right\|_{L^2(\Omega)}^{4/(4-\lambda)}\right)^{(4-\lambda)/\lambda}.\end{aligned} \tag{4.57}$$

Due to the L^∞-L^2-bound for the velocity field obtained in Lemma 3.8, the second factor is bounded. Concerning the first factor, we use Lemma 4.8 and compute

$$\tau\sum_{k=0}^{N-l}\left\|\mathbf{u}_h^{k+l}-\mathbf{u}_h^k\right\|_{(\boldsymbol{H}^1_{0,\mathrm{div}}(\Omega))'}^{4/\lambda} \leq C\tau\sum_{k=0}^{N-l}\sum_{m=1}^{l}\tau^{4/\lambda}\left\|\partial_\tau^-\mathbf{u}_h^{k+m}\right\|_{(\boldsymbol{H}^1_{0,\mathrm{div}}(\Omega))'}^{4/\lambda} \leq C\tau^{4/\lambda}l\,. \tag{4.58}$$

Combining Korn's inequality and Lemma 3.8 shows that the second term on the right-hand side of (4.56) is bounded by $Ch_{\mathbf{x}}^2$, which gives the result. ☐

To conclude this section, we collect the bounds derived so far. In particular, we have

$$\begin{aligned}\max_{k=1,\dots,n}\int_\Omega \left|\nabla_{\mathbf{x}}\phi_h^k\right|^2 + \max_{k=1,\dots,n}\int_\Omega \left|\mathbf{u}_h^k\right| + \max_{k=1,\dots,n}\int_{\Omega\times\mathfrak{D}} (M_h+\mathfrak{m})\left|\hat{\psi}_h^k\right|^2 \\ + \nu^{-1}\max_{k=1,\dots,n}\int_{\Omega\times\mathfrak{D}} (M_h+\mathfrak{m})\mathcal{I}_h^{\mathbf{xq}}\left\{[\hat{\psi}_h^k]_-^2\right\} \\ + \sum_{k=1}^n\int_\Omega\left|\nabla_{\mathbf{x}}\phi_h^k-\nabla_{\mathbf{x}}\phi_h^{k-1}\right|^2 + \sum_{k=1}^n\left|\mathbf{u}_h^k-\mathbf{u}_h^{k-1}\right|^2 + \sum_{k=1}^n\int_{\Omega\times\mathfrak{D}}(M_h+\mathfrak{m})\left|\hat{\psi}_h^k-\hat{\psi}_h^{k-1}\right|^2 \\ + \tau\sum_{k=0}^n\int_\Omega\left|\Delta_h\phi_h^k\right|^2 + \tau\sum_{k=0}^n\left\|\phi_h^k\right\|_{L^\infty(\Omega)}^2 + \tau\sum_{k=1}^n\int_\Omega\left|\nabla_{\mathbf{x}}\mu_{\phi,h}^k\right|^2 + \tau\sum_{k=1}^n\int_\Omega\left|\nabla_{\mathbf{x}}\mathbf{u}_h^k\right|^2 \\ + \tau\sum_{k=0}^n\int_{\Omega\times\mathfrak{D}}M_h\left|\nabla_{\mathbf{x}}\hat{\psi}_h^k\right|^2 + \tau\sum_{k=0}^n\int_{\Omega\times\mathfrak{D}}M_h\left|\nabla_{\mathbf{q}}\hat{\psi}_h^k\right|^2 + \tau\sum_{k=1}^n\left\|\boldsymbol{S}\{\partial_\tau^-\mathbf{u}_h^k\}\right\|_{H^1(\Omega)}^{4/\lambda} \leq C\end{aligned} \tag{4.59a}$$

and

$$\tau\sum_{k=0}^{N-l}\left\|\phi_h^{k+l}-\phi_h^k\right\|_{L^2(\Omega)}^2 \leq Cl\tau,\quad \tau\sum_{k=0}^{N-l}\left\|\boldsymbol{R}_h\{\mathbf{u}_h^{k+l}-\mathbf{u}_h^k\}\right\|_{(\boldsymbol{H}_{0,\mathrm{div}}^1(\Omega))'}^2 \leq C(l\tau)^{\lambda/4}+Ch_{\mathbf{x}}^2 \tag{4.59b}$$

for all $l\in\{1,\dots,N\}$, as $\lambda/4<1$.

5. Passage to the limit

In this section, we simultaneously pass to the limit $(h,\tau,\mathfrak{m},\nu)\searrow 0$. For this purpose, we define time-interpolants of time-discrete functions a^n, $n=0,\dots,N$, and introduce some time-index-free notation as follows.

$$a^\tau(.,t) := \tfrac{t-t^{n-1}}{\tau}a^n(.) + \tfrac{t^n-t}{\tau}a^{n-1}(.) \qquad t\in[t^{n-1},t^n], n\geq 1, \tag{5.1a}$$

$$a^{\tau,+}(.,t) := a^n(.),\quad a^{\tau,-}(.,t) := a^{n-1}(.) \qquad t\in(t^{n-1},t^n], n\geq 1. \tag{5.1b}$$

We want to point out that the time derivative of a^τ coincides with the difference quotient, *i.e.*

$$\partial_t a^\tau = \partial_t\left(\tfrac{t-t^{n-1}}{\tau}a^n + \tfrac{t^n-t}{\tau}a^{n-1}\right) = \tfrac{1}{\tau}a^n - \tfrac{1}{\tau}a^{n-1} = \partial_\tau^- a^n\,. \tag{5.2}$$

If a statement is valid for a^τ, $a^{\tau,+}$, and $a^{\tau,-}$, we will use the abbreviation $a^{\tau,(\pm)}$.

Using these notations and summing (3.4a)–(3.4d) from $n=1$ to N, we restate our set of equations as

$$\int_{\Omega_T}\mathcal{I}_h^{\mathbf{x}}\{\partial_t\phi_h^\tau\theta_h^{\mathbf{x}}\} - \int_{\Omega_T}(\mathbf{u}_h^{\tau,-}-\tau\phi_h^{\tau,-}\nabla_{\mathbf{x}}\mu_{\phi,h}^{\tau,+})\phi_h^{\tau,-}\cdot\nabla_{\mathbf{x}}\theta_h^{\mathbf{x}} + \int_{\Omega_T}\nabla_{\mathbf{x}}\mu_{\phi,h}^{\tau,+}\cdot\nabla_{\mathbf{x}}\theta_h^{\mathbf{x}} = 0 \qquad \forall\theta^{\mathbf{x}}\in L^2(0,T;U_h^{\mathbf{x}}), \tag{5.3a}$$

$$\begin{aligned}\int_{\Omega_T}\mathcal{I}_h^{\mathbf{x}}\left\{\mu_{\phi,h}^{\tau,+}\theta_h^{\mathbf{x}}\right\} = \int_{\Omega_T}\mathcal{I}_h^{\mathbf{x}}\{W_h'(\phi_h^{\tau,+},\phi_h^{\tau,-})\theta_h^{\mathbf{x}}\} + \int_{\Omega_T}(\vartheta\nabla_{\mathbf{x}}\phi_h^{\tau,+}+(1-\vartheta)\nabla_{\mathbf{x}}\phi_h^{\tau,-})\cdot\nabla_{\mathbf{x}}\theta_h^{\mathbf{x}} \\ + \int_{\Omega_T}\mathcal{I}_h^{\mathbf{x}}\left\{\mathcal{J}_h\{\mathcal{I}_h^{\mathbf{x}}\{\beta_{DQ}'(\phi_h^{\tau,+},\phi_h^{\tau,-})\theta_h^{\mathbf{x}}\}\}\int_{\mathfrak{D}}(M_h+\mathfrak{m})\hat{\psi}_h^{\tau,-}\right\} \qquad \forall\theta_h^{\mathbf{x}}\in L^2(0,T;U_h^{\mathbf{x}}),\end{aligned} \tag{5.3b}$$

$$\int_{\Omega_T\times\mathfrak{D}}(M_h+\mathfrak{m})\mathcal{I}_h^{\mathbf{xq}}\Big\{\partial_t\hat{\psi}_h^{\tau}\theta_h\Big\}-\int_{\Omega_T\times\mathfrak{D}}M_h\mathbf{u}_h^{\tau,+}\cdot\mathcal{I}_h^{\mathbf{q}}\Big\{\Lambda_\nu^{\mathbf{x}}[\hat{\psi}_{\mathrm{h}}^{\tau,+}]\nabla_{\mathbf{x}}\theta_h\Big\}$$
$$-\int_{\Omega_T\times\mathfrak{D}}\big(\nabla_{\mathbf{x}}\mathcal{I}_h^{\mathbf{x}}\{\boldsymbol{\mathcal{J}}_h\{\mathbf{u}_h^{\tau,+}\}\}\cdot\mathcal{I}_h^{\mathbf{q}}\{\mathbf{q}M_h\}\big)\cdot\mathcal{I}_h^{\mathbf{x}}\Big\{\Xi_\nu^{\mathbf{q}}[\hat{\psi}_{\mathrm{h}}^{\tau,+}]\nabla_{\mathbf{q}}\theta_h\Big\}$$
$$+\int_{\Omega_T\times\mathfrak{D}}c_{\mathbf{x}}M_h\mathcal{I}_h^{\mathbf{q}}\Big\{\Big(\Big((1-\gamma)\Xi_\nu^{\mathbf{x}}[\hat{\psi}_{\mathrm{h}}^{\tau,+}]+\gamma\Lambda_\nu^{\mathbf{x}}[\hat{\psi}_{\mathrm{h}}^{\tau,+}]\Big)\nabla_{\mathbf{x}}\mu_{\psi,h,\nu}^{\tau,+}\Big)\cdot\nabla_{\mathbf{x}}\theta_h\Big\} \tag{5.3c}$$
$$+\int_{\Omega_T\times\mathfrak{D}}c_{\mathbf{q}}M_h\mathcal{I}_h^{\mathbf{x}}\Big\{\nabla_{\mathbf{q}}\hat{\psi}_h^{\tau,+}\cdot\nabla_{\mathbf{q}}\theta_h\Big\}=0$$
$$\forall\theta_h\in L^2(0,T;\hat{X}_h),$$

$$\int_{\Omega_T}\partial_t\mathbf{u}_h^{\tau}\cdot\mathbf{w}_h-\tfrac{1}{2}\int_{\Omega_T}\Big((\nabla_{\mathbf{x}}\mathbf{w}_h)^T\cdot\mathbf{u}_h^{\tau,+}\Big)\cdot\mathbf{u}_h^{\tau,-}+\tfrac{1}{2}\int_{\Omega_T}\Big((\nabla_{\mathbf{x}}\mathbf{u}_h^{\tau,+})^T\cdot\mathbf{w}_h\Big)\cdot\mathbf{u}_h^{\tau,-}$$
$$+\int_{\Omega_T}2\mathcal{I}_h^{\mathbf{x}}\{\eta(\phi_h^{\tau,+})\}\mathbf{D}\mathbf{u}_h^{\tau,+}:\mathbf{D}\mathbf{w}_h=-\int_{\Omega_T}\phi_h^{\tau,-}\nabla_{\mathbf{x}}\mu_{\phi,h}^{\tau,+}\cdot\mathbf{w}_h$$
$$-\int_{\Omega_T\times\mathfrak{D}}M_h\mathbf{w}_h\cdot\mathcal{I}_h^{\mathbf{q}}\Big\{\Lambda_\nu^{\mathbf{x}}[\hat{\psi}_{\mathrm{h}}^{\tau,+}]\nabla_{\mathbf{x}}\mu_{\psi,h,\nu}^{\tau,+}\Big\}-\int_{\Omega_T\times\mathfrak{D}}(\nabla_{\mathbf{x}}\mathcal{I}_h^{\mathbf{x}}\{\boldsymbol{\mathcal{J}}_h\{\mathbf{w}_h\}\}\cdot\mathcal{I}_h^{\mathbf{q}}\{\mathbf{q}M_h\})\cdot\nabla_{\mathbf{q}}\hat{\psi}_h^{\tau,+}$$
$$\forall\mathbf{w}_h\in L^{4/(4-\lambda)}(0,T;\boldsymbol{W}_{h,\mathrm{div}}), \tag{5.3d}$$

where we again used the abbreviation

$$\mu_{\psi,h,\nu}^{\tau,+}:=\mathcal{I}_h^{\mathbf{xq}}\Big\{g_\nu'(\hat{\psi}_h^{\tau,+})+\mathcal{J}_\varepsilon\{\beta(\phi_h^{\tau,+})\}\Big\}. \tag{5.4}$$

Similarly, we rewrite the bounds from (4.59) as

$$\int_0^{T-l\tau}\big\|\phi_h^{\tau,+}(\cdot+l\tau)-\phi_h^{\tau,+}(\cdot)\big\|_{L^2(\Omega)}^2\leq C(l\tau)\quad\forall l\in\{1,\dots,N\}, \tag{5.5a}$$

$$\int_0^{T-l\tau}\big\|\boldsymbol{R}_h\{\mathbf{u}_h^{\tau,+}(\cdot+l\tau)\}-\boldsymbol{R}_h\{\mathbf{u}_h^{\tau,+}(\cdot)\}\big\|_{(\boldsymbol{H}_{0,\mathrm{div}}^1(\Omega))'}^2\leq C(l\tau)^{\lambda/4}+Ch_{\mathbf{x}}^2$$
$$\forall l\in\{1,\dots,N\}, \tag{5.5b}$$

$$\sup_{t\in[0,T]}\int_\Omega\Big|\nabla_{\mathbf{x}}\phi_h^{\tau,(\pm)}\Big|^2+\tau^{-1}\int_{\Omega_T}\big|\nabla_{\mathbf{x}}\phi_h^{\tau,+}-\nabla_{\mathbf{x}}\phi_h^{\tau,-}\big|^2+\int_{\Omega_T}\Big|\Delta_h\phi_h^{\tau,(\pm)}\Big|^2$$
$$+\int_0^T\Big\|\phi_h^{\tau,(\pm)}\Big\|_{L^\infty(\Omega)}^4+\int_{\Omega_T}\Big|\nabla_{\mathbf{x}}\mu_{\phi,h}^{\tau,+}\Big|^2$$
$$+\sup_{t\in[0,T]}\int_{\Omega_T\times\mathfrak{D}}(M_h+\mathfrak{m})\mathcal{I}_h^{\mathbf{xq}}\Big\{\Big|\hat{\psi}_h^{\tau,(\pm)}\Big|^2\Big\}+\nu^{-1}\sup_{t\in[0,T]}\int_{\Omega\times\mathfrak{D}}(M_h+\mathfrak{m})\mathcal{I}_h^{\mathbf{xq}}\Big\{[\hat{\psi}_h^{\tau,(\pm)}]_-^2\Big\}$$
$$+\tau^{-1}\int_{\Omega_T\times\mathfrak{D}}(M_h+\mathfrak{m})\mathcal{I}_h^{\mathbf{xq}}\Big\{\Big|\hat{\psi}_h^{\tau,+}-\hat{\psi}_h^{\tau,-}\Big|^2\Big\}+\int_{\Omega_T\times\mathfrak{D}}M_h\mathcal{I}_h^{\mathbf{q}}\Big\{\Big|\nabla_{\mathbf{x}}\hat{\psi}_h^{\tau,(\pm)}\Big|^2\Big\}$$
$$+\int_{\Omega_T\times\mathfrak{D}}M_h\mathcal{I}_h^{\mathbf{x}}\Big\{\Big|\nabla_{\mathbf{q}}\hat{\psi}_h^{\tau,(\pm)}\Big|^2\Big\}+\int_{\Omega_T\times\mathfrak{D}}M_h\mathcal{I}_h^{\mathbf{q}}\Big\{\Big(\Xi_\nu^{\mathbf{x}}[\hat{\psi}_{\mathrm{h}}^{\tau,+}]\nabla_{\mathbf{x}}\mu_{\psi,h,\nu}^{\tau,+}\Big)\cdot\nabla_{\mathbf{x}}\mu_{\psi,h,\nu}^{\tau,+}\Big\}$$
$$+\int_{\Omega_T\times\mathfrak{D}}M_h\mathcal{I}_h^{\mathbf{q}}\Big\{\Big(\Lambda_\nu^{\mathbf{x}}[\hat{\psi}_{\mathrm{h}}^{\tau,+}]\nabla_{\mathbf{x}}\mu_{\psi,h,\nu}^{\tau,+}\Big)\cdot\nabla_{\mathbf{x}}\mu_{\psi,h,\nu}^{\tau,+}\Big\}$$

$$+\sup_{t\in[0,T]}\int_\Omega \left|\mathbf{u}_h^{\tau,(\pm)}\right|^2 + \tau^{-1}\int_{\Omega_T}\left|\mathbf{u}_h^{\tau,+}-\mathbf{u}_h^{\tau,-}\right|^2 + \int_{\Omega_T}\left|\mathbf{D}\mathbf{u}_h^{\tau,(\pm)}\right|^2 + \int_0^T \|\boldsymbol{S}\{\partial_t \mathbf{u}_h^\tau\}\|_{H^1(\Omega)}^{4/\lambda}$$
$$\leq C\,. \tag{5.5c}$$

Applying (2.12a)–(2.12c) and noting the results of Lemma 4.3, we additionally obtain

$$\sup_{t\in[0,T]}\int_{\Omega\times\mathfrak{D}}(M_h+\mathfrak{m})\left|\hat\psi_h^{\tau,(\pm)}\right|^2 + \tau^{-1}\int_{\Omega_T\times\mathfrak{D}}(M_h+\mathfrak{m})\left|\hat\psi_h^{\tau,+}-\hat\psi_h^{\tau,-}\right|^2$$
$$+\int_{\Omega_T\times\mathfrak{D}} M_h\left|\nabla_{\mathbf{x}}\hat\psi_h^{\tau,(\pm)}\right|^2 + \int_{\Omega_T\times\mathfrak{D}} M_h\left|\nabla_{\mathbf{q}}\hat\psi_h^{\tau,(\pm)}\right|^2$$
$$+\sup_{t\in[0,T]}\int_{\Omega\times\mathfrak{D}}\hat M\left|\hat\psi_h^{\tau,(\pm)}\right|^2 + \tau^{-1}\int_{\Omega_T\times\mathfrak{D}}\hat M\left|\hat\psi_h^{\tau,+}-\hat\psi_h^{\tau,-}\right|^2 \leq C\,. \tag{5.5d}$$

We use the bounds in (5.5) to show the existence of a subsequence, which is again denoted by $(\phi_h^{\tau,(\pm)},\mu_{\phi,h}^{\tau,(\pm)},\hat\psi_h^{\tau,(\pm)},\mathbf{u}_h^{\tau,(\pm)})_{(h,\tau,\mathfrak{m},\nu)}$, converging towards limit functions in an appropriate sense. As we only have Maxwellian-weighted bounds for the scaled configurational density function $\hat\psi_h^{\tau,(\pm)}$, we may not expect to obtain any information on the limit function outside of D. As we will show in Theorem 5.2, the values of the limit functions on $\Omega_T\times\mathfrak{D}\setminus D$ are negligible, as the integrals over this part of the domain do not contribute to the weak formulation. Therefore, we concentrate on identifying its limit functions on $\Omega_T\times D$. Analogously to the notation $a^{\tau,(\pm)}$, we denote the triple of limit functions $(a,\, a^+,\, a^-)$ by $a^{(\pm)}$.

Lemma 5.1. *Let the assumptions (A1)–(A9) hold true. Then there exists a subsequence (again denoted by* $(\phi_h^{\tau,(\pm)},\mu_{\phi,h}^{\tau,(\pm)},\hat\psi_h^{\tau,(\pm)},\mathbf{u}_h^{\tau,(\pm)})_{(h,\tau,\mathfrak{m},\nu)}$*) and functions* ϕ*,* μ_ϕ*, and* $\mathbf{u}$ *satisfying*

$$\phi\in L^\infty(0,T;H^1(\Omega))\cap L^2(0,T;H^2(\Omega))\cap L^4(0,T;L^\infty(\Omega)), \tag{5.6a}$$
$$\mu_\phi\in L^2(0,T;H^1(\Omega)), \tag{5.6b}$$
$$\mathbf{u}\in L^\infty(0,T;\boldsymbol{L}^2(\Omega))\cap L^2(0,T;\boldsymbol{H}^1_{0,\mathrm{div}}(\Omega))\cap W^{1,4/\lambda}(0,T;(\boldsymbol{H}^1_{0,\mathrm{div}}(\Omega))'), \tag{5.6c}$$

with $\lambda\in(2,4)$*, if* $d=2$*, and* $\lambda=3$*, if* $d=3$*, as well as functions* $\hat\psi$*,* P_1*,* P_2*,* P_3*,* $\boldsymbol{P}_4^{(\pm)}$*,* $\boldsymbol{P}_5^{(\pm)}$ *satisfying*

$$\hat\psi\in L^2(0,T;\hat X_+)\cap L^\infty(0,T;L^2(\Omega\times D;M)), \tag{5.6d}$$
$$P_1,P_2,P_3\in L^\infty(0,T;L^2(\Omega\times\mathfrak{D})), \tag{5.6e}$$
$$\boldsymbol{P}_4^{(\pm)},\boldsymbol{P}_5^{(\pm)}\in L^2(0,T;\boldsymbol{L}^2(\Omega\times\mathfrak{D})), \tag{5.6f}$$

with

$$P_1\big|_{\Omega_T\times D}=P_2\big|_{\Omega_T\times D}=P_3\big|_{\Omega_T\times D}=\sqrt{M}\hat\psi, \tag{5.7a}$$
$$\boldsymbol{P}_4^{(\pm)}\Big|_{\Omega_T\times D}=\sqrt{M}\nabla_{\mathbf{x}}\hat\psi, \tag{5.7b}$$
$$\boldsymbol{P}_5^{(\pm)}\Big|_{\Omega_T\times D}=\sqrt{M}\nabla_{\mathbf{q}}\hat\psi, \tag{5.7c}$$

such that, as $(h, \tau, \mathfrak{m}, \nu) \searrow 0$,

$$\phi_h^{\tau,(\pm)} \overset{*}{\rightharpoonup} \phi \quad \text{in } L^\infty(0,T;H^1(\Omega)), \tag{5.8a}$$
$$\phi_h^{\tau,(\pm)} \overset{*}{\rightharpoonup} \phi \quad \text{in } L^4(0,T;L^\infty(\Omega)), \tag{5.8b}$$
$$\phi_h^{\tau,(\pm)} \rightarrow \phi \quad \text{in } L^p(0,T;L^s(\Omega)), \quad \forall p<\infty,\ s\in[1,\tfrac{2d}{d-2}), \tag{5.8c}$$
$$\Delta_h \phi_h^{\tau,(\pm)} \rightharpoonup \Delta\phi \quad \text{in } L^2(0,T;L^2(\Omega)), \tag{5.8d}$$
$$\mu_{\phi,h}^{\tau,+} \rightharpoonup \mu_\phi \quad \text{in } L^2(0,T;H^1(\Omega)), \tag{5.8e}$$

$$M_h \rightarrow \hat{M} \quad \text{in } L^\infty(\mathfrak{D}), \tag{5.9a}$$
$$\sqrt{\hat{M}}\hat{\psi}_h^{\tau,(\pm)} \overset{*}{\rightharpoonup} P_1 \quad \text{in } L^\infty(0,T;L^2(\Omega\times\mathfrak{D})), \tag{5.9b}$$
$$\sqrt{M_h+\mathfrak{m}}\hat{\psi}_h^{\tau,(\pm)} \overset{*}{\rightharpoonup} P_2 \quad \text{in } L^\infty(0,T;L^2(\Omega\times\mathfrak{D})), \tag{5.9c}$$
$$\sqrt{M_h}\hat{\psi}_h^{\tau,(\pm)} \overset{*}{\rightharpoonup} P_3 \quad \text{in } L^\infty(0,T;L^2(\Omega\times\mathfrak{D})), \tag{5.9d}$$
$$\sqrt{M_h}\nabla_{\mathbf{x}}\hat{\psi}_h^{\tau,(\pm)} \rightharpoonup \boldsymbol{P}_4^{(\pm)} \quad \text{in } L^2(0,T;\boldsymbol{L}^2(\Omega\times\mathfrak{D})), \tag{5.9e}$$
$$\sqrt{M_h}\nabla_{\mathbf{q}}\hat{\psi}_h^{\tau,(\pm)} \rightharpoonup \boldsymbol{P}_5^{(\pm)} \quad \text{in } L^2(0,T;\boldsymbol{L}^2(\Omega\times\mathfrak{D})), \tag{5.9f}$$

$$\mathbf{u}_h^{\tau,(\pm)} \overset{*}{\rightharpoonup} \mathbf{u} \quad \text{in } L^\infty(0,T;\boldsymbol{L}^2(\Omega)), \tag{5.10a}$$
$$\mathbf{u}_h^{\tau,(\pm)} \rightharpoonup \mathbf{u} \quad \text{in } L^2(0,T;\boldsymbol{H}^1_{0,\mathrm{div}}(\Omega)), \tag{5.10b}$$
$$\boldsymbol{S}\{\partial_t \mathbf{u}_h^\tau\} \rightharpoonup \boldsymbol{S}\{\partial_t \mathbf{u}\} \quad \text{in } L^{4/\lambda}(0,T;\boldsymbol{H}^1_{0,\mathrm{div}}(\Omega)), \tag{5.10c}$$
$$\mathbf{u}_h^{\tau,(\pm)} \rightarrow \mathbf{u} \quad \text{in } L^2(0,T;\boldsymbol{L}^s(\Omega)),\ s\in[1,\tfrac{2d}{d-2})\,. \tag{5.10d}$$

In addition, we have

$$\mathcal{I}_h^{\mathbf{x}}\{\mathcal{J}_h\{\mathcal{I}_h^{\mathbf{x}}\{\beta'_{DQ}(\phi_h^{\tau,+},\phi_h^{\tau,-})\theta^{\mathbf{x}}\}\}\} \rightarrow \mathcal{J}_\varepsilon\{\beta'(\phi)\theta^{\mathbf{x}}\} \quad \text{in } L^2(0,T;W^{1,\infty}(\Omega)), \text{ for } \theta^{\mathbf{x}}\in C^\infty(0,T;C^\infty(\overline{\Omega})), \tag{5.11a}$$
$$\mathcal{I}_h^{\mathbf{x}}\Big\{\mathcal{J}_h\Big\{\mathcal{I}_h^{\mathbf{x}}\Big\{\beta(\phi_h^{\tau,(\pm)})\Big\}\Big\}\Big\} \rightarrow \mathcal{J}_\varepsilon\{\beta(\phi)\} \quad \text{in } L^2(0,T;W^{1,\infty}(\Omega)), \tag{5.11b}$$
$$\mathcal{I}_h^{\mathbf{x}}\Big\{\boldsymbol{\mathcal{J}}_h\Big\{\mathbf{u}_h^{\tau,(\pm)}\Big\}\Big\} \rightarrow \boldsymbol{\mathcal{J}}_\varepsilon\{\mathbf{u}\} \quad \text{in } L^2(0,T;\boldsymbol{W}^{1,\infty}(\Omega))\,. \tag{5.11c}$$

Proof. The convergence results stated in (5.8a), (5.8b), (5.8d), and (5.8e) are direct consequences of the bounds in (5.5c). As we can control $\tau^{-1}\int_{\Omega_T}\left|\nabla_{\mathbf{x}}\phi_h^{\tau,+} - \nabla_{\mathbf{x}}\phi_h^{\tau,-}\right|^2$ (*cf.* (5.5c)), it is possible to show that appropriate subsequences of $\phi_h^{\tau,+}$, $\phi_h^{\tau,-}$, and ϕ_h^τ converge towards the same limit function. The strong convergence in (5.8c) follows from Simon's compactness theorem (*cf.* [27]) and the bound in (5.5a).

As proving the convergence expressed in (5.9) and (5.7) is more technical, we provide additional details on this part of the proof. (5.9a) is a direct consequence of Lemma 2.2. The convergence implied by (5.9b) follows from (5.5d). Using

$$\int_{\Omega_T\times\mathfrak{D}} \sqrt{\hat{M}}\hat{\psi}_h^{\tau,+}\theta = \int_{\Omega_T\times\mathfrak{D}} \sqrt{\hat{M}}\hat{\psi}_h^{\tau,-}\theta + \int_{\Omega_T\times\mathfrak{D}} \sqrt{\hat{M}}\Big(\hat{\psi}_h^{\tau,+} - \hat{\psi}_h^{\tau,-}\Big)\theta, \tag{5.12}$$

for all $\theta \in L^1(0,T;L^2(\Omega\times\mathfrak{D}))$, we show that $\sqrt{\hat{M}}\hat{\psi}_h^{\tau,+}$, $\sqrt{\hat{M}}\hat{\psi}_h^{\tau,-}$, and $\sqrt{\hat{M}}\hat{\psi}_h^{\tau}$ converge towards the same limit function P_1 which we use to define the limit function $\hat{\psi}$ on $\Omega_T\times D$. Analogously, we obtain that $\sqrt{M_h+\mathfrak{m}}\hat{\psi}_h^{\tau,(\pm)}$ converge towards the same limit function denoted by P_2. Using the strong convergence of the discrete Maxwellian from (5.9a), we choose a test function $\tilde{\theta} := \sqrt{\hat{M}}\theta$ with $\theta \in L^1(0,T;L^2(\Omega\times\mathfrak{D}))$ and deduce

$$\begin{aligned}\int_{\Omega_T\times\mathfrak{D}} P_2\tilde{\theta} \leftarrow \int_{\Omega_T\times\mathfrak{D}} \sqrt{M_h+\mathfrak{m}}\hat{\psi}_h^{\tau,(\pm)}\tilde{\theta} &= \int_{\Omega_T\times\mathfrak{D}} \sqrt{M_h+\mathfrak{m}}\hat{\psi}_h^{\tau,(\pm)}\sqrt{\hat{M}}\theta \\ &\to \int_{\Omega_T\times\mathfrak{D}} \sqrt{\hat{M}}P_1\theta = \int_{\Omega_T\times\mathfrak{D}} P_1\tilde{\theta},\end{aligned} \tag{5.13}$$

which shows that P_1 and P_2 coincide on $\Omega_T\times D$. Similar arguments yield (5.9d). Choosing a test function $\boldsymbol{\eta}\in L^2(0,T;\boldsymbol{C}_0^\infty(\Omega\times D))$, we obtain

$$\begin{aligned}\int_{\Omega_T\times D} \boldsymbol{P}_4^{(\pm)}\cdot\boldsymbol{\eta} \leftarrow \int_{\Omega_T\times D} \sqrt{M_h}\nabla_{\mathbf{x}}\hat{\psi}_h^{\tau,(\pm)}\cdot\boldsymbol{\eta} &= \int_{\Omega_T\times D} \nabla_{\mathbf{x}}(\sqrt{M_h}\hat{\psi}_h^{\tau,(\pm)})\cdot\boldsymbol{\eta} \\ = -\int_{\Omega_T\times D} \sqrt{M_h}\hat{\psi}_h^{\tau,(\pm)}\,\mathrm{div}_{\mathbf{x}}\{\boldsymbol{\eta}\} &\to -\int_{\Omega_T\times D} P_3\,\mathrm{div}_{\mathbf{x}}\{\boldsymbol{\eta}\} = \int_{\Omega_T\times D}\sqrt{M}\nabla_{\mathbf{x}}\hat{\psi}\cdot\boldsymbol{\eta},\end{aligned} \tag{5.14}$$

which yields (5.9e). Concerning the proof of (5.9f), we infer from the bounds in (5.5d) that the subsequences converge towards limit functions which we denote by $\boldsymbol{P}_5^{(\pm)}$. We prove that $\boldsymbol{P}_5^{(\pm)}$ coincide with $\sqrt{M}\nabla_{\mathbf{q}}\hat{\psi}$ on every compact subset of D. In a first step, we restrict ourselves to subsets $D_\delta := \{\mathbf{q}\in D : \mathrm{dist}\,(\mathbf{q},\partial D)\geq\delta\}$ of D with $\delta > 2h_{\mathbf{q}}$. From (4.6), we have $\hat{M}\leq CM_h$ on D_δ, which implies $\int_{\Omega_T\times D_\delta}\hat{M}\left|\nabla_{\mathbf{q}}\hat{\psi}_h^{\tau,(\pm)}\right|^2\leq C$ and therefore the existence of subsequences converging weakly towards some limit function. Following the approach in [7] (see also [5] and [18]), we choose a test function $\boldsymbol{\eta}\in L^2(0,T;\boldsymbol{C}_0^\infty(\Omega\times D_\delta))$ and compute

$$\begin{aligned}\int_{\Omega_T\times D_\delta}\sqrt{\hat{M}}\nabla_{\mathbf{q}}\hat{\psi}_h^{\tau,(\pm)}\cdot\boldsymbol{\eta} &= -\int_{\Omega_T\times D_\delta}\sqrt{\hat{M}}\hat{\psi}_h^{\tau,(\pm)}\frac{\mathrm{div}_{\mathbf{q}}\left\{\sqrt{\hat{M}}\boldsymbol{\eta}\right\}}{\sqrt{\hat{M}}} \to -\int_{\Omega_T\times D_\delta} P_1\frac{\mathrm{div}_{\mathbf{q}}\left\{\sqrt{\hat{M}}\boldsymbol{\eta}\right\}}{\sqrt{\hat{M}}} \\ &= -\int_{\Omega_T\times D_\delta}\sqrt{\hat{M}}\hat{\psi}\frac{\mathrm{div}_{\mathbf{q}}\left\{\sqrt{\hat{M}}\boldsymbol{\eta}\right\}}{\sqrt{\hat{M}}} = \int_{\Omega_T\times D_\delta}\sqrt{\hat{M}}\nabla_{\mathbf{q}}\hat{\psi}\cdot\boldsymbol{\eta}.\end{aligned} \tag{5.15}$$

In the next step, we choose some test function $\tilde{\boldsymbol{\eta}}\in L^1(0,T;\boldsymbol{C}_0^\infty(\Omega\times D))$. Hence, there exists $\delta>0$ such that $\mathrm{supp}\,\tilde{\boldsymbol{\eta}}\subset\Omega\times D_\delta$, which implies

$$\begin{aligned}\int_{\Omega_T\times\mathfrak{D}}\sqrt{M_h}\nabla_{\mathbf{q}}\hat{\psi}_h^{\tau,(\pm)}\cdot\left(\sqrt{\hat{M}}\tilde{\boldsymbol{\eta}}\right) &= \int_{\Omega_T\times D_\delta}\sqrt{\hat{M}}\nabla_{\mathbf{q}}\hat{\psi}_h^{\tau,(\pm)}\cdot\left(\sqrt{M_h}\tilde{\boldsymbol{\eta}}\right) \\ &\to \int_{\Omega_T\times D_\delta}\sqrt{\hat{M}}\nabla_{\mathbf{q}}\hat{\psi}\cdot\left(\sqrt{\hat{M}}\tilde{\boldsymbol{\eta}}\right),\end{aligned} \tag{5.16}$$

and therefore yields the result.

The nonnegativity of $\hat{\psi}$ on $\Omega_T\times D$ follows from $\sup_{t\in[0,T]}\int_{\Omega\times\mathfrak{D}}(M_h+\mathfrak{m})\mathcal{I}_h^{\mathbf{xq}}\left\{[\hat{\psi}_h^{\tau,(\pm)}]_-^2\right\}\leq\nu C$ (*cf.* (5.5c)).

(5.10a) and (5.10b) follow directly from the bounds in (5.5c). Due to the denseness of $\bigcup_{h>0}U_h^{\mathbf{x}}$ in $L^2(\Omega)$, we have $\mathbf{u}\in L^2(0,T;\boldsymbol{H}^1_{0,\mathrm{div}}(\Omega))$. Noting that $\boldsymbol{S}$ denotes the inverse Riesz-isomorphism on $\boldsymbol{H}^1_{0,\mathrm{div}}(\Omega)$ (*cf.* [5], [18]), we obtain (5.10c), which also implies weak* convergence of $\partial_t\mathbf{u}_h^\tau$ towards $\partial_t\mathbf{u}$. To prove the strong convergence postulated in (5.10d), we show that $\|\mathbf{u}_h^{\tau,(\pm)}-\mathbf{u}\|_{L^2(0,T;L^s(\Omega))}$, which is bounded by

$$\|\mathbf{u}_h^{\tau,(\pm)}-\mathbf{u}_h^{\tau,+}\|_{L^2(0,T;L^s(\Omega))} + \|\mathbf{u}_h^{\tau,+}-\boldsymbol{R}_h\{\mathbf{u}_h^{\tau,+}\}\|_{L^2(0,T;L^s(\Omega))} + \|\boldsymbol{R}_h\{\mathbf{u}_h^{\tau,+}\}-\mathbf{u}\|_{L^2(0,T;L^s(\Omega))}, \tag{5.17}$$

tends to zero. The first two terms vanish due to (5.5c), (4.37b), and the Gagliardo–Nirenberg inequality. The convergence of the third term is a direct consequence of the bound in (5.5b) and the bounds in (5.5c) and a "compactness by pertubation" result by Azérad and Guillén [4] which we cited in Lemma B.2.

To prove (5.11a), we apply the decomposition

$$\begin{aligned}
&\left\|\mathcal{I}_h^{\mathbf{x}}\big\{\mathcal{J}_h\big\{\mathcal{I}_h^{\mathbf{x}}\big\{\beta'_{DQ}(\phi_h^{\tau,+},\phi_h^{\tau,-})\theta^{\mathbf{x}}\big\}\big\}\big\} - \mathcal{J}_\varepsilon\{\beta'(\phi)\theta^{\mathbf{x}}\}\right\|_{L^2(0,T;W^{1,\infty}(\Omega))}\\
&\quad\le \left\|\mathcal{I}_h^{\mathbf{x}}\big\{\mathcal{J}_h\big\{\mathcal{I}_h^{\mathbf{x}}\big\{\beta'_{DQ}(\phi_h^{\tau,+},\phi_h^{\tau,-})\theta^{\mathbf{x}}\big\} - \beta'(\phi)\theta^{\mathbf{x}}\big\}\big\}\right\|_{L^2(0,T;W^{1,\infty}(\Omega))}\\
&\qquad+ \|\mathcal{I}_h^{\mathbf{x}}\{\mathcal{J}_h\{\beta'(\phi)\theta^{\mathbf{x}}\} - \mathcal{J}_\varepsilon\{\beta'(\phi)\theta^{\mathbf{x}}\}\}\|_{L^2(0,T;W^{1,\infty}(\Omega))}\\
&\qquad+ \|\mathcal{I}_h^{\mathbf{x}}\{\mathcal{J}_\varepsilon\{\beta'(\phi)\theta^{\mathbf{x}}\}\} - \mathcal{J}_\varepsilon\{\beta'(\phi)\theta^{\mathbf{x}}\}\|_{L^2(0,T;W^{1,\infty}(\Omega))}
\end{aligned}\tag{5.18}$$

and show that the terms on the right-hand side vanish. Using Lemma 2.10, we compute

$$\begin{aligned}
&\left\|\mathcal{I}_h^{\mathbf{x}}\big\{\mathcal{J}_h\big\{\mathcal{I}_h^{\mathbf{x}}\big\{\beta'_{DQ}(\phi_h^{\tau,+},\phi_h^{\tau,-})\theta^{\mathbf{x}}\big\} - \beta'(\phi)\theta^{\mathbf{x}}\big\}\big\}\right\|_{L^2(0,T;W^{1,\infty}(\Omega))}\\
&\quad\le C(\varepsilon)\left\|\mathcal{I}_h^{\mathbf{x}}\big\{\beta'_{DQ}(\phi_h^{\tau,+},\phi_h^{\tau,-})\theta^{\mathbf{x}}\big\} - \beta'(\phi)\theta^{\mathbf{x}}\right\|_{L^2(0,T;L^1(\Omega))}.
\end{aligned}\tag{5.19}$$

Therefore, the first term vanishes, if $\mathcal{I}_h^{\mathbf{x}}\big\{\beta'_{DQ}(\phi_h^{\tau,+},\phi_h^{\tau,-})\theta^{\mathbf{x}}\big\}$ converges strongly towards $\beta'(\phi)\theta^{\mathbf{x}}$ in $L^2(0,T;L^1(\Omega))$. To prove this convergence, we start with the estimate

$$\begin{aligned}
\int_\Omega \left|\mathcal{I}_h^{\mathbf{x}}\big\{\beta'_{DQ}(\phi_h^{\tau,+},\phi_h^{\tau,-})\theta^{\mathbf{x}}\big\} - \beta'(\phi)\theta^{\mathbf{x}}\right| &\le \int_\Omega \left|\mathcal{I}_h^{\mathbf{x}}\big\{\beta'_{DQ}(\phi_h^{\tau,+},\phi_h^{\tau,-})\theta^{\mathbf{x}} - \beta'(\phi)\theta^{\mathbf{x}}\big\}\right|\\
&\quad+ \int_\Omega |\mathcal{I}_h^{\mathbf{x}}\{\beta'(\phi)\theta^{\mathbf{x}}\} - \beta'(\phi)\theta^{\mathbf{x}}| =: I + II\,.
\end{aligned}\tag{5.20}$$

As we have $\theta^{\mathbf{x}} \in C^\infty(0,T;C^\infty(\overline{\Omega}))$ and $\phi_h^{\tau,+},\phi_h^{\tau,-} \in U_h^{\mathbf{x}}$, we use the mean value theorem to compute

$$\begin{aligned}
I &\le \max_{\mathbf{x}\in\Omega}|\theta^{\mathbf{x}}| \int_\Omega \mathcal{I}_h^{\mathbf{x}}\big\{\big|\beta'_{DQ}(\phi_h^{\tau,+},\phi_h^{\tau,-}) - \beta'(\phi)\big|\big\}\\
&\le C\int_\Omega \mathcal{I}_h^{\mathbf{x}}\big\{\big|\phi_h^{\tau,+}-\phi\big|\big\} + C\int_\Omega \mathcal{I}_h^{\mathbf{x}}\big\{\big|\phi_h^{\tau,-}-\phi\big|\big\}\\
&= C\int_\Omega \mathcal{I}_h^{\mathbf{x}}\big\{\big|\phi_h^{\tau,+}-\mathcal{I}_h^{\mathbf{x}}\{\phi\}\big|\big\} + C\int_\Omega \mathcal{I}_h^{\mathbf{x}}\big\{\big|\phi_h^{\tau,-}-\mathcal{I}_h^{\mathbf{x}}\{\phi\}\big|\big\}.
\end{aligned}\tag{5.21}$$

To deduce the last equality in (5.21), we used in particular that the integrals depend only on the values in the vertices of the simplices. Therefore, it is possible to interchange ϕ and $\mathcal{I}_h^{\mathbf{x}}\{\phi\}$. Combining a discrete version of Hölder's inequality and (2.10) shows

$$\begin{aligned}
\int_\Omega \mathcal{I}_h^{\mathbf{x}}\big\{\big|\phi_h^{\tau,+}-\mathcal{I}_h^{\mathbf{x}}\{\phi\}\big|\big\} &\le C\bigg(\int_\Omega \mathcal{I}_h^{\mathbf{x}}\Big\{\big(\phi_h^{\tau,+}-\mathcal{I}_h^{\mathbf{x}}\{\phi\}\big)^2\Big\}\bigg)^{1/2}\\
&\le C\left\|\phi_h^{\tau,+}-\mathcal{I}_h^{\mathbf{x}}\{\phi\}\right\|_{L^2(\Omega)} \le C\left\|\phi_h^{\tau,+}-\phi\right\|_{L^2(\Omega)} + C\left\|\mathcal{I}_h^{\mathbf{x}}\{\phi\}-\phi\right\|_{L^2(\Omega)} \to 0
\end{aligned}\tag{5.22}$$

due to (5.8c), $\phi \in L^2(0,T;H^2(\Omega))$, and standard error estimates for the nodal interpolation operator (*cf.* [9]). Similar arguments imply

$$\int_\Omega \mathcal{I}_h^{\mathbf{x}}\big\{\big|\phi_h^{\tau,-}-\mathcal{I}_h^{\mathbf{x}}\{\phi\}\big|\big\} \to 0\,.\tag{5.23}$$

From (5.8c), we also infer $II \to 0$. The second term on the right hand side of (5.18) vanishes as we have

$$\begin{aligned}
&\|\mathcal{I}_h^{\mathbf{x}}\{\mathcal{J}_h\{\beta'(\phi)\theta^{\mathbf{x}}\} - \mathcal{J}_\varepsilon\{\beta'(\phi)\theta^{\mathbf{x}}\}\}\|_{L^2(0,T;W^{1,\infty}(\Omega))}\\
&\quad\le \|\mathcal{J}_h\{\beta'(\phi)\theta^{\mathbf{x}}\} - \mathcal{J}_\varepsilon\{\beta'(\phi)\theta^{\mathbf{x}}\}\|_{L^2(0,T;W^{1,\infty}(\Omega))}\\
&\quad\le Ch_{\mathbf{x}}\|\beta'(\phi)\theta^{\mathbf{x}}\|_{L^2(0,T;L^1(\Omega))} \le Ch_{\mathbf{x}}\,.
\end{aligned}\tag{5.24}$$

Combining standard error estimates for the nodal interpolation operator with (1.9f), we compute for the last term on the right hand side of (5.18)

$$\begin{aligned}\left\|\mathcal{I}_h^{\mathbf{x}}\{\mathcal{J}_\varepsilon\{\beta'(\phi)\theta^{\mathbf{x}}\}\} - \mathcal{J}_\varepsilon\{\beta'(\phi)\theta^{\mathbf{x}}\}\right\|_{L^2(0,T;W^{1,\infty}(\Omega))} &\leq Ch_{\mathbf{x}}\left\|\mathcal{J}_\varepsilon\{\beta'(\phi)\theta^{\mathbf{x}}\}\right\|_{L^2(0,T;W^{2,\infty}(\Omega))} \\ &\leq Ch_{\mathbf{x}}\left\|\beta'(\phi)\theta^{\mathbf{x}}\right\|_{L^2(0,T;L^1(\Omega))} \leq Ch_{\mathbf{x}} \to 0\,. \end{aligned} \tag{5.25}$$

Similar arguments provide (5.11b) and (5.11c). □

Using the above mentioned convergence results, we pass to the limit $(h,\tau,\mathfrak{m},\nu)\searrow(0,0,0,0)$ in (5.3) and obtain the following result.

Theorem 5.2. *Let $d\in\{2,3\}$. Under the assumptions (A1)–(A9), there is a quadruple $(\phi,\mu_\phi,\hat{\psi},\mathbf{u})$ which can be obtained from discrete solutions of (5.3) by passing to the limit $(h,\tau,\mathfrak{m},\nu)\searrow(0,0,0,0)$ and which solves the equal-density version of (1.5) in the following weak sense.*

$$\int_{\Omega_T}(\Phi^0-\phi)\partial_t\theta^{\mathbf{x}} - \int_{\Omega_T}\phi\mathbf{u}\cdot\nabla_{\mathbf{x}}\theta^{\mathbf{x}} + \int_{\Omega_T}\nabla_{\mathbf{x}}\mu_\phi\cdot\nabla_{\mathbf{x}}\theta^{\mathbf{x}} = 0$$
$$\forall\theta^{\mathbf{x}}\in C^1([0,T];H^1(\Omega)) \text{ with } \theta^{\mathbf{x}}(.,T)\equiv 0, \tag{5.26a}$$

$$\int_{\Omega_T}\mu_\phi\theta^{\mathbf{x}} = \int_{\Omega_T}\nabla_{\mathbf{x}}\phi\cdot\nabla_{\mathbf{x}}\theta^{\mathbf{x}} + \int_{\Omega_T}W'(\phi)\theta^{\mathbf{x}} + \int_{\Omega_T}\beta'(\phi)\mathcal{J}_\varepsilon\left\{\int_D M\hat{\psi}\right\}\theta^{\mathbf{x}}$$
$$\forall\theta^{\mathbf{x}}\in L^2(0,T;H^1(\Omega)), \tag{5.26b}$$

$$\begin{aligned}\int_{\Omega_T\times D}(\hat{\Psi}^0-\hat{\psi})\partial_t\theta - \int_{\Omega_T\times D}M\hat{\psi}\mathbf{u}\cdot\nabla_{\mathbf{x}}\theta - \int_{\Omega_T\times D}M\hat{\psi}(\nabla_{\mathbf{x}}\boldsymbol{\mathcal{J}}_\varepsilon\{\mathbf{u}\}\cdot\mathbf{q})\cdot\nabla_{\mathbf{q}}\theta \\ + c_{\mathbf{q}}\int_{\Omega_T\times D}M\nabla_{\mathbf{q}}\hat{\psi}\cdot\nabla_{\mathbf{q}}\theta + c_{\mathbf{x}}\int_{\Omega_T\times D}M\nabla_{\mathbf{x}}\hat{\psi}\cdot\nabla_{\mathbf{x}}\theta \\ + c_{\mathbf{x}}\int_{\Omega_T\times D}M\hat{\psi}\nabla_{\mathbf{x}}\mathcal{J}_\varepsilon\{\beta(\phi)\}\cdot\nabla_{\mathbf{x}}\theta = 0 \quad \forall\theta\in C^1([0,T],\hat{X}) \text{ with } \theta(.,T)\equiv 0,\end{aligned} \tag{5.26c}$$

$$\begin{aligned}\int_0^T\langle\partial_t\mathbf{u},\mathbf{w}\rangle + \int_{\Omega_T}(\mathbf{u}\cdot\nabla_{\mathbf{x}})\mathbf{u}\cdot\mathbf{w} + \int_{\Omega_T}2\eta(\phi)\mathbf{D}\mathbf{u}:\mathbf{D}\mathbf{w} \\ = \int_{\Omega_T}\mu_\phi\nabla_{\mathbf{x}}\phi\cdot\mathbf{w} + \int_{\Omega_T}\operatorname{div}_{\mathbf{x}}\left\{\mathfrak{J}_\varepsilon\left\{\int_D M\nabla_{\mathbf{q}}\hat{\psi}\otimes\mathbf{q}\right\}\right\}\cdot\mathbf{w} + \int_{\Omega_T\times D}\mathcal{J}_\varepsilon\{\beta(\phi)\}M\nabla_{\mathbf{x}}\hat{\psi}\cdot\mathbf{w} \\ \forall\mathbf{w}\in L^{4/(4-\lambda)}(0,T;\boldsymbol{H}^1_{0,\mathrm{div}}(\Omega)),\end{aligned} \tag{5.26d}$$

with $\lambda\in(2,4)$, if $d=2$, and $\lambda=3$, if $d=3$. Moreover, the solution has the following regularity properties

$$\phi\in L^\infty(0,T;H^1(\Omega))\cap L^2(0,T;H^2(\Omega))\cap L^4(0,T;L^\infty(\Omega)), \tag{5.27a}$$
$$\mu_\phi\in L^2(0,T;H^1(\Omega)), \tag{5.27b}$$
$$\hat{\psi}\in L^2(0,T;\hat{X}_+)\cap L^\infty(0,T;L^2(\Omega\times D;M)), \tag{5.27c}$$
$$\mathbf{u}\in L^\infty(0,T;\boldsymbol{L}^2(\Omega))\cap L^2(0,T;\boldsymbol{H}^1_{0,\mathrm{div}}(\Omega))\cap W^{1,4/\lambda}(0,T;(\boldsymbol{H}^1_{0,\mathrm{div}}(\Omega))'), \tag{5.27d}$$

with $\lambda\in(2,4)$, if $d=2$, and $\lambda=3$, if $d=3$.

Proof. In order to pass to the limit in (5.3a), we choose $\theta_h^{\mathbf{x}} = \mathcal{I}_h^{\mathbf{x}}\{\theta^{\mathbf{x}}\}$ with $\theta^{\mathbf{x}} \in C^1([0,T], C^\infty(\overline{\Omega}))$ and $\theta^{\mathbf{x}}(.,T) \equiv 0$. Therefore, the first term in (5.3a) can be rewritten as

$$\int_{\Omega_T} \partial_t \phi_h^\tau \mathcal{I}_h^{\mathbf{x}}\{\theta^{\mathbf{x}}\} - \int_\Omega (I - \mathcal{I}_h^{\mathbf{x}})\{\partial_t \phi_h^\tau \mathcal{I}_h^{\mathbf{x}}\{\theta^{\mathbf{x}}\}\} =: I_a + I_b \,. \tag{5.28}$$

Partial integration with respect to time, the assumptions on the initial data, (5.8c), and the strong convergence of $\mathcal{I}_h^{\mathbf{x}}\{\theta^{\mathbf{x}}\}$ towards $\theta^{\mathbf{x}}$ provided by standard estimates on the interpolation error (*cf.* [9]) yield the convergence of $I_a \to \int_{\Omega_T} (\Phi^0 - \phi)\partial_t \theta^{\mathbf{x}}$. I_b vanishes due to the estimates stated in Lemma 2.4. The convergence of the second term in (5.3a) is a direct consequence of the convergence results obtained in Lemma 5.1 and standard interpolation error estimates (*cf.* Thm. 4.4.4 in [9]). From the bounds in (5.5c), we obtain that the third term is bounded by τC and therefore vanishes when passing to the limit. The last convergence of the last term in (5.3a) follows from the weak convergence of $\nabla_{\mathbf{x}} \mu_{\phi,h}^{\tau,+}$ and the strong convergence of $\nabla_{\mathbf{x}} \mathcal{I}_h^{\mathbf{x}}\{\theta^{\mathbf{x}}\} \to \nabla_{\mathbf{x}} \theta^{\mathbf{x}}$.

In order to pass to the limit in (5.3b), we choose $\theta_h^{\mathbf{x}} = \mathcal{I}_h^{\mathbf{x}}\{\theta^{\mathbf{x}}\}$ with $\theta^{\mathbf{x}} \in C^\infty([0,T], C^\infty(\overline{\Omega}))$. Then, the convergence of term on the left-hand side of (5.3b) follows from the weak convergence of $\mu_{\phi,h}^{\tau,+}$ stated in (5.8e) and (2.18). The first term on the right-hand side of (5.3b) can be rewritten as

$$\int_{\Omega_T} \mathcal{I}_h^{\mathbf{x}}\big\{(W_h'(\phi_h^{\tau,+}, \phi_h^{\tau,-}) - W_h'(\phi_h^{\tau,-}, \phi) + W_h'(\phi_h^{\tau,-}, \phi) - W_h'(\phi, \phi))\theta^{\mathbf{x}}\big\} + \int_{\Omega_T} \mathcal{I}_h^{\mathbf{x}}\{W_h'(\phi,\phi)\theta^{\mathbf{x}}\}. \tag{5.29}$$

Thereby, the first term vanishes. In particular, (W5) and the bounds on $\|\phi_h^{\tau,(\pm)}\|_{L^4(0,T;L^\infty(\Omega))}$ and $\|\phi\|_{L^4(0,T;L^\infty(\Omega))}$ show that it is bounded by

$$C\left(\int_0^T \left[\int_\Omega \mathcal{I}_h^{\mathbf{x}}\big\{\big|\phi_h^{\tau,+} - \phi_h^{\tau,-}\big| + \big|\phi_h^{\tau,-} - \phi\big|\big\}\right]^2\right)^{1/2}. \tag{5.30}$$

Due to $\left\|\phi_h^{\tau,-} - \mathcal{I}_h^{\mathbf{x}}\{\phi\}\right\|_{L^2(\Omega)} \le \left\|\phi_h^{\tau,-} - \phi\right\|_{L^2(\Omega)} + C\left\|\phi - \mathcal{I}_h^{\mathbf{x}}\{\phi\}\right\|_{L^\infty(\Omega)}$, (5.30) is bounded by

$$C\left\|\phi_h^{\tau,+} - \phi_h^{\tau,-}\right\|_{L^2(\Omega_T)} + C\left\|\phi_h^{\tau,-} - \phi\right\|_{L^2(\Omega_T)} + Ch_{\mathbf{x}}^{1/2}\left\|\phi\right\|_{L^2(0,T;H^2(\Omega))} \to 0\,. \tag{5.31}$$

The convergence of the second term in (5.29) towards $\int_{\Omega_T} W'(\phi)\theta^{\mathbf{x}}$ follows from (W4) and the estimate $\|\mathcal{I}_h^{\mathbf{x}}\{f\} - f\|_{L^6(\Omega)} \le Ch_{\mathbf{x}} |f|_{W^{1,6}(\Omega)}$ (*cf.* [9]), as we have

$$|W'(\phi)\theta^{\mathbf{x}}|_{L^1(0,T;W^{1,6}(\Omega))} \le C\Big(\|W'(\phi)\|_{L^1(0,T;L^6(\Omega))} + \|W''(\phi)\nabla_{\mathbf{x}}\phi\|_{L^1(0,T;L^6(\Omega))}\Big)\,. \tag{5.32}$$

Due to (W1), the terms on the right-hand side of (5.32) are bounded. The convergence of the third integral in (5.3b) towards $\int_{\Omega_T} \nabla_{\mathbf{x}}\phi \cdot \nabla_{\mathbf{x}}\theta^{\mathbf{x}}$ is a direct consequence of (5.8a), while the convergence of the last term follows from the weak* convergence in (5.9c), the strong convergence in (5.11a), and (2.18). Altogether, we have

$$\int_{\Omega_T} \mu_\phi \theta^{\mathbf{x}} = \int_{\Omega_T} \nabla_{\mathbf{x}}\phi \cdot \nabla_{\mathbf{x}}\theta^{\mathbf{x}} + \int_{\Omega_T} W'(\phi)\theta^{\mathbf{x}} + \int_{\Omega_T \times \mathfrak{D}} \mathcal{J}_\varepsilon\{\beta'(\phi)\}\sqrt{\hat{M}} P_2 \theta^{\mathbf{x}} \qquad \forall \theta^{\mathbf{x}} \in C^\infty([0,T], C^\infty(\overline{\Omega}))\,. \tag{5.33}$$

Noting the estimate

$$\left|\int_{\Omega_T \times (\mathfrak{D}\setminus D)} \mathcal{J}_\varepsilon\{\beta'(\phi)\theta^{\mathbf{x}}\}\sqrt{\hat{M}} P_2\right| \le \left(\int_{\Omega_T} |\mathcal{J}_\varepsilon\{\beta'(\phi)\theta^{\mathbf{x}}\}|^2 \int_{\mathfrak{D}\setminus D} \hat{M}\right)^{1/2} \left(\int_{\Omega_T \times \mathfrak{D}} P_2^2\right)^{1/2} = 0 \tag{5.34}$$

and $P_2\big|_D = \sqrt{M}\hat{\psi}$, shifting the continuous mollifier $\mathcal{J}_\varepsilon$ onto $\int_D M\hat{\psi}$, and recalling the denseness of $C^\infty([0,T],C^\infty(\overline{\Omega}))$ in $L^2(0,T;H^1(\Omega))$, we obtain (5.26b).

To pass to the limit in the Fokker–Planck type equation (5.3c), we again use $\mathcal{I}_h^{\mathbf{xq}}\{\theta\}$ with $\theta \in C^1([0,T];C^\infty(\overline{\Omega\times D}))$ and $\theta(.,T)\equiv 0$ as test function. Applying partial integration with respect to time, we split the first term in (5.3c) into

$$\begin{aligned}
-\int_{\Omega_T\times\mathfrak{D}} M_h\hat{\psi}_h^\tau\partial_t\mathcal{I}_h^{\mathbf{xq}}\{\theta\} + \int_{\Omega_T\times\mathfrak{D}} M_h(I-\mathcal{I}_h^{\mathbf{xq}})\Big\{\hat{\psi}_h^\tau\partial_t\mathcal{I}_h^{\mathbf{xq}}\{\theta\}\Big\}\\
-\mathfrak{m}\int_{\Omega_T\times\mathfrak{D}}\mathcal{I}_h^{\mathbf{xq}}\Big\{\hat{\psi}_h^\tau\partial_t\mathcal{I}_h^{\mathbf{xq}}\{\theta\}\Big\} - \int_{\Omega\times\mathfrak{D}}(M_h+\mathfrak{m})\mathcal{I}_h^{\mathbf{xq}}\Big\{\hat{\psi}_h^0\mathcal{I}_h^{\mathbf{xq}}\{\theta\big|_{t=0}\}\Big\}
\end{aligned}\tag{5.35}$$

The results of the previous lemma provide the convergence of the first term towards $-\int_{\Omega_T\times\mathfrak{D}}\sqrt{\hat{M}}P_3\partial_t\theta$. The second term vanishes due to (2.16c) and the bounds stated in (5.5c). Applying Young's inequality shows that the third term vanishes, too. Recalling the definition of $\hat{\psi}_h^0$ in (4.1), one obtains the convergence of the last term in (5.35) towards $-\int_{\Omega\times\mathfrak{D}}\hat{M}\hat{\Psi}^0\,\theta\big|_{t=0}$.

Concerning the convergence in the second term of (5.3c), we rewrite the term as

$$\int_{\Omega_T\times\mathfrak{D}} M_h\mathbf{u}_h^{\tau,+}\cdot\mathcal{I}_h^{\mathbf{q}}\Big\{\hat{\psi}_h^{\tau,+}\nabla_{\mathbf{x}}\mathcal{I}_h^{\mathbf{xq}}\{\theta\}\Big\} - \int_{\Omega_T\times\mathfrak{D}} M_h\mathbf{u}_h^{\tau,+}\cdot\mathcal{I}_h^{\mathbf{q}}\Big\{\Big(\hat{\psi}_h^{\tau,+}\mathbb{1}-\Lambda_\nu^{\mathbf{x}}[\hat{\psi}_{\mathrm{h}}^{\tau,+}]\Big)\nabla_{\mathbf{x}}\mathcal{I}_h^{\mathbf{xq}}\{\theta\}\Big\}\,. \tag{5.36}$$

As $\Lambda_\nu^{\mathbf{x}}[\hat{\psi}_{\mathrm{h}}^{\tau,+}]$ is an approximation of $\hat{\psi}_h^{\tau,+}$ in the sense of (2.33c), the second term vanishes when passing to the limit, while the first term converges towards $\int_{\Omega_T\times\mathfrak{D}}\sqrt{\hat{M}}P_3\mathbf{u}\cdot\nabla_{\mathbf{x}}\theta$ due to (5.9a), (5.10d), (5.9d), (2.19), and the standard error estimates for the interpolation error.

Similarly, we obtain from (2.33a) and the convergence results established in Lemma 5.1

$$\begin{aligned}
\int_{\Omega_T\times\mathfrak{D}}\big(\nabla_{\mathbf{x}}\mathcal{I}_h^{\mathbf{x}}\{\boldsymbol{\mathcal{J}}_h\{\mathbf{u}_h^{\tau,+}\}\}\cdot\mathcal{I}_h^{\mathbf{x}}\{\mathbf{q}M_h\}\big)\cdot\mathcal{I}_h^{\mathbf{x}}\Big\{\Xi_\nu^{\mathbf{q}}[\hat{\psi}_{\mathrm{h}}^{\tau,+}]\nabla_{\mathbf{q}}\mathcal{I}_h^{\mathbf{xq}}\{\theta\}\Big\}\\
\to\int_{\Omega_T\times\mathfrak{D}}\sqrt{\hat{M}}P_3(\nabla_{\mathbf{x}}\boldsymbol{\mathcal{J}}_\varepsilon\{\mathbf{u}\}\cdot\mathbf{q})\cdot\nabla_{\mathbf{q}}\theta,
\end{aligned}\tag{5.37}$$

where we used in particular the high regularity of the mollified velocity field. Recalling (2.24a), we split the fourth term in (5.3c) into

$$\begin{aligned}
\int_{\Omega_T\times\mathfrak{D}} c_{\mathbf{x}}M_h\mathcal{I}_h^{\mathbf{q}}\Big\{\Big(\Xi_\nu^{\mathbf{x}}[\hat{\psi}_{\mathrm{h}}^{\tau,+}]\nabla_{\mathbf{x}}\mu_{\psi,h,\nu}^{\tau,+}\Big)\cdot\nabla_{\mathbf{x}}\mathcal{I}_h^{\mathbf{x}}\{\theta\}\Big\} = \int_{\Omega_T\times\mathfrak{D}} c_{\mathbf{x}}M_h\mathcal{I}_h^{\mathbf{q}}\Big\{\nabla_{\mathbf{x}}\hat{\psi}_h^{\tau,+}\cdot\nabla_{\mathbf{x}}\mathcal{I}_h^{\mathbf{x}}\{\theta\}\Big\}\\
+\int_{\Omega_T\times\mathfrak{D}} c_{\mathbf{x}}M_h\mathcal{I}_h^{\mathbf{q}}\Big\{\Big(\Xi_\nu^{\mathbf{x}}[\hat{\psi}_{\mathrm{h}}^{\tau,+}]\nabla_{\mathbf{x}}\mathcal{I}_h^{\mathbf{x}}\{\mathcal{J}_h\{\mathcal{I}_h^{\mathbf{x}}\{\beta(\phi_h^{\tau,+})\}\}\}\Big)\cdot\nabla_{\mathbf{x}}\mathcal{I}_h^{\mathbf{x}}\{\theta\}\Big\}\\
=: A+B\,.
\end{aligned}\tag{5.38}$$

The convergence of A follows from (5.9a), (5.9e), and (2.16b), while the convergence of B can be established using Lemma 2.10, (A6), (2.19), (5.9d), (5.11b), (2.12b), and (2.33b). Therefore, we obtain

$$A+B\to\int_{\Omega_T\times\mathfrak{D}} c_{\mathbf{x}}\sqrt{\hat{M}}\boldsymbol{P}_4^+\cdot\nabla_{\mathbf{x}}\theta + \int_{\Omega_T\times\mathfrak{D}} c_{\mathbf{x}}\sqrt{\hat{M}}P_3\nabla_{\mathbf{x}}\mathcal{J}_\varepsilon\{\beta(\phi)\}\cdot\nabla_{\mathbf{x}}\theta\,. \tag{5.39}$$

As the following computations show, we may substitute $\Xi_\nu^{\mathbf{x}}[\hat\psi_{\mathrm{h}}^{\tau,+}]$ by $\Lambda_\nu^{\mathbf{x}}[\hat\psi_{\mathrm{h}}^{\tau,+}]$ without changing the limit, which provides the convergence in the fifth term (*cf.* (5.38), (5.39)).

$$\begin{aligned}&\left|\int_{\Omega_T\times\mathfrak{D}} M_h\mathcal{I}_h^{\mathbf{q}}\Big\{\Big(\Big(\Lambda_\nu^{\mathbf{x}}[\hat\psi_{\mathrm{h}}^{\tau,+}]-\Xi_\nu^{\mathbf{x}}[\hat\psi_{\mathrm{h}}^{\tau,+}]\Big)\nabla_{\mathbf{x}}\mu_{\psi,h,\nu}^{\tau,+}\Big)\cdot\nabla_{\mathbf{x}}\mu_{\psi,h,\nu}^{\tau,+}\Big\}\right|\\ &\quad\le C\left(\nu^{-1}\int_{\Omega_T\times\mathfrak{D}} M_h\mathcal{I}_h^{\mathbf{q}}\left\{\left|\Lambda_\nu^{\mathbf{x}}[\hat\psi_{\mathrm{h}}^{\tau,+}]-\Xi_\nu^{\mathbf{x}}[\hat\psi_{\mathrm{h}}^{\tau,+}]\right|^2\right\}\right)^{1/2}\left(\nu\int_{\Omega_T\times\mathfrak{D}} M_h\mathcal{I}_h^{\mathbf{q}}\left\{\left|\nabla_{\mathbf{x}}\mu_{\psi,h,\nu}^{\tau,+}\right|^2\right\}\right)^{1/2}.\end{aligned}\tag{5.40}$$

As the eigenvalues of $\Xi_\nu^{\mathbf{x}}[\hat\psi_{\mathrm{h}}^{\tau,+}]$ are greater than or equal to ν, we have

$$\nu\int_{\Omega_T\times\mathfrak{D}} M_h\left|\nabla_{\mathbf{x}}\mu_{\psi,h,\nu}^{\tau,+}\right|^2\le\int_{\Omega_T\times\mathfrak{D}} M_h\mathcal{I}_h^{\mathbf{q}}\Big\{\Big(\Xi_\nu^{\mathbf{x}}[\hat\psi_{\mathrm{h}}^{\tau,+}]\nabla_{\mathbf{x}}\mu_{\psi,h,\nu}^{\tau,+}\Big)\cdot\nabla_{\mathbf{x}}\mu_{\psi,h,\nu}^{\tau,+}\Big\}\le C\tag{5.41}$$

due to (5.5c). We obtain from (2.33d) that the first factor on the right-hand side of (5.40) scales with $\frac{h_{\mathbf{x}}^2}{\nu}$. In combination with assumption (A7) and the bounds in (5.5c), we obtain

$$\nu^{-1}\int_{\Omega_T\times\mathfrak{D}} M_h\mathcal{I}_h^{\mathbf{q}}\left\{\left|\Lambda_\nu^{\mathbf{x}}[\hat\psi_{\mathrm{h}}^{\tau,+}]-\Xi_\nu^{\mathbf{x}}[\hat\psi_{\mathrm{h}}^{\tau,+}]\right|^2\right\}\le C\frac{h_{\mathbf{x}}^2}{\nu}\int_{\Omega_T\times\mathfrak{D}} M_h\mathcal{I}_h^{\mathbf{q}}\left\{\left|\nabla_{\mathbf{x}}\hat\psi_h^{\tau,+}\right|^2\right\}\to 0\,.\tag{5.42}$$

The convergence

$$\int_{\Omega_T\times\mathfrak{D}} c_{\mathbf{q}}M_h\mathcal{I}_h^{\mathbf{x}}\Big\{\nabla_{\mathbf{q}}\hat\psi_h^{\tau,+}\cdot\nabla_{\mathbf{q}}\mathcal{I}_h^{\mathbf{xq}}\{\theta\}\Big\}\to\int_{\Omega_T\times\mathfrak{D}} c_{\mathbf{q}}\sqrt{\hat M}\boldsymbol{P}_5^+\cdot\nabla_{\mathbf{q}}\theta\tag{5.43}$$

follows directly from the results of Lemma 5.1 and (2.16a).

Collecting the above result yields

$$\begin{aligned}\int_{\Omega_T\times\mathfrak{D}}(\hat M\hat\Psi^0-\sqrt{\hat M}P_3)\partial_t\theta-\int_{\Omega_T\times\mathfrak{D}}\sqrt{\hat M}P_3\mathbf{u}\cdot\nabla_{\mathbf{x}}\theta-\int_{\Omega_T\times\mathfrak{D}}\sqrt{\hat M}P_3(\nabla_{\mathbf{x}}\boldsymbol{\mathcal{J}}_\varepsilon\{\mathbf{u}\}\cdot\mathbf{q})\cdot\nabla_{\mathbf{q}}\theta&\\ +\int_{\Omega_T\times\mathfrak{D}} c_{\mathbf{x}}\sqrt{\hat M}\boldsymbol{P}_4^+\cdot\nabla_{\mathbf{x}}\theta+\int_{\Omega_T\times\mathfrak{D}} c_{\mathbf{x}}\sqrt{\hat M}P_3\nabla_{\mathbf{x}}\mathcal{J}_\varepsilon\{\beta(\phi)\}\cdot\nabla_{\mathbf{x}}\theta&\\ +\int_{\Omega_T\times\mathfrak{D}} c_{\mathbf{q}}\sqrt{\hat M}\boldsymbol{P}_5^+\cdot\nabla_{\mathbf{q}}\theta=0,&\end{aligned}\tag{5.44}$$

for all $\theta\in C^1([0,T];C^\infty(\overline{\Omega\times\mathfrak{D}}))$ with $\theta(.,T)\equiv 0$. Arguments similar to (5.34) show that the integrals over $\mathfrak{D}\setminus D$ provide no contribution to (5.44). Recalling (5.7) and $\hat M\equiv M$ on D, we obtain (5.26c) as $C^\infty(\overline{\Omega\times D})$ is dense in $\hat X$ (*cf.* [30]).

Recalling the strong convergence of $\mathcal{Q}_h[\mathbf{w}]$ towards $\mathbf{w}$ for all $\mathbf{w}\in\boldsymbol{H}^1_{0,\mathrm{div}}(\Omega)\cap\boldsymbol{H}^2(\Omega)$ (see (TH2)), we choose $\mathbf{w}_h=\mathcal{Q}_h[\mathbf{w}]\in\boldsymbol{W}_{h,\mathrm{div}}$ with some $\mathbf{w}\in C^\infty([0,T];C_0^\infty(\Omega)\cap\boldsymbol{H}^1_{0,\mathrm{div}}(\Omega))$ and pass to the limit in (5.3d). The convergence in the first term follows immediately from the weak* convergence of $\partial_t\mathbf{u}_h^\tau$ in $L^{4/\lambda}(0,T;(\boldsymbol{H}^1_{0,\mathrm{div}}(\Omega))')$ implied by (5.10c) and the aforementioned strong convergence of $\mathcal{Q}_h[\mathbf{w}]$. The convergence in the next four terms also follows directly from the results of Lemma 5.1 in combination with Hölder's inequality, Young's inequality, Poincaré's inequality and the Gagliardo-Nirenberg inequality. In particular, we have

$$\begin{aligned}\tfrac12\int_\Omega\Big(\big(\nabla_{\mathbf{x}}\mathbf{u}_h^{\tau,+}\big)^T\cdot\mathcal{Q}_h[\mathbf{w}]\Big)\cdot\mathbf{u}_h^{\tau,-}-\tfrac12\int_{\Omega_T}\Big((\nabla_{\mathbf{x}}\mathcal{Q}_h[\mathbf{w}])^T\cdot\mathbf{u}_h^{\tau,+}\Big)\cdot\mathbf{u}_h^{\tau,-}&\to\int_{\Omega_T}(\mathbf{u}\cdot\nabla_{\mathbf{x}})\mathbf{u}\cdot\mathbf{w},\\ \int_{\Omega_T}2\mathcal{I}_h^{\mathbf{x}}\{\eta(\phi_h^{\tau,+})\}\mathbf{D}\mathbf{u}_h^{\tau,+}:\mathbf{D}\mathcal{Q}_h[\mathbf{w}]&\to\int_{\Omega_T}2\eta(\phi)\mathbf{D}\mathbf{u}:\mathbf{D}\mathbf{w},\\ -\int_{\Omega_T}\phi_h^{\tau,-}\nabla_{\mathbf{x}}\mu_{\phi,h}^{\tau,+}\cdot\mathcal{Q}_h[\mathbf{w}]&\to-\int_{\Omega_T}\phi\nabla_{\mathbf{x}}\mu_\phi\cdot\mathbf{w}\,.\end{aligned}\tag{5.45}$$

Passing to the limit in the sixth term is more technical due to the operator $\Lambda_\nu^{\mathbf{x}}[.]$. Recalling the ideas of the proof of Lemma 4.8 (in particular (4.49)–(4.51)), we dispose the projection operator $\mathcal{Q}_h$ by computing

$$\left|\int_{\Omega_T\times\mathfrak{D}} M_h(\mathcal{Q}_h[\mathbf{w}]-\mathbf{w})\cdot\mathcal{I}_h^{\mathbf{q}}\Big\{\Lambda_\nu^{\mathbf{x}}[\hat\psi_{\mathrm{h}}^{\tau,+}]\nabla_{\mathbf{x}}\mu_{\psi,h,\nu}^{\tau,+}\Big\}\right| \leq \left(\int_{\Omega_T\times\mathfrak{D}} M_h\left|\mathcal{Q}_h[\mathbf{w}]-\mathbf{w}\right|^2\sigma^{\Lambda_\nu^{\mathbf{x}}[\hat\psi_{\mathrm{h}}^{\tau,+}]}(\mathbf{x},\mathbf{q})\right)^{1/2}$$
$$\times\left(\int_{\Omega_T\times\mathfrak{D}} M_h\mathcal{I}_h^{\mathbf{q}}\Big\{\Big(\Lambda_\nu^{\mathbf{x}}[\hat\psi_{\mathrm{h}}^{\tau,+}]\nabla_{\mathbf{x}}\mu_{\psi,h,\nu}^{\tau,+}\Big)\cdot\nabla_{\mathbf{x}}\mu_{\psi,h,\nu}^{\tau,+}\Big\}\right)^{1/2} \leq C\left\|\mathcal{Q}_h[\mathbf{w}]-\mathbf{w}\right\|_{L^2(0,T;H^1(\Omega))}\to 0\,. \tag{5.46}$$

Recycling the ideas used to establish convergence in the fifth term of (5.3c), we compute

$$\begin{aligned}&\left|\int_{\Omega_T\times\mathfrak{D}} M_h\mathbf{w}\cdot\mathcal{I}_h^{\mathbf{q}}\Big\{\Big(\Lambda_\nu^{\mathbf{x}}[\hat\psi_{\mathrm{h}}^{\tau,+}]-\Xi_\nu^{\mathbf{x}}[\hat\psi_{\mathrm{h}}^{\tau,+}]\Big)\nabla_{\mathbf{x}}\mu_{\psi,h,\nu}^{\tau,+}\Big\}\right|\\&\quad\leq C\left(\nu^{-1}\int_{\Omega_T\times\mathfrak{D}} M_h\mathcal{I}_h^{\mathbf{q}}\Big\{\Big|\Lambda_\nu^{\mathbf{x}}[\hat\psi_{\mathrm{h}}^{\tau,+}]-\Xi_\nu^{\mathbf{x}}[\hat\psi_{\mathrm{h}}^{\tau,+}]\Big|^2\Big\}\right)^{1/2}\left(\int_{\Omega_T\times\mathfrak{D}}\nu M_h\mathcal{I}_h^{\mathbf{q}}\Big\{\Big|\nabla_{\mathbf{x}}\mu_{\psi,h,\nu}^{\tau,+}\Big|^2\Big\}\right)^{1/2}\to 0\end{aligned}\tag{5.47}$$

due to (A7). Therefore, replacing replacing $\Lambda_\nu^{\mathbf{x}}[.]$ by $\Xi_\nu^{\mathbf{x}}[.]$ does not change the limit. Using (2.24a) and the convergence implied by Lemma 5.1, we obtain

$$\begin{aligned}&\int_{\Omega_T\times\mathfrak{D}} M_h\mathbf{w}\cdot\mathcal{I}_h^{\mathbf{q}}\Big\{\Xi_\nu^{\mathbf{x}}[\hat\psi_{\mathrm{h}}^{\tau,+}]\nabla_{\mathbf{x}}\mu_{\psi,h,\nu}^{\tau,+}\Big\}\\&\quad=\int_{\Omega_T\times\mathfrak{D}} M_h\mathbf{w}\cdot\nabla_{\mathbf{x}}\hat\psi_h^{\tau,+}+\int_{\Omega_T\times\mathfrak{D}} M_h\mathbf{w}\cdot\mathcal{I}_h^{\mathbf{q}}\Big\{\Xi_\nu^{\mathbf{x}}[\hat\psi_{\mathrm{h}}^{\tau,+}]\nabla_{\mathbf{x}}\mathcal{I}_h^{\mathbf{xq}}\big\{\mathcal{J}_h\big\{\beta(\phi_h^{\tau,+})\big\}\big\}\Big\}\\&\quad=\int_{\Omega_T\times\mathfrak{D}} M_h\mathbf{w}\cdot\mathcal{I}_h^{\mathbf{q}}\Big\{\hat\psi_h^{\tau,+}\nabla_{\mathbf{x}}\mathcal{I}_h^{\mathbf{xq}}\big\{\mathcal{J}_h\big\{\beta(\phi_h^{\tau,+})\big\}\big\}\Big\}\\&\qquad+\int_{\Omega_T\times\mathfrak{D}} M_h\mathbf{w}\cdot\mathcal{I}_h^{\mathbf{q}}\Big\{(\Xi_\nu^{\mathbf{x}}[\hat\psi_{\mathrm{h}}^{\tau,+}]-\hat\psi_h^{\tau,+}\mathbb{1})\nabla_{\mathbf{x}}\mathcal{I}_h^{\mathbf{xq}}\big\{\mathcal{J}_h\big\{\beta(\phi_h^{\tau,+})\big\}\big\}\Big\}\\&\quad\to\int_{\Omega_T\times\mathfrak{D}}\sqrt{\hat M}P_3\mathbf{w}\cdot\nabla_{\mathbf{x}}\mathcal{J}_\varepsilon\{\beta(\phi)\},\end{aligned}\tag{5.48}$$

as $\mathbf{w}$ is solenoidal. Similarly to (5.11c), we obtain the convergence $\mathcal{I}_h^{\mathbf{x}}\{\boldsymbol{\mathcal{J}}_h\{\mathcal{Q}_h[\mathbf{w}]\}\}\to\boldsymbol{\mathcal{J}}_\varepsilon\{\mathbf{w}\}$ in $L^2(0,T;\boldsymbol{W}^{1,\infty}(\Omega))$ which allows us to show convergence of the last term of (5.3d) towards $\int_{\Omega_T\times\mathfrak{D}}\sqrt{\hat M}(\nabla_{\mathbf{x}}\mathcal{J}_h\{\mathbf{w}\}\cdot\mathbf{q})\cdot\boldsymbol{P}_5^+$. As before, we use Young's inequality to justify the restriction to $\Omega_T\times D$. The final result follows from the denseness of $C^\infty([0,T];C_0^\infty(\Omega)\cap\boldsymbol{H}^1_{0,\mathrm{div}}(\Omega))$ in $L^{4/(4-\lambda)}(0,T;\boldsymbol{H}^1_{0,\mathrm{div}}(\Omega))$. □

Remark 5.3. In [18], the existence of weak solutions with similar regularity properties was established starting from an only time-discrete scheme. The regularity properties of the marginal $\omega:=\int_D M\hat\psi$ established in [18] – namely $\omega\in L^\infty(0,T;L^2(\Omega))\cap L^2(0,T;H^1(\Omega))$ – may be recovered from Theorem 5.2 (*cf.* Rem. 2.2.41 in [25]).

In the presented discrete scheme, the Fokker–Planck type equation was stated on a superset of $\Omega\times D$. While passing to the limit, we restricted ourselves to the original domain $\Omega\times D$. This, however, does not violate the conservation of the number density of the polymer chains.

Corollary 5.4. *Let the assumptions of Theorem 5.2 hold true. Then*

$$\int_{\Omega\times D} M\hat\psi(t)=\int_{\Omega\times D} M\hat\Psi^0$$

holds true for almost every $t\in(0,T)$.

Proof. Combining (3.6) with the computation of $\hat{\psi}_h^0$ stated in (4.1) in (A9), we obtain

$$\int_{\Omega\times\mathfrak{D}} (M_h+\mathfrak{m})\hat{\psi}_h^{\tau,(\pm)} = \int_{\Omega\times\mathfrak{D}} (M_h+\mathfrak{m})\hat{\psi}_h^0 = \int_{\Omega\times\mathfrak{D}} (M_h+\mathfrak{m})\hat{\Psi}^0 \tag{5.49}$$

for every $t\in(0,T)$. The strong convergence $(M_h+\mathfrak{m})\to\hat{M}$ in $L^\infty(D)$ (*cf.* Lem. 2.2) implies

$$\int_{\Omega\times\mathfrak{D}} (M_h+\mathfrak{m})\hat{\Psi}^0 \to \int_{\Omega\times\mathfrak{D}} \hat{M}\hat{\Psi}^0 = \int_{\Omega\times D} M\hat{\Psi}^0\,. \tag{5.50}$$

Passing to the limit on the left-hand side of (5.49) then provides the result (*cf.* [25]). □

6. Numerical simulations

For practical computations, the finite element scheme (3.4) is implemented in the framework of the inhouse code `EconDrop` which is written in `C++` (*cf.* [2, 10, 17]). As a proof of concept, we compute the oscillatory

Table 1. Parameters used in the two-dimensional setting.

σ	δ	m	$\rho\,(\pm1)$	$\eta\,(\pm1)$	$c_{\mathbf{x}}$	$c_{\mathbf{q}}$	ν	$\mathfrak{m}$	γ	$\beta\,(-1)$	$\beta\,(+1)$	ε	ϑ
10	0.01	10^{-4}	2	0.005	0.01	0.1	10^{-7}	10^{-23}	10^{-9}	5	1	0.01	1

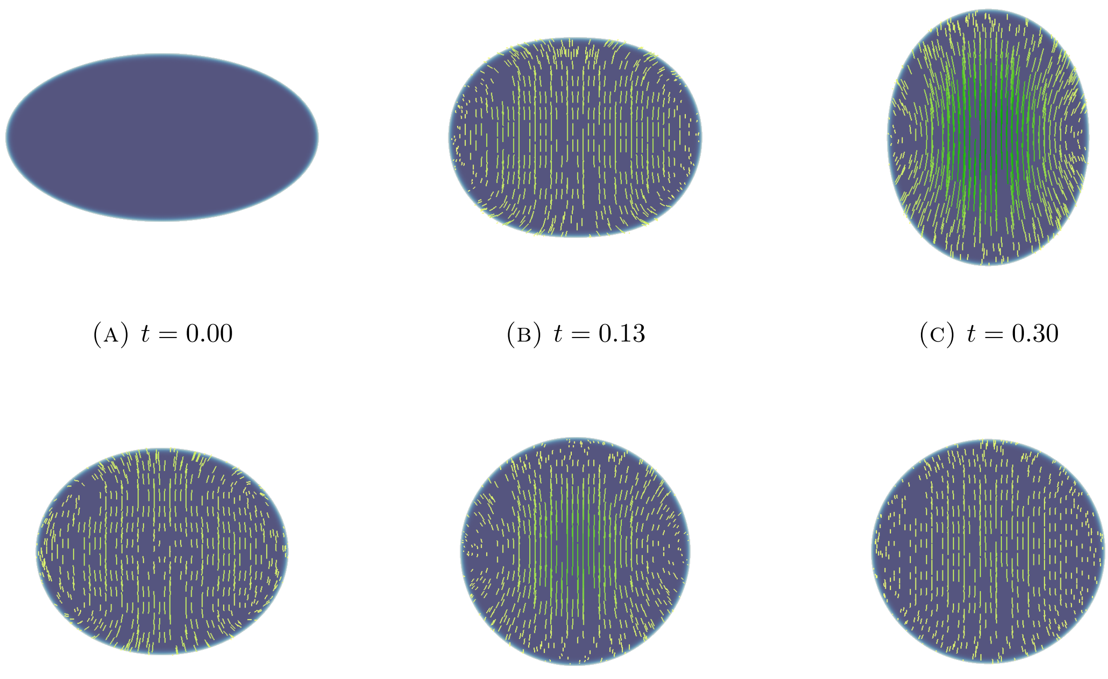

(a) $t=0.00$ (b) $t=0.13$ (c) $t=0.30$

(d) $t=0.60$ (e) $t=0.90$ (f) $t=2.00$

Figure 1. Oscillating droplet

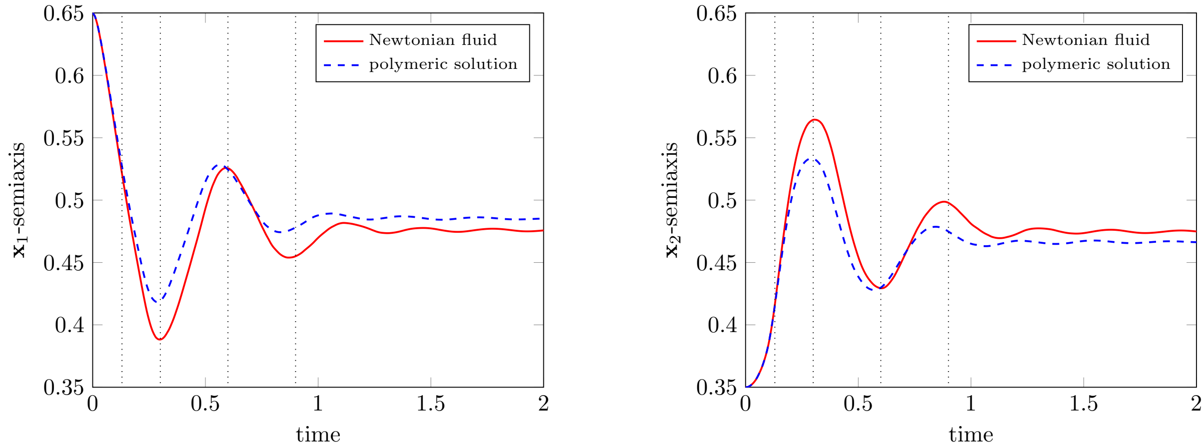

FIGURE 2. Comparison of the length of the semiaxis of oscillating droplets (vertical lines corresponding to shnapshots in Fig. 1).

TABLE 2. Parameters used in the three-dimensional setting.

σ	δ	m	ρ (±1)	η (±1)	$c_{\mathbf{x}}$	$c_{\mathbf{q}}$	ν	$\mathfrak{m}$	γ	β (±1)	τ	ε	ϑ
10	0.02	$2{\cdot}10^{-4}$	2	0.005	0.1	0.2	10^{-7}	10^{-7}	10^{-12}	0	10^{-4}	0.01	1

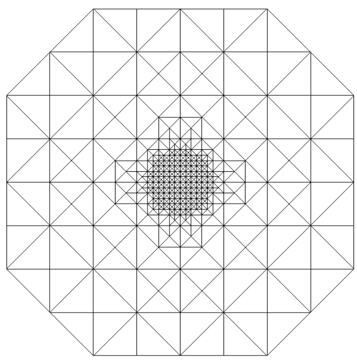

FIGURE 3. Triangulation of $\mathfrak{D}$ $(d = 2)$ adapted to values of M_h.

behaviour of non-Newtonian droplets and compare these results to the behaviour of Newtonian ones. Information concerning the implementation of the discrete scheme can be found in [25]. For a more detailed investigation on the influence of the Deborah number

$$De := \frac{\text{relaxation time}}{\text{typical observation time}}, \tag{6.1}$$

which corresponds to $(2c_{\mathbf{q}})^{-1}$, and the polymer concentration, we also refer to [25].

In a first simulation, we consider a non-Newtonian droplet surrounded by a Newtonian fluid in a two-dimensional set-up, *i.e.* $\Omega \times \mathfrak{D} \subset \mathbb{R}^2 \times \mathbb{R}^2$. For this simulation, we use the following general setting. The

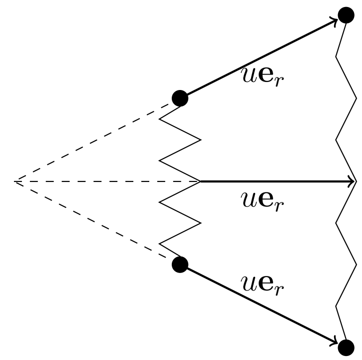

FIGURE 4. Dumbbell subjected to a radial velocity field $u\mathbf{e}_r$.

spatial domain is given as $\Omega = (-1,1)^2$ and discretized using an adaptive triangulation consisting of simplices with diameters between approximately 0.0667 and 0.0083. To evaluate the discrete mollifier which is defined according to (2.38) with $\varepsilon = 0.01$, we choose $\Omega^* = (-1-h_{\mathbf{x}}, 1+h_{\mathbf{x}})^2$ where $h_{\mathbf{x}}$ is the maximal diameter of the simplices (*i.e.* $h_{\mathbf{x}} \approx 0.0667$). Setting $Q_{\max} = 10$, we choose $\mathfrak{D}$ as $\operatorname{supp} M_h \supset D$ on the coarsest triangulation which consists of simplices with a diameter of approximately 3.5355. We refine this triangulation by means of the Maxwellian (*cf.* Fig. 3) such that the smallest simplices have a diamter of approximately 0.3125. Concerning the discretization in time, a fixed time increment $\tau = 10^{-4}$ is used.

Initially, an elliptical shaped droplet (with axes of length 1.3 and 0.7) is placed with its barycenter at $(0,0)$. This droplet, which is indicated by $\phi = 1$, is non-Newtonian and contains polymers with number density $\omega_h^0 = 3$. As the ambient liquid, indicated by $\phi = -1$, is assumed to be Newtonian, we set $\omega_h^0 \equiv 0$ outside of the droplet. Assuming that the polymer chains are in equilibrium at the beginning of the simulations, we set

$$\hat{\psi}_h^0(\mathbf{x},\mathbf{q}) := \omega_h^0(\mathbf{x}) \quad \text{which corresponds to} \quad \psi_h^0(\mathbf{x},\mathbf{q}) := M_h(\mathbf{q})\omega_h^0(\mathbf{x}). \tag{6.2}$$

We restrict the polymers to the droplet by an appropriate β-function which interpolates between $\beta(-1) = 5$ and $\beta(1) = 1$. Concerning the double-well potential, we stick to the prototype (3.2) with $\delta' = 4 \cdot 10^{-3}$ and approximate its derivatives using

$$W_h'(a,b) := \tfrac{1}{4}\big(a^3 + a^2 b + ab^2 + b^3\big) - \tfrac{1}{2}(a+b) + \tfrac{1}{\delta'}\,\tfrac{\mathrm{d}}{\mathrm{d}s}\big|_{s=a} \max\left\{|s|-1, 0\right\}^2. \tag{6.3}$$

The remaining parameters are chosen according to Table 1.

The elliptical shaped droplet tries to attain its energetically optimal, circular shape and starts to contract giving rise to a velocity field. We are interested in the arising non-Newtonian effects – *i.e.* in the arising changes in the polymer configuration and the resulting additional stresses – and in their impact on the rheological behaviour of the droplet. Figure 1 shows the evolution of the non-Newtonian droplet. To illustrate occuring additional stresses, we computed the Kramers tensor $\int_{\mathfrak{D}} M_h \nabla_{\mathbf{q}} \hat{\psi} \otimes \mathbf{q}$ and, if its eigenvalues are real, its eigenvectors and eigenvalues on each $\kappa_{\mathbf{x}} \in \mathcal{T}_h^{\mathbf{x}}$. The eigenvectors to the largest eigenvalue of these tensors are depicted in Figure 1 as yellow and green lines. While the droplet oscillates, the polymer chains build up stresses in mainly vertical direction. To analyze the impact of those stresses, we measure the $\mathbf{x}_1$- and $\mathbf{x}_2$-semiaxis of the droplet and compare them to the ones of a Newtonian droplet.

Figure 2 shows that the oscillation is damped in both cases. Comparing the evolution of the length of the semiaxes, we notice that the oscillation of the non-Newtonian droplet is damped asymmetrically: While the elongation of the $\mathbf{x}_2$-axis (and the contraction of the $\mathbf{x}_1$-axis) of the droplet is significantly more damped in the non-Newtonian case, the amplitudes of the second oscillation are almost identical. This phenomenon can be explained as follows. As the polymer chains are initially in equilibrium, *i.e.* the distribution of their

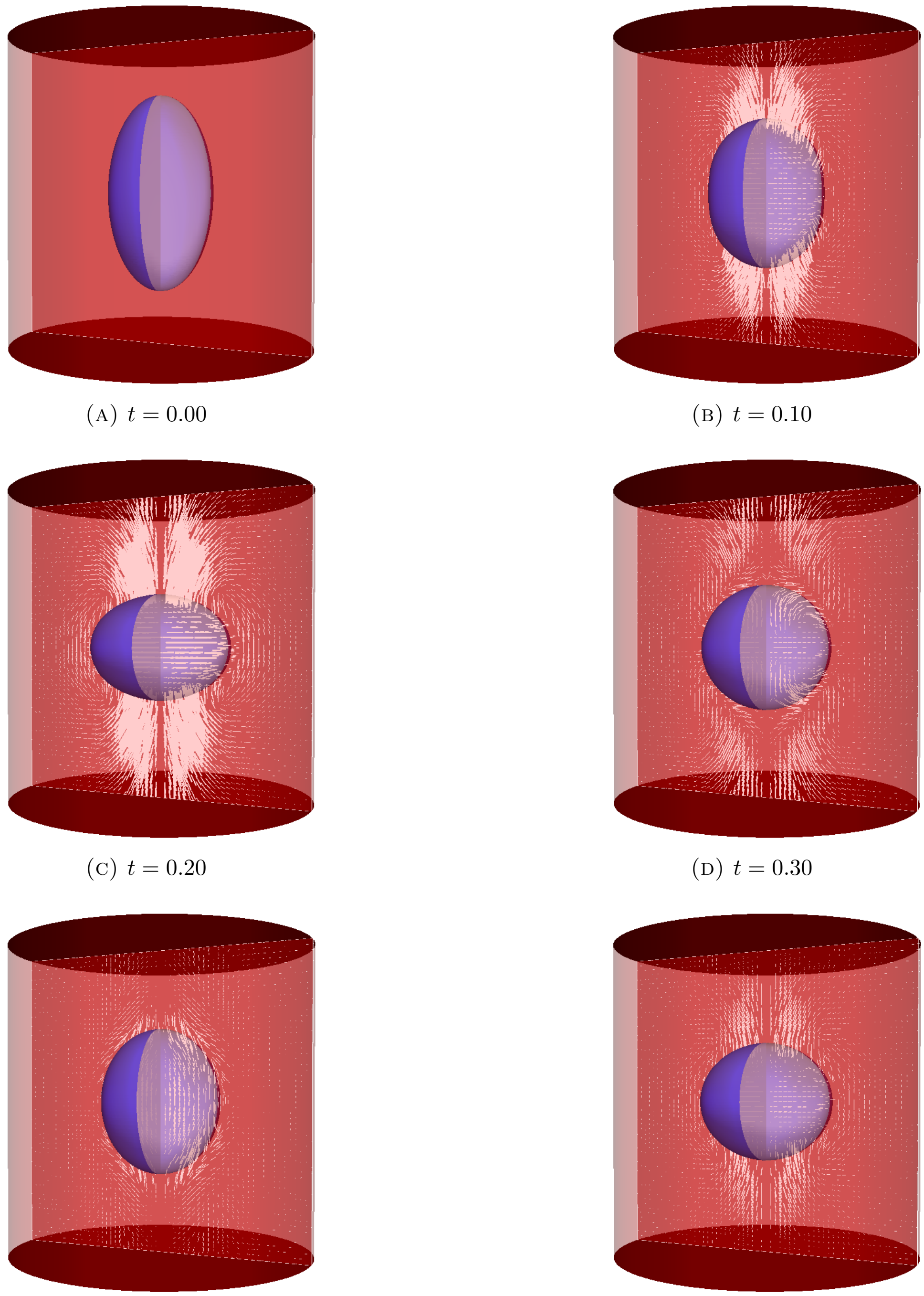

(A) $t = 0.00$ (B) $t = 0.10$

(C) $t = 0.20$ (D) $t = 0.30$

(E) $t = 0.45$ (F) $t = 0.60$

FIGURE 5. Rotationally symmetric, oscillating droplet.

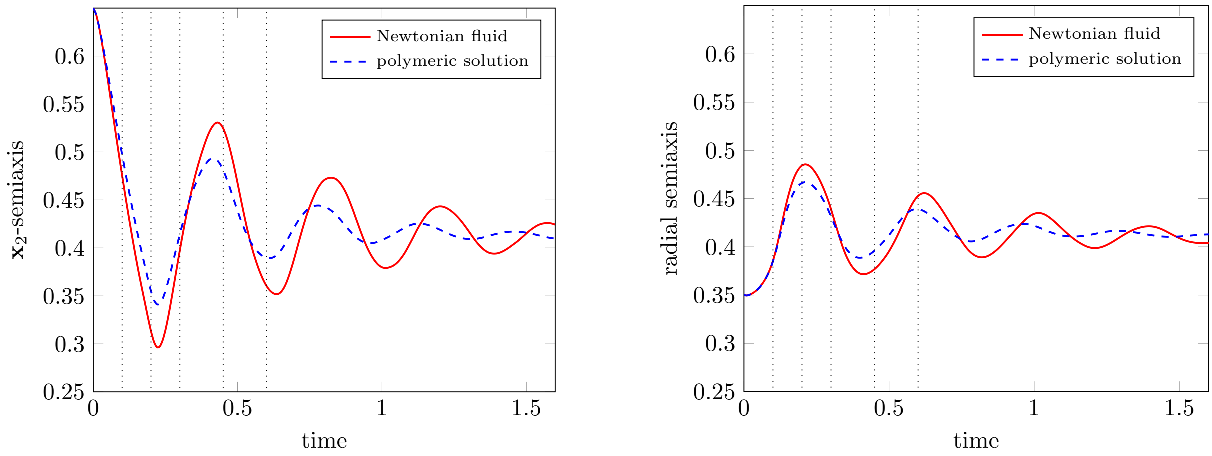

FIGURE 6. Comparison of the length of the semiaxis of oscillating droplets (vertical lines corresponding to shnapshots in Fig. 5).

configurational density is aligned to the Maxwellian, the first oscillation stretches the polymer chains in $\mathbf{x}_2$-direction (*i.e.* vertically). This deflection from equilibrium slows down the oscillation. When swinging back, the oscillation is supported by the polymer chains as it reduces their deviation from their preferred state.

On the long run, both droplets seem to attain a stationary state. Nevertheless, the non-Newtonian one does not attain a perfectly circular shape, but stays slightly elliptical. As Figure 1f shows, there remain still vertical stresses inside of the droplet, which are not dissipated fast enough and therefore still influence the shape of the droplet.

In the second scenario, we consider a non-Newtonian droplet surrounded by an also non-Newtonian fluid. To underline the practicality of the presented scheme, we consider a three-dimensional, rotationally symmetric set-up. We place an ellipsoidal shaped, rotationally symmetric droplet with barycenter at $(0,0,0)$ in the rotationally symmetric, cylindrical domain $\Omega := \{\mathbf{x} \in \mathbb{R}^3 \,:\, -1 < \mathbf{x}_2 < 1,\, \mathbf{x}_1^2 + \mathbf{x}_3^2 < 1\}$. The longest principal axis points in $\mathbf{x}_2$-direction and has length 1.3. The other principal axes are of length 0.7. We parameterize the spatial domain using cylindrical coordinates, *i.e.* it suffices to compute the spatial quantities on a two-dimensional domain $(0,1) \times (-1,1)$ which we discretize using triangles with diameters between approximately 0.0471 and 0.0118. Specifying $Q_{\max} = 10$, we set $\mathfrak{D} := (-10,10)^3$. Adapting the triangulation of $\mathfrak{D}$ to the values of the Maxwellian, we end up with tetrahedrons with diameters between approximately 3.536 and 0.442. In contrast to the last scenario, we consider a two-phase flow consisting of two dilute polymeric solutions. Assuming that the polymer chains are equally soluble in both phases and that the polymer chains are initially in equilibrium, we set $\beta \equiv 0$ and $\hat{\psi}_h^0 \equiv 1$. Similarly to the two-dimensional setting, we use the penalized, polynomial double-well potential introduced in (3.2) with $\delta' = 4 \cdot 10^{-3}$ and approximate its derivatives using (6.3). The remaining parameters are specified in Table 2.

Figure 5 shows the evolution of the droplet. Again, the eigenvectors and eigenvalues of the additional stress tensor are computed. For better readability, we depict the eigenvectors to positive eigenvalues (white lines) of the additional stress tensor only in a cross section of Ω. Although we assumed rotational symmetry, the additional stresses still span a three-dimensional space. In particular, stresses perpendicular to the cross section appear in Figures 5b and 5c on the inside of the droplet, as the radial component of the velocity field may induce elongation of polymer chains in azimuthal direction (*cf.* Fig. 4).

Similar to the first scenario, we compare the evolution of the semiaxes for the case of dilute polymeric solutions and pure Newtonian fluids. As depicted in Figure 6, the oscillation is more damped in the non-Newtonian case than in the Newtonian one. As the Deborah number is chosen larger and the polymer concentration is chosen smaller than in the two-dimensional setting, the additional stresses caused by the polymer chains dissipate faster and have less impact on the evolution of the droplet. Consequently, the damping is not as asymmetric as in the first scenario.

Appendix A. Proofs of Section 2

Proof of Lemma 2.2. (P3) provides $c_3[\mathrm{dist}\,(\mathbf{q},\partial D)]^\kappa \leq M(\mathbf{q}) \leq c_4[\mathrm{dist}\,(\mathbf{q},\partial D)]^\kappa$ on D with $\kappa > 1$ implying the continuity of $\hat{M}$. Recalling the definition of the Maxwellian (see (1.3)), we compute for **q**-derivatives on D

$$\begin{aligned}\left|\partial_{\mathbf{q}_i} M\right| &= C\left|\exp\left(-U(\tfrac{1}{2}\left|\mathbf{q}\right|^2)\right)U'(\tfrac{1}{2}\left|\mathbf{q}\right|^2)\mathbf{q}_i\right| \\ &\leq C\left|M(\mathbf{q})U'(\tfrac{1}{2}\left|\mathbf{q}\right|^2)\right| \leq C[\mathrm{dist}\,(\mathbf{q},\partial D)]^{\kappa-1} \to 0 \end{aligned} \tag{A.1}$$

as $\mathbf{q}\to\partial D$, for $i = 1,\dots,d$. Noting $\hat{M}\equiv 0$ on $\mathfrak{D}\setminus D$, we have $\hat{M}\in C^1(\overline{\mathfrak{D}})$ with $\hat{M}\Big|_{\partial\mathfrak{D}} = 0$.

Due to $\int_{\mathfrak{D}} \mathcal{I}_h^{\mathbf{q}}\{\hat{M}\}\,\mathrm{d}\mathbf{q} \leq |\mathfrak{D}| \max_{\mathbf{q}\in\mathfrak{D}} \hat{M}(\mathbf{q}) \leq C$, there is a constant $c_M > 0$ independent of $h_{\mathbf{q}}$ such that $c_{h_{\mathbf{q}}} \geq c_M$.

Noting $\hat{M}\in C^1(\overline{\mathfrak{D}})$ and applying standard bounds for the interpolation error (*cf.* [9]), we infer

$$\begin{aligned} 1 - \int_{\mathfrak{D}} \mathcal{I}_h^{\mathbf{q}}\left\{\hat{M}\right\}\mathrm{d}\mathbf{q} \leq \left|\int_{\mathfrak{D}} \mathcal{I}_h^{\mathbf{q}}\left\{\hat{M}\right\}\mathrm{d}\mathbf{q} - 1\right| &= \left|\int_{\mathfrak{D}}\left(\mathcal{I}_h^{\mathbf{q}}\left\{\hat{M}\right\} - \hat{M}\right)\mathrm{d}\mathbf{q}\right| \\ &\leq C\left\|\mathcal{I}_h^{\mathbf{q}}\left\{\hat{M}\right\} - \hat{M}\right\|_{L^\infty(\mathfrak{D})} \leq Ch_{\mathbf{q}}\left|\hat{M}\right|_{W^{1,\infty}(\mathfrak{D})} \leq Ch_{\mathbf{q}}, \end{aligned} \tag{A.2}$$

which implies $c_{h_{\mathbf{q}}} \leq \frac{1}{1-Ch_{\mathbf{q}}} \leq C$ for $h_{\mathbf{q}}$ small enough. Computing

$$\begin{aligned} \left\|M_h - \hat{M}\right\|_{L^\infty(\mathfrak{D})} &= \left\|c_{h_{\mathbf{q}}}\mathcal{I}_h^{\mathbf{q}}\left\{\hat{M}\right\} - \hat{M}\right\|_{L^\infty(\mathfrak{D})} \\ &\leq c_{h_{\mathbf{q}}}\left\|\mathcal{I}_h^{\mathbf{q}}\left\{\hat{M}\right\} - \hat{M}\right\|_{L^\infty(\mathfrak{D})} + \left\|\hat{M}\right\|_{L^\infty(\mathfrak{D})} c_{h_{\mathbf{q}}}\left|c_{h_{\mathbf{q}}}^{-1} - 1\right| \\ &\leq c_{h_{\mathbf{q}}}\left\|\mathcal{I}_h^{\mathbf{q}}\left\{\hat{M}\right\} - \hat{M}\right\|_{L^\infty(\mathfrak{D})} + \left\|\hat{M}\right\|_{L^\infty(\mathfrak{D})} c_{h_{\mathbf{q}}}\left|\int_{\mathfrak{D}}\left(\mathcal{I}_h^{\mathbf{q}}\left\{\hat{M}\right\} - \hat{M}\right)\right|. \end{aligned} \tag{A.3}$$

and applying (A.2) completes the proof. □

Proof of Lemma 2.3. As $\hat{\theta}_h, \tilde{\theta}_h \in \hat{X}_h$, $\nabla_{\mathbf{q}}\hat{\theta}_h$ and $\nabla_{\mathbf{q}}\tilde{\theta}_h$ are constant on $\kappa_{\mathbf{x}}\times\kappa_{\mathbf{q}}$ with respect to **q** and $\nabla_{\mathbf{x}}\hat{\theta}_h$ and $\nabla_{\mathbf{x}}\tilde{\theta}_h$ are constant on $\kappa_{\mathbf{x}}\times\kappa_{\mathbf{q}}$ with respect to **x**. We use $\|\mathcal{I}_h^{\mathbf{x}}\{g_{\mathbf{x}}\} - g_{\mathbf{x}}\|_{L^\infty(\kappa_{\mathbf{x}})} \leq Ch_{\mathbf{x}}^2\,|g_{\mathbf{x}}|_{W^{2,\infty}(\kappa_{\mathbf{x}})}$ for $g_{\mathbf{x}}\in W^{2,\infty}(\kappa_{\mathbf{x}})$ (*cf.* [9]) to compute

$$\begin{aligned} &\int_{\kappa_{\mathbf{x}}\times\kappa_{\mathbf{q}}}\left|M_h(I-\mathcal{I}_h^{\mathbf{x}})\left\{\nabla_{\mathbf{q}}\hat{\theta}_h\cdot\nabla_{\mathbf{q}}\tilde{\theta}_h\right\}\right|\,\mathrm{d}\mathbf{q}\,\mathrm{d}\mathbf{x} \\ &\leq \left(\int_{\kappa_{\mathbf{x}}\times\kappa_{\mathbf{q}}} M_h\,\mathrm{d}\mathbf{q}\,\mathrm{d}\mathbf{x}\right)\left\|(I-\mathcal{I}_h^{\mathbf{x}})\left\{\nabla_{\mathbf{q}}\hat{\theta}_h\cdot\nabla_{\mathbf{q}}\tilde{\theta}_h\right\}\right\|_{L^\infty(\kappa_{\mathbf{x}})} \\ &\leq Ch_{\mathbf{x}}^2\left(\int_{\kappa_{\mathbf{x}}\times\kappa_{\mathbf{q}}} M_h\,\mathrm{d}\mathbf{q}\,\mathrm{d}\mathbf{x}\right)\left|\nabla_{\mathbf{q}}\hat{\theta}_h\cdot\nabla_{\mathbf{q}}\tilde{\theta}_h\right|_{W^{2,\infty}(\kappa_{\mathbf{x}})} \\ &\leq Ch_{\mathbf{x}}^2\left(\int_{\kappa_{\mathbf{x}}\times\kappa_{\mathbf{q}}} M_h\,\mathrm{d}\mathbf{q}\,\mathrm{d}\mathbf{x}\right)\sum_{i,j,k=1}^d\left|\partial_{\mathbf{x}_j}\partial_{\mathbf{q}_i}\hat{\theta}_h\partial_{\mathbf{x}_k}\partial_{\mathbf{q}_i}\tilde{\theta}_h\right| \end{aligned} \tag{A.4}$$

as $\hat{\theta}_h, \tilde{\theta}_h \in \hat{X}_h$and $\partial_{\mathbf{x}_i}\partial_{\mathbf{x}_j}\hat{\theta}_h = \partial_{\mathbf{x}_i}\partial_{\mathbf{x}_j}\tilde{\theta}_h = 0$ $(i,j = 1,\dots,d)$. Since $\partial_{\mathbf{x}_j}\partial_{\mathbf{q}_i}\hat{\theta}_h$ and $\partial_{\mathbf{x}_j}\partial_{\mathbf{q}_i}\tilde{\theta}_h$ are constant on $\kappa_{\mathbf{x}} \times \kappa_{\mathbf{q}}$ for $i,j = 1,\dots,d$, we obtain that the right-hand side of (A.4) is bounded by

$$Ch_{\mathbf{x}}^2 \sum_{i,j,k=1}^{d} \left(\int_{\kappa_{\mathbf{x}}\times\kappa_{\mathbf{q}}} M_h \left| \partial_{\mathbf{x}_j}\partial_{\mathbf{q}_i}\hat{\theta}_h \right|^2 \, \mathrm{d}\mathbf{q}\,\mathrm{d}\mathbf{x} \right)^{1/2} \left(\int_{\kappa_{\mathbf{x}}\times\kappa_{\mathbf{q}}} M_h \left| \partial_{\mathbf{x}_k}\partial_{\mathbf{q}_i}\tilde{\theta}_h \right|^2 \, \mathrm{d}\mathbf{q}\,\mathrm{d}\mathbf{x} \right)^{1/2}. \tag{A.5}$$

We apply (2.13c) to the first integral in (A.5) and obtain

$$\begin{aligned} \sum_{i,j=1}^{d} \left(\int_{\kappa_{\mathbf{x}}\times\kappa_{\mathbf{q}}} M_h \left| \partial_{\mathbf{x}_j}\partial_{\mathbf{q}_i}\hat{\theta}_h \right|^2 \, \mathrm{d}\mathbf{q}\,\mathrm{d}\mathbf{x} \right)^{1/2} &\le C \sum_{i=1}^{d} \left(\int_{\kappa_{\mathbf{q}}} M_h \int_{\kappa_{\mathbf{x}}} \left| \nabla_{\mathbf{x}}(\partial_{\mathbf{q}_i}\hat{\theta}_h) \right|^2 \, \mathrm{d}\mathbf{x}\,\mathrm{d}\mathbf{q} \right)^{1/2} \\ \le Ch_{\mathbf{x}}^{-1} \sum_{i=1}^{d} \left(\int_{\kappa_{\mathbf{x}}\times\kappa_{\mathbf{q}}} M_h \left| \partial_{\mathbf{q}_i}\hat{\theta}_h \right|^2 \, \mathrm{d}\mathbf{q}\,\mathrm{d}\mathbf{x} \right)^{1/2} &\le Ch_{\mathbf{x}}^{-1} \left(\int_{\kappa_{\mathbf{x}}\times\kappa_{\mathbf{q}}} M_h \left| \nabla_{\mathbf{q}}\hat{\theta}_h \right|^2 \, \mathrm{d}\mathbf{q}\,\mathrm{d}\mathbf{x} \right)^{1/2}, \end{aligned} \tag{A.6}$$

which yields (2.16a). Analogous computations provide a bound similar to (A.5) for the left-hand side of (2.16b) with $h_{\mathbf{x}}$ substituted by $h_{\mathbf{q}}$. We apply (A.6) to the first integral and use $\frac{h_{\mathbf{q}}}{h_{\mathbf{x}}} \le C$ (*cf.* (2.1)) to complete the proof of (2.16b).
To prove the last inequality, we use that the left-hand side of (2.16c) is bounded by

$$\int_{\kappa_{\mathbf{x}}\times\kappa_{\mathbf{q}}} \left| M_h (I - \mathcal{I}_h^{\mathbf{x}}) \left\{ \hat{\theta}_h \tilde{\theta}_h \right\} \right| \, \mathrm{d}\mathbf{q}\,\mathrm{d}\mathbf{x} + \int_{\kappa_{\mathbf{x}}\times\kappa_{\mathbf{q}}} \left| M_h (I - \mathcal{I}_h^{\mathbf{q}}) \left\{ \mathcal{I}_h^{\mathbf{x}} \left\{ \hat{\theta}_h \tilde{\theta}_h \right\} \right\} \right| \, \mathrm{d}\mathbf{q}\,\mathrm{d}\mathbf{x} \\ =: I + II\,. \tag{A.7}$$

As before, we use that $\hat{\theta}_h$ and $\tilde{\theta}_h$ are affine linear with respect to $\mathbf{x}$ on $\kappa_{\mathbf{x}}$ and compute

$$\begin{aligned} I &\le \int_{\kappa_{\mathbf{x}}\times\kappa_{\mathbf{q}}} M_h \left\| (I - \mathcal{I}_h^{\mathbf{x}}) \left\{ \hat{\theta}_h \tilde{\theta}_h \right\} \right\|_{L^\infty(\kappa_{\mathbf{x}})} \, \mathrm{d}\mathbf{q}\,\mathrm{d}\mathbf{x} \le Ch_{\mathbf{x}}^2 \int_{\kappa_{\mathbf{x}}\times\kappa_{\mathbf{q}}} M_h \left| \hat{\theta}_h \tilde{\theta}_h \right|_{W^{2,\infty}(\kappa_{\mathbf{x}})} \, \mathrm{d}\mathbf{q}\,\mathrm{d}\mathbf{x} \\ &\le Ch_{\mathbf{x}}^2 \int_{\kappa_{\mathbf{x}}\times\kappa_{\mathbf{q}}} M_h \sum_{i,j=1}^{d} \left| \partial_{\mathbf{x}_i}\hat{\theta}_h \partial_{\mathbf{x}_j}\tilde{\theta}_h \right| \, \mathrm{d}\mathbf{q}\,\mathrm{d}\mathbf{x} \\ &\le Ch_{\mathbf{x}}^2 \left(\int_{\kappa_{\mathbf{x}}\times\kappa_{\mathbf{q}}} M_h \left| \nabla_{\mathbf{x}}\hat{\theta}_h \right|^2 \, \mathrm{d}\mathbf{q}\,\mathrm{d}\mathbf{x} \right)^{1/2} \left(\int_{\kappa_{\mathbf{x}}\times\kappa_{\mathbf{q}}} M_h \left| \nabla_{\mathbf{x}}\tilde{\theta}_h \right|^2 \, \mathrm{d}\mathbf{q}\,\mathrm{d}\mathbf{x} \right)^{1/2} \end{aligned} \tag{A.8}$$

and

$$\begin{aligned} II \le& \left(\int_{\kappa_{\mathbf{x}}\times\kappa_{\mathbf{q}}} M_h \, \mathrm{d}\mathbf{q}\,\mathrm{d}\mathbf{x} \right) \left\| (I - \mathcal{I}_h^{\mathbf{q}}) \left\{ \mathcal{I}_h^{\mathbf{x}} \left\{ \hat{\theta}_h \tilde{\theta}_h \right\} \right\} \right\|_{L^\infty(\kappa_{\mathbf{x}}\times\kappa_{\mathbf{q}})} \\ \le& Ch_{\mathbf{q}}^2 \left(\int_{\kappa_{\mathbf{x}}\times\kappa_{\mathbf{q}}} M_h \, \mathrm{d}\mathbf{q}\,\mathrm{d}\mathbf{x} \right) \left\| \nabla_{\mathbf{q}}\hat{\theta}_h \right\|_{L^\infty(\kappa_{\mathbf{x}})} \left\| \nabla_{\mathbf{q}}\tilde{\theta}_h \right\|_{L^\infty(\kappa_{\mathbf{x}})} . \end{aligned} \tag{A.9}$$

As $\nabla_{\mathbf{q}}\hat{\theta}_h$ and $\nabla_{\mathbf{q}}\tilde{\theta}_h$ are affine linear with respect to $\mathbf{x}$, they will attain their maximum in one of the vertices of $\kappa_{\mathbf{x}}$, which are denoted by $\{\mathbf{P}_{\kappa_{\mathbf{x}},i}\}_{i=0,\dots,d}$. Therefore, we may compute

$$\begin{aligned}
&\left(\int_{\kappa_{\mathbf{x}}\times\kappa_{\mathbf{q}}} M_h \,\mathrm{d}\mathbf{q}\,\mathrm{d}\mathbf{x}\right)\left\|\nabla_{\mathbf{q}}\hat{\theta}_h\right\|_{L^\infty(\kappa_{\mathbf{x}})}\left\|\nabla_{\mathbf{q}}\tilde{\theta}_h\right\|_{L^\infty(\kappa_{\mathbf{x}})} \\
&\leq \int_{\kappa_{\mathbf{x}}\times\kappa_{\mathbf{q}}} M_h \sum_{i=0}^{d}\left|\nabla_{\mathbf{q}}\hat{\theta}_h(\mathbf{P}_{\kappa_{\mathbf{x}},i},\mathbf{q})\right|\sum_{j=0}^{d}\left|\nabla_{\mathbf{q}}\tilde{\theta}_h(\mathbf{P}_{\kappa_{\mathbf{x}},j},\mathbf{q})\right| \,\mathrm{d}\mathbf{q}\,\mathrm{d}\mathbf{x} \\
&\leq \left(\int_{\kappa_{\mathbf{x}}\times\kappa_{\mathbf{q}}} M_h\left(\sum_{i=0}^{d}\left|\nabla_{\mathbf{q}}\hat{\theta}_h(\mathbf{P}_{\kappa_{\mathbf{x}},i},\mathbf{q})\right|\right)^2 \,\mathrm{d}\mathbf{q}\,\mathrm{d}\mathbf{x}\right)^{1/2} \\
&\leq C\left(\int_{\kappa_{\mathbf{x}}\times\kappa_{\mathbf{q}}} M_h\left|\nabla_{\mathbf{q}}\hat{\theta}_h\right|^2 \,\mathrm{d}\mathbf{q}\,\mathrm{d}\mathbf{x}\right)^{1/2}\left(\int_{\kappa_{\mathbf{x}}\times\kappa_{\mathbf{q}}} M_h\left|\nabla_{\mathbf{q}}\tilde{\theta}_h\right|^2 \,\mathrm{d}\mathbf{q}\,\mathrm{d}\mathbf{x}\right)^{1/2}.
\end{aligned} \tag{A.10}$$

Combining (A.7)–(A.10) yields (2.16c). ☐

Appendix B. Miscellaneous

Lemma B.1. *Let ϕ, $\hat{\psi}$, and $\mathbf{u}$ satisfy (1.5) on a formal level. Then the energy $\mathcal{E}$ defined in (1.7) satisfies*

$$\begin{aligned}
&\mathcal{E}(\phi,\hat{\psi},\mathbf{u})\Big|_{t=T} + \int_{\Omega_T\times D} M\hat{\psi}\left|\nabla_{\mathbf{q}}g'(\hat{\psi})\right|^2 + \int_{\Omega_T\times D} M\hat{\psi}\left|\nabla_{\mathbf{x}}\Big(g'(\hat{\psi})+\mathcal{J}_\varepsilon\{\beta(\phi)\}\Big)\right|^2 \\
&\quad + \int_{\Omega_T}\left|\nabla_{\mathbf{x}}\mu_\phi\right|^2 + \int_{\Omega_T} 2\eta(\phi)\left|\mathbf{D}\mathbf{u}\right|^2 = \mathcal{E}(\phi,\hat{\psi},\mathbf{u})\Big|_{t=0},
\end{aligned} \tag{B.1}$$

for all $T\geq 0$ In particular, we have $\mathcal{E}(\phi,\hat{\psi},\mathbf{u})\Big|_{t=T} \leq \mathcal{E}(\phi,\hat{\psi},\mathbf{u})\Big|_{t=0}$.

Proof. Testing (1.5a) by μ_ϕ and (1.5b) by $\partial_t\phi$ and integrating by parts yields

$$\int_\Omega \partial_t\phi\mu_\phi - \int_\Omega \phi\mathbf{u}\cdot\nabla_{\mathbf{x}}\mu_\phi + \int_\Omega \left|\nabla_{\mathbf{x}}\mu_\phi\right|^2 = 0, \tag{B.2}$$

$$\int_\Omega \partial_t\phi\mu_\phi = \int_\Omega \tfrac{1}{2}\partial_t\left|\nabla_{\mathbf{x}}\phi\right|^2 + \int_\Omega \partial_t W(\phi) + \int_{\Omega\times D}\mathcal{J}_\varepsilon\{\partial_t\beta(\phi)\}M\hat{\psi}\,. \tag{B.3}$$

In the next step, we test (1.5c) by the chemical potential $(g'(\hat{\psi})+\mathcal{J}_\varepsilon\{\beta(\phi)\})$. Using the identity $\hat{\psi}\nabla_{\mathbf{q}}g'(\hat{\psi}) = \nabla_{\mathbf{q}}\hat{\psi}$ and the fact that $\mathcal{J}_\varepsilon\{\beta(\phi)\}$ is independent of $\mathbf{q}$, we obtain

$$\begin{aligned}
&\int_{\Omega\times D} M\partial_t g(\hat{\psi}) + \int_{\Omega\times D}\mathcal{J}_\varepsilon\{\beta(\phi)\}\partial_t\hat{\psi} - \int_{\Omega\times D} M\hat{\psi}\nabla_{\mathbf{x}}\Big(g'(\hat{\psi})+\mathcal{J}_\varepsilon\{\beta(\phi)\}\Big)\cdot\mathbf{u} \\
&\quad - \int_{\Omega\times D} M(\nabla_{\mathbf{x}}\boldsymbol{\mathcal{J}}_\varepsilon\{\mathbf{u}\}\cdot\mathbf{q})\cdot\nabla_{\mathbf{q}}\hat{\psi} + \int_{\Omega\times D} c_{\mathbf{q}}M\hat{\psi}\left|\nabla_{\mathbf{q}}g'(\hat{\psi})\right|^2 + \int_{\Omega\times D} c_{\mathbf{x}}M\hat{\psi}\left|\nabla_{\mathbf{x}}\Big(g'(\hat{\psi})+\mathcal{J}_\varepsilon\{\beta(\phi)\}\Big)\right|^2 = 0 \\
&.
\end{aligned} \tag{B.4}$$

Testing (1.5d) by $\mathbf{u}$ and integrating by parts with respect to $\mathbf{x}$, we obtain

$$\begin{aligned}
&\int_\Omega \tfrac{1}{2}\rho(\phi)\partial_t\left|\mathbf{u}\right|^2 + \int_\Omega \tfrac{1}{2}\rho(\phi)\mathbf{u}\cdot\nabla_{\mathbf{x}}\left|\mathbf{u}\right|^2 - \int_\Omega \tfrac{1}{2}\rho'(\phi)m(\phi)\nabla_{\mathbf{x}}\mu_\phi\cdot\nabla_{\mathbf{x}}\left|\mathbf{u}\right|^2 + \int_\Omega 2\eta(\phi)\left|\mathbf{D}\mathbf{u}\right|^2 \\
&\quad = -\int_\Omega \phi\nabla_{\mathbf{x}}\mu_\phi\cdot\mathbf{u} - \int_{\Omega\times D} M\hat{\psi}\nabla_{\mathbf{x}}\Big(g'(\hat{\psi})+\mathcal{J}_\varepsilon\{\beta(\phi)\}\Big)\cdot\mathbf{u} - \int_{\Omega\times D} M(\nabla_{\mathbf{x}}\boldsymbol{\mathcal{J}}_\varepsilon\{\mathbf{u}\}\cdot\mathbf{q})\cdot\nabla_{\mathbf{q}}\hat{\psi}\,.
\end{aligned} \tag{B.5}$$

In order to get rid of the second and third term in (B.5), we additionally test (1.5a) by $\frac{1}{2}\rho'(\phi)\left|\mathbf{u}\right|^2$. Using the fact that ρ' is constant and that the convection terms in (B.2) and (B.4) reappear on the right-hand side of (B.5), we add the equations above and end up with

$$\begin{aligned}&\int_{\Omega\times D} M\partial_t g(\hat{\psi}) + \int_{\Omega\times D} M\partial_t\Big(\mathcal{J}_\varepsilon\{\beta(\phi)\}\hat{\psi}\Big) + \int_\Omega \tfrac{1}{2}\partial_t\left|\nabla_{\mathbf{x}}\phi\right|^2 + \int_\Omega \partial_t W(\phi) + \int_\Omega \tfrac{1}{2}\partial_t\left|\mathbf{u}\right|^2\\ &\quad+\int_{\Omega\times D} M\hat{\psi}\left|\nabla_{\mathbf{q}} g'(\hat{\psi})\right|^2 + \int_{\Omega\times D} M\hat{\psi}\left|\nabla_{\mathbf{x}}\Big(g'(\hat{\psi}) + \mathcal{J}_\varepsilon\{\beta(\phi)\}\Big)\right|^2 + \int_\Omega\left|\nabla_{\mathbf{x}}\mu_\phi\right|^2 + \int_\Omega 2\eta(\phi)\left|\mathbf{Du}\right|^2 = 0\\ &.\end{aligned} \tag{B.6}$$

As M is time-independent an integration with respect to time yields (B.1). □

For the reader's convenience, we cite a compactness result by Azérad and Guillén (*cf.* [4]).

Lemma B.2. *Let $T > 0$, and let the Banach spaces $\mathbf{X} \overset{compact}{\hookrightarrow} \mathbf{B} \hookrightarrow \mathbf{Y}$. Let $(f_\epsilon)_{\epsilon>0}$ be a family of functions of $L^p(0,T;\mathbf{X})$, $1 \le p \le \infty$, with the extra condition $(f_\epsilon)_{\epsilon>0} \subset C(0,T;\mathbf{Y})$ if $p = \infty$, such that*

- *$(f_\epsilon)_{\epsilon>0}$ is bounded in $L^p(0,T;\mathbf{X})$,*
- *$\|f_\epsilon(\cdot+\tau) - f_\epsilon(\cdot)\|_{L^p(0,T-\tau;\mathbf{Y})} \le \varphi(\tau) + \psi(\epsilon)$ with $\lim_{\tau\to 0}\varphi(\tau) = 0 = \lim_{\epsilon\to 0}\psi(\epsilon)$.*

Then the family $(f_\epsilon)_{\epsilon>0}$ posses a cluster point in $L^p(0,T;\mathbf{B})$ and also in $C(0,T;\mathbf{B})$ if $p = \infty$, as $\epsilon \to 0$.

Acknowledgements. This research has been supported by Deutsche Forschungsgemeinschaft (German Science Foundation) through the Priority Programme 1506 "Transport processes at fluidic interfaces".

References

[1] H. Abels, H. Garcke and G. Grün, Thermodynamically consistent, frame indifferent diffuse interface models for incompressible two-phase flows with different densities. *Math. Models Methods Appl. Sci.* **22** (2012) 1150013.

[2] S. Aland, S. Boden, A. Hahn, F. Klingbeil, M. Weismann and S. Weller, Quantitative comparison of Taylor flow simulations based on sharp-interface and diffuse-interface models. *Int. J. Numer. Methods Fluids* **73** (2013) 344–361.

[3] F. Armero and J.C. Simo, Formulation of a new class of fractional-step methods for the incompressible MHD equations that retains the long-term dissipativity of the continuum dynamical system. *Fields Inst. Commun.* **10** (1996) 1–24.

[4] P. Azêrad and F. Guilln, Mathematical justification of the hydrostatic approximation in the primitive equations of geophysical fluid dynamics. *SIAM J. Math. Anal.* **33** (2001) 847–859.

[5] J.W. Barrett and E. Süli, Existence of global weak solutions to some regularized kinetic models for dilute polymers. *Multiscale Model. Simul.* **6** (2007) 506–546.

[6] J.W. Barrett and E. Süli, Existence and equilibration of global weak solutions to kinetic models for dilute polymers. I: Finitely extensible nonlinear bead-spring chains. *M3AS* **21** (2011) 1211–1289.

[7] J.W. Barrett and E. Süli, Finite element approximation of kinetic dilute polymer models with microscopic cut-off. *ESAIM M2AN* **45** (2011) 39–89.

[8] J.W. Barrett and E. Süli, Finite element approximation of finitely extensible nonlinear elastic dumbbell models for dilute polymers. *ESAIM M2AN* **46** (2012) 949–978.

[9] S.C. Brenner and L.R. Scott, The mathematical theory of finite element methods. Springer (2002).

[10] E. Campillo-Funollet, G. Grün and F. Klingbeil, On modeling and simulation of electrokinetic phenomena in two-phase flow with general mass densities. *SIAM J. App. Math.* **72** (2012) 1899–1925.

[11] Ph.G. Ciarlet, The finite element method for elliptic problems. North-Holland (1978).

[12] M. Dauge, Stationary stokes and Navier–Stokes systems on two- or three-dimensional domains with corners. Part I. Linearized equations. *SIAM J. Math. Anal.* **20** (1989) 74–97.

[13] F.M. Guillén-González and J.V. Gutiérrez-Santacreu, A linear mixed finite element scheme for a nematic ericksenleslie liquid crystal model. *ESAIM: M2AN* **47** (2013) 1433–1464.

[14] V. Girault and P. Raviard, Finite element methods for Navier–Stokes equations. In Vol. 5 of *Springer Series in Computational Mathematics.* Springer (1986).

[15] G. Grün, On convergent schemes for diffuse interface models for two-phase flow of incompressible fluids with general mass densities. *SIAM J. Numer. Anal.* **51** (2013) 3036–3061.

[16] G. Grün, F. Guillén-González and S. Metzger, On fully decoupled, convergent schemes for diffuse interface models for two-phase flow with general mass densities. *CiCP* **19** (2016) 1473–1502.

[17] G. Grün and F. Klingbeil, Two-phase flow with mass density contrast: stable schemes for a thermodynamic consistent and frame-indifferent diffuse-interface model. *J. Comput. Phys.* **257** Part A (2014) 708–725.

[18] G. Grün and S. Metzger, On micro-macro-models for two-phase flow with dilute polymeric solutions – modeling and analysis. *Math. Model. Methods Appl. Sci.* **26** (2016), 823–866.

[19] G. Grün and M. Rumpf, Nonnegativity preserving convergent schemes for the thin film equation. *Numer. Math* **87** (2000) 113–152.

[20] F. Guillén-González and G. Tierra, Splitting schemes for a Navier–Stokes–Cahn–Hilliard model for two fluids with different densities. *J. Comput. Math.* **32** (2014) 643–664.

[21] J.G. Heywood and R. Rannacher, Finite element approximation of the nonstationary Navier–Stokes problem. I. Regularity of solutions and second-order error estimates for spatial discretization. *SIAM J. Numer. Anal.* **19** (1982) 275–311.

[22] C. Le Bris and T. Lelièvre, Multiscale modelling of complex fluids: a mathematical initiation, in Multiscale modeling and simulation in science, edited by B. Engquist, P. Lötstedt and O. Runborg. In Vol. 66 of *Lecture Notes in Computational Science and Engineering*. Springer (2009) 49–137.

[23] N. Masmoudi, Well-posedness for the fene dumbbell model of polymeric flows. *Commun. Pure Appl. Math.* **61** (2008) 1685–1714.

[24] N. Masmoudi, Global existence of weak solutions to the FENE dumbbell model of polymeric flows. *Invent. Math.* **191** (2013) 427–500.

[25] S. Metzger, *Diffuse interface models for complex flow scenarios: modeling, analysis and simulations*; Ph.D. Thesis, Friedrich-Alexander-Universität Erlangen-Nürnberg (2017).

[26] S. Minjeaud, An unconditionally stable uncoupled scheme for a triphasic Cahn–Hilliard/Navier-Stokes model. *Numer Methods Partial Differ Equ.* **29** (2013) 584–618.

[27] J. Simon, Compact sets in the space $L^p(0,T;B)$. *Ann. Mat. Pura Appl.* (IV) **146** (1987) 65–96.

[28] R. Temam, Navier–Stokes equations: theory and numerical analysis, Reprint. with corr. AMS Chelsea Publ. (2001).

[29] V. Thomée, Galerkin finite element methods for parabolic problems. Springer (1984).

[30] H. Triebel, Interpolation theory, function spaces, differential operators. North-Holland Publ. (1978).

[31] H. Werner and H. Arndt, Gewöhnliche Differentialgleichungen. Springer Verlag (1991).

On stable, dissipation reducing splitting schemes for two-phase flow of electrolyte solutions

Stefan Metzger

Numerical Algorithms

ISSN 1017-1398

Numer Algor
DOI 10.1007/s11075-018-0530-2

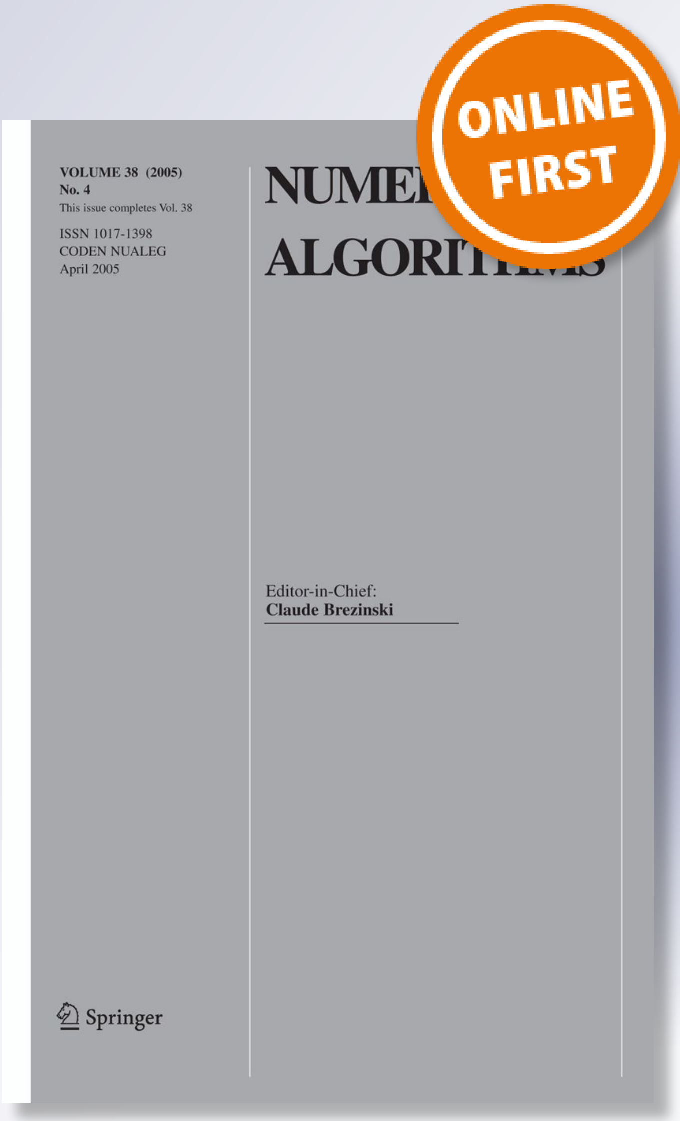

Numer Algor
https://doi.org/10.1007/s11075-018-0530-2

ORIGINAL PAPER

On stable, dissipation reducing splitting schemes for two-phase flow of electrolyte solutions

Stefan Metzger[1]

Received: 22 August 2017 / Accepted: 9 April 2018

Abstract In this paper, we are concerned with the numerical treatment of a recent diffuse interface model for two-phase flow of electrolyte solutions (Campillo-Funollet et al., SIAM J. Appl. Math. **72**(6), 1899–1925, 2012) . This model consists of a Nernst–Planck-system describing the evolution of the ion densities and the electrostatic potential which is coupled to a Cahn–Hilliard–Navier–Stokes-system describing the evolution of phase-field, velocity field, and pressure. In the first part, we present a stable, fully discrete splitting scheme, which allows to split the governing equations into different blocks, which may be treated sequentially and thereby reduces the computational costs significantly. This scheme comprises different mechanisms to reduce the induced numerical dissipation. In the second part, we investigate the impact of these mechanisms on the scheme's sensitivity to the size of the time increment using the example of a falling droplet. Finally, we shall present simulations showing ion induced changes in the topology of charged droplets serving as a qualitative validation for our discretization and the underlying model.

Keywords Electrolyte solutions · Phase-field model · Navier–Stokes equations · Cahn–Hilliard equation · Nernst–Planck equations · Finite element scheme · Splitting scheme

Mathematics Subject Classification (2010) 35Q35 · 65M60 · 65M12 · 76D05 · 76T99 · 76W05

✉ Stefan Metzger
stefan.metzger@fau.de

[1] Department Mathematik, Friedrich-Alexander-Universität Erlangen-Nürnberg, Cauerstr. 11, 91058 Erlangen, Germany

Published online: 23 April 2018

1 Introduction

In this paper, we are concerned with the numerical treatment of a diffuse interface model for two-phase flow of electrolyte solutions (cf. [5]) The model describes the evolution of two immiscible fluids with several dissolved species differing in valence and solubility properties. It is based on a diffuse interface description with a solenoidal, volume-averaged velocity field u (cf. [1]), and reads as follows.

$$\partial_t(\rho(\phi)u) + \operatorname{div}\{\rho(\phi)u\otimes u\} - \operatorname{div}\left\{u\otimes\rho'(\phi)m(\phi)\nabla\mu_\phi\right\} - \operatorname{div}\{2\eta(\phi)Du\} + \nabla p$$
$$= \mu_\phi\nabla\phi + \sum_{j=1}^{K}\mu_{\omega_j}\nabla\omega_j - \sum_{j=1}^{K} z_j\omega_j\nabla V\,, \tag{1.1a}$$

$$\operatorname{div} u = 0\,, \tag{1.1b}$$

$$\partial_t\phi + u\cdot\nabla\phi - \operatorname{div}\left\{m(\phi)\nabla\mu_\phi\right\} = 0\,, \tag{1.1c}$$

$$\mu_\phi = \frac{\partial f(\phi,\nabla\phi)}{\partial\phi} - \operatorname{div}\left\{\frac{\partial f(\phi,\nabla\phi)}{\partial\nabla\phi}\right\} + \sum_{j=1}^{K}\beta_j'(\phi)\omega_j - \tfrac{1}{2}\partial_\phi\epsilon\,|\nabla V|\,, \tag{1.1d}$$

$$\partial_t\omega_i + u\cdot\nabla\omega_i - \operatorname{div}\left\{k(\phi)\omega_i\nabla(\mu_{\omega_i} + z_iV)\right\} = R_i\,, \tag{1.1e}$$
$$\mu_{\omega_i} = g'(\omega_i) + \beta_i(\phi) \qquad (i = 1, ..., K) \tag{1.1f}$$

on $\Omega\times\mathbb{R}^+$, together with

$$-\operatorname{div}\{\epsilon[\phi]\nabla V\} = \sum_{j=1}^{K} z_j\omega_j\chi_\Omega \tag{1.1g}$$

on $\Omega^*\times\mathbb{R}^+$, completed with the boundary conditions

$$u = 0\,,\quad m(\phi)\nabla\mu_\phi\cdot n = 0\,,\quad k(\phi)\omega_i\nabla(\mu_{\omega_i}+z_iV)\cdot n = 0 \quad \text{on } \partial\Omega\times\mathbb{R}^+\,, \tag{1.1h}$$

$$\frac{\partial f}{\partial\nabla\phi}\cdot n = -\alpha\partial_t\phi - \gamma_{fs}'(\phi) \qquad \text{on } \partial\Omega\times\mathbb{R}^+\,, \tag{1.1i}$$
$$V = \overline{V} \qquad \text{on } \partial\Omega^*\times\mathbb{R}^+\,. \tag{1.1j}$$

The (1.1a)–(1.1d) represent the phase-field description of the balance of mass (depending linearly on the phase-field parameter ϕ via $\rho(\phi) = \frac{1}{2}(\tilde\rho_2+\tilde\rho_1) + \frac{1}{2}(\tilde\rho_2-\tilde\rho_1)\phi$ with $\tilde\rho_1$ and $\tilde\rho_2$ denoting the mass densities of the pure phases) and momentum of two immiscible fluids which are confined to the domain $\Omega\subset\mathbb{R}^d$, $d = 2$ or 3. Thereby, m is the mobility. The Nernst–Planck-system (1.1e)–(1.1g) describes the evolution of the electrostatic potential V and of the number densities $\{\omega_i\}_{i=1,\dots,K}$ of the K dissolved species having valence z_i $(i = 1, .., K)$ and individual solubility properties described by a solubility energy of the form $\int_\Omega\beta_i(\phi)\omega_i$ $(i = 1, \dots, K)$. Thereby, the electrostatic potential V is considered on a larger domain $\Omega^*\supset\Omega$ (cf. Fig. 1) to reduce the bias caused by the finite domain. Assuming

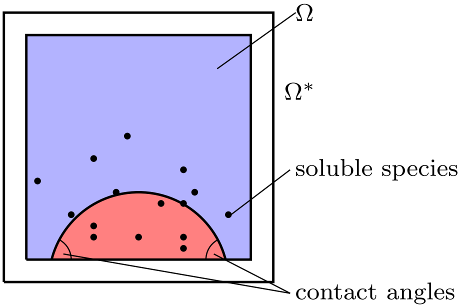

Fig. 1 Fluidic domain $\Omega \subset \Omega^*$ containing two fluids and soluble species

relatively small movements of electric charges, which do not create a substantial magnetic field, magnetic effects are neglected and the electric field equals the negative gradient of the electrostatic potential V.

While k_i are nonnegative coefficient functions depending solely on the fluids, the positive dielectric permittivity ϵ is also x-dependent, i.e., it depends on the fluids inside of Ω, but may also vary between Ω and $\Omega^*\backslash\Omega$. In particular, we use the notation

$$\epsilon[\phi](x) := \begin{cases} \tilde{\epsilon}(\phi(x)) & \text{if } x \in \overline{\Omega}, \\ \epsilon^*(x) & \text{if } x \in \overline{\Omega^*}\backslash\overline{\Omega} \end{cases} \tag{1.2}$$

with a fluid dependent permittivity $\tilde{\epsilon} : \mathbb{R} \to \mathbb{R}^+$ and a space dependent permittivity function $\epsilon^* : \overline{\Omega^*}\backslash\overline{\Omega} \to \mathbb{R}^+$.

Formal computations show that an energy of form

$$\begin{aligned} \mathcal{E}(\phi, \{\omega_i\}_{i=1,\ldots,K}, V, u) := & \int_\Omega f(\phi, \nabla\phi) + \int_{\partial\Omega} \gamma_{fs}(\phi) + \sum_{i=1}^{K} \int_\Omega g(\omega_i) \\ & + \sum_{i=1}^{K} \int_\Omega \beta_i(\phi)\omega_i + \int_{\Omega^*} \epsilon[\phi](x) \left|\nabla V\right|^2 \\ & + \int_\Omega \tfrac{1}{2}\rho \left|u\right|^2 , \end{aligned} \tag{1.3}$$

acts as a Lyapunov functional (cf. [5]). Thereby, the Cahn–Hilliard free energy $\int_\Omega f(\phi, \nabla\phi)$ describes the fluid-fluid contact energy, while the second component models the fluid-solid contact energy with some ϕ-dependent energy density γ_{fs}. The next two ingredients describe the contributions of the species. In particular, there is an entropic component $\int_\Omega g(\omega_i)$ with $g(s) := s \log s - s$ and the solubility energy $\int_\Omega \beta_i(\phi)\omega_i$ for each species. The last two terms in (1.3) describe the contribution of the electrostatic potential and the kinetic energy.

Throughout this paper, we assume the Cahn–Hilliard free energy density to be of the form $f(\phi, \nabla\phi) := \frac{\sigma\delta}{2}\left|\nabla\phi\right|^2 + \frac{\sigma}{\delta}W(\phi)$, where the parameter σ corresponds to the surface tension, the parameter δ describes the width of the diffuse interface, and W is double-well potential with minima in $\pm$ 1. In this case, boundary condition (1.1i) reads

$$\delta\sigma\nabla\phi \cdot n = -\alpha\partial_t\phi - \gamma_{fs}'(\phi). \tag{1.3}$$

The meaning of this boundary condition was elucidated of [17] (with reference to [22]). For $\alpha = 0$, Young's formula for the contact angle between the wall and the moving interface may be recovered. For an application of this boundary condition, we refer to [2], where a suitable choice of γ_{fs} was successfully used to prevent a rising bubble from sticking to the wall of a narrow channel. The choice $\alpha > 0$ allows for contact angle hysteresis (cf. [5, 22]), i.e., the advancing contact angle is larger than the static contact angle, and the latter is larger than the receding contact angle.

In the original model in [5], the electrostatic potential V is subjected to Dirichlet boundary conditions on $\partial\Omega^*$. Nevertheless, it was already suggested in Section 7.2.4 of that publication to consider Dirichlet boundary data only on a nonempty subset Γ_D of $\partial\Omega^*$ and to impose homogeneous Neumann boundary conditions on $\partial\Omega^* \setminus \Gamma_D$. As expatiated in [17], the Dirichlet boundary mimics a (maybe grounded) electrode, whereas the Neumann boundary is chosen to reduce the bias caused by considering the electric field only on a finite domain. With this in mind, we replace (1.1j) by

$$V = \overline{V} \qquad \text{on } \Gamma_D \times \mathbb{R}^+ , \tag{1.5a}$$

$$\nabla V \cdot n = 0 \qquad \text{on } (\partial\Omega^* \backslash \Gamma_D) \times \mathbb{R}^+ . \tag{1.5b}$$

The reaction terms R_i in (1.1e) are suggested to obey a generalization of the law of mass action. Namely, they may be written as

$$R_i(\{\mu_{\omega_j}\}_{j=1,\ldots,K}, V) := \zeta_i \left[\exp\left(\sum_{\zeta_j < 0} |\zeta_j| \left(\mu_{\omega_j} + z_j V\right) \right) - \exp\left(\sum_{\zeta_j \geq 0} \zeta_j \left(\mu_{\omega_j} + z_j V\right) \right) \right] . \tag{1.6}$$

To simplify the notation, we suppressed the dependency of R_i on $\{\mu_{\omega_j}\}_{j=1,\ldots,K}$ and V in (1.1a). The coefficients ζ_i ($i = 1, \ldots, K$) in (1.6) depend on the stoichiometric coefficients.

Other modeling approaches can be found, e.g. in [8] and [9]. The model investigated in the latter one also states evolution equations for different species which are coupled via reaction terms. However, it omits the energetic description of the solubility properties. Instead, degenerate coefficient functions were used to confine the species to one phase. The model presented in [8] also uses a degenerate coefficient function, but considers only one evolution equation for the charge density.

In Section 7 of [5], a simplified version of (1.1) was derived: Using a quadratic entropic functional instead of the logarithmic one linearizes the balance equations for the species concentrations and allows to combine them to one balance equation for the charge density. Omitting an energetic description of solubility properties, they confined the electric charges to one phase by introducing a suitable, degenerate coefficient function in the third term of (1.1e) (see also, e.g. [8]). First, numerical results for this simplified model based on finite element and finite volume approaches have already been published in [5]. A further investigation of discrete schemes for the aforementioned model was done in [17], where F. Klingbeil proved convergence of a finite element scheme for the case of homogeneous Dirichlet boundary conditions for the electrostatic potential.

A similar approach can also be found in [21], where the authors combined Cahn–Hilliard and Navier–Stokes type equations with a Nernst–Planck-system for the evolution of the charge density and the electric field. In [21], Nochetto et al. also proposed a coupled discrete scheme for the model and proved the stability of the scheme, as well as the existence of solutions. However, in order to perform simulations, the scheme was linearized with time-lagging of the variables.

In this paper, we propose a stable, fully discrete splitting scheme for (1.1). Splitting (1.1) into different blocks, which may be treated sequentially, allows to compute discrete solutions efficiently by omitting an iterative approach on the complete system. Similar splitting ideas have previously been used in [3, 20], and [15] for a model of magnetohydrodynamics and for diffuse interface models for multi-phase flows, respectively. In contrast to other splitting approaches—cf. [16], where a two-step scheme for Cahn–Hilliard–Navier–Stokes-systems was proposed—the presented schemes relies only on the data of the last time step. The presented scheme is an extension of the prototype suggested in [18]. In contrast to that prototype, the scheme presented in this publication omits the application of a cutoff function in the solubility energy and comprises different mechanisms to reduce the induced numerical dissipation, which are investigated by studying the example of a falling droplet.

The outline of the paper is as follows. In Section 2, we introduce the discrete function spaces and interpolation operators and state the discrete scheme. In Section 3, we establish the stability of the scheme for the general case of inhomogeneous Dirichlet boundary data $\overline{V}$ by proving that the discrete version of the energy is bounded from above by a positive constant which is independent of the discretization parameters. Based on this a priori estimate, we use Brouwer's fixed point theorem to show the existence of discrete solutions. A numerical investigation of the dissipation reducing mechanisms can be found in Section 4.1. Simulations serving as a qualitative validation of the presented scheme and the underlying model can be found in Sections 4.2 and 4.3.

The results presented in the following sections are excerpts from the author's Ph.D. thesis [19].

Notation To simplify the notation, we will assume that the mobility m and the coefficient functions k_i $(i = 1, ..., K)$ are constant (w.l.o.g. $m \equiv 1$, $k_i \equiv 1$ for $i = 1, ..., K$) for the remainder of this paper. However, the presented results are valid as long as these functions are nonnegative. We also set $\delta = \sigma = 1$ to simplify the notation.

By "·", we denote the Euclidean scalar product on $\mathbb{R}^d$. For a given domain $\Omega \subset \mathbb{R}^d$ with $d \in \{2, 3\}$, we denote the space of k-times weakly differentiable functions with weak derivatives in $L^p(\Omega)$ by $W^{k,p}(\Omega)$. The symbol $W_0^{k,p}(\Omega)$ stands for the closure of $C_0^\infty(\Omega)$ in $W^{k,p}(\Omega)$. For $p = 2$, we will denote $W^{k,2}(\Omega)$ by $H^k(\Omega)$ and $W_0^{k,2}(\Omega)$ by $H_0^k(\Omega)$. Corresponding spaces of vector- and matrix-valued functions are denoted in boldface. For a Banach space Y and a time interval I, the symbol $L^p(I; Y)$ stands for the parabolic space of L^p-integrable functions on I with values in Y. Sometimes, we write Ω_T for the space-time cylinder $\Omega \times (0, T)$. The discrete function spaces will be introduced in Section 2.

2 A stable discrete splitting scheme

In this section, we present a fully discrete finite element scheme. Concerning the discretization in space and time, we assume that

(T) the time interval $I := [0, T)$ is subdivided in intervals $I_k := [t_k, t_{k+1})$ with $t_{k+1} = t_k + \tau_k$ for time increments $\tau_k > 0$ and $k = 0, ..., N-1$ with $t_N = T$. For simplicity, we take $\tau_k \equiv \tau = \frac{T}{N}$ for $k = 0, ..., N-1$.

The triangulations $\mathcal{T}_h^*$ and $\mathcal{T}_h$ of Ω^* and Ω are supposed to satisfy the following assumptions.

(S1) Let $\left\{\mathcal{T}_h^*\right\}_{h>0}$ be a quasiuniform family (in the sense of [4]) of partitions of Ω^* into disjoint, open simplices κ, so that

$$\overline{\Omega^*} \equiv \bigcup_{\kappa \in \mathcal{T}_h^*} \overline{\kappa} \quad \text{with} \quad h := \max_{\kappa \in \mathcal{T}_h^*} \operatorname{diam}(\kappa)\,.$$

(S2) Let $\{\mathcal{T}_h\}_{h>0}$ be a quasiuniform family of partitions of Ω into simplices with $\mathcal{T}_h \subset \mathcal{T}_h^*$, so that $\overline{\Omega} \equiv \bigcup_{\kappa \in \mathcal{T}_h} \overline{\kappa}$.

Furthermore, we assume that the electrodes are not arbitrarily close to the fluidic domain.

(S3) The non-empty subset Γ_D of $\partial\Omega^*$ has a certain h-independent distance to Ω, i.e., there is a constant $c_\Gamma > 0$ such that $\operatorname{dist}(\Gamma_D, \Omega) \geq c_\Gamma$.

We use the standard reference simplex $\tilde{\kappa}$ with vertices $\{\tilde{P}_i\}_{i=0,\ldots,d}$, where $\tilde{P}_0$ is the origin and the $\tilde{P}_i$ are such that the jth component of $\tilde{P}_i$ is δ_{ij} for $i, j = 1, ..., d$. Furthermore, we denote the vertices of an element $\kappa \in \mathcal{T}_h^*$ by $\{P_{\kappa,i}\}_{i=0,\ldots,d}$ and define $\mathbf{B}_\kappa \in \mathbb{R}^{d \times d}$ such that the mapping $\mathcal{B}_\kappa : \mathbb{R}^d \ni y \mapsto P_{\kappa,0} + \mathbf{B}_\kappa y$ maps the vertex $\tilde{P}_i$ to $P_{\kappa,i}$ $(i = 0, ..., d)$ and hence $\tilde{\kappa}$ to κ.

Concerning the discrete function spaces, we denote the space of continuous, piecewise linear finite element functions on $\mathcal{T}_h$ by U_h and the extension to $\mathcal{T}_h^*$ by U_h^*. By $U_{h,0}^*$, we denote the subspace of U_h^* containing functions which vanish on $\Gamma_D \subset \partial\Omega^*$. Pressure and velocity field are approximated with the lowest order Taylor–Hood elements, i.e. S_h is the subspace of U_h containing only functions with zero mean and the space of continuous, piecewise quadratic, vector-valued finite element functions on $\mathcal{T}_h$ is denoted by $\boldsymbol{W}_h$, while $\boldsymbol{W}_{h,\mathrm{div}}$ denotes the subspace of weakly solenoidal vector-fields. In particular, we have

$$S_h := \left\{\theta_h \in U_h \; : \; \int_\Omega \theta_h \, \mathrm{d}\mathbf{x} = 0\right\}, \tag{2.1}$$

$$\boldsymbol{W}_{h,\mathrm{div}} := \left\{w_h \in \boldsymbol{W}_h \; : \; \int_\Omega \operatorname{div} w_h \theta_h = 0 \;\; \forall \theta_h \in S_h\right\}. \tag{2.2}$$

To project continuous functions onto U_h^* or U_h, we use the nodal interpolation operator $\mathcal{I}_h$ from $C^0(\overline{\Omega^*})$ to U_h^* which is defined by

$$\mathcal{I}_h\{a\} := \sum_{i=1}^{\dim U_h^*} a(x_i)\chi_{h,i} \,, \tag{2.3}$$

where the functions $\{\chi_{h,i}\}_{i=1,\dots,\dim U_h^*}$ form a dual basis to the vertices $\{x_i\}_{i=1,\dots,\dim U_h^*}$ of $\mathcal{T}_h^*$, i.e. $\chi_{h,i}(x_j) = \delta_{ij}$ for $i, j = 1, \dots, \dim U_h^*$. In a slight misuse of notation, we will denote the interpolation operator from $C^0(\overline{\Omega})$ to U_h also by $\mathcal{I}_h$. The backward difference quotient in time is denoted by ∂_τ^-.
As we are not able to guarantee the nonnegativity of the discrete number densities of the species $\omega_{h,i}$ $(i = 1, \dots, K)$ in the discrete setting, we define a regularized version of the entropic functional g via

$$g_\nu(s) := \begin{cases} s\log s - s & \text{if } s \geq \nu\,, \\ \frac{s^2-\nu^2}{2\nu} + (\log\nu - 1)s & \text{if } s < \nu\,, \end{cases} \tag{2.4a}$$

$$g_\nu'(s) = \begin{cases} \log s & \text{if } s \geq \nu\,, \\ \frac{s}{\nu} + \log\nu - 1 & \text{if } s < \nu\,, \end{cases} \tag{2.4b}$$

$$g_\nu''(s) = \max\{\nu, s\}^{-1}\,, \tag{2.4c}$$

for all $s \in \mathbb{R}$ and some regularization parameter $\nu > 0$. Using the ideas from [14], we define for a given function $\theta_h \in U_h$ and a given element $\kappa \in \mathcal{T}_h$ a diagonal matrix $\hat{\Xi}_\nu[\theta_h]$ by

$$\left[\hat{\Xi}_\nu[\theta_h]\right]_{ii} = \begin{cases} \frac{\theta_h(P_{\kappa,i})-\theta_h(P_{\kappa,0})}{g_\nu'(\theta_h(P_{\kappa,i}))-g_\nu'(\theta_h(P_{\kappa,0}))} & \text{if } \theta_h\big(P_{\kappa,i}\big) \neq \theta_h\big(P_{\kappa,0}\big)\,, \\ \frac{1}{g_\nu''(\theta_h(P_{\kappa,0}))} & \text{if } \theta_h\big(P_{\kappa,i}\big) = \theta_h\big(P_{\kappa,0}\big)\,, \end{cases} . \tag{2.5a}$$

Incorporating the affine mapping from $\tilde{\kappa}$ to κ, we define the matrix-valued operator $\Xi_\nu[.]$ via

$$\Xi_\nu[\theta_h]\big|_\kappa := \mathbf{B}_\kappa^{-T}\,\hat{\Xi}_\nu[\theta_h]\,\mathbf{B}_\kappa^T \tag{2.5b}$$

for $\theta_h \in U_h$. A straight forward computation shows that this operator satisfies

$$\Xi_\nu[\theta_h]\nabla\mathcal{I}_h\left\{g_\nu'(\theta_h)\right\} = \nabla\theta_h \tag{2.6}$$

on Ω with $\theta_h \in U_h$. To guarantee positivity of the mass density, we use the regularized mass density function $\overline{\rho}$ satisfying

$$\overline{\rho}(\phi)\big|_{(-\overline{\phi},+\overline{\phi})} = \tfrac{\tilde{\rho}_2+\tilde{\rho}_1}{2} - \tfrac{\tilde{\rho}_2-\tilde{\rho}_1}{2}\phi\,, \tag{2.7a}$$

$$\overline{\rho}(\phi)\big|_{(-\infty,-\overline{\phi}]} \equiv \text{const}\,, \quad \overline{\rho}(\phi)\big|_{[+\overline{\phi},+\infty)} \equiv \text{const}\,, \tag{2.7b}$$

with $\overline{\phi} > 1$ small enough. As the original mass density ρ depends affine linearly on the phase-field parameter, we introduce $\frac{\delta\overline{\rho}}{\delta\phi} := \frac{\tilde{\rho}_2-\tilde{\rho}_1}{2}$ as an approximation of $\overline{\rho}'$ (cf. [11]).

Concerning the double-well potential W, we make assumptions similar to the ones used in [12], i.e.,

(W1) $W \in C^1(\mathbb{R};\mathbb{R}_0^+)$ with $\left|W(s)s^{-3}\right| \to \infty$ for $|s| \to \infty$ such that W' is piecewise C^1 and that its derivatives have at most quadratic growth for $|s| \to \infty$.

Considering different discrete approximations of W' denoted by $W_h' : \mathbb{R}^2 \to \mathbb{R}_0^+$, we assume the following conditions to hold true.

(W2) There is a positive constant C such that for all $a, b \in \mathbb{R}$

$$\left|W_h'(a,b)\right| \leq C\left(1 + |a|^3 + |b|^3\right).$$

(W3) $W_h'(a,b)(a-b) \geq W(a) - W(b)$ for all $a, b \in \mathbb{R}$.
(W4) $W_h'(a,a) = W'(a)$ for all $a \in \mathbb{R}$.
(W5) There is a positive constant C, such that for all $a, b, c \in \mathbb{R}$

$$\left|W_h'(a,b) - W_h'(b,c)\right| \leq C(a^2+b^2+c^2)(|a-b| + |b-c|).$$

For instance, these conditions hold true for a polynomial double-well potential $\frac{1}{4}(1-\phi^2)^2$ with W_h' based on a difference quotient (cf. [12]). For numerical schemes based on a logarithmic-type double-well potential, we refer to [7]. Moreover, we define the difference quotients on $\overline{\Omega}$

$$\beta_{i,DQ}'(a,b) := \begin{cases} \frac{\beta_i(a)-\beta_i(b)}{a-b} & \text{if } a \neq b, \\ \beta_i'(a) & \text{if } a = b, \end{cases} \quad \forall i \in \{1, \ldots, K\}, \tag{2.8}$$

$$\gamma_{fs,DQ}'(a,b) := \begin{cases} \frac{\gamma_{fs}(a)-\gamma_{fs}(b)}{a-b} & \text{if } a \neq b, \\ \gamma_{fs}'(a) & \text{if } a = b, \end{cases} \tag{2.9}$$

$$\epsilon_{DQ}'(a,b) := \begin{cases} \frac{\tilde{\epsilon}(a)-\tilde{\epsilon}(b)}{a-b} & \text{if } a \neq b, \\ \partial_\phi \tilde{\epsilon}(\phi)\big|_{\phi=a} & \text{if } a = b. \end{cases} \tag{2.10}$$

The last difference quotient can naturally be extended to $\overline{\Omega^*}$ via $\epsilon_{DQ}'(a,b) \equiv 0$ on $\overline{\Omega^*}\setminus\overline{\Omega}$.

Using the abbreviations $\overline{\rho}_h^n := \mathcal{I}_h\left\{\overline{\rho}(\phi_h^n)\right\}$, $\epsilon_h^n := \mathcal{I}_h\left\{\epsilon[\phi_h^n](x)\right\}$, and

$$\begin{aligned} R_{i,h}^n := R_{i,h}(\phi_h^n, (\omega_h^n)^K, V_h^n) := \mathcal{I}_h\Bigg\{\zeta_i\Bigg[&\exp\left(\sum_{\zeta_j<0}|\zeta_j|\left(g_\nu'(\omega_{j,h}^n) + \beta_j(\phi_h^n) + z_j V_h^n\right)\right) \\ &- \exp\left(\sum_{\zeta_j\geq 0}\zeta_j\left(g_\nu'(\omega_{j,h}^n) + \beta_j(\phi_h^n) + z_j V_h^n\right)\right)\Bigg]\Bigg\}, \end{aligned} \tag{2.11}$$

we state the following discrete scheme. For better readability, we write $(\theta_h)^K \in (U_h)^K$ for the tuple $(\theta_{i,h})_{i=1,\ldots,K}$ with $\theta_{i,h} \in U_h$ for $i = 1, \ldots, K$.

Given $(\phi_h^{n-1}, (\omega_h^{n-1})^K, u_h^{n-1}) \in U_h \times (U_h)^K \times \boldsymbol{W}_{h,\mathrm{div}}$, and $\overline{V}_h^n \in U_h^*$, which defines the Dirichlet data of the electrostatic potential, find $(\phi_h^n, \mu_{\phi,h}^n, (\omega_h^n)^K, V_h^n - \overline{V}_h^n, u_h^n) \in U_h \times U_h \times (U_h)^K \times U_{h,0}^* \times \boldsymbol{W}_{h,\mathrm{div}}$ such that

$$\int_\Omega \mathcal{I}_h\{\partial_\tau^- \phi_h^n \theta_h\} - \int_\Omega \phi_h^{n-1} u_h^{n-1} \cdot \nabla\theta_h + \tau \int_\Omega (\min \overline{\rho}_h^{n-1})^{-1} \left|\phi_h^{n-1}\right|^2 \nabla\mu_{\phi,h}^n \cdot \nabla\theta_h + \int_\Omega \nabla\mu_{\phi,h}^n \cdot \nabla\theta_h = 0 \qquad \forall\theta_h \in U_h\,, \tag{2.12a}$$

$$\begin{aligned}\int_\Omega \mathcal{I}_h\left\{\mu_{\phi,h}^n \theta_h\right\} &= \int_\Omega (\vartheta\nabla\phi_h^n + (1-\vartheta)\nabla\phi_h^{n-1}) \cdot \nabla\theta_h + \int_\Omega \mathcal{I}_h\left\{W_h'(\phi_h^n, \phi_h^{n-1})\theta_h\right\} \\ &\quad + \int_{\partial\Omega} \mathcal{I}_h\left\{\gamma_{fs,DQ}'(\phi_h^n, \phi_h^{n-1})\theta_h\right\} + \alpha \int_{\partial\Omega} \mathcal{I}_h\{\partial_\tau^- \phi_h^n \theta_h\} \\ &\quad + \int_\Omega \mathcal{I}_h\left\{\sum_{j=1}^K \beta_{j,DQ}'(\phi_h^n, \phi_h^{n-1})\omega_{j,h}^{n-1}\theta_h\right\} - \tfrac{1}{2}\int_\Omega \mathcal{I}_h\left\{\epsilon_{DQ}'(\phi_h^n, \phi_h^{n-1})\theta_h\right\} \left|\nabla V_h^n\right|^2 \qquad \forall\theta_h \in U_h\,,\end{aligned} \tag{2.12b}$$

$$\begin{aligned}&\int_\Omega \mathcal{I}_h\{\partial_\tau^- \omega_{i,h}^n \theta_h\} - \int_\Omega \omega_{i,h}^{n-1} u_h^{n-1} \cdot \nabla\theta_h \\ &\quad + \tau K \int_\Omega (\min \overline{\rho}_h^{n-1})^{-1} \left|\omega_{i,h}^{n-1}\right|^2 \nabla\mathcal{I}_h\{g_\nu'(\omega_{i,h}^n) + \beta_i(\phi_h^n) + z_i V_h^n\} \cdot \nabla\theta_h \\ &\quad + \int_\Omega \left(\Xi_\nu[\omega_{i,h}^n]\nabla\mathcal{I}_h\{g_\nu'(\omega_{i,h}^n) + \beta_i(\phi_h^n) + z_i V_h^n\}\right) \cdot \nabla\theta_h = \int_\Omega \mathcal{I}_h\{R_{i,h}^n \theta_h\} \qquad \forall\theta_h \in U_h\,,\end{aligned} \tag{2.12c}$$

$$\int_{\Omega^*} \epsilon_h^n \nabla V_h^n \cdot \nabla\theta_h = \int_\Omega \mathcal{I}_h\left\{\sum_{j=1}^K z_j \omega_{j,h}^n \theta_h\right\} \qquad \forall\theta_h \in U_{h,0}^*\,, \tag{2.12d}$$

$$\begin{aligned}&\int_\Omega \tfrac{1}{2}\left(\overline{\rho}_h^n + \overline{\rho}_h^{n-1}\right)\partial_\tau^- u_h^n \cdot w_h + \tfrac{1}{2}\int_\Omega \partial_\tau^- \overline{\rho}_h^n u_h^{n-1} \cdot w_h \\ &\quad + \tfrac{1}{2}\int_\Omega \overline{\rho}_h^n\left(\left(\nabla u_h^n\right)^T \cdot w_h\right) \cdot u_h^{n-1} - \tfrac{1}{2}\int_\Omega \overline{\rho}_h^n\left((\nabla w_h)^T \cdot u_h^n\right) \cdot u_h^{n-1} \\ &\quad + \tfrac{1}{2}\int_\Omega \tfrac{\delta\overline{\rho}}{\delta\phi}\left(\left(\nabla u_h^n\right)^T \cdot w_h\right) \cdot \nabla\mu_{\phi,h}^n - \tfrac{1}{2}\int_\Omega \tfrac{\delta\overline{\rho}}{\delta\phi}\left((\nabla w_h)^T \cdot u_h^n\right) \cdot \nabla\mu_{\phi,h}^n \\ &\quad + \int_\Omega 2\mathcal{I}_h\{\eta(\phi_h^n)\} D u_h^n : D w_h = -\int_\Omega \phi_h^{n-1}\nabla\mu_{\phi,h}^n \cdot w_h \\ &\quad - \sum_{j=1}^K \int_\Omega \omega_{j,h}^{n-1}\nabla\mathcal{I}_h\left\{g_\nu'(\omega_{j,h}^n) + \beta_j(\phi_h^n) + z_j V_h^n\right\} \cdot w_h \qquad \forall w_h \in \boldsymbol{W}_{h,\mathrm{div}}\end{aligned} \tag{2.12e}$$

with $\alpha \geq 0$ describing contact angle hysteresis and the parameter $\vartheta \in [0.5, 1]$, which allows to reduce the numerical dissipation (cf. Section 4.1).

Remark 2.1 As the (2.12a)-(2.12d) are independent of u_h^n, we may compute ϕ_h^n, $\mu_{\phi,h}^n$, $(\omega_h^n)^K$ and V_h^n before solving the saddle-point problem (2.12e). If the dielectric permittivity ϵ is independent of the fluids, the last integral in (2.12b) vanishes allowing us to split (2.12) into three blocks which may be treated sequentially: The phase-field equations (2.12a) and (2.12b), the Nernst–Planck-system (2.12c) and (2.12d), and the momentum equations (2.12e).
The application of $\Xi_\nu[.]$ allows to rewrite the fourth term in (2.12c) as

$$\int_\Omega \nabla\omega_{i,h}^n \cdot \nabla\theta_h + \int_\Omega \left(\Xi_\nu[\omega_{i,h}^n]\nabla\mathcal{I}_h\left\{\beta_i(\phi_h^n) + z_i V_h^n\right\}\right) \cdot \nabla\theta_h\,. \tag{2.13}$$

As this is not required for the stability of the scheme, a further reduction of the computational costs may be achieved by replacing $\Xi_\nu[\omega_{i,h}^n]$ in (2.12c) by an explicit, nonnegative expression like $\mathcal{I}_h\left\{(g_\nu''(\omega_{i,h}^{n-1}))^{-1}\right\}$.
A convergence result for this splitting approach applied to pure two-phase flows with different mass densities, i.e., sole Navier–Stokes–Cahn–Hilliard-systems, can be found in [12].

Straight forward computations show that the phase-field parameter and the number densities of species which do not participate in any reaction are conserved, i.e.,

$$\int_\Omega \phi_h^n = \int_\Omega \phi_h^{n-1} \quad\text{and}\quad \int_\Omega \omega_{i,h}^n = \int_\Omega \omega_{i,h}^{n-1} \quad \text{for all } i \in \{1, ..., K\} \text{ satisfying } \zeta_i = 0. \tag{2.14}$$

Under the additional assumption $\sum_{i=1}^K \zeta_i z_i = 0$, i.e., the considered reaction conserves the total charge of the involved molecules, the overall charge of the fluids $\int_\Omega \sum_{i=1}^K \omega_{i,h}^n z_i$ is also conserved.

3 Stability and existence of discrete solutions

This section is devoted to the stability properties of the splitting scheme introduced in (2.12). We prove that—under appropriate assumptions which are listed below—the aforementioned splitting scheme is stable. Based on this a priori stability result, we establish the existence of discrete solutions.
To prove the stability of the scheme and the existence of discrete solutions, we make the following general assumptions.

(E1) Ω^* and Ω are open, bounded, convex polygonal (or polyhedral), and the discretization in space and time satisfies (T), (S1), (S2), and (S3).
(E2) Assumptions (W1)–(W5) apply to the double-well potential W and W_h'.
(E3) $\beta, \eta \in C^\infty(\mathbb{R}) \cap W^{1,\infty}(\mathbb{R})$ satisfying $0 \leq \beta(s)$ and $\eta(s) \geq c > 0$ for all $s \in \mathbb{R}$.
(E4) The liquid-solid interfacial energy is described by $\gamma_{fs} \in C^\infty(\mathbb{R}) \cap W^{1,\infty}(\mathbb{R})$.
(E5) The dielectric permittivity is defined via (1.2). It is bounded from above and below by positive constants $\epsilon_{\min}$ and $\epsilon_{\max}$. $\tilde{\epsilon} \in C^1(\mathbb{R})$ is piecewise constant

in $\mathbb{R}\setminus(-2,2)$. For technical reasons, let $\left|\frac{1}{2}(\tilde{\epsilon}(1)-\tilde{\epsilon}(-1))\right| = \sup\left|\tilde{\epsilon}'\right|$ and $\tilde{\epsilon}(0) = \frac{1}{2}(\tilde{\epsilon}(-1)+\tilde{\epsilon}(1))$ (cf. [17]).

(E6) The Dirichlet data for the electrostatic potential is given by the trace of functions $\overline{V}_h \in U_h^*$, which are bounded in $H^1(0,T;H^1(\Omega^*))$ independently of h, τ, and ν.

(E7) Initial data $\phi_h^0 \in U_h$, $\omega_{i,h}^0 \in U_h$ $(i=1,...,K)$, and $u_h^0 \in \boldsymbol{W}_{h,\mathrm{div}}$ is given such that

$$\int_\Omega \left|\nabla\phi_h^0\right|^2 + \int_\Omega \mathcal{I}_h\left\{W(\phi_h^0)\right\} + \int_\Omega \left|u_h^0\right|^2 + \sum_{i=1}^K \int_\Omega \left|\omega_{i,h}^0\right|^2 \le C \quad (3.1)$$

with $C>0$ independent of h, τ, and ν and $\omega_{i,h}^0 \ge 0$ $(i=1,...,K)$.

Furthermore, we define the initial electrostatic potential V_h^0 as the solution of

$$\int_{\Omega^*} \mathcal{I}_h\left\{\epsilon[\phi_h^0](x)\right\}\nabla V_h^0\cdot\nabla\theta_h = \int_\Omega \mathcal{I}_h\left\{\sum_{j=1}^K z_j\omega_{j,h}^0\theta_h\right\} \quad (3.2)$$

for all $\theta_h \in U_{h,0}^*$ under the constraint $V_h^0 = \overline{V}_h^0$ on Γ_D.

In order to prove the stability of (2.12) even for inhomogeneous Dirichlet data for the electrostatic potential, we introduce a cutoff function. Recalling assumption (S3), we define the set $\Omega_{c_\Gamma} := \{x\in\overline{\Omega^*} : \mathrm{dist}\,(x,\Gamma_D)\ge c_\Gamma\}$ and obtain the inclusions

$$\Omega \subset \Omega_{c_\Gamma} \subset \overline{\Omega^*}\,. \quad (3.3)$$

We continue by defining a weight function ς mapping $\overline{\Omega^*}$ on the interval $[0,1]$ via

$$\varsigma(x) := \begin{cases} 1 & \text{if } x\in\Omega_{c_\Gamma}\,, \\ c_\Gamma^{-1}\,\mathrm{dist}\,(x,\Gamma_D) & \text{if } x\in\overline{\Omega^*}\setminus\Omega_{c_\Gamma}\,. \end{cases} \quad (3.4)$$

Finally, we define a discrete cut-off function $\Pi_{c_\Gamma} : U_h^* \to U_{h,0}^*$ via

$$\Pi_{c_\Gamma}(A_h) := \mathcal{I}_h\{\varsigma A_h\} \quad \text{for all} A_h \in U_h^*\,. \quad (3.5)$$

Lemma 3.1 *Let the Assumptions (S1), (S2), and (S3) hold true. Furthermore, let ς and Π_{c_Γ} be defined according to (3.4) and (3.5). Then, ς is Lipschitz continuous with Lipschitz constant c_Γ^{-1} and for any $A_h\in U_h^*$ the following pointwise estimate holds true on $\overline{\Omega^*}$.*

$$\left|\nabla\Pi_{c_\Gamma}(A_h)\right| \le C\left[\left|\nabla A_h\right| + c_\Gamma^{-1}\left|A_h\right|\right]. \quad (3.6)$$

Proof The Lipschitz continuity follows from

$$|\varsigma(x)-\varsigma(y)| \le c_\Gamma^{-1}\,|\mathrm{dist}\,(x,\Gamma_D)-\mathrm{dist}\,(y,\Gamma_D)| \le c_\Gamma^{-1}\,|x-y| \quad (3.7)$$

for $x,y\in\overline{\Omega^*}$.

As ς is Lipschitz continuous, the estimate (3.6) may be proven following the lines of [10], Lemma 2.3. For the readers convenience, we summarize the proof. In a first step, we consider a simplex $\kappa \in \mathcal{T}_h^*$ with vertices $\{P_{\kappa,i}\}_{i=0,\ldots,d}$ and establish an analogous estimate for directional derivatives along the edges starting at $P_{\kappa,0}$. Parameterizing the edge between $P_{\kappa,0}$ and $P_{\kappa,i}$ by

$$c_i(s) := P_{\kappa,0} + s\frac{P_{\kappa,i} - P_{\kappa,0}}{\operatorname{dist}(P_{\kappa,i}, P_{\kappa,0})} =: P_{\kappa,0} + sv_i \quad s \in [0, \operatorname{dist}(P_{\kappa,i}, P_{\kappa,0})]\,, \tag{3.8}$$

and denoting the dual basis to the vertices $\{P_{\kappa,i}\}_{i=0,\ldots,d}$ by $\{\chi_{h,i}\}_{i=0,\ldots,d}$, we compute the directional derivative along v_i

$$\partial_{v_i} A_h\big|_{c_i(s)} = A_h(P_{\kappa,0})\nabla\chi_{h,0}(c_i(s)) \cdot v_i + A_h(P_{\kappa,i})\nabla\chi_{h,i}(c_i(s)) \cdot v_i \tag{3.9}$$

for any $A_h \in U_h^*$ and $i = 1, \ldots, d$. To simplify the notation, we introduce $\varsigma_i := \varsigma(P_{\kappa,i})$ and $A_{h,i} := A_h(P_{\kappa,i})$ for $i = 0, \ldots, d$. In this notation, the directional derivatives of $\Pi_{c_\Gamma}(A_h)$ satisfy

$$\begin{aligned} &\left|\partial_{v_i}\Pi_{c_\Gamma}(A_h)\right| = \left|\varsigma_0 A_{h,0}\nabla\chi_{h,0} \cdot v_i - \varsigma_i A_{h,i}\nabla\chi_{h,i} \cdot v_i\right| \\ &\leq \left|(A_{h,i} - A_{h,0})\nabla\chi_{h,i} \cdot v_i\right| + \left|A_{h,0}\right| \left|(\varsigma_i - \varsigma_0)\nabla\chi_{h,i} \cdot v_i\right| \leq \left|\partial_{v_i} A_h\right| + c_\Gamma^{-1}\left|A_{h,0}\right|. \end{aligned} \tag{3.10}$$

To generalize (3.10) to estimates for the gradient of $\Pi_{c_\Gamma}(A_h)$, we define the invertible matrix $T := (v_1, \ldots, v_d)$ to obtain

$$\nabla\Pi_{c_\Gamma}(A_h) \cdot T = \left(\partial_{v_1}\Pi_{c_\Gamma}(A_h), \ldots, \partial_{v_d}\Pi_{c_\Gamma}(A_h)\right), \tag{3.11}$$

and consequently

$$\left\|\nabla\Pi_{c_\Gamma}(A_h)\right\|_1 \leq \left\|\left(\partial_{v_1}\Pi_{c_\Gamma}(A_h), \ldots, \partial_{v_d}\Pi_{c_\Gamma}(A_h)\right)\right\|_1 \left\|T^{-1}\right\|, \tag{3.12}$$

$$\left\|\left(\partial_{v_1}\Pi_{c_\Gamma}(A_h), \ldots, \partial_{v_d}\Pi_{c_\Gamma}(A_h)\right)\right\|_1 \leq \left\|\nabla\Pi_{c_\Gamma}(A_h)\right\|_1 \|T\|, \tag{3.13}$$

where $\|.\|$ is the matrix norm induced by the l^1 vector norm $\|.\|_1$. Combining (3.10), (3.12), and (3.13) provides

$$\begin{aligned} \left\|\nabla\Pi_{c_\Gamma}(A_h)\right\|_1 &\leq \left\|\left(\partial_{v_1} A_h, \ldots, \partial_{v_d} A_h\right)\right\|_1 \left\|T^{-1}\right\| + dc_\Gamma^{-1}\left|A_{h,0}\right| \left\|T^{-1}\right\| \\ &\leq \|T\| \left\|T^{-1}\right\| \|\nabla A_h\|_1 + dc_\Gamma^{-1}\left\|T^{-1}\right\| \left|A_{h,0}\right|. \end{aligned} \tag{3.14}$$

Using the affine linearity of A_h on κ, we choose $x \in \kappa$ and derive

$$\left|A_{h,0}\right| = \left|A_h(x) + \nabla A_h \cdot (P_{\kappa,0} - x)\right| \leq |A_h(x)| + Ch\,\|\nabla A_h\|_1 \tag{3.15}$$

making (3.14) independent of $A_h(P_{\kappa,0})$. To complete the proof, it remains to show that there is a constant $C > 0$ independent of h such that $\|T\| + \left\|T^{-1}\right\| \leq C$.
We want to emphasize that T does not belong to some affine transformation, which is mapping the reference simplex to an arbitrary simplex $\kappa \in \mathcal{T}_h^*$, as its column vectors $\{v_i\}_{i=1,\ldots,d}$ have length one. Instead, T can be seen as a part of a function mapping the reference simplex to a stretched version of a simplex $\kappa \in \mathcal{T}_h^*$ with d edges of length one. Due to standard estimates (see, e.g. Theorem 3.1.3. in [6]), the norm of T and T^{-1} is bounded independently of h. For further details, we refer to the proof of Lemma 2.3 in [10]. □

Lemma 3.2 *Let Assumptions (E1)-(E7) hold true. Under the assumption that a discrete solution* $(\phi_h^n, \mu_{\phi,h}^n, (\omega_h^n)^K, V_h^n, u_h^n)_{n\geq 1}$ *to* (2.12) *exists, this solution satisfies*

$$\begin{aligned}
&\int_\Omega |\nabla\phi_h^n|^2 + \int_\Omega \mathcal{I}_h\{W(\phi_h^n)\} + \int_{\partial\Omega} \mathcal{I}_h\{\gamma_{fs}(\phi_h^n)\} + \sum_{j=1}^K \int_\Omega \mathcal{I}_h\left\{g_\nu(\omega_{j,h}^n)\right\} + \sum_{j=1}^K \int_\Omega \mathcal{I}_h\left\{[\omega_{j,h}^n]_-^2\right\} \\
&\quad + \int_{\Omega^*} \epsilon_h^n |\nabla V_h^n|^2 + \int_\Omega \overline{\rho}_h^n |u_h^n|^2 + \tfrac{2\vartheta-1}{2} \sum_{k=1}^n \int_\Omega \left|\nabla\phi_h^k - \nabla\phi_h^{k-1}\right|^2 \\
&\quad + \sum_{k=1}^n \int_{\Omega^*} \epsilon_h^{k-1} \left|\nabla V_h^k - \nabla V_h^{k-1}\right|^2 + \tau \sum_{k=1}^n \int_\Omega \left|\nabla\mu_{\phi,h}^k\right|^2 + \alpha\tau \sum_{k=1}^n \int_{\partial\Omega} \mathcal{I}_h\left\{\left|\partial_\tau^-\phi_h^k\right|^2\right\} \\
&\quad + \tau \sum_{k=1}^n \int_\Omega 2\mathcal{I}_h\left\{\eta(\phi_h^k)\right\} \left|Du_h^k\right|^2 \\
&\quad + \tau \sum_{k=1}^n \sum_{j=1}^K \int_\Omega \left(\Xi_\nu[\omega_{j,h}^k]\nabla\left(\mu_{\omega_j,h}^k + z_j V_h^k\right)\right) \cdot \nabla\left(\mu_{\omega_j,h}^k + z_j V_h^k\right) \leq C, \qquad (3.16)
\end{aligned}$$

for $n \geq 1$*, where the abbreviation* $\mu_{\omega_i,h}^n := \mathcal{I}_h\left\{g_\nu'(\omega_{i,h}^n) + \beta_i(\phi_h^n)\right\}$ $(i = 1, \ldots, K)$ *for the discrete chemical potentials of the species was used.*

Proof We start by testing (2.12a) by $\mu_{\phi,h}^n$, (2.12b) by $\partial_\tau^-\phi_h^n$, (2.12c) by the sum of the chemical potential and the electrostatic potential $\mu_{\omega_i,h}^n + z_i V_h^n = \mathcal{I}_h\left\{g_\nu'(\omega_{i,h}^n) + \beta_i(\phi_h^n) + z_i V_h^n\right\}$, and (2.12e) by u_h^n. Adding the results and applying Young's inequality yields

$$\begin{aligned}
0 \geq\ & \tfrac{1}{2}\int_\Omega \partial_\tau^- |\nabla\phi_h^n|^2 + \int_\Omega \mathcal{I}_h\{\partial_\tau^- W(\phi_h^n)\} + \int_{\partial\Omega} \mathcal{I}_h\{\partial_\tau^-\gamma_{fs}(\phi_h^n)\} \\
&+ \sum_{i=1}^K \int_\Omega \mathcal{I}_h\{\partial_\tau^- g_\nu(\omega_{i,h}^n)\} + \sum_{i=1}^K \int_\Omega \mathcal{I}_h\left\{\partial_\tau^-\beta_i(\phi_h^n)\omega_{i,h}^{n-1}\right\} + \sum_{i=1}^K \int_\Omega \mathcal{I}_h\{\beta_i(\phi_h^n)\partial_\tau^-\omega_{i,h}^n\} \\
&+ \tfrac{1}{2}\int_{\Omega^*} \partial_\tau^-\epsilon_h^n |\nabla V_h^n|^2 + \tfrac{1}{2}\int_{\Omega^*} \epsilon_h^{n-1}\partial_\tau^- |\nabla V_h^n|^2 + \tfrac{1}{2}\int_\Omega \partial_\tau^-\left(\overline{\rho}_h^n |u_h^n|^2\right) \\
&+ \tfrac{2\vartheta-1}{2\tau}\int_\Omega \left|\nabla\phi_h^n - \nabla\phi_h^{n-1}\right|^2 + \tfrac{1}{2\tau}\int_{\Omega^*} \epsilon_h^{n-1}\left|\nabla V_h^n - \nabla V_h^{n-1}\right|^2 \\
&+ \int_\Omega \left|\nabla\mu_{\phi,h}^n\right|^2 + \alpha\int_{\partial\Omega} \mathcal{I}_h\left\{\left|\partial_\tau^-\phi_h^n\right|^2\right\} + \int_\Omega 2\mathcal{I}_h\{\eta(\phi_h^n)\}\left|Du_h^n\right|^2 \\
&+ \sum_{i=1}^K \int_\Omega \left(\Xi_\nu[\omega_{i,h}^n]\nabla(\mu_{\omega_i,h}^n + z_i V_h^n)\right) \cdot \nabla(\mu_{\omega_i,h}^n + z_i V_h^n) \\
&- \sum_{i=1}^K \int_\Omega \mathcal{I}_h\left\{R_{i,h}^n(\mu_{\omega_i,h}^n + z_i V_h^n)\right\} - \int_{\Omega^*} \partial_\tau^-\left(\epsilon_h^n\nabla V_h^n\right) \cdot \nabla\overline{V}_h^n \\
&+ \int_\Omega \mathcal{I}_h\left\{\sum_{i=1}^K z_i\partial_\tau^-\omega_{i,h}^n\overline{V}_h^n\right\}. \qquad (3.17)
\end{aligned}$$

The first three lines in (3.17) are the time difference quotient of the discrete energy. As the terms in lines four to six are nonnegative, we have to focus on the treatment of the last three terms. Recalling the definition of $R_{i,h}$ from (2.11), we obtain the identity

$$-\sum_{i=1}^{K} R^n_{i,h}(\mu^n_{\omega_i,h} + z_i V^n_h) = \left[\exp\left(\sum_{\zeta_j<0} |\zeta_j| (\mu^n_{\omega_j,h} + z_j V^n_h)\right) - \exp\left(\sum_{\zeta_j\geq 0} \zeta_j (\mu^n_{\omega_j,h} + z_j V^n_h)\right)\right] \times \left(\sum_{\zeta_i<0} |\zeta_i| \left(\mu^n_{\omega_i,h} + z_i V^n_h\right) - \sum_{\zeta_i\geq 0} \zeta_i (\mu^n_{\omega_i,h} + z_i V^n_h)\right) \quad (3.18)$$

on every vertex of the underlying triangulation. Since exp is a monotone increasing function, (3.18) provides $-\sum_{i=1}^{K}\int_\Omega \mathcal{I}_h\left\{R^n_{i,h}(\mu^n_{\omega_i,h} + z_i V^n_h)\right\} \geq 0$.
Therefore, we infer from (3.17) after a discrete integration with respect to time

$$\begin{aligned}
&\tfrac{1}{2}\int_\Omega \left|\nabla\phi^n_h\right|^2 + \int_\Omega \mathcal{I}_h\{W(\phi^n_h)\} + \int_{\partial\Omega} \mathcal{I}_h\{\gamma_{fs}(\phi^n_h)\} + \sum_{i=1}^{K}\int_\Omega \mathcal{I}_h\{g_\nu(\omega^n_{i,h})\} \\
&\quad + \sum_{i=1}^{K}\int_\Omega \mathcal{I}_h\{\beta_i(\phi^n_h)\omega^n_{i,h}\} + \tfrac{1}{2}\int_{\Omega^*} \epsilon^n_h \left|\nabla V^n_h\right|^2 + \tfrac{1}{2}\int_\Omega \overline{\rho}^n_h \left|u^n_h\right|^2 \\
&\quad + \tfrac{2\vartheta-1}{2}\sum_{k=1}^{n}\int_\Omega \left|\nabla\phi^k_h - \nabla\phi^{k-1}_h\right|^2 + \tfrac{1}{2}\sum_{k=1}^{n}\int_{\Omega^*} \epsilon^{k-1}_h \left|\nabla V^k_h - \nabla V^{k-1}_h\right|^2 \\
&\quad + \tau\sum_{k=1}^{n}\int_\Omega \left|\nabla\mu^k_{\phi,h}\right|^2 + \alpha\tau\sum_{k=1}^{n}\int_{\partial\Omega} \mathcal{I}_h\left\{\left|\partial^-_\tau\phi^k_h\right|^2\right\} + \tau\sum_{k=1}^{n}\int_\Omega 2\mathcal{I}_h\left\{\eta(\phi^k_h)\right\}\left|Du^k_h\right|^2 \\
&\quad + \tau\sum_{k=1}^{n}\sum_{i=1}^{K}\int_\Omega \left(\Xi_\nu[\omega^k_{i,h}]\nabla(\mu^k_{\omega_i,h} + z_i V^k_h)\right)\cdot\nabla(\mu^k_{\omega_i,h} + z_i V^k_h) \\
&\quad \leq C(\phi^0_h, (\omega^0_h)^K, u^0_h) \\
&\quad + \tau\sum_{k=1}^{n}\int_{\Omega^*} \partial^-_\tau\left(\epsilon^k_h\nabla V^k_h\right)\cdot\nabla\overline{V}^k_h - \tau\sum_{k=1}^{n}\int_\Omega \mathcal{I}_h\left\{\sum_{i=1}^{K} z_i\,\partial^-_\tau\omega^k_{i,h}\overline{V}^k_h\right\}
\end{aligned} \quad (3.19)$$

As $\omega_{i,h}$ may become negative, we have to absorb $\int_\Omega \mathcal{I}_h\left\{\beta_i(\phi^n_h)\omega^n_{i,h}\right\}$ in $\int_\Omega \mathcal{I}_h\left\{g_\nu(\omega^n_{i,h})\right\}$. For this reason, we consider a dual basis to the nodes $\{x_j\}_{j=1,\ldots,\dim U_h}$ which is denoted by $\{\chi_{h,j}\}_{j=1,\ldots,\dim U_h}$. Furthermore, we define positive weights $\lambda_j := \int_\Omega \chi_{h,j}$ for all $j \in \{1, \ldots, \dim U_h\}$. We compute

$$\begin{aligned}
\tfrac{1}{2}\int_\Omega \mathcal{I}_h\{g_\nu(\omega^n_{i,h})\} &= \tfrac{1}{2}\sum_{j=1}^{\dim U_h} \lambda_j g_\nu(\omega^n_{i,h}(P_j)) = \tfrac{1}{2}\sum_{j:\omega^n_{i,h}(P_j)\geq 0} \lambda_j g_\nu(\omega^n_{i,h}(P_j)) \\
&\quad + \tfrac{1}{2}\sum_{j:\omega^n_{i,h}(P_j)<0} \lambda_j g_\nu(\omega^n_{i,h}(P_j)) \geq -C + \frac{1}{4\nu}\int_\Omega \mathcal{I}_h\left\{[\omega^n_{i,h}]^2_-\right\},
\end{aligned} \quad (3.20)$$

due to (2.4a). Applying Young's inequality finally shows that

$$\tfrac{1}{2}\int_\Omega \mathcal{I}_h\{g_\nu(\omega^n_{i,h})\} + \int_\Omega \mathcal{I}_h\{\beta_i(\phi^n_h)\omega^n_{i,h}\} + C \geq \left(\tfrac{1}{4\nu} - \delta\right)\int_\Omega \mathcal{I}_h\left\{[\omega^n_{i,h}]^2_-\right\} \quad (3.21)$$

holds true for $i = 1, ..., K$ with some C and with $0 < \delta \ll 1$ independent of the discrete solutions. Therefore, the left-hand side of (3.16) is bounded from above by

$$C + C\left(\tau \sum_{k=1}^{n} \int_{\Omega^*} \partial_\tau^- \left(\epsilon_h^k \nabla V_h^k\right) \cdot \nabla \overline{V}_h^k - \tau \sum_{k=1}^{n} \int_{\Omega} \mathcal{I}_h \left\{ \sum_{i=1}^{K} z_i \partial_\tau^- \omega_{i,h}^k \overline{V}_h^k \right\}\right). \quad (3.22)$$

Although the last two terms look similar to (2.12d), they do not vanish in general, as $\overline{V}_h^k \neq 0$ on Γ_D. Applying the cutoff function Π_{c_Γ} defined in (3.5), we introduce the function $\overline{\mathcal{V}}_h^k := \Pi_{c_\Gamma}(\overline{V}_h^k)$. As $\overline{\mathcal{V}}_h^k = 0$ on Γ_D and $\overline{\mathcal{V}}_h^k = \overline{V}_h^k$ on Ω, we may use (2.12d) to rewrite (3.22) as

$$C + C\tau \sum_{k=1}^{n} \int_{\Omega^*} \partial_\tau^- \left(\epsilon_h^k \nabla V_h^k\right) \cdot \nabla \left(\overline{V}_h^k - \overline{\mathcal{V}}_h^k\right). \quad (3.23)$$

Applying a discrete partial integration with respect to time and Young's inequality, we compute

$$\begin{aligned}
& C\tau \sum_{k=1}^{n} \int_{\Omega^*} \partial_\tau^- \left(\epsilon_h^k \nabla V_h^k\right) \cdot \nabla \left(\overline{V}_h^k - \overline{\mathcal{V}}_h^k\right) \\
\leq\ & C\tau \int_{\Omega^*} \epsilon_h^n \nabla V_h^n \cdot \nabla \left(\overline{V}_h^n - \overline{\mathcal{V}}_h^n\right) - C\tau \sum_{k=1}^{n} \int_{\Omega^*} \left(\epsilon_h^{k-1} \nabla V_h^{k-1}\right) \cdot \nabla \partial_\tau^- \left(\overline{V}_h^k - \overline{\mathcal{V}}_h^k\right) \\
& - C\tau \int_{\Omega^*} \epsilon_h^0 \nabla V_h^0 \cdot \nabla \left(\overline{V}_h^0 - \overline{\mathcal{V}}_h^0\right) \\
\leq\ & \tfrac{1}{4} \int_{\Omega^*} \epsilon_h^n \left|\nabla V_h^n\right|^2 + C\tau \int_{\Omega^*} \left|\nabla \overline{V}_h^n\right|^2 + C\tau \int_{\Omega^*} \left|\nabla \overline{\mathcal{V}}_h^n\right|^2 + C\tau \sum_{k=1}^{n} \int_{\Omega^*} \epsilon_h^{k-1} \left|\nabla V_h^{k-1}\right|^2 \\
& + C\tau \sum_{k=1}^{n} \int_{\Omega^*} \left|\nabla \partial_\tau^- \overline{V}_h^k\right|^2 + C\tau \sum_{k=1}^{n} \int_{\Omega^*} \left|\nabla \partial_\tau^- \overline{\mathcal{V}}_h^k\right|^2 + C\tau \int_{\Omega^*} \epsilon_h^0 \left|\nabla V_h^0\right|^2 \\
& + C\tau \int_{\Omega^*} \left|\nabla \overline{V}_h^0\right|^2 + C\tau \int_{\Omega^*} \left|\nabla \overline{\mathcal{V}}_h^0\right|^2,
\end{aligned} \quad (3.24)$$

as ϵ is bounded. Recalling the estimates on Π_{c_Γ} (see Lemma 3.1) and the regularity assumptions on $\overline{V}_h$ (see (E6)), we complete the proof by absorbing the first term on the right-hand side and by applying a discrete version of Gronwall's lemma (cf., e.g. [23]). □

Using the a priori estimate stated in the lemma above, we will now establish the existence of discrete solutions. For this purpose, we need an auxiliary result which was proven in Lemma 2.11 in [17].

Lemma 3.3 *Let ϵ satisfy (E5). Then*

$$\epsilon[a](x) + \epsilon[b](x) - \epsilon'_{DQ}(a, b)b \geq 0 \quad (3.25)$$

holds true for every $a, b \in \mathbb{R}$ and $x \in \Omega$.

Lemma 3.4 *Let the Assumptions (E1)–(E7) hold true. Then, for given*

$$(\phi_h^{n-1}, (\omega_h^{n-1})^K, V_h^{n-1} - \overline{V}_h^{n-1}, u_h^{n-1}) \in U_h \times (U_h)^K \times U_{h,0}^* \times \boldsymbol{W}_{h,\mathrm{div}}\,,$$

there exists at least one tuple $(\phi_h^n, \mu_{\phi,h}^n, (\omega_h^n)^K, V_h^n - \overline{V}_h^n, u_h^n) \in U_h \times U_h \times (U_h)^K \times U_{h,0}^* \times \boldsymbol{W}_{h,\mathrm{div}}$ *solving* (2.12).

Proof The structure of the (2.12d) and (2.12b) provides the existence of unique V_h^n and $\mu_{\phi,h}^n$ for any given ϕ_h^n and $(\omega_h^n)^K$. Consequently, we may treat V_h^n and $\mu_{\phi,h}^n$ as functions depending on the quantities ϕ_h^n and $(\omega_h^n)^K$. In general, we will write $V_h(\phi_h, (\omega_h)^K) \in U_h^*$ and $\mu_{\phi,h}(\phi_h, (\omega_h)^K) \in U_h$ for the solutions of

$$\int_{\Omega^*} \mathcal{I}_h\{\epsilon[\phi_h](\mathbf{x})\}\nabla V_h(\phi_h, (\omega_h)^K) \cdot \nabla\theta_h = \int_\Omega \mathcal{I}_h\left\{\sum_{j=1}^K z_j\omega_{j,h}\theta_h\right\} \tag{3.26}$$

for all $\theta_h \in U_{h,0}^*$, subjected to the constraint $V_h(\phi_h, (\omega_h)^K) = \overline{V}_h^n$ on Γ_D and

$$\begin{aligned}\int_\Omega \mathcal{I}_h\left\{\mu_{\phi,h}(\phi_h, (\omega_h)^K)\theta_h\right\} = &\int_\Omega (\vartheta\nabla\phi_h + (1-\vartheta)\nabla\phi_h^{n-1})\cdot\nabla\theta_h + \int_\Omega \mathcal{I}_h\left\{W_h'(\phi_h, \phi_h^{n-1})\theta_h\right\}\\ &+ \int_{\partial\Omega} \mathcal{I}_h\left\{\gamma_{fs,DQ}'(\phi_h, \phi_h^{n-1})\theta_h\right\} + \alpha\tau^{-1}\int_{\partial\Omega}\mathcal{I}_h\left\{(\phi_h - \phi_h^{n-1})\theta_h\right\}\\ &+ \int_\Omega \mathcal{I}_h\left\{\sum_{j=1}^K \beta_{j,DQ}'(\phi_h, \phi_h^{n-1})\omega_{j,h}^{n-1}\theta_h\right\}\\ &- \tfrac{1}{2}\int_\Omega \mathcal{I}_h\left\{\epsilon_{DQ}'(\phi_h, \phi_h^{n-1})\theta_h\right\}\left|\nabla V_h(\phi_h, (\omega_h)^K)\right|^2 \ \forall\theta_h \in U_h\,.\end{aligned} \tag{3.27}$$

To prove the existence of the remaining quantities, we proceed as follows. We assume the nonexistence of solutions and use Brouwer's fixed point theorem to construct a contradiction. To omit clumsy notation, we assume w.l.o.g. $\int_\Omega \phi_h^n = \int_\Omega \phi_h^{n-1} = 0$, i.e., we look for solutions Φ_h^n in the space $S_h \subset U_h$. We define an inner product $(\!(.,.)\!)$ on $S_h \times (U_h)^K \times \boldsymbol{W}_{h,\mathrm{div}}$ via

$$(\!((\phi_h, (\omega_h)^K, u_h), (\psi_h, (\theta_h)^K, w_h))\!) := \int_\Omega \mathcal{I}_h\{\phi_h\psi_h\} + \sum_{j=1}^K \int_\Omega \mathcal{I}_h\{\omega_{j,h}\theta_{j,h}\} + \int_\Omega u_h \cdot w_h \tag{3.28}$$

for all $(\phi_h, (\omega_h)^K, u_h), (\psi_h, (\theta_h)^K, w_h) \in S_h \times (U_h)^K \times \boldsymbol{W}_{h,\mathrm{div}}$. Given $(\phi_h^{n-1}, (\omega_h^{n-1})^K, u_h^{n-1}) \in S_h \times (U_h)^K \times \boldsymbol{W}_{h,\mathrm{div}}$, we define a mapping $\mathcal{H} := \left(\mathcal{F}_\phi, \{\mathcal{F}_{\omega_i}\}_{i=1,\dots,K}, \boldsymbol{\mathcal{F}}_u\right)$ mapping $S_h \times (U_h)^K \times \boldsymbol{W}_{h,\mathrm{div}}$ onto itself. These functions are the residual of (2.12) and defined via

$$\begin{aligned}\int_\Omega \mathcal{I}_h\left\{\mathcal{F}_\phi(\phi_h, (\omega_h)^K, u_h)\psi_h\right\} = \int_\Omega \mathcal{I}_h\left\{(\phi_h - \phi_h^{n-1})\psi_h\right\} - \tau\int_\Omega \phi_h^{n-1}u_h^{n-1}\cdot\nabla\psi_h\\ + \tau\int_\Omega \left(\tau(\min\overline{\rho}_h^{n-1})^{-1}|\phi_h^{n-1}|^2 + 1\right)\nabla\mu_{\phi,h}(\phi_h, (\omega_h)^K)\cdot\nabla\psi_h\,,\end{aligned} \tag{3.29a}$$

$$
\begin{aligned}
&\int_\Omega \mathcal{I}_h\Big\{\mathcal{F}_{\omega_i}(\phi_h,(\omega_h)^K,u_h)\theta_h\Big\} = \int_\Omega \mathcal{I}_h\Big\{(\omega_{i,h}-\omega_{i,h}^{n-1})\theta_h\Big\} - \tau\int_\Omega \omega_{i,h}^{n-1}u_h^{n-1}\cdot\nabla\theta_h \\
&+\tau^2 K\int_\Omega (\min\overline{\rho}_h^{n-1})^{-1}|\omega_{i,h}|^2\nabla\mathcal{I}_h\Big\{g_\nu'(\omega_{i,h})+\beta_i(\phi_h)+z_i V_h(\phi_h,(\omega_h)^K)\Big\}\cdot\nabla\theta_h \\
&+\tau\int_\Omega \Big(\Xi_\nu[\omega_{i,h}]\nabla\mathcal{I}_h\Big\{g_\nu'(\omega_{i,h})+\beta_i(\phi_h)+z_i V_h(\phi_h,(\omega_h)^K)\Big\}\Big)\cdot\nabla\theta_h \\
&-\tau\int_\Omega \mathcal{I}_h\Big\{R_{i,h}(\phi_h,(\omega_h)^K,V_h(\phi_h,(\omega_h)^K))\theta_h\Big\}, \qquad (3.29b)
\end{aligned}
$$

$$
\begin{aligned}
&\int_\Omega \boldsymbol{\mathcal{F}}_u(\phi_h,(\omega_h)^K,u_h)\cdot w_h = \int_\Omega \tfrac12(\overline{\rho}_h+\overline{\rho}_h^{n-1})(u_h-u_h^{n-1})\cdot w_h + \tfrac12\int_\Omega(\overline{\rho}_h-\overline{\rho}_h^{n-1})u_h^{n-1}\cdot w_h \\
&+\tfrac12\tau\int_\Omega \overline{\rho}_h\Big((\nabla u_h)^T\cdot w_h\Big)\cdot u_h^{n-1} - \tfrac12\tau\int_\Omega \overline{\rho}_h\Big((\nabla w_h)^T\cdot u_h\Big)\cdot u_h^{n-1} \\
&+\tfrac12\tau\int_\Omega \tfrac{\delta\overline{\rho}}{\delta\phi}\Big((\nabla u_h)^T\cdot w_h\Big)\cdot\nabla\mu_{\phi,h}(\phi_h,(\omega_h)^K) - \tfrac12\tau\int_\Omega \tfrac{\delta\overline{\rho}}{\delta\phi}\Big((\nabla w_h)^T\cdot u_h\Big)\cdot\nabla\mu_{\phi,h}(\phi_h,(\omega_h)^K) \\
&+\tau\int_\Omega 2\mathcal{I}_h\{\eta(\phi_h)\}Du_h : Dw_h + \tau\int_\Omega \phi_h^{n-1}\nabla\mu_{\phi,h}(\phi_h,(\omega_h)^K)\cdot w_h \\
&+\tau\sum_{j=1}^K\int_\Omega \omega_{j,h}^{n-1}\nabla\mathcal{I}_h\Big\{g_\nu'(\omega_{j,h})+\beta_j(\phi_h)+z_j V_h(\phi_h,(\omega_h)^K)\Big\}\cdot w_h\,, \qquad (3.29c)
\end{aligned}
$$

for all $\psi_h\in S_h$, $\theta_h\in U_h$, $w_h\in \boldsymbol{W}_{h,\mathrm{div}}$, and $i\in\{1,\ldots,K\}$ with $\overline{\rho}_h:=\mathcal{I}_h\{\overline{\rho}(\phi_h)\}$. Therefore, the existence of a root to $\mathcal{H}$ is equivalent to the existence of solutions to (2.12). Assuming $\mathcal{H}\neq 0$ on

$$
B_R := \Big\{(\psi_h,(\theta_h)^K,w_h)\in S_h\times(U_h)^K\times\boldsymbol{W}_{h,\mathrm{div}} : \Big\|\Big|(\psi_h,(\theta_h)^K,w_h)\Big\|\Big|\le R\Big\} \qquad (3.30)
$$

with $|\!|\!|.|\!|\!| = \sqrt{(\!(.,.)\!)}$, the continuous mapping $\mathcal{G} : B_R\to B_R$ defined by

$$
\mathcal{G}\Big(\psi_h,(\theta_h)^K,w_h\Big) := -R\frac{\mathcal{H}(\psi_h,(\theta_h)^K,w_h)}{|\!|\!|\mathcal{H}(\psi_h,(\theta_h)^K,w_h)|\!|\!|} \qquad (3.31)
$$

has—due to Brouwer's fixed point theorem—at least one fixed point, which we denote by $(\hat{\phi}_h,(\hat{\omega}_h)^K,\hat{u}_h)$. We will now show that for a suitable choice of $\hat{\psi}_h$, $(\hat{\theta}_h)^K$, and $\hat{\mathbf{w}}_h$

$$
0 < (\!((\hat{\phi}_h,(\hat{\omega}_h)^K,\hat{u}_h),(\hat{\psi}_h,(\hat{\theta}_h)^K,\hat{w}_h))\!) < 0 \qquad (3.32)
$$

holds true for R large enough. This contradiction then provides the desired result. We choose $\hat{\psi}_h$, $(\hat{\theta}_h)^K$, and $\hat{w}_h$ as follows. Abbreviating $V_h(\hat{\phi}_h,(\hat{\omega}_h)^K)$ by $\hat{V}_h$ and the chemical potential $\mu_{\phi,h}(\hat{\phi}_h,(\hat{\omega}_h)^K)$ by $\hat{\mu}_{\phi,h}$, we define

$$
\begin{aligned}
\hat{\psi}_h &:= \hat{\mu}_{\phi,h} - \tfrac{1}{|\Omega|}\int_\Omega \hat{\mu}_{\phi,h} \in S_h\,, && (3.33a)\\
\hat{\theta}_{i,h} &:= \mathcal{I}_h\Big\{g_\nu'(\hat{\omega}_{i,h})+\beta_i(\hat{\phi}_h)+z_i\hat{V}_h\Big\}\in U_h\,, && (3.33b)\\
\hat{w}_h &:= \hat{u}_h \in \boldsymbol{W}_{h,\mathrm{div}}\,. && (3.33c)
\end{aligned}
$$

We start by proving the first inequality in (3.32). As $\hat{\phi}_h$ has zero mean, we apply Young's inequality with $0 < \delta \ll 1$ and compute

$$
\begin{aligned}
&\int_\Omega \mathcal{I}_h\left\{\hat{\phi}_h\hat{\psi}_h\right\} = \int_\Omega \mathcal{I}_h\left\{\hat{\phi}_h\hat{\mu}_{\phi,h}\right\} \\
\geq\ & \vartheta\int_\Omega |\nabla\hat{\phi}_h|^2 - \delta\int_\Omega |\nabla\hat{\phi}_h|^2 - C_\delta\int_\Omega \left|\nabla\phi_h^{n-1}\right|^2 + \int_\Omega \mathcal{I}_h\left\{W_h'(\hat{\phi}_h,\phi_h^{n-1})\hat{\phi}_h\right\} \\
&+ \int_{\partial\Omega}\mathcal{I}_h\left\{\gamma'_{fs,DQ}(\hat{\phi}_h,\phi_h^{n-1})\hat{\phi}_h\right\} + \tfrac{\alpha}{2\tau}\int_{\partial\Omega}\mathcal{I}_h\left\{|\hat{\phi}_h|^2 + |\hat{\phi}_h - \phi_h^{n-1}|^2 - \left|\phi_h^{n-1}\right|^2\right\} \\
&+ \int_\Omega \mathcal{I}_h\left\{\sum_{j=1}^K \beta'_{j,DQ}(\hat{\phi}_h,\phi_h^{n-1})\omega_{j,h}^{n-1}\hat{\phi}_h\right\} - \tfrac{1}{2}\int_\Omega \mathcal{I}_h\left\{\epsilon'_{DQ}(\hat{\phi}_h,\phi_h^{n-1})\hat{\phi}_h\right\}\left|\nabla\hat{V}_h\right|^2 \\
=:\ & I_\phi + II_\phi + III_\phi + IV_\phi + V_\phi + VI_\phi + VII_\phi + VIII_\phi\,. \qquad (3.34)
\end{aligned}
$$

Obviously, we have $III_\phi \geq -C$, $VI_\phi \geq -C$, and $IV_\phi \geq -C$ due to (W1). From (E3) and (E4), we obtain also $V_\phi \geq -C$ and $VII_\phi \geq -C$.
As g_ν is a convex function, we obtain for $i = 1, \ldots, K$

$$
\begin{aligned}
\int_\Omega \mathcal{I}_h\left\{\hat{\omega}_{i,h}\hat{\theta}_{i,h}\right\} &= \int_\Omega \mathcal{I}_h\left\{\hat{\omega}_{i,h}(g_\nu'(\hat{\omega}_{i,h}) + \beta_i(\hat{\phi}_h) + z_i\hat{V}_h)\right\} \\
&\geq \int_\Omega \mathcal{I}_h\{g_\nu(\hat{\omega}_{i,h}) - g_\nu(0)\} + \int_\Omega \mathcal{I}_h\left\{\beta_i(\hat{\phi})\hat{\omega}_{i,h}\right\} \\
&+ \int_\Omega \mathcal{I}_h\left\{\hat{\omega}_{i,h}z_i\hat{V}_h\right\} := I_{\omega_i} + II_{\omega_i} + III_{\omega_i}. \qquad (3.35)
\end{aligned}
$$

Recalling the arguments used in the proof of Lemma 3.2 to deduce (3.21) yields $\frac{1}{2}I_{\omega_i} + II_{\omega_i} \geq -C$.
Using $\overline{V}_h^n - \Pi_{c\Gamma}(\overline{V}_h^n) \equiv 0$ on Ω, $\hat{V}_h - \overline{V}_h^n + \Pi_{c\Gamma}(\overline{V}_h^n) \equiv 0$ on Γ_D and (3.26), we compute

$$
\begin{aligned}
&\sum_{i=1}^K III_{\omega_i} = \sum_{i=1}^K \int_\Omega \mathcal{I}_h\left\{\hat{\omega}_{i,h}z_i\left(\hat{V}_h - \overline{V}_h^n + \Pi_{c\Gamma}(\overline{V}_h^n)\right)\right\} \\
&= \int_{\Omega^*}\mathcal{I}_h\left\{\epsilon[\hat{\phi}_h](x)\right\}\nabla\hat{V}_h\cdot\nabla\hat{V}_h - \int_{\Omega^*\setminus\Omega}\mathcal{I}_h\left\{\epsilon[\hat{\phi}_h](x)\right\}\nabla\hat{V}_h\cdot\nabla\left(\overline{V}_h^n - \Pi_{c\Gamma}(\overline{V}_h^n)\right). \\
&\qquad (3.36)
\end{aligned}
$$

Combining (3.36) and $VIII_\phi$ shows

$$
\begin{aligned}
&\sum_{i=1}^K III_{\omega_i} + VIII_\phi = \tfrac{1}{2}\int_\Omega \mathcal{I}_h\left\{\epsilon[\hat{\phi}_h](x) + \epsilon[\phi_h^{n-1}](x) - \epsilon'_{DQ}(\hat{\phi}_h,\phi_h^{n-1})\phi_h^{n-1}\right\}\left|\nabla\hat{V}_h\right|^2 \\
&+ \int_{\Omega^*\setminus\Omega}\mathcal{I}_h\left\{\epsilon[\hat{\phi}_h](x)\right\}\nabla\hat{V}_h\cdot\nabla\hat{V}_h - \int_{\Omega^*\setminus\Omega}\mathcal{I}_h\left\{\epsilon[\hat{\phi}_h](x)\right\}\nabla\hat{V}_h\cdot\nabla\left(\overline{V}_h^n - \Pi_{c\Gamma}(\overline{V}_h^n)\right). \quad (3.37)
\end{aligned}
$$

According to Lemma 3.3, the first term is nonnegative. Due to Young's inequality and Lemma 3.1, the first two terms are bounded from below by $-C$ depending on $\overline{V}_h^n$ but not on the fixed point.

Noting $\int_\Omega |\hat{u}_h|^2 \cdot \hat{w}_h = \int_\Omega |\hat{u}_h|^2$, we deduce

$$(((\hat{\phi}_h, (\hat{\omega}_h)^K, \hat{u}_h), (\hat{\psi}_h, (\hat{\theta}_h)^K, \hat{w}_h))) \geq (\vartheta - \delta) \int_\Omega \left|\nabla \hat{\phi}_h\right|^2 + \tfrac{1}{2} \sum_{j=1}^{K} \int_\Omega \mathcal{I}_h\{g_\nu(\hat{\omega}_{j,h})\} + \int_\Omega |\hat{u}_h|^2 - C\,. \tag{3.38}$$

As $g_\nu(s) \geq |s| - C$ for $s \in \mathbb{R}$ and $\hat{\phi}_h \in S_h$, we may use the equivalence of norms on finite dimensional spaces to deduce the first inequality in (3.32) for R large enough. To prove the second inequality in (3.32), we follow the lines of the proof of Lemma 3.2 to deduce

$$\begin{aligned}
&((\mathcal{H}(\hat{\phi}_h, (\hat{\omega}_h)^K, \hat{u}_h), (\hat{\psi}_h, (\hat{\theta}_h)^K, \hat{\mathbf{w}}_h)))\\
&\geq -C + \tfrac{1}{2} \int_\Omega \left|\nabla \hat{\phi}_h\right|^2 + \tfrac{1}{2} \sum_{j=1}^{K} \int_\Omega \mathcal{I}_h\{g_\nu(\hat{\omega}_{j,h})\} + \tfrac{1}{2} \int_{\Omega^*} \mathcal{I}_h\left\{\epsilon[\hat{\phi}_h](x)\right\} \left|\nabla \hat{V}_h\right|^2\\
&\quad + \tfrac{1}{2} \min_{s\in\mathbb{R}} \overline{\rho}(s) \int_\Omega |\hat{u}_h|^2 - \int_{\Omega^*} \left(\mathcal{I}_h\left\{\epsilon[\hat{\phi}_h](x)\right\}\nabla \hat{V}_h - \mathcal{I}_h\left\{\epsilon[\phi_h^{n-1}](\mathbf{x})\right\}\nabla V_h^{n-1}\right) \cdot \nabla \overline{V}_h^n\\
&\quad + \sum_{j=1}^{K} \int_\Omega \mathcal{I}_h\left\{z_j(\hat{\omega}_{j,h} - \omega_{j,h}^{n-1})\overline{V}_h^n\right\}\\
&\geq -C + \tfrac{1}{2} \int_\Omega \left|\nabla \hat{\phi}_h\right|^2 + \tfrac{1}{2} \sum_{j=1}^{K} \int_\Omega \mathcal{I}_h\{g_\nu(\hat{\omega}_{j,h})\}\\
&\quad + \tfrac{1}{2} \min_{s\in\mathbb{R}} \overline{\rho}(s) \int_\Omega |\hat{u}_h|^2 - C \sum_{j=1}^{K} \int_\Omega \mathcal{I}_h\{|\hat{\omega}_{j,h}|\}\,,
\end{aligned} \tag{3.39}$$

as $\overline{V}_h^n$ is sufficiently regular (cf. (E6)). As g_ν has superlinear growth, $\frac{1}{4} g_\nu(s) \geq C|s|$ holds true for s larger than some critical value $\tilde{\omega}$ which is independent of R. Hence,

$$\begin{aligned}
\tfrac{1}{4} \int_\Omega \mathcal{I}_h\{g_\nu(\hat{\omega}_{j,h})\} - C \int_\Omega \mathcal{I}_h\{|\hat{\omega}_{j,h}|\} &\geq -C \int_\Omega \mathcal{I}_h\{\min\{\tilde{\omega}, |\hat{\omega}_{j,h}|\}\} - C\\
&\geq -C|\Omega|\tilde{\omega} - C
\end{aligned} \tag{3.40}$$

holds true for $j = 1, ..., K$. Therefore, similar arguments as in the last step imply the positivity of the right-hand side for R large enough. Recalling that $(\hat{\phi}_h, (\hat{\omega}_h)^K, \hat{u}_h)$ is a fixed point of $\mathcal{G}$, (3.31) completes the proof. □

4 Numerical experiments

For practical computations, the finite element scheme (2.12) is implemented in the framework of the inhouse code `EconDrop` which is written in `C++` (cf. [2, 5, 13]). In this section, we present and discuss simulations based on the presented scheme. In Section 4.1, we use the simulation of a falling droplet as an example to illustrate the effect of the different discretization techniques introduced in Section 2 to reduce the numerical dissipation. In Sections 4.2 and 4.3, we present simulations of ion induced droplet deformations to validate the basic functionality of the model and the discrete scheme.

4.1 Numerical dissipation

Simulations published in [12] already indicated that numerical dissipation may affect the falling velocity of droplets. Generally, one may derive an energy inequality of the form

$$\text{energy}(t^n) \;+\; \text{dissipation} \leq \; \text{energy}(t^{n-1}) \;+\; \text{external forces}\,, \tag{4.1}$$

i.e., external forces may increase the energy of the system, while dissipation withdraws energy from the system. As the energy of pure two-phase flows (in absence of dissolved species) consists of a kinetic term $\frac{1}{2}\int_\Omega \rho\,|u|^2$ and terms describing the fluid-fluid and fluid-wall contact energies (cf. (1.3)), an energy reduction may be obtained either by optimizing the shape of the droplet or by reducing the velocity.
The scheme presented in Section 2 includes several mechanisms to reduce the numerical dissipation and therefore the artificial loss of energy: First, the parameter ϑ allows to interpolate between time discretizations of the discrete Laplacian introducing a different amount of numerical dissipation. In particular, we combine the following identities.

$$\nabla\phi_h^n \cdot \nabla\partial_\tau^-\phi_h^n \;=\; \tfrac{1}{2\tau}\left|\nabla\phi_h^n\right|^2 + \tfrac{1}{2\tau}\left|\nabla\phi_h^n - \nabla\phi_h^{n-1}\right|^2 - \tfrac{1}{2\tau}\left|\nabla\phi_h^{n-1}\right|^2 \tag{4.2a}$$

$$\tfrac{1}{2}\left(\nabla\phi_h^n + \nabla\phi_h^{n-1}\right)\cdot\nabla\partial_\tau^-\phi_h^n \;=\; \tfrac{1}{2\tau}\left|\nabla\phi_h^n\right|^2 - \tfrac{1}{2\tau}\left|\nabla\phi_h^{n-1}\right|^2 . \tag{4.2b}$$

Secondly, the assumptions (W1)–(W5) allow for different approximations of W'. In particular, we will use a polynomial double-well potential with penalty term (cf. [12])

$$W(\phi) := \tfrac{1}{4}(1-\phi^2)^2 + \tfrac{1}{\delta'}\max\{|\phi|-1,\ 0\}^2 \tag{4.3}$$

with $\delta' = 4\cdot 10^{-3}$ and compare the following approaches.

(CC) Given a convex-concave decomposition $W = W_{\text{conv}} + W_{\text{conc}}$, we set

$$W_h'(a,b) := W_{\text{conv}}'(a) + W_{\text{conc}}'(b)\,.$$

(DQ) We compute the difference quotient of the polynomial part and set

$$W_h'(a,b) := \tfrac{1}{4}\left(a^3+a^2b+ab^2+b^3\right) - \tfrac{1}{2}(a+b) + \tfrac{1}{\delta'}\left.\tfrac{\mathrm{d}}{\mathrm{d}s}\right|_{s=a}\max\{|s|-1,0\}^2\,.$$

(IM) Combining the ideas of (CC) and (DQ), we set

$$W_h'(a,b) := W'(a) + \tfrac{a-b}{2}\,.$$

While (DQ) is expected to be the least dissipative approximation, (IM) is constructed as an intermediate between (CC) and (DQ), i.e., starting from a suitable convex-concave decomposition of W, the derivative of the concave part is approximated using a difference quotient.
To investigate the influence of the numerical dissipation, we decide on a simple experiment. A comparison of (IM) and (DQ) in a more sophisticated setting can be found in [12]. Given the rectangular domain $(-1,1)\times(-1,5)$ filled with a fluid of mass density 1, we position a circular droplet with radius 0.3, barycenter at

(0, 4) and mass density 3 (cf. Figure 2 and Table 1). We include gravity by adding $-\int_\Omega \overline{\rho}_h^n g e_{x_2} \cdot w$ with the gravitational acceleration $g = 10$ on the right-hand side of (2.12e), which results in the droplet falling downwards. By choosing a relatively high surface energy density $\sigma = 10$, we prevent the droplet from deforming. Therefore, tracking the position of its barycenter provides a good indication for the droplet's position.
The mesh is adaptive, i.e., it is relatively coarse in the pure fluids while providing a fine resolution in the interfacial area. It consists of simplices with diameter between approximately 0.067 and 0.008. Concerning the boundary conditions, $u = 0$ and $\nabla\phi \cdot n$ are imposed on $\partial\Omega \times \mathbb{R}^+$. For the remaining parameters, we refer to Table 1.

We start by investigating the influence of the time increment on the results computed using (DQ) and $\vartheta = 0.5$ which corresponds to the least dissipative scheme. For this reason, we track the droplet's barycenter and compute the kinetic energy $\mathcal{E}_{\mathrm{kin}}(\phi_h^n, u_h^n) := \int_\Omega \mathcal{I}_h\{\rho(\phi_h^n)\}|u_h^n|^2$ of the system. As it turns out, the computed positions of the droplet vary only little when decreasing the time increment. The variations in the kinetic energy are slightly larger. However, Fig. 3 suggests that a further reduction of the time increment will not improve the results significantly. Therefore, the results based on (DQ) and $\vartheta = 0.5$ may serve as reference solutions in the comparison with the other approaches.
In the next step, we compare the results of different schemes for time increments $\tau = 1.0 \cdot 10^{-4}$ and $\tau = 2.5 \cdot 10^{-5}$. The results are depicted in Figs. 4 and 5. The differences between the results obtained with the most dissipative scheme ((CC), $\vartheta = 1.0$) and the least dissipative scheme are evident. As predicted by (4.1), larger numerical dissipation reduces the kinetic energy significantly and thereby inhibits large velocities. Consequently, different schemes compute different droplet positions. While the first, most dissipative scheme suggest a final droplet position at height 3 ($\tau = 1.0 \cdot 10^{-4}$) or height 2 ($\tau = 2.5 \cdot 10^{-4}$), respectively, the reference solutions yield approx. 0.6 as the height of the barycenter at time 2.
Concerning the impact of the aforementioned mechanisms, Figs. 4 and 5 indicate that using a discretization of W' which induces only little numerical dissipation is inevitable for improving the quality of the approximation. Nevertheless, a reduction of ϑ is also necessary to obtain reliable results, as the comparison of $((DQ),\ \vartheta = 0.5)$ and $((DQ),\ \vartheta = 1.0)$ shows. While the first approach provides already a good approximation of the droplet position using $\tau = 1.0 \cdot 10^{-4}$, the results obtained with the second one are still unsatisfactory.

4.2 Droplet movement and contact angles

In the remaining subsections, we present simulations serving as a qualitative validation of the presented discrete scheme. In this subsection, we present a simulation of a two-dimensional charged droplet which is influenced by an external electrode. Thereby, we focus on the contact angles of the droplet and the confinement of the dissolved ions to the droplet.
Given the fluidic domain $\Omega := (-5, 5) \times (0.625, 5)$, we place a semicircular shaped droplet with radius 1 and midpoint $(1, 0.625)$ on the lower boundary of Ω. The

Fig. 2 Initial triangulation

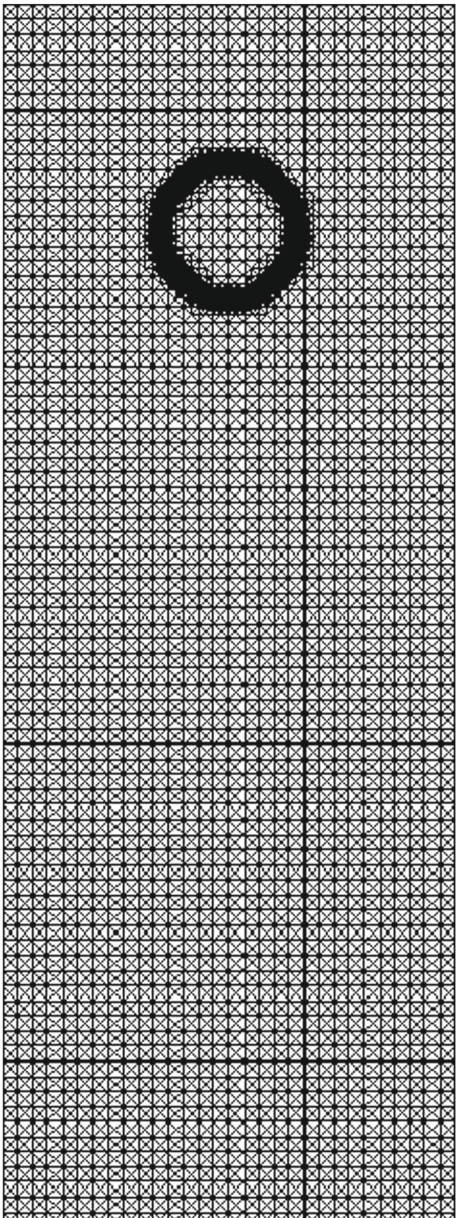

Table 1 Parameters used in Section 4.1

δ	σ	m	$\gamma_{fs}(\pm 1)$	α	$\rho(+1)$	$\rho(-1)$	$\eta(\pm 1)$
0.01	10	10^{-4}	0	0	3	1	0.05

droplet has the same density and viscosity as the ambient liquid (cf. Table 2). The choice $\sigma = 3$ allows for deformation of the droplet while still preventing breakup. The width of the fluid-fluid interface is given by $\delta = 0.02$. The stationary contact angle between interface and wall is prescribed by $\gamma_{fs} \equiv 0$ which corresponds to a contact angle of 90°. By setting $\alpha = 0.0002$, we allow the dynamic contact angles to deviate from the stationary ones. The droplet contains positively charged ions. On a semicircle with radius 0.5 and midpoint $(1, 0.625)$ we prescribe $\omega_h^0 = 10$. To avoid jumps in the initial ion concentration (indicated in gray in Fig. 6a), the number density decays linearly until it vanishes on a sphere with radius 0.75 around the midpoint $(1, 0.625)$. The ions are supposed to be soluble only in the droplet, which is achieved by setting $\beta = 1$ inside of the droplet and $\beta = 10$ in the ambient fluid (and interpolating in the interfacial region using an appropriate sin-function). The diffusivity of the ions is given by $k \equiv 5$.

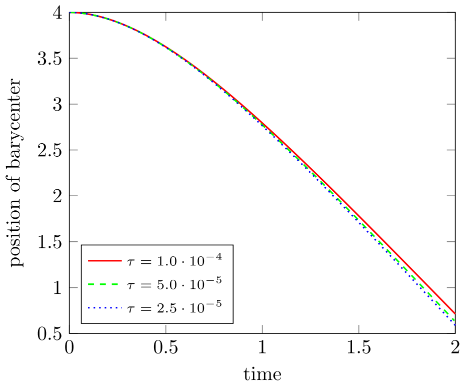

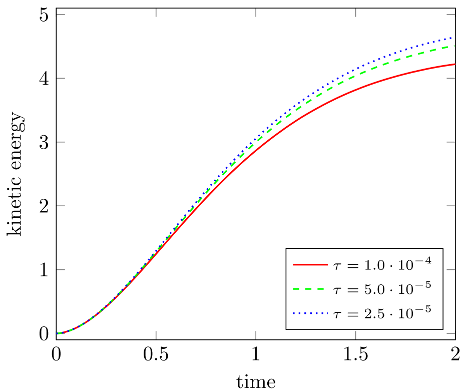

Fig. 3 Position of the droplet's barycenter and kinetic energy; computed using (DQ), $\vartheta = 0.5$

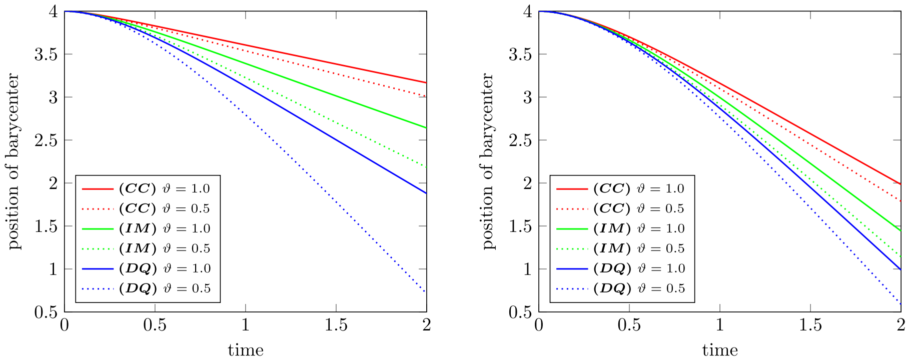

Fig. 4 Position of the droplet's barycenter computed using $\tau = 1.0 \cdot 10^{-4}$ (left) and $\tau = 2.5 \cdot 10^{-5}$ (right)

To manipulate the droplet, we place electrodes below it, i.e., we consider $\Omega^* := (-5, 5) \times (0, 10)$ and assume Dirichlet conditions on $\Gamma_b := [-5, 5] \times \{0\}$ and $\Gamma_t := [-5, 5] \times \{10\}$. While imposing homogeneous Dirichlet data on Γ_t and on most parts of Γ_b, the electrode is represented by $\overline{V} = -20$. Initially, it is placed right below the droplet, i.e. ,$\overline{V} = -20$ on $[0.5, 1.5] \times \{0\}$. Later (at $t = 0.001$) this electrode is shifted to $[-1.5, -0.5] \times \{0\}$ before returning to its original position at $t = 0.03$. On the left and right boundary of Ω^*, we impose homogeneous Neumann conditions.

The discretization parameters are chosen as follows. We use an adaptive mesh consisting of simplices with diameters between approximately 0.110 and 0.014. The fixed time increment is set to $\tau = 5 \cdot 10^{-6}$. The polynomial double-well potential is extended by a penalty term with $\delta' = 4 \cdot 10^{-3}$ (cf. (4.3)). The derivatives of the double-well potential are discretized using (DQ). Choosing $\vartheta = 0.625$, we expect the Cahn-Hilliard type equations to introduce only little numerical dissipation. For the remaining parameters, we refer to Table 2.

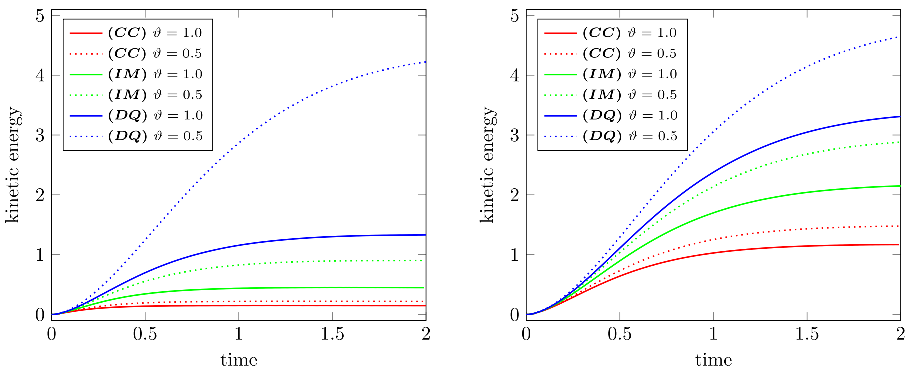

Fig. 5 Kinetic energy computed using $\tau = 1.0 \cdot 10^{-4}$ (left) and $\tau = 2.5 \cdot 10^{-5}$ (right)

Table 2 Parameters used in the simulation in Section 4.2.

σ	δ	m	$\gamma_{fs}(\pm 1)$	α	ϑ	$\rho(\pm 1)$	$\eta(\pm 1)$	ϵ	ν	τ
3	0.02	0.1	0	$2 \cdot 10^{-4}$	0.625	10^{-4}	$5 \cdot 10^{-4}$	1	10^{-7}	$5 \cdot 10^{-6}$

The position of the droplet and the distribution of the ions are depicted in Fig. 6. The black rectangle represents the fluidic domain Ω. The position of the droplet is indicated by a black curve representing the equipotential line $\phi = 0$, while the position of the electrode is marked by the thick black line below Ω. The gray shading in the background indicates the spatial distribution of the ions.

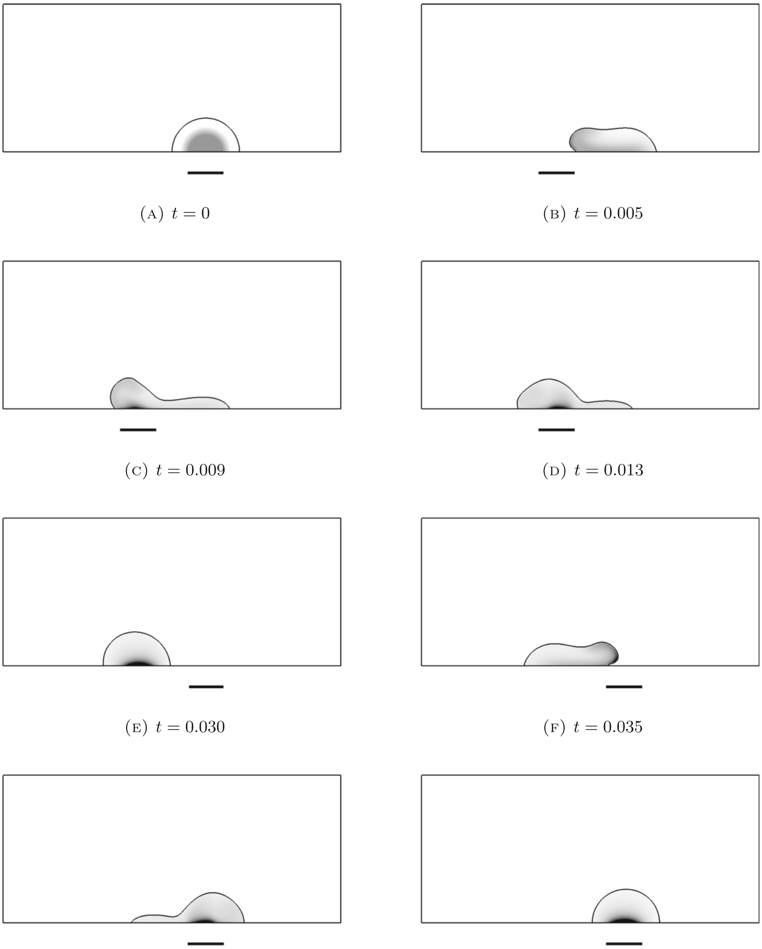

(A) $t = 0$ (B) $t = 0.005$ (C) $t = 0.009$ (D) $t = 0.013$ (E) $t = 0.030$ (F) $t = 0.035$ (G) $t = 0.043$ (H) $t = 0.070$

Fig. 6 Ion-induced droplet movement

Initially, the ions are placed right above the electrode. After shifting the electrode to the left, the ions try to follow the electrode carrying a portion of droplet with them (see Fig. 6a–d). As the surface tension is high enough to prevent rupture, the entire droplet moves to the left and attains a nearly semicircular shape above the new position of the electrode.

At time $t = 0.03$, the electrode is shifted back to its former position (see Fig. 6e). Consequently, the ions—and therefore the entire droplet—also move back to the right-hand side of the domain (cf. Fig. 6f–h), where the droplet finally attains a semicircular shape above the electrode.

We want to highlight two details occuring in this simulation. First, we want to point out the contact angle hysteresis at the bottom of Ω. While the droplet is moving, the contact angles of the droplet deviate significantly from the stationary one which was prescribed as $\frac{\pi}{2}$ (cf. Fig. 6c–d and f–g). In the stationary state (see Fig. 6h), the stationary contact angle of $\frac{\pi}{2}$ is recovered, as the droplet is at rest. Secondly, we want to recall that we used only an energetic argument to confine the ions to the droplet. As this simulations shows, the energetic penalization suffices to prevent the ions from leaving the droplet, although they are subjected to relatively strong forces.

4.3 Ion-induced droplet deformation

In this subsection, we consider several kinds of species and focus on topological changes like droplet breakup or droplet coalescence.

In the first scenario, we position a circular droplet ($\phi = 1$) with radius 0.3 and barycenter at $(0, 0, 0)$ in a cylindrical domain $\Omega := \{x \in \mathbb{R}^3 : -1.75 < x_1 < 1.75,\ x_2^2 + x_3^2 < 1\}$. In this simulation three different types of species are included. On the right-hand side of Fig. 7, the uncharged molecules, negatively charged ions, and positively charged ions are indicated in green, blue, and red, respectively. All three considered species types are assumed to be soluble only in the droplet, which is achieved by choosing $\beta_i(1) = 1$ (droplet), $\beta_i(-1) = 10$ (ambient liquid), and using an appropriate sin-function to interpolate between those values in the interfacial region ($i = 1, 2, 3$). The properties of the species types are specified in Table 3. The droplet initially contains only uncharged molecules, i.e., $\omega^0_{1,h} = 2$ in an origin centered ball with radius 0.1 and decays linearly until it vanishes on the origin centered sphere with radius 0.29, while $\omega^0_{2,h} \equiv \omega^0_{3,h} \equiv 0$. The uncharged molecules may decompose into charged ions. The rate of decomposition and recombination is prescribed by the coefficients $\zeta_1 = -2$, $\zeta_2 = \zeta_3 = 2$ (cf. Table 3).

The electrostatic potential V is computed on $\Omega^* := \{x \in \mathbb{R}^3 : -2 < x_1 < 2,\ x_2^2 + x_3^2 < 1\}$. The base surfaces of this cylinder are assumed to be electrodes, i.e., we prescribe inhomogeneous Dirichlet data $\overline{V} = 5$ on $\{x \in \partial\Omega^* : x_1 = -2\}$ and $\overline{V} = -5$ on $\{x \in \partial\Omega^* : x_1 = 2\}$. Matching to the representation of the ion number densities, the electrodes in Fig. 7 are colored in red (positive) and blue (negative). On the lateral area of Ω^*, we impose $\nabla V \cdot n = 0$.

In this simulation, we use a penalized polynomial double-well potential (see (4.3)) with a penalty parameter $\delta' = 4 \cdot 10^{-3}$. Its derivatives are approximated using (DQ). For the remaining parameters, we refer to Table 4.

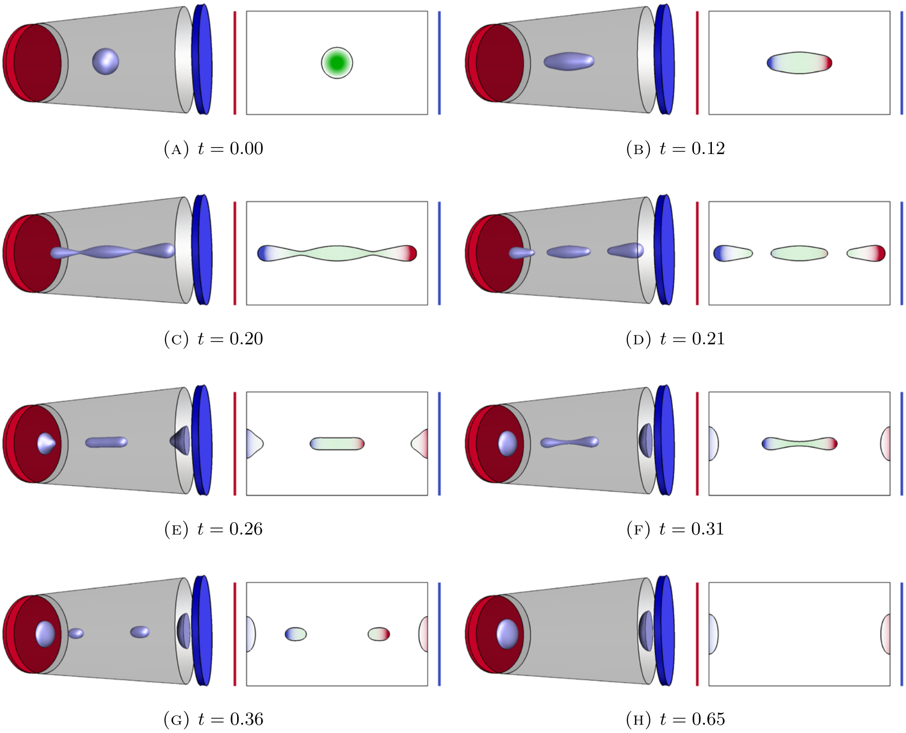

Fig. 7 Ion-induced droplet breakup. Left: droplet shape. Right: cross-section showing species distributions

Assuming rotational symmetry, we may describe the setting using cylindrical coordinates and use a two-dimensional, adaptive mesh consisting of simplices with diameters between 0.0625 and approximately 0.0055. The simulation was performed using a fixed time increment $\tau = 10^{-4}$.

Figure 7 shows the evolution of the droplet and the dissolved species. The evolution of the three-dimensional droplet is depicted on the left-hand side. The right-hand side of Fig. 7 shows a cross-section of Ω^*.

As depicted in Fig. 7b, the molecules start decomposing into ions which move towards the electrodes. As the species are only soluble in the droplet, this movement causes the droplet to stretch—resulting in neckings (see Fig. 7c) and finally in the

Table 3 Species parameters used in the simulation in Section 4.3

species	z_i	$k_i(\pm 1)$	ζ_i	$\beta_i(-1)$	$\beta_i(+1)$
$i = 1$	0	2	-2	10	1
$i = 2$	-3	2	2	10	1
$i = 3$	3	2	2	10	1

Table 4 Parameters used in the simulation in Section 4.3

σ	δ	m	$\gamma_{fs}(\pm 1)$	α	ϑ	$\rho(\pm\, 1)$	$\eta(\pm\, 1)$	ϵ	ν	τ
0.1	0.01	0.05	0	0	1	10^{-4}	0.05	0.5	10^{-5}	10^{-4}

breakup of the droplet (see Fig. 7d). As most of the ions are located in the detached satellite droplets, the central droplet, which still contains uncharged molecules, is hardly affected by the electric field for a short period of time and therefore tries to recover a circular shape. At the same time, the satellite droplets continue drifting towards the electrodes. Since the decomposition of the molecules continues, the ion concentration in the central droplet rises again—resulting once again in stretching, necking and rupture of the droplet (see Fig. 7e–g). At the end of the simulation (see Fig. 7h), there are two charged droplets positioned at the base surfaces of Ω. Although the droplets try to minimize their surface, they do not attain a hemispherical shape, as they also try to maximize the contact area with $\partial\Omega$ in order to allow the ions to get as close to the electrodes as possible without piling up.

In the first scenario, the influence of the ions on the electrostatic potential was negligible in comparison to the influence of the prescribed boundary data. In the second scenario, we reduce the impact of the boundary conditions by choosing grounded electrodes which are placed further away from the fluidic domain, i.e., we choose $\Omega^* := \{x \in \mathbb{R}^3 : -3 < x_1 < 3,\ x_2^2 + x_3^2 < 1\}$ with homogeneous Dirichlet conditions on the base surfaces. Again, on the lateral area $\nabla V \cdot n = 0$ is imposed. We position circular droplets with radius 0.3 and barycenters at $(\pm\, 0.5, 0, 0)$. Initially, these droplets contain ions. Similarly to the last scenario, we prescribe $\omega_{2,h}^0 = 2$ and $\omega_{3,h}^0 = 2$ in a ball with radius 0.1 and assume linear decay until the number density vanishes on a sphere with radius 0.29 (see Fig. 7a). The positively charged ions are placed in the left droplet, i.e., the barycenter of their number density is at $(-\, 0.5, 0, 0)$, and the negatively charged ions are placed around $(0.5, 0, 0)$. The initial number density of the uncharged molecules is set to zero. The remaining parameters stay unchanged and can be found in Tables 3 and 4. Again, the derivatives of the penalized, polynomial double-well potential with $\delta' = 4 \cdot 10^{-3}$ are approximated using (DQ).

Figure 8 shows the evolution of the droplet and the dissolved species. Thereby, some figures show the three-dimensional droplets, while others show a cross-section. The grounded electrodes which are placed farther from the fluidic domain are not depicted. The color of the droplets in Fig. 8a, d, and h indicates the electrostatic potential on the zero level line of the phase-field (red: positive; blue: negative; green: ≈ 0). In the figures depicting the cross-section, the colors indicate the number densities of the species ($\omega_{1,h}$: green; $\omega_{2,h}$: blue; $\omega_{3,h}$: red). The arrows visualize the electric field, i.e. $-\nabla V$. The grounded electrodes are placed outside of the picture. As depicted in Fig. 8, the droplets move towards each other, collide, and finally merge. As soon as the droplets merge, the electrical charges equilibrate causing the disappearance of the electric field (see Fig. 8f–g). At the same time the reaction starts and

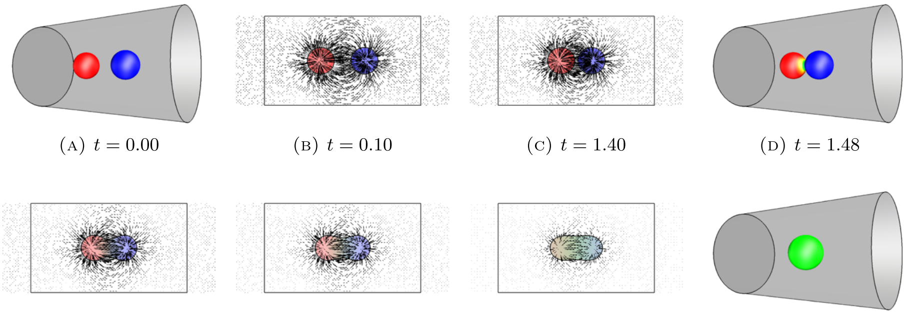

(A) $t = 0.00$ (B) $t = 0.10$ (C) $t = 1.40$ (D) $t = 1.48$

(E) $t = 1.51$ (F) $t = 1.53$ (G) $t = 1.58$ (H) $t = 2.58$

Fig. 8 Ion-induced droplet coalescence

produces uncharged molecules. After some time only one uncharged, circular shaped droplet remains (see Fig. 8h). This droplet still contains a significant amount of ions, but as the ion charges cancel out each other, the entire droplet is uncharged.

Funding information This research has been supported by Deutsche Forschungsgemeinschaft (German Science Foundation) through the Priority Programme 1506 "Transport processes at fluidic interfaces".

References

1. Abels, H., Garcke, H., Grün, G.: Thermodynamically consistent, frame indifferent diffuse interface models for incompressible two-phase flows with different densities. Math. Model. Methods Appl. Sci. **22**(3), 1150013 (2012)
2. Aland, S., Boden, S., Hahn, A., Klingbeil, F., Weismann, M., Weller, S.: Quantitative comparison of Taylor flow simulations based on sharp-interface and diffuse-interface models. Int. J. Numer. Methods Fluids **73**(4), 344–361 (2013)
3. Armero, F., Simo, J.C.: Formulation of a new class of fractional-step methods for the incompressible MHD equations that retains the long-term dissipativity of the continuum dynamical system. Fields Inst Commun **10**, 1–24 (1996)
4. Brenner, S.C., Scott, L.R.: The mathematical theory of finite element methods. Springer, Berlin (2002)
5. Campillo-Funollet, E., Grün, G., Klingbeil, F.: On modeling and simulation of electrokinetic phenomena in two-phase flow with general mass densities. SIAM J. Appl. Math. **72**(6), 1899–1925 (2012). https://doi.org/10.1137/120861333
6. Ciarlet, Ph.G.: The finite element method for elliptic problems. North-Holland, Amsterdam (1978)
7. Copetti, M.I.M., Elliott, C.M.: Numerical analysis of the Cahn–Hilliard equation with a logarithmic free Energy. Numer. Math. **63**, 39–65 (1992)
8. Eck, C., Fontelos, M.A., Grün, G., Klingbeil, F., Vantzos, O.: On a phase-field model for electrowetting. Interfaces Free Boundaries **11**, 259–290 (2009)
9. Fontelos, M.A., Grün, G., Jörres, S.: On a phase-field model for electrowetting and other electrokinetic phenomena. SIAM J. Math. Anal. **43**(1), 527–563 (2011)
10. Grün, G.: Partiell gleichmäßige Konvergenz finiter Elemente bei quasikonvexen Variationsintegralen. Diploma Thesis (Universität Bonn), Bonn (1991)
11. Grün, G.: On convergent schemes for diffuse interface models for two-phase flow of incompressible fluids with general mass densities. SIAM J. Numer. Anal. **6**, 3036–3061 (2013)
12. Grün, G., Guillén-González, F., Metzger, S.: On fully decoupled, convergent schemes for diffuse interface models for two-phase flow with general mass densities. Commun. Comput. Phys. **19**(5), 1473–1502 (2016). https://doi.org/10.4208/cicp.scpde14.39s

13. Grün, G., Klingbeil, F.: Two-phase flow with mass density contrast: stable schemes for a thermodynamic consistent and frame-indifferent diffuse-interface model. J. Comput. Phys. **257, Part A**, 708–725 (2014)
14. Grün, G., Rumpf, M.: Nonnegativity preserving convergent schemes for the thin film equation. Numer. Math. **87**, 113–152 (2000). MR 1800156 (2002h:76108)
15. Guillén-González, F., Tierra, G.: Splitting schemes for a Navier–Stokes–Cahn–Hilliard model for two fluids with different densities. J. Comput. Math. **32**(6), 643–664 (2014)
16. Garcke, C., Kahle, H., Hinze, M.: A stable and linear time discretization for a thermodynamically consistent model for two-phase incompressible flow. Hamburger beiträge zur Angewandte Mathematik (2014)
17. Klingbeil, F.: On the numerics of diffuse-interface models for two-phase flow with species transport. Ph.D. thesis, friedrich-alexander-universität erlangen-nürnberg, Erlangen (2014)
18. Metzger, S.: On numerical schemes for phase-field models for electrowetting with electrolyte solutions. PAMM **15**(1), 715–718 (2015). https://doi.org/10.1002/pamm.201510346
19. Metzger, S.: Diffuse interface models for complex flow scenarios: modeling, analysis and simulations. Ph.D. thesis, Friedrich-Alexander-Universität Erlangen-Nürnberg, Erlangen (2017)
20. Minjeaud, S.: An unconditionally stable uncoupled scheme for a triphasic Cahn–Hilliard/Navier-Stokes model. Num. Methods PDE **29**(2), 584–618 (2013)
21. Nochetto, R.H., Salgado, A.J., Walker, S.W.: A diffuse interface model for electrowetting with moving contact lines. Math. Model Methods Appl. Sci. **24**(1), 67–111 (2014)
22. Qian, T., Wang, X., Sheng, P.: A variational approach to the moving contact line hydrodynamics. J. Fluid Mech. **564**, 333–360 (2006)
23. Werner, H., Arndt, H.: Gewöhnliche Differentialgleichungen. Springer, Berlin–Heidelberg (1991)